AD-778 012

MATERIALS FOR RADIATION DETECTION

National Materials Advisory Board (NAS-NAE)

Prepared for:

Office, Defense Research and Engineering

January 1974

REPORT DOCUMENTATION PAGE		READ INSTRUCTIONS BEFORE COMPLETING FORM
1. REPORT NUMBER NMAB-287	2. GOVT ACCESSION NO.	3. RECIPIENT'S CATALOG NUMBER AD 778012
4. TITLE *(and Subtitle)* "Materials for Radiation Detection"		5. TYPE OF REPORT & PERIOD COVERED FINAL
		6. PERFORMING ORG. REPORT NUMBER
7. AUTHOR(s) NMAB ad hoc Committee on Materials for Radiation Detection Devices		8. CONTRACT OR GRANT NUMBER(s) DA-49-083-OSA-3131
9. PERFORMING ORGANIZATION NAME AND ADDRESS National Materials Advisory Board Division of Engineering-National Research Council National Academy of Sciences-National Academy of Engineering 2101 Constitution Ave., Washington, D.C., 20418		10. PROGRAM ELEMENT, PROJECT, TASK AREA & WORK UNIT NUMBERS
11. CONTROLLING OFFICE NAME AND ADDRESS ODDR&E, Department of Defense The Pentagon, Washington, D. C.		12. REPORT DATE January 1974
		13. NUMBER OF PAGES 359
14. MONITORING AGENCY NAME & ADDRESS*(if different from Controlling Office)*		15. SECURITY CLASS. *(of this report)* Unclassified
		15a. DECLASSIFICATION DOWNGRADING SCHEDULE

16. DISTRIBUTION STATEMENT *(of this Report)*

This document has been approved for publication release and sale; its distribution is unlimited.

17. DISTRIBUTION STATEMENT *(of the abstract entered in Block 20, if different from Report)*

18. SUPPLEMENTARY NOTES

19. KEY WORDS *(Continue on reverse side if necessary and identify by block number)*

See table of contents

Reproduced by
NATIONAL TECHNICAL
INFORMATION SERVICE
U S Department of Commerce
Springfield VA 22151

20. ABSTRACT *(Continue on reverse side if necessary and identify by block number)*

This report surveys the available information (complete through 1971) on detectors for the electromagnetic radiation spectrum in the wavelength range 10^{-10} to 1 cm. The detectors are divided according to wavelength range into four groups: (1) sensors for x-rays and gamma-rays; (2) sensors for ultraviolet, visible and near-infrared radiation; (3) detectors for infrared radiation from 2 to 200 micrometers; (4) detectors for far-infrared and millimeter wave radiation.

DD $_{1\ JAN\ 73}^{FORM}$ 1473   EDITION OF 1 NOV 65 IS OBSOLETE   UNCLASSIFIED

Progress on a broad front in the understanding of materials and the production of devices useful in radiation detection is recognized, but limitatio s both in the quality and properties of available material and in fundamental understanding require intensive effort in a number of areas. Conclusions and recommendations are made for (a) fundamental studies, (b) research on specific materials with definite applications, and (c) the establishment of two groups for continuing review and further study of specific problems. Priorities have been assigned to the various recommendations, based on the Committee's judgment of the importance of the required need and the probability of success in a research and development effort aimed at satisfying that need.
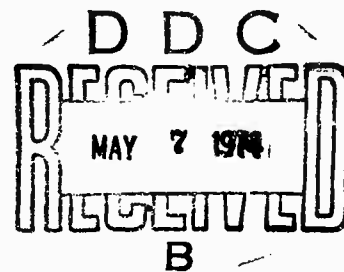
MATERIALS FOR RADIATION DETECTION

REPORT OF THE AD HOC
COMMITTEE ON MATERIALS FOR RADIATION DETECTION DEVICES

NATIONAL MATERIALS ADVISORY BOARD
DIVISION OF ENGINEERING - NATIONAL RESEARCH COUNCIL

Approved for Public Release
Distribution Unlimited

D D C
RECEIVED
MAY 7 1974
B

January, 1974
Publication NMAB 287
National Academy of Sciences - National Academy of Engineering
2101 Constitution Avenue, N. W.
Washington, D. C., 20418

ib

NOTICE

The project which is the subject of this report was approved by the Governing Board of the National Research Council, acting in behalf of the National Academy of Sciences. Such approval reflects the Board's judgment that the project is of national importance and appropriate with respect to both the purposes and resources of the National Research Council.

The members of the committee selected to undertake this project and prepare this report were chosen for recognized scholarly competence and with due consideration for the balance of disciplines appropriate to the project. Responsibility for the detailed aspects of this report rests with that committee.

Each report issuing from a study committee of the National Research Council is reviewed by an independent group of qualified individuals according to procedures established and monitored by the Report Review Committee of the National Academy of Sciences. Distribution of the report is approved, by the President of the Academy, upon satisfactory completion of the review process.

———

Members of the National Materials Advisory Board study groups serve as individuals contributing their personal knowledge and judgments and not as representatives of any organizatic n in which they are employed or with which they may be associated.

The quantitative data published in this report are intended only to illustrate the scope and substance of information considered in the study and should not be used for any other purpose, such as in specifications or in design, unless so stated.

NATIONAL MATERIALS ADVISORY BOARD
DIVISION OF ENGINEERING – NATIONAL RESEARCH COUNCIL
AD HOC COMMITTEE ON MATERIALS FOR RADIATION DETECTION DEVICES

Chairman: Maurice Glicksman, University Professor, Division of Engineering, Brown University, Providence, R. I.,, 02912

Members: Elias Burstein, Professor, Department of Physics, University of Pennsylvania, Phialdelphia, Pa., 19104

John W. Cleland, Physicist, Solid State Division, Oak Ridge National Laboratories. Box X, Oak Ridge, Tennessee, 37830

Ali Javan, Professor, Department of Physics, Massachusetts Institute of Technology, Cambridge, Massachusetts, 02139

Paul W. Kruse, Jr., Senior Staff Scientist, Corporate Research Center, Honeywell, Inc., 10701 Lyndale Ave. S., Bloomington, Minnesota, 55420

James W. Mayer, Professor, Department of Electrical Engineering, California Institute of Technology, 1201 E. California Blvd., Pasadena, California, 91109

Karl H. Zaininger, Head, Solid State Device Technology, David Sarnoff Laboratories, Radio Corporation of America, Princeton, New Jersey, 08540

NMAB
Staff: Robert S. Shane, Staff Scientist, National Materials Advisory Board, National Academy of Sciences, 2101 Constitution Ave., N. W., Washington, D. C., 20418

Liaison Representatives

DoD Jerome Persh, Staff Specialist for Materials and Structures (Engineering Technology) ODDR&E, Department of Defense, Washington, D. C., 20301

George H. Heilmeier, Assistant Director (Electronics and Computer Sciences) ODDR&E, Department of Defense, Washington, D. C., 20301

iii

ARPA   C. M. Stickley, Director, Materials Science, Defense Advanced Research Projects Agency, 1400 Wilson Blvd., Arlington, VA 22209

Dept. of   Stanley Kronenberg, Institute of Exploratory Research,
Army   U. S. Army Electronics Command, Ft. Monmouth, N. J. 07703

        Karl Thomas, Night Vision Laboratory, U. S. Army Mobility Equipment Research and Development Center, Ft. Belvoir, VA 22060

Dept. of   James Willis, Electronics Scientist, Code AIR-310, Naval
Navy   Air Systems Command, Washington, D.C. 20360

Dept. of   Freeman Shephers, U. S. Air Force Cambridge Research
Air Force Laboratory, Hanscom Field, Bedford, MA 01730

NASA   Bernard Rubin, NASA Headquarters, Code REE, 600 Indepencence Ave., Washington, D.C. 20546

Dept. of   David Sawyer, National Bureau of Standards, Washington,
Commerce D. C., 20234

ABSTRACT

This report surveys the available information (complete through 1971) on detectors for the electromagnetic radiation spectrum in the wavelength range 10^{-10} to 1 cm. The detectors are divided according to wavelength range into four groups: (1) sensors for x-rays and gamma-rays; (2) sensors for ultraviolet, visible and near-infrared radiation; (3) detectors for infrared radiation from 2 to 200 micrometers; (4) detectors for far-infrared and millimeter wave radiation. Progress on a broad front in the understanding of materials and the production of devices useful in radiation detection is recognized, but limitations both in the quality and properties of available material and in fundamental understanding require intensive effort in a number of areas. Conclusions and recommendations are made for (a) fundamental studies, (b) research on specific materials with definite applications, and (c) the establishment of two groups for continuing review and further study of specific problems. Priorities have been assigned to the various recommendations, based on the Committee's judgment of the importance of the required need and the probability of success in a research and development effort aimed at satisfying that need.

PREFACE

This study originated pursuant to a request for information from the Department of Defense, Office of the Director of Defense Research and Engineering.

The National Materials Advisory Board (NMAB) undertook the task of initiating a survey of materials for electromagnetic radiation detection devices (over the range of wavelengths from 10^{-10} cm to 1.0 cm) in order to define the needs, opportunities, limitations, and problems involved in advancing current technology, including an R & D program to permit satisfying the needs and exploiting the opportunities.

The National Materials Advisory Board Constituted an ad hoc Committee to conduct the study of "Materials for Radiation (electromagnetic) Detection Devices." This Committee reviewed the initial task, listened to statements of federal agency liaison personnel on problem areas, decided on areas of interest, received presentations by experts in specified areas of the field of study, collected information, discussed conclusions and recommendations, and drafted this report. The report is written from a materials rather than a processing viewpoint.

This report is organized to meet the needs of several categories of readers. To serve managers it presents a summary of the more important conclusions and recommendations. The information which served as a basis for the conclusions and recommendations as well as a detailed presentation of them, along with a list of references, is presented in subsequent chapters. The table of contents is quite detailed since it is also designed to serve as a subject index.

ACKNOWLEDGMENTS

CONTENTS

GENERAL INTRODUCTION

1.1 Objectives

The Committee was originally asked to conduct a survey of materials for radiation detection devices (in the range of wavelengths from 10^{-9} to 1.0 cm) to define the needs, opportunities, fundamental limitations, and problems involved in advancing current technology. This would include discussion of research and development programs which would allow the satisfaction of currently known needs, and exploit opportunities that could generate advanced applications.

After considering government needs, the range of wavelengths was modified to 10^{-10} cm to 1.0 cm (10^{-6} μm to 10^{4} μm). High priority was assigned to development of suggestions for research on specific topics in the wavelength ranges of interest. Emphasis was placed on the newer detection mechanisms and the materials requirements involved.

Great importance was assigned to presentation of the current state of knowledge of detector materials, not only to put the study in proper perspective, but also to provide a reference source for those who may be approached for support of research on materials science problems that may already have been solved.

Finally, the Committee emphasized materials problems rather than device development, while recognizing that materials are ultimately evaluated when incorporated in a device.

1.2 Scope

The Committee decided that its purview consisted of material properties and allied processing within a framework of device utilization and applications. From the point of view of detector applications, it appeared most useful to structure the study according to wavelength range, rather than in terms of materials or physical phenomena. The study was carried out in five parts that are reviewed in separate chapters of this report:

- Fundamentals of electromagnetic radiation detection.
- Sensors for wavelength range 10^{-6} to 10^{-1} μm (quantum energy range: 1.24 MeV to 12.4 eV).
- Sensors for wavelength range 10^{-1} to 2.0 μm.
- Sensors for wavelength range 2.0 to 200 μm.
- Sensors for wavelength range 200 to 10^4 μm.

The needs and programs of the Department of Defense (DoD), National Aeronautics and Space Administration (NASA) and Atomic Energy Commission (AEC) were considered during the work of the Committee.

Since some of the applications and desirable characteristics of several detectors are in the classified literature (as are also some current state of the art data), it was necessary for the Committee to hold several meetings that involved classified information. Even so, the Committee felt that it was unable to obtain a complete understanding of the relative importance of various classified goals and needs because of the difficulties in evaluating incomplete presentations.

The Committee planned its study to ascertain the various mechanisms and physical phenomena that could be of use in radiation detection. For each of these the Committee attempted to determine:

- Fundamental limitations inherent in the mechanism or phenomenon.
- State of the art with regard to materials used in these ways and the prospect of approaching fundamental limitations.
- Environmental interactions and their effects on detector performance.
- Desirable material properties and the possible new materials or necessary changes in old materials that could match the requirements.

1.3 Exclusions and Caveats

Although this Committee discussed the relative priority of its conclusions and recommendations, this report does not attempt to advise managers of resources how they should allocate those resources among the various fields of inquiry. The approach the Committee took in attempting to give high or low priority to its recommendations is discussed in 1.4.

The Defense Nuclear Agency (DNA) was invited to participate in the work of the Committee. DNA representatives attended one meeting; thereafter the agency did not participate, stating that the work of this Committee had no relevance to the assigned mission of DNA.

Specific exclusions from this report include inter alia, vulnerability and hardening of materials and devices to nuclear weapon radiation and other effects as well as: information processing; mosaics (but see 6.6.3 and 2.3.2.3.6-8); specific device design improvement; chemical detectors (e.g., photographic film); most aspects of integrating mode detectors for X-rays (a problem was recognized in this area – see 4.3); and, coherent amplifying devices in the microwave region (e.g., travelling wave tubes).

1.4 Committee Approach

The Committee recognized that this report could have only four principal accomplishments:

- Delineation of the state of the art in detector materials and detectors.
- Identification of problem areas and possible opportunities.
- Identification of possible avenues of approach to solve these problems and exploit the opportunities.
- Recommendation of choices among the possible avenues of approach.

In several cases, the Committee found somewhat divergent views regarding the relative importance of several competing types of detectors. It has attempted to present a fair picture of the current understanding and has taken what it believes to be the best view in making its recommendations.

In assessing priorities, the major factors considered were the importance of users' needs, the probability of success in research and development, and the relative effect such success would have in achieving the goals for devices which are desired. Opinions on the conclusions drawn were solicited from experts in device use and materials preparation and characterization. The Committee considered these and then reached the consensus presented in this report. Whatever quantification procedure might have been used, the basic relative weightings would still contain a major sub-jective input; even so, the Committee felt that some recommended relative priority was desirable.

1.5 Committee Viewpoints

The members of this Committee are involved with materials research and development, rather than device making and using. Thus, the Committee was interested in input information, germane to evaluation of materials research needs, from device makers and users and attempted to solicit as much of this information as possible in the limited time available. Less attention was given to processing or specific device matters.

1.6 Committee Termination Date

The Committee essentially completed its survey of the state of the art by the end of 1971. Literature references beyond that date are not included except for unpublished work that came to the Committee's attention.

SUMMARY: MAJOR CONCLUSIONS AND RECOMMENDATIONS

2.1 Introduction

The problem of clearly detecting the presence and character of electro-magnetic energy has become increasingly important in recent years. Devices that can detect radiation in the visible and infrared ranges of the spectrum with sensiti-vity and contrast approaching fundamental limits are available, but generally radi-ation is not detected with such sensitivity. This report surveys the available infor-mation or detector operation over a wide range of wavelengths (10^{-10} to 1 cm), ex-amines the basic principles of operation and the limitations on performance of de-tectors, and discusses areas of research wherein improvements might be effected.

It must be stressed that the interest here is primarily in the materials used in such detectors. and particularly the materials that perform the primary act of detection. The devices, connections, etc. involved in the processing of informa-tion coming from the detector(s) and the problems of multi-dimensional arrays of detector devices are not considered, except for several clear cases in which prob-lems in such areas of study have close bearing on individual detector-material choices. Detection involves the conversion of the photons of electromagnetic energy into a form that can be processed further, usually of an electrical or chemical nature. The photons may excite charge carriers from immobile states to states in which they and/or their progeny can be collected at contacts or electrodes; they may modify the conduction of carriers already mobile; they may heat the detector material or part of the detector complex, resulting in a change in electrical, optical, or mechanical properties; they may provide the energy necessary to cause a local chemical reaction; they may (on absorption) change the state of an atomic complex so as to change its physical properties. A comparison of the performance of materials known to operate in one or more of these modes is necessary for some understanding of the desirable direction of future work.

It is of interest to note that the principal superior devices for electro-
magnetic radiation detection (especially in the γ-ray and infrared ranges) utilize
semiconductors as the detector material. Development of improved detectors will
depend on continuing research effort on the processing of existing semiconductors
to improve bulk material properties, bulk homogeneity, and, most important for
many applications, the surface and interface conditions of the material, as well as
research to develop desirable new semiconducting materials. It should be recog-
nized that the requirements for the production of semiconductor materials for other
device applications are not the same as those for detectors. Thus, development of
satisfactory material for detector use requires further study of presently available
material that may be eminently satisfactory for other semiconductor component
applications.

The current state of the art of detectors is reviewed in each of the
chapters, and where appropriate, summarized in graphic and tabular form (e.g.,
see 6.1.2 for the 1–1000 μm range). The next section provides an overview of
recent accomplishments in the field, and the problem areas that need to be attacked.
A summary of the most important conclusions and recommendations completes
this chapter.

2.2 Recent Accomplishments and Present Problems

As a result of extensive effort supported by agencies of the U. S.
Government, and a considerable investment by industrial laboratories and develop-
ment groups, there has been progress on a broad front in the understanding of ma-
terials and the production of devices useful for electromagnetic radiation detection.
Among the significant results are:

- The development of detectors f X-rays and γ-rays with
  very good energy resolution. These detectors, which must
  be stored and operated at low temperatures, use germanium.
  (Some of the success in this effort is a spin-off from develop-
  ments made to advance detectors useful in nuclear spectroscopy.)

- The development of detectors with very high sensitivity to visible radiation and capable of good spatial resolution in imaging applications. The most recent detectors use III-V* compounds and alloys for operation in the near-infrared. In recent years, this effort has yielded very good imaging detectors in the near-infrared, as a result of the application of techniques like that of negative electron affinity (NEA) to imaging structures.

- The development of single-element detectors and one-dimensional arrays with very good sensitivity to infrared radiation. These use a number of different semiconductors and semiconductor alloys.

- The development of very good detectors of far-infrared and millimeter-wave radiation, although the applications in this wavelength range are, as yet, limited in number and importance.

- The development of useful detectors of infrared radiation that are of lower sensitivity, but have the advantage of operating at room temperature. These have been made possible by the development of new pyroelectric materials such as triglycine sulfate.

- Basic studies that have yielded understanding of the direct effects of incoming electromagnetic radiation on detector material. (The sources of noise in high-quality detector materials and the characteristics of the material that affect the resulting signal in a number of specific devices have been identified.) This understanding applies most successfully to devices using silicon or germanium as intrinsic or extrinsic photoconductors.

As a result of effort in recent years, a wide range of materials of fairly good quality (in some cases excellent quality) has become available, and these have permitted substantial progress in the development of good detectors. It is clear that much improvement in the quality of useful materials, in most cases requiring improved understanding of the material and its properties, as well as some effort in finding new materials for specific special needs, are needed. The Committee addressed itself to the needs for improved materials for detectors, especially in the following

---

* Roman numerals are used throughout this report to denote the Group or Family in the Table of Periodic Properties of the Elements.

8

areas:

- Development of improved materials that can be used in detectors for high-energy X-rays and γ-rays. These detectors should not only achieve the required resolution, but also be capable of being stored without refrigeration and functioning satisfactorily thereafter.

- Development of materials for highly sensitive infrared detectors, capable of operating advantageously in the presence of a "cold" background.

- Development of appropriate materials and combinations of materials that can be used in very sensitive imaging detectors capable of operating at wavelengths in the near-infrared and mid-infrared. To achieve these goals will require work with composite structures (e.g., semiconductors with surfaces modified by metal atoms and other elements); an important problem is the poor control of the materials at the interfaces.

- Development of materials for use in arrays, designed to perform an imaging function at infrared wavelengths. A major problem in the attainment of this goal is the inhomogeneity of the present materials. This inhomogeneity is due in part to the fact that they are semiconducting alloys, and alloys are very difficult to produce in homogeneous form.

- The development of suitable materials for use in detection of laser radiation in the near-infrared (1-2 μm region of wavelength), as well as in the 5 to 10 μm region. These have applications relevant to star tracking, information gathering, and communication systems.

- An understanding of the properties of semiconducting materials, particularly heterogeneous materials (involving contacts, surfaces, and internal defects), as they affect the signal that results from electromagnetic radiation falling on the detector made from such materials. (Such an understanding is essential information for decision-making in achieving the previously listed goals.)

It is important to recognize the role that basic studies can play in a successful attack on many of the problems discussed in this report. Among the most vital of these is the need to characterize and control the properties of surfaces and interfaces especially in the compound semiconductors that play a major role in detectors throughout the spectral range of study. It is fair to say that the state of knowledge of surface and interface properties today can be compared to that of bulk semiconductors in the early 1950's. A concerted effort to improve our understanding of and ability to control surfaces and defects in semiconductors should pay off in many ways. Not least among these would be an improvement of the government's ability to procure electromagnetic-radiation detection devices at minimum cost.

Enough is now known to attack the problems effectively. The approach used in the past has been empirical, with the usual result that the solution of a specific problem yielded little that could be generally applied to other related problems. There is sound reason for confidence in the development of a predictive capability if the fundamental problems are attacked with determination and ability.

2.3   Summary of Conclusions and Recommendations

Detailed conclusions and recommendations are contained in each of the following chapters (except for Chapter 3). The Committee has attempted to assign some priority to these recommendations within each of the wavelength regions considered. This is reflected in the order of presentation of the conclusions and recommendations in the summary. Those having high (Priority 1) or moderate (Priority 2) priority are more briefly summarized in this chapter than in the respective chapters from which they come. Those considered to have lower priority (Priority 3) remain in the individual chapters. In this section, the recommendations are divided into three categories:

- fundamental studies
- materials research (mostly specific materials)
- administrative recommendations

10

Priorities are assigned in each of the categories, so that Priority 1 recommendations appear in each section and sub-section. The reader should refer to the individual chapters for all the conclusions and recommendations.

The recommendations for fundamental studies are basic and derive from problems encountered in several of the chapters. They are presented only in this chapter.

2.3.1 Fundamental Studies

2.3.1.1 Conclusions on Surface Studies (cf. Chapters 5 and 6)

Much fundamental understanding of bulk phenomena in homogeneous semiconductors is available. But the useful devices of today and of the foreseeable future, for the processes of photon detection, are made up of inhomogeneous, surface-dominated materials in many cases. Limited understanding of such systems has inhibited the development of efficient devices.

A sound scientific basis for engineering applications of surface properties has yet to be established. The outstanding need in surface physics and chemistry appears to be the development of a satisfactory microscopic (atomistic) phenomenological description. Progress toward this goal will demand painstaking effort and excellent cooperation among carefully chosen research teams addressing systems that can be more easily treated theoretically and that have a strong practical interest.

Recommendation (Priority 1)

Fundamental studies of the surfaces of solids and the interfaces between solids should be supported. Included in such studies would be determination of local potentials at the surface, the effect of surface environment and prior history, and the effects of chemical ambients, the electronic states, and bonding at the surface.

Theoretical studies would involve, *inter alia*, the electronic surface states, changes in work functions, surface chemical bonding, and film-growth processes. Experiments should make use of fairly simple material systems under very well controlled conditions; experimental techniques should include electron diffraction (particularly low-energy electron diffraction (LEED)), inelastic and Auger electron spectroscopy, and photoelectron spectroscopy. Effort on compound semiconducting materials should be emphasized.

2.3.1.2 Conclusion on Recombination and Trapping (cf. Chapters 4 and 6)

Common to many of the devices described in this report are problems with charge-carrier dynamics. These involve recombination processes and trapping mechanisms.

Recommendation (Priority 1)

Fundamental studies of the source of trapping in semiconductors should be supported. The relation of trapping effects to the impurity character and distribution (paring), the influence of surface bonds, and the effect of non-stoichiometric compound formation should be included in these studies.

2.3.1.3 Conclusion on Contacts (cf. Chapters 4, 5, and 6)

Many of the detectors discussed in this report have contacts used for the flow of current or the measurement of voltage. The metal-semiconductor interface has properties that are not fundamentally understood and is characterized by parameters that have to be empirically determined. What part of this uncertainty is due to material impurities at the interface (compound formation or other impurities that may be present) is not well understood.

Recommendation (Priority 2)

Research aimed at understanding the role of contacts in device performance should be supported. Included in such studies would be the physical and mechanical properties of the interfaces, recombination due to states in the interface, and the role such effects play in the noise of device in operation.

2.3.2 Materials Research

2.3.2.1 X-Ray and Gamma Ray Detectors (10^{-6} to $0.1\,\mu m$)

2.3.2.1.1 Conclusion on Detector Material Evaluation (cf. 4.4.2)

Commercial organizations have not found it profitable to support materials research of the type required for the development of detectors in this short wave-length region.

Recommendation (Priority 1)

Support should be provided for the development of detector quality materials, the maintenance of the capability of instrumentation and detector development groups, and the investigation of physical and electrical properties useful in materials evaluation.

2.3.2.1.2 Conclusion on High-Purity Germanium (cf. 4.4.4)

Germanium is the principal material used in gamma-ray detectors; however, when lithium drifting is used in fabrication, it requires low-temperature storage and operation. High-purity germanium suitable for use without lithium drifting is available in small quantities from one supplier and shows promise of being detector quality material. Commercial justification for continuing development of the high-quality germanium is uncertain.

Recommendation (Priority 1)

Developmental work on the production of high-purity germanium should be continued and expanded to provide two competent sources. Research aimed at improving quality and characterizing the material should be supported.

2.3.2.1.3 Conclusion on Cadmium Telluride (cf. 4.4.5)

A need for gamma-ray detectors that can operate at temperatures up to 100° C appears to be satisfied by cadmium telluride detectors. Significant advances in the material properties have resulted from research aimed at its use in electro-optic modulation as well as in detectors. The performance of present devices is limited by the concentration of trapping centers and material inhomogeneity.

Recommendation (Priority 2)

Support research on cadmium telluride aimed at providing improved material and characterizing it for use in high-energy photon detectors.

2.3.2.1.4 Conclusion on Gallium Arsenide (cf. 4.4.6)

Gamma-ray detectors for use in spectroscopy and in medical probes, involving photons of energy below 100 keV, have been made from epitaxial gallium arsenide. These detectors have excellent resolution and show promise but are limited, at present, to quite thin layers (100 μm thick) because of severe trapping in thicker layers. Future use depends on availability of layers of higher purity and lower trap density; there is no program in the United States at this time on the application of epitaxial GaAs for this use.

Recommendation (Priority 2)

Develop a program to provide higher-purity epitaxial layers of gallium arsenide for gamma-ray detectors.

2.3.2.1.5 Conclusion on Materials Containing Elements of High Nuclear Charge (cf. 4.4.7)

Materials of high nuclear charge Z and larger band gaps than germanium or silicon have potential application in short-wavelength detectors. Lead oxide, lead iodide, and mercury iodide have been used to demonstrate the possibility of gamma-ray detection.

Recommendation (Priority 2)

Exploratory work on high-Z materials potentially useful in high energy photon detection should be supported.

2.3.2.2 Ultraviolet, Visible, and Near Infrared Detectors (0.1 - 2 μm)

2.3.2.2.1 Conclusion on GaAs Photocathodes (cf. 5.6.1.1)

The semitransparent negative electron affinity (NEA) photocathodes, using single crystal material for both active detector and its substrate, have shown considerable promise under laboratory conditions. The gallium arsenide photocathode with alloy substrates (gallium-aluminum arsenide or gallium-indium phosphide) is well along in the research and development cycle. A remaining significant materials problem is the uniformity of the photocathode; this non-uniformity is much affected by problems with the substrate.

Recommendation (Priority 1)

Continued materials research on the GaAs photocathode is recommended. Specific studies should include investigation of: preparation techniques for GaAlAs and GaInP substrates and their surfaces; the uniformity of resistivity and optical transmission; and the growth of GaAs on these substrates by vapor and liquid phase epitaxy. Techniques for sealing GaAs to glass faceplates and of etch-thinning GaAs wafers should be investigated with the aim of eliminating the expensive GaP substrate and, consequently, reducing photocathode costs.

2.3.2.2.2 Conclusion on the Alloy GaInAsP (cf. 5.6.1.2)

The quaternary alloy gallium-indium arsenide-phosphide appears to offer a useful alternative to InAsP and GaInAs as a NEA photocathode sensitive to 1.1 μm. It is expected that the activation process and the stability of the material should be much like those in the corresponding ternary alloys.

Recommendation (Priority 1)

A study of the growth and transport properties of the quaternary alloy GaInAsP should be supported over the range of compositions from InAsP to GaInAs corresponding to a band gap of 1.1 eV. Work on other quaternary alloys that may also operate in this range should be supported.

2.3.2.2.3 Conclusion on Ternary III - V Compound Alloys (cf. 5.6.1.3)

Negative electron affinity photocathodes, sensitive at $1.06 \mu m$, use the ternary III-V alloys $InAs_x P_{1-x}$ and $Ga_x In_{1-x} As$ (with $x \overset{\sim}{=} 0.15$) as the active layer; InAsP produces the best results. InP and GaAs are the best substrates for semi-transparent operation, but they are narrow band, particularly InAsP on InP. They are ideal for applications where narrow band response is desired. The only obvious broad-band response substrate for InAsP is $AlAs_x Sb_{1-x}$, with $x \overset{\sim}{=} 0.5$, which tends to oxidize in air. For GaInAs, GaInP could be used as a substrate. Considerable decay in performance with time, which may be related to lack of cleanliness in processing, has been observed for these photocathodes. The character of the Cs:O layer is not well understood for the ternary alloy photocathodes.

Recommendation (Priority 1)

The alloy AlAsSb should be investiaged as a broad-band substrate for InAsP to improve the airglow efficiency of the NEA photocathode. A more thorough investiga-tion should be made of the stability of this cathode, with particular emphasis on the effect that small levels of surface and ambient contaminants have on the sensitizing Cs:O layer. This should be complemented by more definitive studies of the character of the Cs:O layer and the nature of the activation process itself.

Recommendation (Priority 1)

Studies of GaInP as a substrate for the GaInAs NEA photocathode should be supported with emphasis on the substrate surface chemistry and the growth dynamics of the GaInAs layer. As with the InAsP photocathode, the stability of the activation process, the effects of surface and ambient contamination, and the character of the sensitizing layer should be investigated to reduce this photocathode to a practical device.

2.3.2.2.4 Conclusion on Silicon Charge-Coupled Devices (cf. 5.6.1.4)

Within the past few years silicon charge-coupled devices have developed into the most promising approach to solid-state imaging available at this time. The basic feasibility of this approach has been demonstrated for small numbers of image elements and for correspondingly low scan rates. These devices put considerably more strain on silicon metal-oxide-semiconductors (MOS) technology than metal-oxide-semiconductor field effect transistor (MOSFET) devices since the acceptable surface-state density is lower. The surface states constitute an additional noise source that masks the others present and reduces the transfer efficiencies that can be achieved. Unless this limitation can be removed, either array densities will remain small or scan rates must be reduced to maintain transfer efficiency. In either case, image resolution and acceptability will be sacrificed.

Recommendation (Priority 1)

Support is recommended for development of high-efficiency, high-density silicon charge-coupled devices (CCD) for imaging at standard video rates and with element numbers of at least 500 x 500 per device.

2.3.2.2.5 Conclusion on Materials for Field-Assisted Photocathodes (cf. 5.6.1.5)

In principle, it is possible to obtain photoemission beyond the limit of Cs:O covered surfaces (1.1 or 1.2 μm) by applying a bias to the sample--a process known as field-assisted photoemission. Sufficient work has not yet been done to single out a single material and approach to accomplish this. The most promising materials are germanium, gallium antimonide, gallium-indium arsenide, and indium arsenide-phosphide. Active layer thicknesses of 5 to 10 μm are required to optimize response and resolution.

Recommendation (Priority 1)

Research on materials for field-assisted photocathodes in the 1-2 μm region should be supported. The prime candidates are Ge, GaSb, GaInAs, and InAsP for the detector layer. The key areas of investigation should include substrate selection

and preparation, growth and doping parameters for the active layer, and transport properties within the active layer.

2.3.2.2.6 Conclusion on Heterojunction Diodes (cf. 5.6.1.6)

Although a field-assisted photocathode with two different materials in the active layer (heterojunction) is promising, achievement is retarded by the difficulties of mechanical matching of the materials. Recent results with liquid-phase epitaxy and close-spaced vapor-phase epitaxial growth appear to have potential for solving these problems.

Recommendation (Priority 2)

Studies of the growth and electrical characteristics of heterojunction diodes should be supported. The narrow-band-gap, p-type semiconductor should be chosen as the detector material for detection to $2\,\mu m$. Carrier transport across the diode, interface states, and the quantum efficiency should be investigated to determine combinations of materials. Similar studies should be supported on double-heterojunction samples.

2.3.2.2.7 Conclusion on Insulator Material (cf. 5.6.1.7)

Thin insulator films constitute special problems in materials technology; examples of such materials are silicon nitride (Si_3N_4) and aluminum oxide (Al_2O_3). The application for tunneling photocathodes contributes additional conditions (barrier height, small thickness) to those already present in insulators for passivation and insulation on semiconductors.

Recommendation (Priority 2)

A study of insulator materials suitable for tunneling barriers should be supported in connection with field-assisted photocathode applications. Insulator properties such as dielectric field strength, barrier height, uniformity, and interface state density at the semiconductor/insulator boundary should be investigated. It is recommended that available deposition methods be studied for a given semiconductor and insulator combination in order to develop the optimum deposition technique

compatible with low interface state densities, including fixed charge in the insulator, semiconductor thermal stability, and insulator uniformity.

2.3.2.2.8 Conclusion on Compound Semiconductors for Avalanche Diodes (cf. 5.6.2.1 and 5.6.2.2)

Research with indium arsenide-phosphide/indium phosphide has shown that good internal quantum efficiency can be obtained at 1.06 μm. Avalanche diodes using this material combination (or many others like it) with light entering through the substrate side are potential replacements for silicon devices. The improvement in quantum efficiency is potentially a factor of 3. Noise and dark current should be smaller than in silicon. Other possible combinations including gallium-indium arsenide/gallium arsenide, gallium arsenide-antimonide/gallium arsenide, and mercury-cadmium telluride/cadmium telluride. A number of III-V and II-VI alloy avalanche diodes could be used in the 1.4 to 1.6 μm range.

Recommendation (Priority 2)

A design analysis should be performed to determine the feasibility and expected performance of III-V and II-VI avalanche diodes in comparison with silicon, for 1.06 μm laser tracking applications. A similar analysis for materials to work in the eye-safe laser region (1.4 to 1.6 μm) also should be undertaken. These analyses should consider the system advantages as well. Work on selected alloy material should be supported to evaluate carrier mobilities, lifetimes, ionization coefficients and leakage current levels. Avalanche diodes using the selected material should be fabricated, passivated, and tested. Such a program should precede and guide any decision on a more substantial effort to develop practical devices.

2.3.2.2.9 Conclusion on Germanium Avalanche Diodes (cf. 5.6.2.3)

Single-element avalanche diodes that are sensitive to both the 1.06 μm and the 1.54 μm laser lines have been built using germanium. In addition to normal bulk-generated current, excessive leakage current, generated through impurities in the depletion region and through surface states, limits the effectiveness of these

devices. Cooling would be required to match the performance of silicon devices at
1.06 μm (with improved germanium material); thus germanium is not a viable candidate at that frequency. It is, however, a viable candidate for detection of the 1.54 μm laser radiation.

Recommendation (Priority 2)

Work on germanium avalanche diodes for detection in the eye-safe region
(1.4 to 1.6 μm) should be supported only if a final system decision is made to shift laser tracking operations into that wavelength range. Exclusion of copper contamination from the starting material and during processing and development of an adequate passivation technique should receive primary emphasis in any consequent work on device technology.

2.3.2.2.10 Conclusion on Materials for Star-Tracking Applications (cf. 5.6.2.4 and 5.6.2.5

Detectors for star-tracking applications can profitably employ materials having wider bandgaps than Si so as to provide lower dark currents and higher detectivities. An avalanche-diode detector potentially could withstand without loss of sensitivity a wider range of environmental extremes in terms of temperature and acceleration than a vacuum device. GaP and III-V compounds with similar band gaps are likely selections, but device technology is the principal limitation. Major areas requiring study are growth of the junction materials and passivating the junction surface (including guard rings). GaP has some promise, although there are disadvantages in a few areas, when compared with other III-V compounds.

Recommendation (Priority 2)

The materials technology for GaP avalanche diodes to be used in star-tracking applications should be developed. Study areas should include the growth of high-purity materials and the development of passivation and diffusion materials and technology. Coincident studies of device parameters such as carrier mobilities, lifetimes, and ionization coefficients should be made. Avalanche-diode performance parameters such as quantum efficiency, leakage current, and multiplication gain

and noise should be measured.

Recommendation (Priority 2)

The III-V compounds AlP and AlAs should be investigated as possible competitors with GaP for star-tracking applications. Main study areas should include materials growth and purity as well as passivation and diffusion materials and techniques. Device parameters such as carrier mobilities, lifetimes, and ionization coefficients should be measured. Avalanche-diode performance parameters such as quantum efficiency, dark current, and avalanche gain and noise should be studied. Techniques to protect the surface of these materials from humid ambients should be devised.

2.3.2.3 Infrared and Far-Infrared Detectors (2 to 200 μm)

2.3.2.3.1 Conclusion on HgCdTe Alloys (cf. 6.7.2)

In the infrared, the 1-to-3 μm range is of interest for rocket-plume and engine-tailpipe detection and for multispectral radiometry for earth resources mapping. The 3-to-5 μm range is of interest for rocket-plume detection and thermal imagery of terrain and ambient-temperature objects. The 8-to-14 μm range is the primary one for thermal imagery of terrain and ambient temperature objects. The 20-to-30 μm interval is of interest for detecting objects against cold space backgrounds.

HgCdTe is the best material for use in the 8-to-14 μm thermal-mapping application. In the photoconductive mode at 77° K, it is background limited in operation. The major problem is providing large areas, 1 cm^2 or more, of sufficient uniformity of composition and purity so that the performance of detectors in an array varies by no more than 10 %. In the other wavelength ranges, it appears that HgCdTe is either the best or one of the best materials. The problems in these ranges are the same as for the 8-to-14 μm interval.

Recommendation (Priority 1)

Research on HgCdTe alloys should be supported. It should aim at exploiting all ranges of composition; special emphasis should be placed on those ranges providing response in the 1-to-3 μm, 3-to-5 μm, 8-to-14 μm, and 20-to-30 μm intervals of the spectrum. The fundamental electrical and optical properties of the alloys in all compositional ranges should be studied with empahsis on determining the trapping and recombination mechanisms. For application to high-density arrays, grow.h methods should be developed to provide crystals of at least 1 inch in diameter of uniform high purity and uniform composition.

2.3.2.3.2 Conclusion on PbSnTe Alloys (cf. 6.7.3)

PbSnTe alloy detectors can operate well in the 8-to-14 μm and 20-to-30 μm ranges; they are operated in the photovoltaic mode because it has not been possible to purify them sufficiently for photoconductive operation. Background-limited infra-red photoconductor (BLIP cf. 3.3.1.1) operation occurs for the 8-to-14 μm detectors. The problems are similar to those with the HgCdTe alloys and involve uniformity of composition and purity.

Recommendation (Priority 1)

Research on PbSnTe alloys should be supported. It should aim at exploiting all ranges of composition; special attention should be given to performance in the 8-to-14 μm and 20-to-30 μm spectral intervals. The fundamental electrical and optical properties of the alloy in all compositional ranges should be studied with emphasis on determining the trapping and recombination mechanisms. For application to high-density arrays, growth methods should be developed to provide crystals of at least 1 inch in diameter of sufficiently high purity and very uniform in both composition and purity.

2.3.2.3.3 Conclusion on Doped Silicon Extrinsic Photoconductors (cf. 6.7.4)

The most important extrinsic materials of current interest in the infrared are silicon doped with phosphorus, arsenic, antimony, bismuth, boron, aluminum, gallium, or indium. All except the Si:In respond in the wavelength range between

15 and 30 μm and are of use in cold-background applications. The relatively high concentrations of dopants allowed in the detectors (compared to germanium) make possible 100 μm thick detector elements.

Recommendation (Priority 1)

Research directed toward exploiting the high-density array-integrated circuit potential of extrinsic photoconductors of Si:P, Si:As, Si:Sb, Si:Bi, Si:B, Si:Al, Si:Ga, and Si:In should be supported. The research should seek to determine the best material for the 20-to-30 μm application. Methods of preparing broad area (1 cm^2) single crystals of the best material and evaluating the potential for large high-density arrays should be supported. The development of integrated circuits within the array chip, operating at the array temperature, also should be supported.

2.3.2.3.4 Conclusion on Doped Germanium Extrinsic Photoconductors (cf. 6.7.5)

The most important extrinsic germanium detector is made from mercury-doped germanium and responds in the 8-to-14 μm region. It must be cooled below 30° K, while the alloy detectors operate at 77° K. Cadmium-doped germanium and copper-doped germanium operate in the 20-to-30 μm interval and do not have the cooling disadvantage with regard to alloy detectors since all have to be cooled below 77° K. Extrinsic germanium detector materials cannot be as heavily doped as those of silicon, thus requiring much thicker detectors. The germanium detectors can have their response times adjusted by compensating doping, an advantage not enjoyed by the intrinsic alloy detectors.

Recommendation (Priority 2)

Research on extrinsic germanium for use in the 8-to-14 μm and 20-to-30 μm intervals should be continued. The materials of primary interest are Ge:Hg for the former, and Ge:Cd and Ge:Cu for the latter. The need for resistance to pulsed radiation should be kept in mind. Studies should concentrate on recombination and trapping.

2.3.2.3.5 Conclusion on Ternary Diamond-Like Semiconductors (cf. 6.7.6)

A new class of materials of potential importance to infrared detection is the group of ternary diamond-like semiconductors that include members of the following classes: $A^{II}B^{IV}C_2^V$, $A_2^I B^{IV}C_3^{VI}$, $A^I B^{III}C_2^{VI}$, $A_3^I B^V C_4^{VI}$, and $A^I B^{IV}C_3^V$. Because of their simple nature, the preparation of uniform arrays of these materials at lower cost than the arrays of alloy semiconductors ultimately should be possible. Basic studies of growth and evaluation of the electrical and optical properties of many of these compounds have not been made.

Recommendation (Priority 2)

An intensive program should be initiated to explore methods of preparing single crystals of promising ternary diamond-like semiconductors whose energy gaps permit operation as detectors in the 1-to-3, 3-to-5, 8-to-14 and 20-to-30 μm spectral intervals; at least four compounds would, thus, be required. The studies should emphasize growth of crystals sufficiently uniform to yield high-density detector arrays over an area of approximately 1 cm^2. Electrical and optical properties of the materials should be evaluated as functions of temperature, and the recombination and trapping mechanisms should be elucidated. P-n junctions should be prepared and evaluated. The potential of the compounds for use in photoconductive and photovoltaic detectors should be determined. Throughout the program, the ultimate need for uniform, low cost, high-density arrays for each of the four spectral regions should weight the decisions on choice of materials, methods of growth, modes of detector operation, etc.

2.3.2.3.6 Conclusion on InSb and InAs Arrays (cf. 6.7.7)

Indium arsenide and indium antimonide are of interest for detector applications in the 1-to-3 μm and 3-to-5 μm regions, respectively. High-density detector arrays of high performance and uniformity are required. A present limitation is the fluctuation in purity obtained. Liquid-phase epitaxy is a promising growth method.

Recommendation (Priority 2)

Research should be supported in the use of liquid-phase epitaxy to produce single crystals of InSb and InAs of at least 1 cm^2 area for use in high-density arrays of both materials. The purity required is of the order of 10^{12} cm^{-3} for photoconductive detectors and 10^{15} cm^{-3} for photovoltaic ones. Methods of preparing p-n junctions in the epitaxial layers should be explored. The electrical and optical properties of the layers should be evaluated, with emphasis on an understanding of the recombination and trapping mechanisms.

2.3.2.3.7 Conclusion on Pyroelectric Detector Materials (cf. 6.7.8)

The most promising uncooled, wavelength-independent detector is the pyroelectric detector that finds application not only as a single element but also in arrays and vidicons. It is of particular use for thermal-imaging applications. Materials of interest are triglycine sulfate (TGS), the most common one, and deuterated TGS, triglycine fluoberyllate (TGFB), strontium barium niobate (SBN), and lanthanum-doped lead zirconate titanate (PLZT). The best detectors today are about one order of magnitude away from the ambient-temperature-background limit.

Recommendation (Priority 2)

Research should be supported on a search for new ferroelectric materials for use in pyroelectric detectors. Emphasis should be on materials useful for large-array, thermal-imaging applications. The detectivity should approach the background limit for thermal detectors against an earth background. Research on methods of preparing single-crystal and polycrystalline samples, attaching electrodes, and evaluating their performance as detectors should be supported.

2.3.2.3.8 Conclusion on Materials for Thermal Imaging (cf. 6.7.9)

A need exists for two-dimensional arrays, or mosaics, for use in imaging applications. The 8-to-14 μm interval is most important for thermal imaging. It is desirable that the associated electronics be fabricated within the same chip, but this will not be accomplished in the near future in the materials other than silicon.

Among the newer methods of signal detection and read out are the bucket-brigade and charge-coupled devices.

<u>Recommendation</u> (Priority 2)

Long-term support should be given to research on methods and materials suitable for thermal-imaging mosaics. New signal read out schemes, such as charge-coupled devices and bucket-brigades, should be investigated. The materials of interest are the small-band-gap semiconductors including HgCdTe and PbSnTe. Research should be directed toward establishing methods of preparing the associated electronics within the mosaic chip, analagous to large-scale integration as employed for silicon circuits.

2.3.2.3.9 <u>Conclusion on Materials for Laser Detectors in 5 μm and 10 μm Wavelength Regions (cf. 6.7.10)</u>

A need exists for laser detectors in the 5 and 10 μm regions where the detector has a high speed of response. To use high-sensitivity detection techniques, tunable infrared lasers with high continuous wave powers are required. One way of achieving this requires high-quality single crystals with large electro-optic coefficients for modulation; another makes use of upconversion by phase-matching and requires good-quality crystals appropriately birefringent.

<u>Recommendation</u> (Priority 2)

Support should be provided for the development of high-speed detectors to work as laser detectors in the 5 and 10 μm regions. Research on high-purity single-crystal GaAs and CdTe should be supported to make material of high resistivity and low loss in the 5 and 10 μm region that could be used in modulators. Research aimed at establishing the full potential of the <u>infrared</u> metal-metal oxide-metal tunnel diode detector should be supported. Exploratory research should aim at understanding the detailed mechanism of operation and the exact material needs. The questions of ruggedness of the device and its potential for array placement, and the coupling of the device to the radiation should be studied. Research on nonlinear

optical materials for use in phase-matched upconvertors should be supported. Work on the III-V compounds (purification) and on several promising ternary diamond-like compounds (e.g., $ZnGeP_2$) should be supported.

2.3.2.4 Detectors for the 200 μm to 1 cm Region

Section 7.6 of this report carries conclusions and recommendations on this spectral range of detectors. In its deliberations the Committee did not uncover currently urgent needs in this spectral range. There was only one recommendation, related to part of the recommendations of 2.3.2.3.9, that appeared to warrant inclusion in this chapter.

2.3.2.4.1 Conclusion on Metallic Far-Infrared Detectors (cf. 7.6.1)

Two important devices in this spectral range, with attractive capabilities, are the Josephson junction (working at liquid helium temperatures) and the room-temperature metal-metal oxide-metal tunnel diodes used as mixer elements for sub-millimeter receivers.

Recommendation (Priority 2)

Research on techniques for making rugged metal-oxide-metal diodes (or Josephson junctions) and understanding their performance as circuit elements should be supported.

2.3.3. Administrative Recommendations

2.3.3.1 Conclusion on Working Group for X-Ray and Gamma-Ray Detectors (cf. 4.4.1)

Detectors for this wavelength range are used by the Department of Defense in advanced systems for short-wavelength detection and identification; in addition there are growing applications in biology, nuclear medicine, geology, criminology, and industrial processing. A long-range overview of the field must be maintained due to the considerable time lag in materials development. Needs should be projected some 10 years into the future for effective planning.

Recommendation (Priority 1)

A working group should be established to provide a continuing review of present and future directions and evaluation of the detector state of the art on a regular basis. One mechanism would be to reactivate the semiconductor nuclear detector panel of the National Academy of Sciences Subcommittee on Instrumentation and Techniques.

2.3.3.2 Conclusion on Need for Study of Integrating-Mode Devices for X-Ray Detection (cf. 4.4.3)

In spite of a clear requirement for integrating-mode devices, there appear to be no suitable solid-state materials that can satisfy present day needs. This Committee was not able to relate the integrating-mode requirements to existing material parameters in sufficient detail to provide specific guidance for materials development.

Recommendation (Priority 1)

A group should be established to examine materials requirements for integrating-mode devices for the detection of X-rays and to make appropriate recommendations for research support.

FUNDAMENTALS OF ELECTROMAGNETIC-RADIATION DETECTION

3.1 Introduction

In this chapter the essential features of the detection of electromagnetic radiation are reviewed, with emphasis on the material properties important to the detection process. The process of detection of radiation can be divided into two parts: the input signal, the direct effect of the radiation on the material; and the output signal, the result of the transformation of the direct effect of the radiation into a different form. Dependence of the detection process on the wavelengths of the input and the response time of the detector are determined by the material properties and by the particular mechanisms used for the output. Noise (i.e., fluctuations in the output signal) determines the sensitivity of the detection process; it arises from fluctuation in the incoming radiation and in the detection process.

The major features of the detection process are presented here to provide the reader with an overall view of the subject. Detailed discussions of specific detector materials and processes of importance to the various wavelength ranges are presented in the chapters that follow.

3.2 The Input Signal

The input signal corresponds to the direct effect of the electromagnetic radiation on the material. There are three fundamental effects that can occur:

- Net electronic excitation of the material.
- Change in the temperature of the material (i.e., thermal excitation).
- Modulation of the state of the material by the electromagnetic wave fields.

3.2.1 Electronic Excitations

Electronic excitations involve the direct change of an electronic state of the material as the result of the absorption of photons. They include:

- The g eration of electron-hole pairs (intrinsic photoionization).

- The ionization of impurity levels, either directly or through thermal ionization of a photo-excited state (extrinsic photoionization).

- Excitation of free carriers to higher energy states.

The first two processes occur in semiconductors and insulators; the third process can occur in metals as well as in semiconductors. In the case of high-energy photons (X-rays and γ-rays), electron-hole pairs are generated as a result of photo-electron, compton, and direct-pair production events. Detectors making use of all these processes are called photon detectors.

The long wavelength limits (λ_c) of the intrinsic and extrinsic photoionization processes are determined respectively by the energy gap (E_g) of the semiconductor $(\lambda_c = hc/E_g)$ and the ionization energy (E_i) of the impurity $(\lambda_c = hc/E_g)$. However, free-carrier excitation does not have a long wavelength limit.

3.2.2 Thermal Excitation

The absorption of electromagnetic radiation can lead to a net change in temperature of the material that is independent of the mechanism of the absorption. Detectors whose operation depends on a temperature change are called thermal detectors.

There is no long wavelength cut-off for the detection process in thermal detectors.

3.2.3 Classical Field Effects

In some cases electromagnetic field amplitudes play a role. Detectors that are based on this effect involve:

- The non-linear optical properties of a material (parametric mixing of the signal with a high-frequency applied energy source (pump)).

- Josephson tunneling junctions in which the vector potential of the electromagnetic field modifies the phase of the Cooper pairs* in the superconductors. These detectors will be called electromagnetic-field detectors.

3.3   The Output Signal

The output signal form depends on the nature of the effect of the electromagnetic radiation (input signal) on the material. It is convenient to structure the discussion of the output signal in terms of the three classes of detectors:

- photon detectors.
- thermal detectors.
- electromagnetic-field detectors.

3.3.1   Photon Detectors

3.3.1.1   Conductivity Modulation

Extrinsic and intrinsic photoionization and free carrier excitation all lead to a change in the conductivity of the material. The photoionization processes lead to a change in the electron (n) and/or hole (p) carrier density; the free-carrier excitation leads to a change in the electron (μ_n) or hole (μ_p) mobility.[1]** Detectors operating in this mode are called photoconductors. An output signal is obtained by applying a constant voltage to the material and reading the change in current or by applying a constant current and reading the change in voltage. In either case, the signal is proportional to the fractional change in conductivity, $\Delta\sigma/\sigma_o$. The steady-state conductivity under operating conditions, σ_o, is determined either by the temperature of the detecting material, as is frequently the case in infrared photoconductors, or by the intensity of the electromagnetic radiation incident on the sample. When σ_o and other significant properties of the infrared photoconductor are determined by the intensity of background (i.e., non-signal) radiation, the detectors are termed background limited infrared photoconductors (BLIP).[2]

---

*"Cooper pair" is a pair of electrons whose momentum and spin are correlated.

**See 3.5 for references.

In intrinsic and extrinsic photoconductors, the speed of response of the detector is determined either by the lifetime of the generated carriers or the dielectric relaxation time. The latter is particularly important when the steady-state carrier density is low, so that the dielectric relaxation time, $\tau = \kappa \epsilon_0 / \sigma$, is long. ϵ_0 is the dielectric permittivity of free space, κ is the dielectric constant of the material and σ is the conductivity. In free-carrier photoconductors, the speed of response is determined by the scattering relaxation time of the carriers.

A mode of operation that increases the sensitivity and discriminates against background radiation makes use of optical heterodyning.[3] An optical beam having a frequency close to that of the signal is used as a local oscillator; the photon absorption process is the non-linear mixing process. As a result, the conductivity is modulated at a frequency equal to the difference between signal and local oscillator frequencies. This discriminates against background radiation at frequencies different from the signal frequency.

3.3.1.2 Junction-Type Detectors

This mode of operation applies to intrinsic photoionization excitations. The simplest form is a p-n junction. Schottky-barrier devices (metal-semiconductor junctions) also can be operated in this mode.

Electron-hole pairs are produced near the junction. They diffuse to the barrier, where the minority carrier is collected, leading to a photovoltage (i.e., photovoltaic effect) or a photocurrent under a back-biasing potential. P-n junction detectors and Schottky-barrier devices operated in this way are therefore minority carrier devices. In the phototransistor, a photodiode is used as the emitter of a transistor structure; transistor gain provides an amplification of the photosignal. Gain can also be achieved in a p-n junction detector by operating it at a back bias sufficient to cause the photo-created minority carriers to initiate avalanching during their transit across the junction. Such avalanche diodes are finding increased application where their larger output is of advantage.

In the case of heterojunctions, that is, junctions between two materials of different energy band gap, it is possible to have both electrons and holes produced in the larger gap material collected at the junction. In this case, the carriers produced in the material with the smaller band gap are not collected.

3.3.1.3 Carrier-Collection Detectors

Carrier-collection is of particular importance in the detection of high-energy photons and the measurement of their energy distribution. Across an intrinsic or high-resistivity material a voltage of sufficient strength is applied to "sweep" all the electrons and holes produced by the photon to the contacts before recombination or trapping can occur. It is essential that the contacts not inject carriers. The device that best meets this requirement is a p-i-n structure, where the p-i contact collects holes and the n-i contact collects electrons. The thickness of the detector is tailored to the range of the photon of energy being detected and the secondary electrons produced. The total charge collected for one event is directly related to the energy of the photon.

3.3.1.4 Photoemitters

The simplest form of photoemitter is a photocathode, consisting of a semiconductor or a metal-vacuum interface. Photons are absorbed by the electrons in the material, giving them sufficient energy to surmount the potential barrier at the interface with the vacuum. In the case of metals, the long wavelength limit (λ_m) is determined by $hc/\lambda_m = \Phi$, where Φ is the work function, defined as the height of the surface energy barrier above the Fermi level in the metal. In the case of semiconductors, electrons can be excited from the valence band. The long wavelength limit for non-degenerate semiconductors is then determined by the height of the barrier above the valence band; for degenerate p-type semiconductors, λ_m is determined by the work function. In the case of non-degenerate semiconductors, λ_m is determined by the band gap E_g and the electron affinity E_A defined as the height of the barrier above the conduction band edge:

34

$$\frac{hc}{\lambda_m} = E_g + E_A.$$

The work function is characteristic of the material. It can be reduced
(and the long wave length limit thus increased) by changing the composition of the
surface (e.g., by depositing a layer of another material, like cesium, on the sur-
face). In the case of semiconductors, decreasing the work function corresponds to
a decrease in the electron affinity. The presence of charge at the semiconductor
surface modifies the potential energy of the electrons and causes a "bending" of the
electron energy bands (i.e., the position of the band edges relative to the Fermi
level differs from that in the semiconductor interior). There is then an effective
electron affinity E_A^{eff}, for electrons that come to the surface from the interior
without loss of energy, given by:

$$E_A^{eff} = E_A - (E_c - E_{cs}),$$

where $E_c - E_{cs}$ is the amount of bending of the conduction band edge. The long
wavelength limit may then be increased for $E_c - E_{cs} > 0$, that corresponds to a
downward bending of the electron energy bands. If $E_c - E_{cs} > E_A$, E_A^{eff} is negative.
In this case, a photon of energy less than the semiconductor band gap can produce
a photoelectron in the vacuum.

To achieve a long wavelength response for semiconductor photocathodes,
a p-type material and surface coating that bends the bands downwards and yields a
low work function surface are used. Band bending can also be produced by the application
of an external electric field between the surface and the interior.

A Schottky-barrier diode can be used as a photoemitter; here the photo-
carriers produced in one material are emitted into a second material, rather than
into a vacuum. This process is called "internal photoemission." The electrons
(holes), photoexcited in the metal, surmount the electron (hole) metal-semiconductor
barrier. These carriers are collected at an ohmic contact to the semiconductor.

Since bulk metals reflect most of the incident light, it is necessary to use thin metallic films--about as thick as the photon wavelength in the metal. For photoemission of electrons an n-type semiconductor is used; the height of the barrier is determined by the position of the conduction band at the interface, relative to the Fermi level. For holes, a p-type semiconductor is used; the barrier height is determined by the position of the valence band relative to the Fermi level. By appropriate choice of metal and semiconductor, it is possible to have the Fermi level at the surface lie in the forbidden gap, thus giving a potential barrier smaller than the band gap. If the band-bending region is sufficiently narrow, the effective barrier height corresponds to the energy at which appreciable tunneling occurs (i.e., the energy at which electrons traverse the barrier quantum mechanically with a reasonable probability).

Tunneling of electrons between two metals separated by a thin insulating film or of unpaired electrons between two superconductors is also a form of photoemission. In the latter case a photon breaks up a Cooper pair in one superconductor, and the unpaired electrons tunnel into the other superconductor. The long wavelength limit is then determined by the superconducting energy gap. In the case of the normal metal junctions, the photons produce energetic electrons that have a greater tunneling probability, thereby producing an enhanced tunneling current. In these tunneling devices, the junction thickness must be of the order of the photon wavelength in the metal to produce appreciable absorption of the incident radiation.

3.3.2 Thermal Detectors (Bolometers)

There are two general types of thermal detectors: in one the temperature change (ΔT) produces a change in some macroscopic properties, and in the second a temperature gradient (grad T) is produced that leads to heat flow and to thermo-electric-type output signals. The magnitude of the signal produced and the response time of the detectors depend on the volume and specific heat of the active materials and their contact with a "constant" temperature thermal reservoir.

3.3.2.1 Temperature Change (∆ T) Detectors

The properties used in ∆ T thermal detectors include:

- Resistance or conductance. These make use of the temperature coefficient of resistance of metals or semiconductors.

- Dielectric constant or magnetic permeability. Changes in dielectric constant and permeability arise (e.g., from thermally-induced changes in the material density) and can be observed as changes in the capacitance or inductance of circuit elements (i.e. capacitors or inductors containing the detector).

- Optical properties. Changes in the refractive index caused by a temperature change can be observed by interferometric techniques. Shifts in the absorption edge caused by a temperature change can be observed as a charge in optical transmission using a monochromatic source.

- Pyroelectric and pyromagnetic effects. Here the permanent electric moment or permanent magnetic moment of a material is dependent on the temperature. Crystals exhibiting a permanent electric moment lack a center of symmetry and have a unique axis. Ferroelectric materials are one of the classes of material exhibiting the pyroelectric effect. A change in electric moment of the pyroelectric material, due to a temperature change, leads to a change in electric potential across the crystal. Optimum signal strength requires material of high resistivity. Pyromagnetic materials are either ferromagnetic or ferrimagnetic. The pyromagnetic effect is utilized in a similar fashion: a change in temperature produces a change in magnetization and thus a change in the magnetic field.

3.3.2.2 Temperature Gradient (Grad T) Detectors

The thermoelectric effects used in grad T detectors include the Seebeck effect (i.e., an emf proportional to the temperature gradient is produced parallel to the temperature gradient) and the Nernst effect (i.e., an emf proportional to the temperature gradient and the intensity of a magnetic field transverse to the temperature gradient is produced in a direction perpendicular to both the temperature gradient and the magnetic field). In detectors based on the Seebeck effect, an emf is produced by the difference in temperature of two junctions of dissimilar metals or semiconductors; the temperature gradient occurs as the result of absorption of radiation by one of the junctions. In detectors based on the Nernst effect, it is only necessary to use a single metal or semiconductor in which a temperature gradient occurs as a result of absorption of radiation.

3.3.3 Electromagnetic-Field Detectors

3.3.3.1 Parametric Mixers

The parametric mixing of the input signal at a low frequency, f_s, with an intense energy source at a much higher frequency, f_o, produces radiation at the frequency $f_o \pm f_s$. This is accomplished in a material having non-linear optical co-efficients arranged in a configuration giving essentially complete "conversion" of the input signal. The low-frequency signal is thereby converted into a high-frequency signal, that can be efficiently detected by a photon detector sensitive only to the radiation at $f_o + f_s$ or $f_o - f_s$. The energy source can be discriminated against by the use of narrow band filters. This process is called "up-conversion."

3.3.3.2 Josephson Tunneling Junctions

In the Josephson effect, Cooper pairs flow or tunnel from one superconductor to another through a barrier (weak link). This is in the form of a geometrical constriction or a dielectric film. The Josephson junction current depends on the difference in phase, ϕ, of the Cooper pair wave functions on opposite sides of the barrier. ϕ is a constant when the voltage across the junction is zero, and its magnitude determines the maximum value of the zero-bias (dc) Josephson current that can be

driven through the junction. When a bias, V, is applied to the junction, ϕ varies linearly with time and causes an ac Josephson current to flow at a frequency that is proportional to the voltage, $w_j = 2eV/h$. Electromagnetic radiation affects the Josephson current in the following ways:

- The maximum value of the zero-bias dc Josephson current is decreased.

- The magnitude of the ac Josephson current is modified and its frequency is modulated.

- The phase of the Cooper pairs is modulated by the vector potential, leading to interference effects in the tunneling current.

3.4 Detectivity and Noise

The merit of a photodetector is determined by the relative magnitudes of the signal and the noise. The performance of a detector is described by the detectivity, D, which is equal to the signal-to-noise ratio divided by the incident radiation signal power. Its reciprocal 1/D is equal to the noise equivalent power, NEP. For comparison of different types of detectors, the quantity D* is used:

$$D^* = D \ (\Delta f)^{\frac{1}{2}} \ A^{\frac{1}{2}}$$

where Δf is the frequency band width and A is the detector area. D*, therefore, normalizes the detectivity to unit area and unit band width.

There are various sources of noise[4,5] ;these can be divided into input noise and detector noise.

3.4.1 Input Noise

Input noise arises from the radiation flux incident on the detector and includes fluctuations in the radiation signal and in the background radiation. These fluctuations give output noise by the same mechanisms that convert the input radiation signal to the output signal. These noise processes are generally called photon noise; their magnitude is characterized by the statistical fluctuation in photon density.

3.4.2 Detector Noise

Detector noise is of two types. One type, Nyquist or Johnson noise, appears even in the absence of flow of current in the detector. It manifests itself as a fluctuation of voltage across the detector, and its magnitude is determined by temperature and resistance as well as by the detector bandwidth.

The second type of detector noise occurs only when current flows through the detector. It includes:

* Generation-recombination noise arising from the fluctuation in the rate of thermal generation and recombination of carriers in the material

* Shot noise arising from the discrete nature of the electron charge, which leads to current pulses when carriers cross interfaces

* 1/f noise, which, as its name implies, varies inversely with the frequency. 1/f noise arises from material inhomogeneities and conditions at surfaces and interfaces

3.5 References

1. T. S. Moss, J. Phys. Chem. Solids 22, 117 (1961).

2. E. Burstein and G. S. Picus, IRIS Meeting, Feb. 3, 1958. For treatment, see P. W. Kruse, L. D. McGlauchlin, and R. B. McQuistan, Elements of Infrared Technology, J. Wiley and Co., New York, 1962, Chapter 9.

3. M. C. Teich, R. J. Keyes, and R. H. Kingston, Appl. Phys. Lett. 9, 357 (1956).

4. P. W. Kruse, L. D. McGlauchlin, and R. B. McQuistan, Elements of Infrared Technology, J. Wiley and Co., New York, 1962.

5. R. A. Smith, F. E. Jones, and R. P. Chasmar, The Detection and Measurement of Infrared Radiation, Clarendon Press, Oxford, 1957.

SENSORS FOR X-RAY AND GAMMA RAYS (10^{-6} TO 10^{-1} μm)

4.1   Introduction

The development of semiconductor devices for the detection of X-rays, gamma rays, and nuclear particles has resulted in revolutionary improvements in radiation spectroscopy.[1-13*] These semiconductor detectors have virtually replaced gaseous ionization or scintillation detectors in nuclear spectroscopy experiments because they provide outstanding energy resolution over a very wide range of energies and for many different types of radiation. Although these devices were developed primarily for research in nuclear physics, there have been important applications in other areas such as biology, nuclear medicine, geology, criminology, defense, and industrial processes. It is in these areas of application that many of the demands for new detector materials are being made. These areas of application also represent a clear example of the benefits of technology transfer of instrumentation techniques that were initially used almost exclusively in nuclear research. However, these areas are outside the scope of this report.

Presently, no detectors meet all the advanced requirements of the Department of Defense, other government agencies, or the wide variety of potential industrial applications. While germanium and silicon have been used extensively in the past, both have basic limitations that cannot be exceeded. Other materials might be suitable for some of the advanced requirements in the future; however, present-day detectors fabricated from these materials do not have the detection efficiency and energy resolution required for these particular applications. It should be noted that for specific cases (medical probes, fuel gauges) CdTe devices have met the energy resolution and detection efficiency requirements for room-temperature gamma detectors.

---

*See 4.5 for references

Many factors militate against the development of new semiconductor materials for detector applications. The first and most straightforward consideration is that the demands on crystal purity and perfection are exceedingly high. In general a period of five to ten years is required before sufficiently high-quality materials can be grown. This can be seen directly in the experience with germanium and cadmium telluride. Since a material of extremely high resistivity and perfection lies outside the mainstream of effort for typical electronic devices, there is little commercial interest in developing materials for detector applications. The volume of material required is not enough to provide a reasonable profit for companies to invest the necessary development time to make this material. This means that government or other non-commercial support is required if development of these materials is to be continued.

An important consideration in the allocation of research and development effort is the fact that present silicon and germanium devices are adequate for most of the needs of the nuclear physicist. Since nuclear research requirements provided a large part of the incentive for the early development of semiconductor nuclear detectors, there is now no driving force within the national laboratories to push toward the development of room temperature-operated detectors and the research effort has diminished. Cutbacks in funding have resulted in a decrease in size of the instrumentation groups associated with the national laboratories.

On a practical basis this means that there are only three or four development programs currently under way that are designed to lead to detectors other than the lithium drift silicon and germanium devices. These involve high-purity germanium, cadmium telluride, gallium arsenide, and silicon avalanche detectors.

There are two distinct modes of operation of X- and γ-ray detectors:

- The pulse-counting mode (utilized in radiation spectroscopy) where the energy deposited by single photons in the detector is measured.

- The integrating mode (often utilized in dosimetry and
  in surveillance of radiation environments) where only
  the average rate of energy dep~sition, not individual
  events, is measured.

Material requirements and the device structures for operation in the two modes
are generally not the same. In this report we have concentrated primarily on the
pulse-counting mode because many of the high-priority applications require dis-
crimination between radiation of different energies. The material requirements,
while stringent, can be delineated and related to the present state of the art in
materials technology. The integrating mode covers a broad spectrum from tissue
equivalent chambers through photoconductors to photographic films and screens;
the material requirements tend to be more specific in terms of application and in-
formation display.

The semiconductor detector operating in the pulse-counting mode is
basically a simple device resembling a p-n junction under reverse bias or an
insulator with a large electric field applied across it. Incident radiation creates
electron-hole pairs that are swept apart by the action of the electric field creating
a voltage pulse. Although the structure is simple, the requriements imposed on
the materials used are exceedingly great. The basic principles were recognized
in the late 1940s, but it was not until the early 1960s that detectors, suitable for
gamma-ray spectroscopy, were made.

The development of semiconductor detectors had its roots in the work
done by Van Heerden in the early 1940s on alkali-halide counters.[10] This work
did not lead to a practical device but it demonstrated the feasibility of using solid
state devices for radiation detection. Hofstadter[11] made a search of a number of
materials to determine if any were suitable for radiation spectroscopy. This
study pointed out that the state of the art of material growth in 1948-49 was not
adequate to produce materials suitable for nuclear spectroscopy. There was then

a hiatus of about 10 years until it was demonstrated that silicon and germanium surface-barrier detectors could respond linearly to the energy of incident alpha particles. From this point onward there was an explosion in the effort to produce larger-volume devices with improved energy resolution. The active volume of these devices was increased by about a factor of 10^6 while the ability to resolve the energy of the incident radiation improved by about an order of magnitude. Silicon and germanium were the two materials used, and the primary emphasis of the development work was to obtain higher purity and higher crystal perfection.

Currently, virtually all X- and γ-ray detectors for spectroscopy are made from silicon or germanium using the lithium drift process to reduce the net carrier density. Silicon devices, although extensively used in X-ray analysis, are generally not used for energies above 50 keV because of the low atomic number of silicon. However, in the energy region above 2 MeV, electron-positron pair production is important, and the advantage of using a higher Z material such as germanium (Z = 32) as opposed to silicon (Z = 14) is not as great as for low energies, where the photoelectric cross section is utilized. Germanium lithium drift detectors must be operated at low temperatures (due to the small band gap) and stored at low temperatures to avoid lithium precipitation. The need for low-temperature storage is eliminated with high-purity germanium, which does not require lithium drift techniques in detector fabrication. However, the maximum volume ($\simeq 10 \text{ cm}^3$) of devices made from such material is less than that routinely available in lithium drift detectors and the operating temperature required for best results is still below 150° K. A major need remains for a gamma-ray detector that can be operated at room temperature. Work with CdTe, GaAs, and other materials has shown promise but large-volume devices capable of good energy resolution have not been developed.

In reviewing the development of the semiconductor nuclear particle detector over the past decade, two important facts emerge. The first is that the major thrust in development was carried out by instrumentation groups associated with nuclear physics efforts at national laboratories. As noted, these instrumentation groups have experienced major funding reductions and, with only one or two

exceptions, have largely abandoned their role in the development (as opposed to fabrication) of semiconductor detectors. The second fact is that, as far as U. S. semiconductor suppliers are concerned, it has not been economical to develop a special material just for application in radiation-detection devices. There is no profit incentive for an industrial company to support five or ten years of intensive material development, unless this occurs because of spin-off from another program. As a result, the main suppliers of detector-quality silicon and germanium are in Europe. Fabrication of detectors has thus been hampered by a chronic problem in obtaining high-quality material. Almost all silicon exhibits trapping effects and spectrum degradation, and this situation has not changed in the past five years. Germanium must be over-bought (often by a factor of 5) to find acceptable portions of an ingot for large-volume detectors. This situation is aggravated by the fact that no adequate evaluation procedure has been found for predicting detector performance from measured characteristics of ingot material. Of course, major guidelines, such as oxygen and gross impurity content, have emerged but in general, a detector must first be made to determine if the material is suitable. This is both tedious and expensive.

If gamma-ray detectors are to be available to meet the advanced detector requirements, it is incumbent upon the government agencies to carefully examine their future needs over a period of five to ten years. If these needs can be delineated, then it is necessary to consult with semiconductor-material and particle-detector specialists to determine a likely approach to achieving these goals. One mechanism to accomplish this would be to reestablish a body like the former semiconductor nuclear detector panel of the National Academy of Sciences Committee on Nuclear Science, Subcommittee on Instrumentation and Techniques. Such a body could serve as an advisory group to government agencies and to materials specialists to relate needs and availability of material.

Based on past experience, the trend over the next five years in detector development can be roughly predicted on the assumption that there is no change in the present pattern of funding. For photon energies up to 60 keV, commercial silicon (lithium) detectors will be used where high resolution is required and low-temperature operation is possible. The major source of silicon will become domestic instead of continuing to be, as now, Wacher Chemie (W. Germany).

For room-temperature applications where small-volume detectors are required (in vivo counting) epitaxial GaAs detectors may be used. There will be no intensive development of ultra-high-purity epitaxial GaAs for gamma detector applications and hence the maximum thickness of the detectors will be between 100 and 500 μm. Development of cadmium telluride will continue and units up to 1 cm^3 in volume will be made for applications where only minimal requirements on energy resolution are imposed. Smaller-volume devices will exhibit better resolution and will be used in place of GaAs where higher detection efficiencies are required.

Germanium (lithium) detectors will continue to dominate in applications where large volumes and high resolutions are required. Hoboken (Belgium) will continue as the major supplier. High-purity germanium detectors will take on a more important role as larger devices are made. There is a real possibility that Hoboken will develop high-purity germanium and replace General Electric Company as the supplier of this material for the present low-volume market.

The sporadic attempts to develop other materials for gamma-detector applications will probably not be successful enough to displace GaAs or CdTe. Avalanche-mode detectors will be used more extensively for in vivo counting applications, but development of large area devices may be hampered by non-uniformities in the silicon-base material.

4.2   Pulse-Counting Devices and Materials

4.2.1 Carrier-Collection Devices

A basic method of detecting and measuring radiation using solid state devices depends on ionizing a material to produce positive and negative free charges. A charged particle interacts with atomic electrons via Coulomb forces, and each freed electron produces a number of electron-hole pairs. Electromagnetic radiation, such as gamma rays, interacts with material by way of a photoelectric interaction, a Compton collision, or pair production, and these also produce electron-hole pairs. Direct collection of the charge, or scintillation (light emission) after excitation, is then used to determine the amount and/or energy of the incident radiation.

The ultimate performance of any given detector material depends on:

- What fraction of the incident and internally created radiation is absorbed

- What fraction of the energy goes into thermal vibrations

- The mean energy, ε, required to produce an electron-hole pair

- The ability to collect and measure the total internal charge

The structure of a typical detector consists of a block of pure (nearly intrinsic) material with electrical contacts on opposite faces. Charge collection is accomplished by applying a voltage. Bulk free-carrier densities, crystal imperfections, trapping centers, scattering centers, contact injection, internal charge generation, side surface generation, and carrier transit time must be minimized, and the mobility and carrier lifetime must be maximized.

Application of a voltage produces an electric field in the material. Full depletion exists when this field extends from contact to contact. Partial depletion exists when the field drives free carriers away from a region called the 'depletion layer.' This layer forms the sensitive region from which charged carriers are collected, and the width of this layer is proportional to the square root of the applied voltage.

The basic ingredients of any detector material are:

- A high-field region requiring low net concentration of free-charge carriers

- Good collection efficiency, requiring low density of trapping or scattering centers

- A minimum free-charge current under applied voltage requiring a small number of both thermally generated carriers and non-injecting contacts

Materials with constituents of high atomic number (Z) are also desirable since they are more effective absorbers of radiation.

There are a large number of medical, surveillance, defense, and industrial applications that require a material of high atomic number $(Z > 50)$ and demand room-temperature operation (i.e., a material with a large band gap $(> 1.5$ to 20 eV)). Further requirements might be listed as:

- Sensitive region: net doping density $\leq 10^{10}$ atoms cm^{-3} to obtain active volumes 0.5 to 1.0 cm thick

- Good collection efficiency: this requires a low density of trapping sites, $N_T \leq 10^{12}$ cm^{-3} and a reasonable carrier mobility $(>100$ $cm^2 V^{-1} sec^{-1})$

- Small $(\leq 50-100$ nA $cm^{-2})$ d.c. currents: This requires both a small number of thermally generated carriers (achieved in silicon and germanium by cooling) and non-injecting contacts (achieved by the use of reverse biased junctions or surface barriers)

- Good resolution (3 keV or better) and high efficiency $(>10\%)$: these can be relaxed in specific cases

Low leakage currents require non-injecting contacts. These can easily be achieved with lithium drift devices. However, to obtain thin windows (thin contact regions) or to make contacts to high-purity germanium (where process temperatures less than 350° C may be required), new techniques such as ion implantation may be necessary. In any event, for operation at room temperature and above semiconductors with a band gap greater than that of silicon are required to maintain a low value of the thermally generated current.

In silicon and germanium detectors, the standard method of obtaining a low net doping concentration is to compensate the doping impurities with lithium. Reasonable thickness can be achieved since lithium is interstitial (high diffusion constant) and a shallow donor (does not introduce trapping effects at liquid nitrogen temperatures). Due to the low solubility and high diffusion coefficient of lithium in germanium, the lithium drifted germanium (Ge(Li)) detectors degrade when held at room temperature for even short periods of time because of precipitation of the lithium. This problem is not as severe in Si(Li) detectors. For germanium this problem has been attacked (at present for ~ 10 cm^3 devices) by growing high-purity material that does not require lithium for compensation. With compound semiconducting materials such as GaAs or CdTe, lithium drift techniques have not been successful and compensation is achieved by introduction of native defects (such as vacancies) by means of heat treatment or incorporation of other impurities. These compensating centers generally act as trapping centers and degrade detector performance.

The presence of trapping centers or crystal imperfections such as dislocations can degrade detector performance. The carrier-transit time required (typically 10^{-7} sec) is about 2 orders of magnitude less than the trapping time. This leads to an upper limit on the number of singly ionized trapping centers (cross section $\sigma \approx 10^{-14}$ to 10^{-15} cm^2) of the order of 10^{12} to 10^{13} cm^{-3}. This level is difficult to achieve in silicon and germanium and has not been obtained in semi-insulating compound semiconductors to date.

Trapping effects play a dominant role in nuclear-particle detectors because carriers must traverse large distances (0.1 to 1 cm). From an operational standpoint, not only trapping but also the thermal release (detrapping) of carriers must be considered. If the detrapping time is sufficiently small, then trapping effects will not significantly reduce the number of carriers that are collected. Since detrapping times are proportional to exp (E_T/kT) where E_T is the trap energy level, there is a range of temperature where detrapping effects will influence charge collection. Further the electric field can influence both trapping and detrapping times.

4.2.1.1 Silicon and Germanium

Silicon (Z = 14) and germanium (Z = 32) have been employed as base materials in many types of detectors. Major attention has been given to the problem of growing large, pure, uniform low-dislocation-content single crystals, mainly by the Czochralski technique. Similar attention has been given to obtaining a low net carrier concentration by compensation using lithium-drift techniques. Large depleted regions can be achieved since lithium has a high diffusion constant. Since lithium is interstitial and of low solubility, it will precipitate at ambient temperatures and lithium-drifted germanium (Ge(Li)) detectors must be used and stored at low temperatures. This problem is not so severe for Si(Li) detectors.

At present Si(Li) and Ge(Li) detectors are available as X- and γ- ray detectors when operated at low temperatures, typically liquid nitrogen. The operational requirements impose severe constraints on the material in terms of purity and crystal perfection. Si(Li) detectors are generally used for detection of radiation of energies up to 60 keV (and may be used for energies above 2 MeV), and Ge(Li) detectors with volumes greater than 10 cm^3 are required for 1 MeV gamma rays to obtain adequate detection efficiency.

These large-volume Ge(Li) detectors require ingots with high lithium-diffusion coefficients and small concentrations of trapping centers. There have been periodic crises when no detector-grade germanium was available. Laboratories

(Oak Ridge National Laboratory and Lawrence Radiation Laboratory, Berkeley) established facilities to develop techniques for growing better-quality germanium.[14] To do so it is necessary to understand the mechanisms of lithium compensation and to grow germanium that is optimized for the fabrication of large-volume lithium drifted detectors. These programs continue. Infrared absorption and detection response measurements have been developed to reveal apparent strain in the crystal and the presence of localized precipitation centers.

A program at the National Bureau of Standards was set up to develop diagnostic techniques that would characterize the materials and could be correlated with detector performance. Conventional bulk materials measurements such as Hall effect, photoconductivity, etc., were found useful but by no means sufficient for detector-material characterization. Studies of lithium driftability at Oak Ridge National Laboratory, etch-pit density distribution at the University of California (Berkeley), and infrared response at the University of California (Livermore) were examined. The results of the Berkeley study could not be confirmed; the Livermore infrared response technique was improved to detect impurities and defects in germanium having densities of the order of 10^{11} cm^{-3}. Characterization and detector studies are continuing.

As a result of noteworthy pioneering development work at General Electric Company,[14-17] and more recently at other laboratories, high-purity germanium has been produced by repeated chemical purification and crystal growth to an electrically active impurity concentration of ~10^{10} atoms cm^{-3}. This material does not require lithium drifting for charge compensation, and does not suffer from lithium precipitation if warmed to ambient temperatures. Devices of ~10 cm^{3} volume and 1 cm depletion depth have been made and 50 mm diameter devices with 2 cm depletion depth are anticipated. Further reduction in the electrically active impurity content may eliminate almost all requirements for lithium drifting in detector fabrication and further refinements in lateral and longitudinal homogeneity may permit the fabrication of much larger detectors.

52

Investigation of compensation of n-type germanium by gamma irradiation as a means of making moderately good detectors has been conducted at Brookhaven National Laboratory.[18] So far this technique has not yielded good resolution, large volume detectors. Hole trapping effects are commonly found even with starting material of high purity. Investigation of the mechanisms that produce compensation in gamma irradiated germanium is under way at Oak Ridge National Laboratory.

Ultrapure, high resistivity (9-15°K ohm-cm), long minority-carrier lifetime silicon is required for detector applications, but present-day* material suffers from trapping, low collection yield, and large leakage currents. A factor of 10 reduction in the free-charge carrier concentration (dark current) would expand the demand for Si(Li) detectors for X-ray fluorescence analyses.

The major problems associated with Si(Li), Ge(Li), and ultrapure Si and Ge are those of materials purification, crystal perfection, homogeneity, and a lack of an adequate evaluation procedure. Work should be continued on purification, crystal growth, and characterization of those defects that lead to a degraded performance. Some effort should also be given to problems of:

- Removing those chemical impurities or lattice defects that still remain after normal crystal growth

- Purposeful doping with impurities to achieve better compensation

- Studying radiation effects on detector materials to attempt to improve radiation stability

Silicon and germanium will probably be used in X- and gamma ray detectors for years to come.

4.2.1.2 Cadmium Telluride

In a 1965 review of semiconductor materials for gamma ray spectroscopy, it was pointed out that cadmium telluride had many of the desirable characteristics for detector material. The band gap was large ($E_g \sim 1.4$ eV) so that room-temperature

---

* A United States producer has made, under U.S.A.F. contract, silicon of detector grade quality with 10°K ohm-cm resistivity and minority carrier lifetime of 10^{-3} seconds, (AFML-TR-71-130) "High Purity Silicon Manufacturing Facility" Contract F-33615-69-C-1829, Texas Instruments, Inc.)

operation could be achieved. Carrier mobilities were sufficiently high ($\mu_n \sim 1,000$, $\mu_p \sim 100$ cm^2/V-sec) so that carrier collection could be achieved. The atomic number was high ($Z_{AV} \sim 50$) so that high photo cross sections could be obtained. High-resistivity material was available. Subsequently, it was demonstrated that cadmium telluride could respond to α-particles and had reasonable resolution. The problem, at that time, was that trapping effects in this high-resistivity material caused substantial degradation in response to gamma radiation. Since then the material has been substantially improved. The most recent summary of the progress in cadmium telluride was presented at an international symposium on cadmium telluride as a material for gamma ray detectors held at Strasbourg in June 1971. [19] At that meeting, it was evident that there were intensive development efforts on cadmium telluride for gamma ray detector applications in France and the Soviet Union as well as in the United States.

The reason for this increased interest is evident from Figure 4.1 which shows the pulse height spectra for the response to Co^{57} (122 keV) for three years 1967, 1970, and 1971. These spectra were obtained on semi-insulating cadmium telluride with a 1.5 mm thick active region and a surface area of about 10 mm^2. In 1967, the first year in which gamma-spectra were obtained, the response to gamma rays indicated that full carrier collection was not achieved. Trapping effects in these devices were severe, so that the pulse height was only about $\frac{1}{4}$ of that to be expected for full collection. In 1970, a photopeak was clearly resolved although a tail of the spectrum indicated that there were inhomogeneities in the material. In 1971, the resolution was 9 keV for a preamplifier-amplifier system with 5 keV resolution.

The improvement in performance can be put on a more quantitative basis by comparing values of the mobility-trapping time product $\mu\tau$, for these three years. The average distance a carrier moves across a region with an electric field, E, is given by $\mu\tau E$. Values for $\mu\tau$ improved by more than one order of magnitude between 1967 and 1971, to 10^{-3} cm^2/V for electrons and 10^{-4} cm^2/V for holes. (Values as high as 10^{-3} cm^2/V for holes have been reported in recent
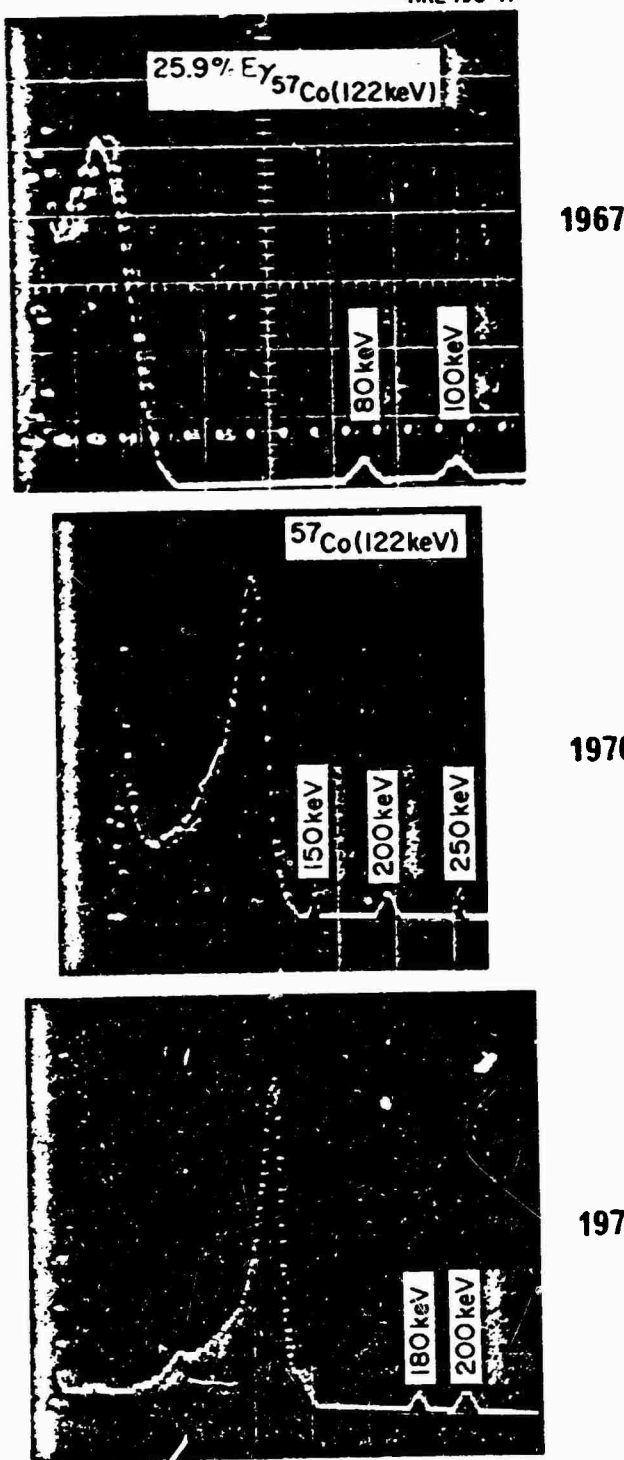
FIGURE 4.1   Pulse-height spectra for 1.5 mm thick semi-insulating CdTe detectors at room
temperature.   The labeled peaks are markers produced by a pulse generator.

measurements (1972)). As a result, resolution improved to 7% full width at half maximum. A $\mu\tau$ product for holes greater than 10^{-3} cm^2/V must be obtained on a routine basis if large-volume (greater than 100 mm^3) and large depletion width (1 to 2 mm) devices are to be made. This improvement can only come about by an increase in the mean trapping time for holes since substantial changes in hole mobility are not expected. It is on improved hole collection that most of the current efforts focus. It should be stressed at this point that if 1 cm^3 volume devices with 3 to 6 keV resolution are required, then both the electron and hole $\mu\tau$ products must be increased to a value of about 10^{-2} cm^2 per volt. Achieving this goal will probably require considerable development time.

At the present time cadmium telluride devices operate satisfactorily for several applications. Small-volume (active area of about 3.3 mm^2 and thickness of 1.4 mm) detectors have been fabricated for medical probes. These probes had a count rate for 122 keV gammas about a factor of 150 greater than standard silicon (Li) probes. Larger-area devices (approximately 200 mm^2) have been tested for application in zero gravity fuel gauge applications. These devices exhibit a photo peak with a peak-to-valley ratio of greater than 2 to 1 for response to ^{137}Cs. This energy resolution is adequate for many gauging applications; however, larger-volume devices are desirable.

Thus, regarding the gamma-ray capabilities of cadmium telluride, it is clear that present material has demonstrated the capability of energy resolution in small-volume devices[20-23] and the present material is adequate for larger-volume devices where good energy resolution is not required. Further improvement in the material is necessary if 1 cm^3 devices with good resolution are to be obtained.

The use of gamma rays in evaluating cadmium telluride detectors provides a good test of the overall capabilities of the device. However, the gamma response is not a good diagnostic technique to evaluate detector-grade material, since it is difficult to separate the individual contributions of holes and electrons.

From an operational standpoint it is necessary to obtain parametric information on the carrier drift velocity, carrier trapping times, and material homogeneity. This information can be obtained in a rather direct fashion by the use of transient charge techniques whereby holes and electrons are generated by other nuclear particles or by a pulsed beam of electrons. In addition to measurement of the hole and electron mobility and trapping time, it is possible to deduce the energy level and the density of traps from these transient charge techniques.

The carrier drift velocity, and therefore its mobility, is computed from the time required for carriers created at one electrode to cross the crystal. The width of the current pulse is a measure of the transit time, while the decay in the current pulse allows calculation of the trapping time. Thus, in one measurement it is possible to obtain directly the mobility and trapping time. Samples with longer trapping times have higher mobilities at low temperatures. The semi-insulating cadmium telluride currently used for gamma detector applications is semi-insulating, not because of high purity, but because of compensating centers. The main thrust in the development of materials for gamma ray detectors is to reduce the number of impurity centers. Experience in the past has been that a reduction in the number of impurities has led to a reduction in the number of trapping centers.

In judging materials with trapping centers one of the major problems is to determine the homogeneity of the sample. One method that has been applied successfully is to evaluate the response of the material using α-particles incident on either of the two electrodes. Presently, the lack of material homogeneity is the major limitation in the production of large-area devices.

In the evaluation of semi-insulating cadmium telluride, most attention has been focused on nuclear or transient charge techniques, because these give direct information on the parameters of interest for applications in gamma ray spectroscopy. Some basic metallurgical and electrical measurements of cadmium telluride have been made in the past. The Proceedings of the Strasbourg Conference[19]

and in particular the review by Strauss, gives a very good summary of electrical measurements on low-resistivity material. There is a problem in relating the properties of low-resistivity cadmium telluride on which Hall and resistivity measurements were made, to the properties of semi-insulating cadmium telluride, on which transient charge measurements are made. At this time, there has been almost no correlation between the two sets of measurements.

Semi-insulating cadmium telluride also has application as an infrared modulator and window. This application has stimulated research effort on semi-insulating cadmium telluride. Past experience has shown that requirements for high-energy radiation detection do not provide a sufficient commercial stimulus for extensive material development. In the United States, at present, there are two laboratories (Tyco and Hughes Research Laboratories) pursuing the development of cadmium telluride for gamma-ray detectors. Both have produced semi-insulating cadmium telluride of detector-grade quality, although each uses a different growth technique and it is not clear which approach will eventually lead to the highest quality detector material. It appears reasonable to continue the material developments at both laboratories to meet advanced requirements of the Department of Defense.

4.2.1.3 Gallium Arsenide

In many respects gallium arsenide should be superior to cadmium telluride as a nuclear particle detector. The electron and hole mobilities are greater than those in cadmium telluride and there has been considerably more development effort on crystal growth. Both materials have comparable energy gaps (~ 1.45 eV) and consequently each can be used for room-temperature applications. Cadmium telluride has one significant advantage over gallium arsenide in that the atomic number is considerably greater which should lead to more efficient detection of photo events.

Although the desirability of epitaxial layers of gallium arsenide for particle detection was recognized as early as 1966, it was not until recently that Tavendale et al,[24] demonstrated the capability of n-type gallium arsenide for nuclear

radiation detection. Their detectors have exhibited better than 3 keV resolution with room-temperature operation.

Conventional melt-grown gallium arsenide is not sufficiently pure to allow fabrication of detectors with good energy resolution. Semi-insulating gallium arsenide that had been evaluated for gamma-ray detection application exhibited severe trapping effects.

Undoped (uncompensated), high-resistivity n-type GaAs was made reproducibly by liquid-phase epitaxy on high-resistivity substrates. The films were several micrometers thick with carrier concentration about 10^{14} cm^{-3}.

Vapor-phase-grown (homo-epitaxial) films (MIT, RCA) are even better detectors. The films have doping levels in the mid 10^{13} cm^{-3} range. Epitaxial growth from the liquid or vapor phase has provided materials with impurity levels less than 10^{14} cm^{-3}; however, this dopant concentration level is not low enough for large-volume detectors and consequently the active thickness of the detectors must be of the order of 100 μm for reasonable values of applied bias. Presently, detectors are made with gold surface barriers on epitaxial material grown on heavily doped gallium arsenide substrates. The units are typically operated so that the epitaxial layer is totally depleted. The presence of an insulating layer at the interface between the epitaxial layer and the n^{+} substrate is thought to be responsible for some anomalous features in detector performance.

An important step in the fabrication of detectors is the forming of contacts, both rectifying (Schottky barrier) and ohmic (non-injecting). For a good device both of these contacts are necessary. In the present state of the art, it is much easier to construct Schottky barriers than low-resistance contacts. Ion implantation may be developed sufficiently in the next few years to allow its use in junction fabrication.

Since surface leakage and high surface recombination velocity have to be avoided, passivation of GaAs surfaces must be under control. At present, no passivation technique (such as SiO_2 for Si-surfaces) exists. Thermal oxidation of GaAs has not been feasible; the best results to date were obtained with deposited Al_2O_3 films. However, surface state densities are still high. Proton bombardment to make semi-insulating GaAs on top of GaAs has been used to make a GaAs field-effect transistor and this has shown some promise.

The response to gamma rays of small-area surface barriers (up to 2 or 3 mm in diameter) on epitaxial layers exhibits good energy resolution. The resolution full width at half maximum (FWHM) at 300° K was 2.5 keV for 122 keV gamma rays and the best resolution was 640 eV (122°K) for 59.54 keV gamma rays. Since the detector active layers are thin, only low-energy photons of the order of 100 keV or less produce photo-peaks. Figure 4.2 shows the room-temperature response for a liquid epitaxial layer which gave a resolution for ^{57}Co of 2.5 keV. At 373° K the resolution was 9.7 keV for 59.54 gamma rays. This detector was stable over a period of six months. This work showed that good resolution can be obtained in material with a direct band gap.

The major problem in the present GaAs devices seems to be associated with the presence of a high-resistivity layer at the interface between the epitaxial layer and the heavily doped substrate. This layer leads to variations in pulse height with bias and multiple peaking over certain bias ranges. This problem with the interface may be overcome if more research attention is paid to the growth near the interface.

If gallium arsenide is to be fully exploited, large volume detectors must be developed.[24-25] This requires an increase in area, accompanied by improved homogeneity of the epitaxial layer, and an increase in thickness, accompanied by improved purity in the epitaxial layers. While the thickness of a gallium arsenide layer grown by liquid-phase epitaxy is usually less than 100μ m, samples up to
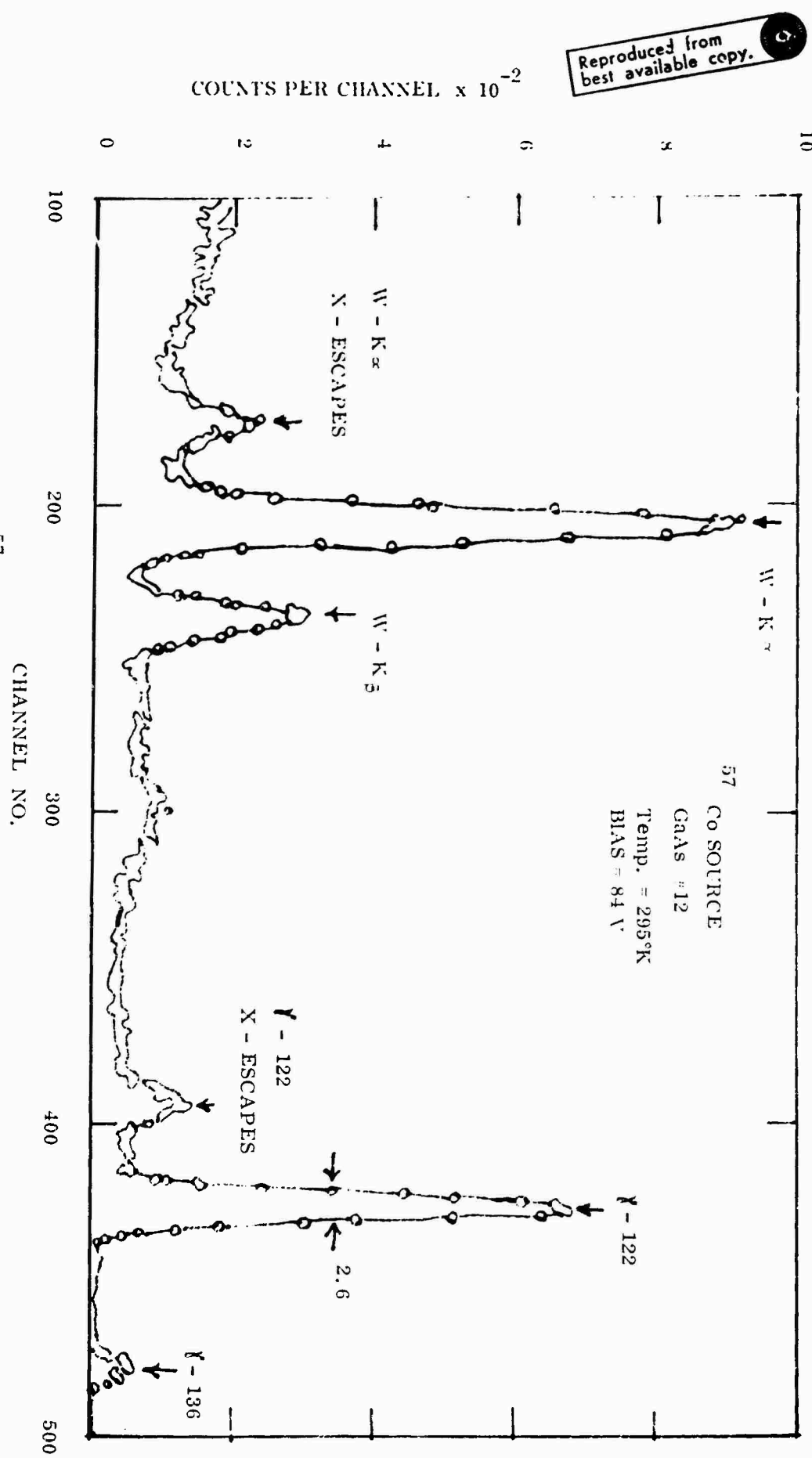
FIGURE 4.2   Response of a GaAs detector to ^{57}Co γ-rays. Epitaxial layer thickness 60 to 80 μm and 2 mm diameter
Au contact on front surface.

400 μm thick have been produced. In principle, it seems that layer thicknesses up to 1 mm can be produced and perhaps greater thicknesses could be obtained by multiple liquid epitaxial cycles.

The commercial interest in GaAs (and its alloys) is presently based on those devices that cannot be made of silicon, such as electroluminescent diodes (incoherent and lasers), electron emission devices (photoemission and secondary emission), microwave devices (transferred electron oscillators, Schottky-barrier, avalanche, and transit-time (IMPATT) oscillators). Industrial development has been insufficient to achieve the required:

- Material purity and perfection (low doping of either n or p)

- Uniformity of doping density within a single epitaxial layer (both in area and thickness)

- Uniformity and control of doping density among epitaxial layers grown from similar substrate materials

- Proper contact technology (ohmic, rectifying)

- Passivation of GaAs (surface chemistry)

- Control of interface (low interface state density, etc.) for GaAs-insulator interface

- Diffusion or implantation technology

- Correlation between device performance and materials properties

In this connection, it must be remarked that all U. S. data on gallium arsenide detectors has essentially been collected in one laboratory that used material not especially grown for gamma-detector applications. However, equivalent results have been obtained in three other laboratories outside the U.S. Extraoplating from the experience with cadmium telluride, it appears that an effort directed toward the improvement of gallium arsenide epitaxial layers for gamma detection applications would result in improved performance. It should be noted that there is no program at present on this application of epitaxial GaAs in the United States. The Department of Defense should review carefully its requirements for gamma-ray

detectors at energies of 100 keV or less to determine if such a program is warranted. It is the Committee's judgment that an appropriate R & D program on gallium arsenide should be encouraged.

4.2.1.4 High-Atomic-Number Semiconductors

The resolution obtained with gallium arsenide and cadmium telluride indicates that gamma detectors can be made from compound semiconductors. In these two materials the major problem is to obtain high purity and reduce the number of trapping centers. It may be that good energy resolution (< 10 keV) gamma detectors from these two materials may be made with thicknesses only up to 3 mm. This suggests an examination of other semiconductor materials with a higher atomic number (e.g., compound semiconductors containing components such as gold, mercury, thallium, or lead). If materials can be grown with sufficient purity and crystal perfection such that devices 1 to 2 mm thick can be made, an increase in photopeak efficiency is expected.

Periodic attempts have been made to determine if suitable candidates exist. The first attempt was made by Hofstadter in 1948 and at that time the results were not encouraging. After the development of silicon and germanium detectors, new materials were not seriously sought until the mid 1960s when cadmium telluride emerged as a logical choice to investigate. More recently the group at Siemens (Erlangen, W. Germany) has investigated[27, 28] a number of high-atomic-number materials such as lead oxide, lead iodide, mercuric iodide, and mercuric sulfide. All of these materials responded to α-particles and gamma rays. For example, in lead iodide gamma rays have been counted in the temperature range from -200 to +130° C.

Mercury iodide (HgI_2) now appears to offer the most promise of the high-atomic-number materials that have been investigated.[26, 27, 29] Single crystals of semi-insulating mercuric iodide have been grown from organic solutions or by vapor transport. These methods produce crystals typically 1 to 3 mm in thickness

and 3 to 10 mm on a side. It has been noted that in the growth of single crystal from saturated solutions of acetone or other solvents, the purity of the starting materials is very important. It does not appear to be difficult to grow crystals but the optical quality shows large variation from sample to sample. Mercury iodide detectors can be operated at room temperature; however, there is a transformation from a tetragonal to an orthorhombic crystal structure at 127° C which limits the higher temperature usefulness of these materials.

The Siemens group prepared cleaved crystals approximately 0.5 mm in thickness and about 4 mm^2 in area. Bias voltage was applied along the (001) direction with contacts made of evaporated carbon layers. For applied fields about 4000 V/cm, good response to ^{60}Co gamma radiation was observed with an energy resolution of about 10% (133 keV). Experiments at other laboratories have indicated that there is gamma detection but photo-peaks were not observed. The shape of the transient response of gamma detectors indicated that inclusions in the material were a major problem.

The work with high-atomic-number semiconductors demonstrates that gamma response can be obtained. The experience with the development of other materials for gamma detection indicates that a lengthy development effort will be required to obtain suitable crystals.[28-30] Presently, it is not obvious which material will produce the best gamma detector. Work on these high-Z materials at Siemens Erlangen has been terminated; only sporadic efforts have been made in U. S. laboratories. This area offers interesting possibilities for the development of a new class of materials for gamma detectors. Further exploratory work is needed before a large-scale development effort should be made on any one material.

4.2.1.5 Silicon Carbide, Diamond

These wide-band-gap materials have been considered for charged particle detectors operated at elevated temperatures (> 200° C). The Lebedev Institute in Moscow[30] has made such detectors from diamond (semi-insulating platelets 100 μm thick)

that operate up to 300° C. Detectors made from silicon carbide (SiC) and diamond would only be satisfactory for low energy γ-rays because of the low Z; further it is difficult to obtain a supply of high-purity, high-resistivity material. However, such material would provide a good approximation in density to body tissue and might then be useful in dosimetry applications. Progress in this field will depend on crystal-growth capability. If high-temperature detector operation is required, the Committee recommends evaluation of material availability and a cautious approach to a detector program.

4.2.1.6 Germanium-Silicon Alloys

Semiconductor mixed-crystal systems such as $Ge_x Si_{1-x}$ form solid solutions throughout the entire alloy range with the band gap varying continuously with composition. Due to the low thermal conductivity of the Ge-Si alloys there has been interest in the application of heavily doped materials to thermo-electric power generation systems. For gamma-ray detection the object is to obtain a wider band gap than that of Ge and hence a higher operating temperature. Since the material is not as pure as either high-quality Ge or Si, lithium drift techniques are required to obtain large active volumes.

The feasibility of using GeSi alloys has been demonstrated by the group at Teledyne. Lithium drift techniques were used to produce 1 mm thick compensated regions in Si rich ($x \approx 0.1$) alloys obtained from Hoboken (Belgium). Energy resolution of about 3 keV was obtained operating at temperatures of about 77° K. The lithium drift rate was relatively low suggesting the presence of oxygen in the alloy. This work has since been terminated.

At present, there is no large-scale program in the United States directed toward growth of high-purity Ge-Si alloys that would be adequate for radiation detector applications. A five- to ten-year development program would be required to produce material suitable for large volume detectors. Since the primary advantage over high-purity Ge detectors is in a possible higher operating temperature (but cooling will still be required), a major development effort does not seem justified

at this time.

4.2.2 Silicon Avalanche-Mode Detectors

A typical avalanche detector consists of a gallium-diffused p-n junction in $\approx 50\,\Omega$-cm, n-type Si with a junction depth of 25 to 75 μm. Surface contouring allows high reverse bias voltages (about 1500-2000 V) without surface breakdown.[31-32] The internal field strength leads to internal multiplication gains of about 100 to 200 (some units have exhibited average gains of 500). A 10 keV X-ray, for example, produces an output signal equivalent to 1 MeV or greater while the measured detector noise level at body temperature (37° C) is less than 100 keV.

Due to the concentration gradient in the diffused p-region, there is a drift field of about 50 V/cm. Electrons created in the diffused region will drift to the high-field junction region in 30 to 100 nsec. The electrons are then swept across the high field regions and additional hole-electron pairs are created by the avalanche process. There are two important characteristics of this avalanche process: the multiplication factor for electrons is greater than that for holes, and the decrease in the electric field with depth results in a multiplication factor that decreases with depth. Consequently the maximum multiplication is achieved by electrons arriving at the high field region near the junction. Electron-hole pairs generated thermally within the space-charge region do not experience, on the average, as large a multiplication gain as that of electrons arriving at the junction. Therefore, a signal-to-noise enhancement is achieved if the incident radiation creates electron-hole pairs within the p-type, diffused region which has a drift field. In these units the active region is about 25 to 75 μm thick.

The electric field profile varies across the detector due to variations in the resistivity of the silicon. This leads to variations of four orders of magnitude in avalanche gain in extreme cases. This non-uniform gain causes a serious loss in energy resolution, making the device unsuitable for spectroscopy applications.

The development of avalanche detectors has been carried out primarily at General Electric Company Space Systems Division.* In most applications the output signal of the avalanche detector drives a tunnel diode which is not triggered by noise pulses, and the tunnel diode system is therefore almost completely immune to noise while able to respond to X-rays at energies as low as 0.6 keV. Due to the fast response of both detector and tunnel diode, rates up to 10^8 counts/sec can be measured. Because the amplifiers are simple, multiple arrays are feasible. High quantum efficiency is attained in the energy region from 1-8 keV and drops with energy; at 17 keV energy, the quantum efficiency is 2 to 4%. The active areas of the devices range from about 10^{-2} to 1 cm^2 and they can be operated at temperatures up to 130° C.

At present the major applications of these devices are in medical fields for detection of β-particles or X-rays. The major limitation in spectroscopy applications is in the silicon material. Development work on the avalanche-detector concept should be continued.

4.2.3 Scintillator Photoconductors

The use of scintillators plus silicon or GaAs photodiodes could lead to high-efficiency gamma detection with operation at room temperature. For scintillators, the problem is to combine fast decay times with efficient light production at wavelengths suitable for the detector. For the detector, the problem is to obtain good light coupling and good signal-to-noise ratios. The disadvantage of the power resolution expected for this two-stage detection system as compared to the germanium gamma detector might be offset by the capability of operating at higher temperatures. Enhanced signal-to-noise ratios can be provided by internal amplification in avalanche detectors.

---

* King of Prussia, Pennsylvania

Several new material concepts have been explored for scintillators. Semiconductors with isoelectronic dopants (CdS doped with Te and ZnTe doped with oxygen) have shown response to gamma radiation.[32-33] Isoelectronic dopants provide centers at which both holes and electrons are captured (rapid recombination rates) and do not provide excess holes and electrons (hence, no increase in non-radiative Auger recombination). Platelets of CdS and bulk crystals of ZnTe were grown and scintillation data obtained at Bell Telephone Laboratories.[33] Preliminary results indicated linearity of response between 7 keV and 5 MeV at 100° K and decay time about the same as for NaI:Tl. Progress in obtaining large volumes will depend on obtaining crystals of high chemical purity and crystallographic perfection; a long development time probably will be required. Further study is required in the basic mechanisms of recombination and in the evaluation of the emission at room temperature.

However, a semiconductor utilized as a phosphor will always suffer from problems imposed by light collection and detector inefficiencies. Lockheed Research Laboratories have been studying scintillators of high atomic number, high luminescence efficiency, and fast response time. The most promising materials are lanthanum oxysulfide and gadolinium oxysulfide activated with ytterbium or cerium. The major problem is obtaining large single crystals of these refractory-type materials; however, progress is being made in cooperation with Sandia Laboratories. This development work should be continued.

Semiconductor photodetectors have significant advantages over photo-multipliers in compactness, insensitivity to magnetic fields, and low operating voltage. Most of the work in this field has concentrated on the detection of high-energy (greater than a few MeV) charged particles. For CsI scintillators coupled with surface barrier detectors, resolutions of ≈ 15 keV have been obtained for 5 MeV alpha particles. Improvements in performance might be obtained with scintillators of longer wavelength output. There has been no development work to utilize a scintillator-photodetector combination for gamma-ray detection

Tuzzolino at the University of Chicago suggests that 400 keV might be the low energy cutoff for useful detection.[32] This might be an extremely attractive detector combination for gamma rays of energies above 1 MeV. If such high-energy detection is required evaluation of scintillator-photodetector systems should be encouraged.

Scintillators can be coupled with avalanche detectors.[34] At present large area silicon avalanche diodes have a spectral response peak in the 8000 to 9000 Å region; available fast scintillators emit efficiently at shorter wavelengths.[35] The study at Lockheed suggests that the best combination for the detection of X- or γ-ray radiation involving a scintillator is a combination of a conventional scintillator (CsI:Tl) with a shallow-junction silicon avalanche detector. The useful range might be extended down to 25 keV. Further experimentation is required.

4.3   Integrating-Mode Devices and Materials

The basic method of detecting radiation with integrating-mode devices depends on the production of electron-hole pairs, direct collection of the charge, or scintillation (light emission) after excitation.[36] However, here interest is in the average rate of energy deposition or total absorbed dose. A low-Z material resembling the z of human tissue is often desired, and large size is an advantage only if it is not accompanied by an increase in leakage current. Room-temperature operation is essential for many applications.

The primary use of an integrating detector is as a solid-state replacement for a Geiger tube or ion chamber. Dose rates of gamma rays can be monitored independently and accurately by means of the ion current produced in an ion chamber, but the volume of chambers of required sensitivity is too large for some applications. Considerable reduction in weight and size could be achieved if suitable solid state materials were available.

The substitution of low-Z solid-state devices for ion chambers and Geiger-Müller counters to obtain useful readouts in doses in the required mrad hr^{-1}

range presents difficulties with respect to sensitivity, stability, current build-up time, and signal-to-noise ratio. These difficulties have not yet been resolved.

Detection of the emission of low-energy secondary electrons from a metallic layer placed on the surface of a hydrogenous material in vacuum is required for tactical dosimetry and for dose rate measurements at high radiation intensities (as high as 10^{12} rads per second). Outgassing is a serious problem. Hence there is a need for a hydrogenous material like a plastic or a hydride of a low-atomic-number metal that does not outgas or deteriorate under radiation. Materials whose surfaces have a high yield for secondary electron emission and are conductive (so that no surface charge build-up occurs) are needed, but they are not now available.

There has been a marked improvement in the quality of such thermoluminescent materials as LiF, LiBr, CaF_2, but serious problems regarding their energy dependence, low upper limit before saturation, and annealing characteristics remain unsolved. Thermoluminescent device materials and glasses with varied composition also are needed to aid in determining the spectrum of incident radiation.

Materials used for the measurement of dose rate and spectra as a function of time in fast-pulsed radiation environments are ceramics like lead zirconium titanate. The time resolution and sensitivity are both near optimum values, but more basic knowledge of their fundamental parameters is needed to permit usage without prior calibration. Curie point, pyroelectric coefficient, specific heat, dielectric constant, and energy absorption coefficients are some of the physical bulk parameters for which better data are needed.

4.4 Conclusions and Recommendations

4.4.1 Conclusion on Working Group for X-Ray and Gamma-Ray Detection

One of the primary facts emerging from this study of materials for detection of X- and γ-rays is that a clear definition of needs by detector users is absolutely necessary. There has been a tremendous upsurge of interest in detector

applications in recent years in such areas as biology, nuclear medicine, geology, crimnology, and industrial processing. The Committee did not attempt to delineate the needs for detection with regard to other governmental agencies (e.g., the Postal Service, Federal Aviation Authority, Department of Justice, Department of Commerce, Department of Health, Education and Welfare). But it is clear that there should be a continuing long-range overview of this field, because of the long time required to implement goals. No detector materials are currently available that meet the advanced needs of the Department of Defense in the spectral range covered in this chapter. Purification of materials, crystal growth, characterization, and detector fabrication have generally not been successful when attempted as a crash program. Materials developed for standard electronic or optical components seldom meet the requirements for detector materials. Experience with high-purity Ge and CdTe indicates a minimum of five to ten years effort for a two to three man team. If gamma-ray detectors are to be available to meet the advanced requirements, it is incumbent upon government agencies to examine carefully their needs at least ten years into the future and to interact with semiconductor material and particle detector specialists.

Recommendation (Priority 1)

A panel like the semiconductor nuclear detector panel of the National Academy of Sciences Subcommittee on Instrumentation and Techniques should be established to provide a continuing review of present and future directions and an evaluation of the detector state of the art on a regular basis.

4.4.2 Conclusion on Detector Materials Evaluation

Commercial organizations apparently have not found it profitable to conduct materials research required for the development of detectors. If government needs are to be met, funding must be made available to develop new materials, maintain instrumentation and detector development groups, and support efforts to characterize detector performance in terms of materials parameters.

Recommendation (Priority 1)

Support should be provided for development of detector-quality materials, maintenance of the capability of instrumentation and detector development groups, and investigation of physical and electrical properties useful in detector materials evaluation.

4.4.3 Conclusion on a Need for Study of Integrating-Mode Devices for X-Ray Detection

There is a clear requirement for integrating-mode devices; however, no solid state materials suitable for present day needs appear to be available. No continuous major effort has been carried out to develop these materials. At present it is not possible to relate the integrating-mode requirements to existing material parameters in sufficient detail to provide specific guidance for materials development.

Recommendation (Priority 1)

A group should be established to examine materials requirements for integrating mode devices and to make appropriate recommendations for research support.

4.4.4 Conclusion on High Purity Germanium

Germanium is used for the bulk of gamma ray spectroscopy applications. Because the energy band gap is relatively small, these large-volume detectors must be cooled below $150°$ K to reduce the leakage current to a level suitable for high-resolution performance. A continuing problem exists in that the primary source of detection-quality material is from Belgium. Presently, most detectors are fabricated by lithium drift techniques, but it is anticipated that continued improvement in the purity and perfection of germanium may serve to eliminate the necessity of lithium drifting. This would provide a major advantage in application of these detectors, since it would eliminate the need for low-temperature storage to prevent lithium precipitation and subsequent detector degradation. Detectors made from

72

present high-purity germanium have an active volume (≤ 10 cm^3) smaller than that desired for many detector requirements. While a commercial source of high-purity Ge exists in the United States, the economic justification for industrial production of high-purity germanium remains uncertain.

Recommendation (Priority 1)

Work on the production of high-purity germanium should be continued and expanded to assure a domestic source and, if possible, to provide a competent second source. Research aimed at improving quality and characterizing the material should be supported.

4.4.5 Conclusion on Cadmium Telluride

One of the outstanding requirements for gamma-ray detectors is to obtain materials suitable for operation at temperatures up to ~ 100° C. The atomic number of these materials should be comparable to, or greater than, that of Ge to assure high photo-peak efficiency. The results obtained with two materials, gallium arsenide and cadmium telluride, indicate that this goal can be reached. For many years cadmium telluride has been considered one of the promising materials for room-temperature gamma-ray spectroscopy. A major funding effort to produce semi-insulating CdTe for application as an electro-optic modulator has been encouraging and has added major support to the materials effort. Significant advances in materials growth, material analysis, and detector performance have been made, and a limit in material improvement has not yet been reached. The performance of currently available devices is limited by the concentration of trapping centers and material inhomogeneity.

Recommendation (Priority 2)

Support research on cadmium telluride aimed at providing improved material and characterizing it for use in high energy photon detectors.

4.4.6 Conclusion on Gallium Arsenide

Gamma detectors have been fabricated from epitaxial gallium arsenide and have been found to exhibit excellent resolution for low-energy gamma rays. Current devices are basically Schottky barriers on high-purity gallium arsenide ($\leq 100\ \mu m$ thick). Devices of thicker dimensions exhibit severe trapping effects but have potential application in medical probes and areas where spectroscopy is required for gamma energies of 100 keV or less. Future developments of this material depend primarily on the availability of epitaxial layers of higher purity and lower trap density. There is no U. S. program at present on this application of epitaxial GaAs.

Recommendation (Priority 2)

Develop a program to provide higher-purity epitaxial layers of GaAs for gamma-ray detectors.

4.4.7 Conclusion on Materials Containing Elements of High Nuclear Charge

The results with CdTe demonstrate that higher Z and larger band gap materials offer promise for detector application. Work in Germany on PbO, PbI_2, and HgI_2 has shown that alpha-particle spectroscopy and gamma ray detection is possible. This work has been terminated, and only sporadic efforts have been made in the United States.

Recommendation (Priority 2)

Exploratory work on high-Z materials potentially useful in high-energy photon detection should be supported.

4.4.8 Conclusion on Silicon

Silicon is used primarily for X-ray spectroscopy for energies less than 50 keV. There has been no marked improvement in material suitable for lithium drift in the past five years; trapping effects are found during low-temperature operation. Improvement in this situation is not anticipated.

Enough high-quality detectors can be selected from present sources to meet foreseeable future demands. Silicon diffused p-n junctions have been used in the avalanche mode as X-ray and low-energy gamma ray detectors. The active regions are thin; hence, the detectors are most useful in the 1 to 10 keV energy region. The primary difficulty in obtaining large area or uniform internal gain is resistivity variations (microstrations) in the silicon.

Recommendation (Priority 3)

Support research on Si aimed at improving homogeneity in avalanche mode devices for use in X-ray detection.

4.4.9 Conclusion on Silicon Carbide and Diamond

The capabilities of SiC and diamond as charged-particle detectors at elevated temperatures ($\sim 200^\circ$ C) have been demonstrated in the U.S.S.R. Use of these materials depends on the availability of suitable crystals. These refractory materials are very difficult to obtain with sufficient purity with large detection volume without trapping effects.

Recommendation (Priority 3)

Support a materials preparation exploratory investigation on SiC and/or diamond only if sufficiently strong needs for high-temperature detector operations can be demonstrated.

4.4.10 Conclusion on Germanium - Silicon Alloys

A potential advantage of Ge-Si alloys is that operating temperatures higher than those possible with Ge detectors might be achieved. At present no large-scale U.S. program is directed toward growth of Ge-Si alloys of detector quality, and a long-term development would be required to obtain suitable material. It is not certain that the advantage of a larger band gap would outweigh the disadvantage of lower purity which would require lithium drifting.

Recommendation (Priority 3)

No program of research on Ge-Si alloys is recommended at the present time.

4.4.11 Conclusion on Scintillator - Photoconductor Combination Detectors

There are other possible detector configurations. The use of scintillator-photodiode combinations appears to offer prospects for applications where energy resolution can be sacrificed for high detection efficiency and higher operating temperatures. There are several new material concepts that will require long-term investigation, and experimental evaluation of scintillator-avalanche diode combinations is needed.

Recommendation (Priority 3)

Support research on materials useful for scintillator-photoconductor combination detectors and the evaluation of their detector performance.

4.5 References

4.5.1 General and Historical References

1. F. S. Goulding and Y. Stone, Semiconductor Radiation Detectors, Science 170, 280 (1970).

2. Semiconductor Nuclear Particle Detectors and Circuits, National Academy of Sciences Publication 1593 (1969). Washington, D. C., 20418.

3. G. Bertolini and A. Coche, Semiconductor Detectors, North Holland, (1968).

4. G. Dearnaley and D. C. Northrop, Semiconductor Counters for Nuclear Radiations, Second Edition, Wiley, N. Y. (1966).

5. R. K. Willardson and A. Beer, Semiconductors and Semimetals, Vols. 1-5, Academic Press, N. Y. (1966-1970).

6. J. M. McKenzie, Index to the Literature of Semiconductor Detectors, National Academy of Sciences, Washington, D. C. (1969).

7. A. H. Sommer, Photoemissive Materials, Preparation, Properties and Uses, John Wiley, N. Y. (1968).

8. S. M. Ryvkin, Photoelectric Effects in Semiconductors, Consultants Bureau, N. Y. (1964).

9. J. Fowler, Radiation Dosimetry, Vol. 11, Academic Press (1966).

10. P. J. Van Heerden, Physica, 16, 505 (1950).

11. R. H. Hofstadter, Nucleonics, 4, 2 (1949).

12. G. T. Ewan and A. J. Tavendale, Can. J. Phys. 42, 2286 (1964).

13. M. Martini, J. W. Mayer, and K. R. Zanio, "Drift Velocity and Trapping in Semiconductors", Applied Solid State Science, Vol. 3, Academic Press, N. Y. (1972).

4.5.2 Specific Materials - Pulse Mode

4.5.2.1 Germanium and Silicon

14. Recent progress in the growth and characterization of germanium for lithium drift and ultrapurification of germanium for detector fabrication is best understood by examining the Annual Reports to the U. S. Atomic Energy Commission of (a) R. N. Hall, et.al., General Electric Company; (b) W. Hansen, et.al., Lawrence Berkeley; (c) G. Armantrout, et.al., Lawrence Livermore; (d) R. D. Westbrook, et.al., Oak Ridge National Laboratories. For copies, address U. S. Atomic Energy Commission, Washington, D. C., 20545.

15. R. D. Baertsch and R. N. Hall, IEEE Trans. Nucl. Sci. NS-17 235 (1970).

16. R. N. Hall and J. T. Soltys, IEEE Trans. NS-18, 160 (1971).

17. W. L. Hansen and E. E. Haller, IEEE Trans. NS-19, 260 (1972); E. E. Haller, W. L. Hansen, and F. S. Goulding, IEEE Trans. NS-20, 481, (1973).

18. Recent Progress in the characterization of germanium by radiation experiments is best understood by examining recent reports to the U. S. Atomic Energy Commission by: (a) J. Llacer and H. Kraner, Brookhaven (BNL-16246, 16142); (b) J. Blankenship, Oak Ridge (to be submitted).* See also (c) J. Llacer, IEEE Trans. NS-19, 295 (1972).

4.5.2.2 Cadmium Telluride

19. The most recent survey is: Proceedings of the International Symposium on CdTe, A Material for Gamma Ray Detectors, June 1971, Strasbourg, France: Available from Dr. Paul Siffert, Centre de Recherches Nucleaires, Rue du Loess, Strasbourg, Cronenbourg, France.

---

* See reference 14 for source of reports.

20. C. Canali, et. al., Transport Properties of CdTe, Phys. Rev. B-4, 422 (1971).

21. R. O. Bell, N. Hemmat, F. Waid, Phys. Stat. Sol. (a) 1, 375 (1970).

22. W. Akutagawa and K. Zanio, J. Appl. Phys. 40, 3838 (1971).

23. K. Zanio, W. Akutagawa and H. Montano, IEEE Trans. NS-19, 257 (1972).

4.5.2.3 Gallium Arsenide

24. J. E. Eberhardt, R. D. Ryan and A. J. Tavendale. Nucl. Instr. and Method, 94, 463 (1971).

25. P. E. Gibbons and J. H. Howes; also T. Kobayashi, et. al.: IEEE Trans. NS-19, 324 (1972).

4.5.2.4 High Z Materials

26. (HgI_2) R. H. Bube, Phys. Rev. 106, 703 (1957).

27. (HgI_2) W R. Willig, Nucl. Inst. and Meth., to be published.

28. (PbI_2) S. Roth and W. R. Willig, Appl. Phys. Lett. 18, 328 (1971).

29. (HgI_2) H. L. Malm, IEEE Trans. NS-19, 263 (1972).

4.5.2.5 Diamond

30. E. K. Konorova and S. F. Kozlov, Sov Phys. Semicond. 4, 1600 (1971).

31. J. E. Bateman, Nucl. Instr. and Meth. 71, 261 (1969).

32. A. J. Trizzolino, et. al., J. Appl. Phys. 33, 148 (1962).

33. T. C. Madden, et. al., IEEE Trans. NS-15, (No. 3), 47, (1968). (Isoelectronic traps-scintillators).

4.5.2.7 Avalanche Photodiodes

34. Recent progress is best understood by examining the contract reports,
   Research on Avalanche Semiconductors for Radiation Detectors, by
   G. C. Huth, to the U. S. Atomic Energy Commission, Division of
   Biology and Medicine, H. Wasson, Director, (Contract No. AT-(30-1)
   3246.*

35. R. J. Lockyer and G. C. Huth, Appl. Phys. Letter 9, 227 (1966).

4.5.3 Specific Materials - Integrating Mode

36. United States Army Research and Development Series, Vol. 3, A
   Monograph on High Intensity Radiation Dosimetry With SemiRad,
   by S. Kronenberg, U. S. Army Electronics Command, Ft. Monmouth,
   N. J. (1966).

---

* See reference 14 for source

SENSORS FOR ULTRAVIOLET, VISIBLE AND NEAR-INFRARED (0.1 to 2.0 μm)

5.1 Introduction

This chapter deals with detector materials sensitive to electromagnetic radiation with wavelength between 0.1 and 2.0 μm. The subdivision of this wavelength band into ultraviolet, visible and near infrared is historically due to the response of the human eye to radiation between 0.4 and 0.7 μm, the so-called visible portion of the spectrum. Wavelengths shorter than 0.4 μm have become known as the ultraviolet while wavelengths longer than 0.7 μm are called infrared, with those nearer the visible region being appropriately called near infrared. These distinctions are less important in the case of nonbiological detectors where the spectral response may extend over a significantly larger fraction of the band and the detector functions may be either substantially simpler or of a completely different nature than that performed by the eye. This is increasingly true of visible-infrared detectors such as silicon avalanche photodiodes that respond well from 0.3 to 1.1 μm. Ultraviolet detectors are still in a somewhat separate class due to requirements on window materials and specific details of application such as solar "blindness" where response beyond 0.3 μm is undesirable.

Practical detector devices for the 0.1 to 2.0 μm spectral range fall naturally into four classes:

- Vacuum devices such as photomultipliers and image intensifiers.

- Gas-filled devices such as Geiger Müller tubes and proportional counters.

- Solid state devices such as photoconductors, phodiodes, and phototransistors.

- Hybrid devices, principally television camera tubes such as the vidicon.

These devices are considered in more detail below. The key detector element in vacuum devices is the photocathode where incoming radiation is converted into electrons which are emitted into vacuum for subsequent processing. It is the

photocathode, therefore, which receives emphasis in the discussion of vacuum devices rather than the devices themselves.

Several detector devices that respond in this spectral range are omitted from the discussion for reasons peculiar to the devices themselves. Thermopiles for example, are frequently used to measure power output from lamps at wavelengths down to the absorption threshold of the window materials in the optical path, but they have a response time far too slow for most other detector requirements. Quantum counters have been examined for many detector applications, including imaging, but are relatively inefficient and have an optical detection bandwidth too narrow for most applications.

Several important advances have been made in recent years in materials and device technology for detectors in this spectral range. Examples are the introduction of the negative electron affinity photocathode[1], the development of the silicon diode array vidicon[2], and the low-noise, high-gain silicon avalanche photodiodes[3], and the demonstration of surface charge-coupled imaging arrays[4]. These developments have led to an increasing degree of commonality in the materials technology applicable to both vacuum and solid state devices. For example, negative electron affinity photocathodes with gallium arsenide sensing layers can be described by the same diffusion model for carrier transport as would be gallium arsenide p-n junction photodiodes. This is in contrast to conventional multialkali antimonide photocathodes whose operation has largely defied all but the crudest analytical treatment. This has been an important factor in the developing materials technology of the new photocathodes. The rapid development of planar integrated circuit technology has affected the size and quality of pre-amplifier and amplifier packages for detector elements and television cameras and of power supplies for image intensifiers and detectors alike and is responsible for the fabrication technology for silicon diode array vidicon targets. Finally, the surface charge-coupled devices offer a highly flexible technique for self-scanned, imaging detector arrays with the possibilities of low-noise operation and integrated signal processing.

To deal with detector materials for the 0.1 to 2.0 μm range, this chapter is organized to consider first the performance and criteria for detector devices and the limitations on their operation imposed by fundamental and environmental considerations. The methods of material and device preparation are discussed next, followed by a review of the status of performance of devices and the materials in them at the time this report was prepared. Finally, foreseeable trends in detector materials and devices are discussed, followed by the conclusions and recommendations that can be drawn from the information available.

5.2 Performance Criteria and Limitations

5.2.1 Photon-Detection Processes

The process of photocarrier generation and transport in detector materials is discussed in the chapter on Fundamentals of Electromagnetic Radiation Detection. To gain some perspective on the material parameters influencing the performance of many detectors, the main features of the diffusion model for photocarrier transport are discussed below. Fundamentally, carrier diffusion currents produce a net transport of carriers from a region of higher concentration to one of lower. Since charges in the solid are generally created in pairs, significant separation of opposite charges results in an electric field retarding the separation unless provision is made for removing the generated excess charge in some preferential manner.

The schematic model for the carrier diffusion problem is illustrated in Figure 5.1. The detector material (Region II) is assumed to have a thickness, d, parallel to the x-axis of the figure and to have dimensions normal to this axis large compared to d. The material is characterized by an absorption coefficient α_z, which is a function of the wavelength of the incident radiation and by mobilities, μ_n and μ_p, and lifetimes τ_n and τ_p, for electrons and holes, respectively. The material is assumed homogeneous. Regions I and III may be vacuum, substrates, or the second half of a p-n junction but are assumed passive for this discussion with respect to carrier generation and transport. They are characterized by optical absorption

82
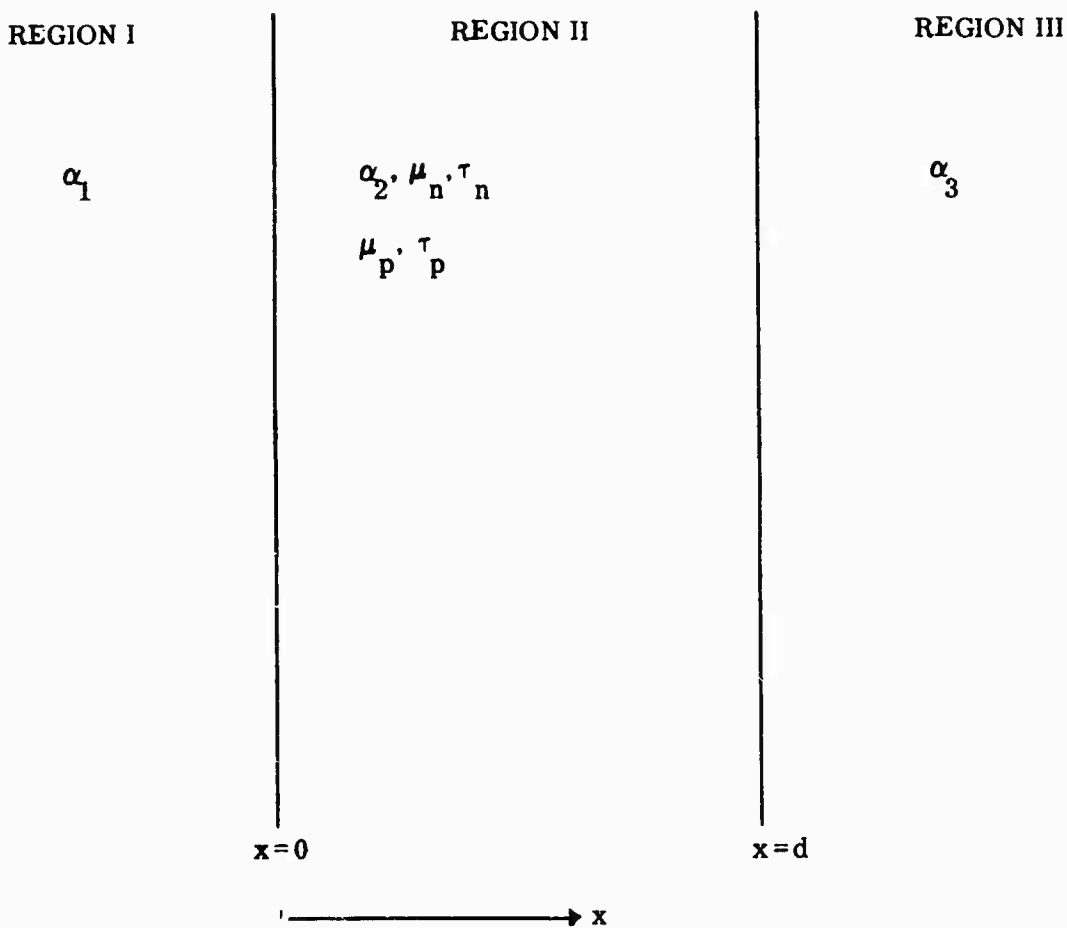
FIGURE 5.1   Schematic model for calculation of detector efficiency from the diffusion equation.

coefficients α_1 and α_3 respectively. Interface I-II is characterized by a reflection coefficient R_1 and interface II-III by reflection coefficient R_2. Light may be incident from either side but it is assumed that photo-generated carriers contribute to the signal only when collected at interface II-III (single-carrier process).

The important performance parameter for detectors is the quantum efficiency η (electrons emitted per incident photon), which is generally a function of the two spatial coordinates y, z, transverse to the detector thickness (x-axis $\stackrel{\text{.}}{.}$ Figure 5. 1), the time, t, and the wavelength, λ, of the incident radiation. The detector material could be a p-type, n-type, or intrinsic semiconductor. Consequently, the general formulation of the model includes both electrons and holes. For many purposes, the semiconductor is of predominantly one type with the photo-generated majority-carrier density a small fraction of the total. The signal then will be due to excess minority-carriers generated by the incident radiation. This current is calculated from a solution of the diffusion equation[5] with appropriate boundary conditions on the excess minority carrier density and/or its derivative.

An important factor influencing detector efficiency is the surface recombination velocity, S, at interface I-II. The interface states responsible for this loss mechanism are directly related to the quality of the interface; high-quality bulk material alone is insufficient to insure efficient detectors.

An electric field also may be present in the detector material. This electric field may result from fixed-charge distributions, mobile charges, or from bias applied externally across the detector. Whatever their source, electric fields may either aid or retard the diffusion current by setting up an independent drift component in the particle motion. The carriers will gain energy from the field. If the energy gained becomes appreciable, the carriers "heat up" and the diffusion equation can no longer be used to describe accurately the behavior of the excess carrier current.

84

Normally fields in excess of 10^4 V/cm, the value depending on the carrier type and material, are required for this to be important. Since diffusion processes are relatively slow, small electric fields that sweep the carriers out of the detector also are applied where fast detector response is desired.

In carrier transport by diffusion, the diffusion length, L, of the carrier is important. It can be defined as $L^2 = D\tau$, where D is the diffusion constant, generally equal to $kT\mu/e$.* The diffusion length is the radius of a sphere, concentric with a point source of excess minority-carriers in a homogeneous material, on which the carrier density has decreased to e^{-1} of its original value through recombination processes. This parameter can be used as a fair characterization of material quality and is intimately related to the shape of detector spectral response curves.

The results of this model can be illustrated by the spectral quantum efficiency of a semitransparent (light incident from Region I) negative affinity photocathode. The photocathode detector material is assumed p-type and is in Region II (Figure 5.1). Regions I and III are assumed to be vacuum with reflection coefficients, R_1 and R_2, at the respective interfaces. Surface recombination at interface I-II gives rise to a parameter in the quantum efficiency:

$$U = SL/D = S\tau/L$$

where S = surface recombination velocity, L = diffusion length, D = diffusion constant and τ = lifetime. The carrier density at x = d is assumed to vanish since the surface acts as a sink for photoelectrons which escape with probability, P. Region II is assumed to have infinite extent in the yz-plane, and function dependence on y, z, and t is suppressed (the zero frequency case). The quantum efficiency at a given wavelength is then given for the semitransparent case by:

* T is the temperature, k is Boltzmann's constant, μ is mobility.

$$\eta_T = \frac{\alpha L}{1 - \alpha^2 L^2} \left[e^{-\alpha d} \left[\frac{\tanh \frac{d}{L} + U}{1 + U \tanh \frac{d}{L}} + \alpha L \right] \right.$$

$$\left. - \frac{\alpha L + U}{\cosh \frac{d}{L} (1 + U \tanh \frac{d}{L})} \right] (1 - R_1) P,$$

Equation 5.1 (a)

and for the opaque case (light incident from Region III) by:

$$\eta_R = \frac{\alpha L}{1 - \alpha^2 L^2} \left[\frac{\tanh \frac{d}{L} + U}{1 + U \tanh \frac{d}{L}} + \frac{e^{-\alpha d}}{\cosh \frac{d}{L}} \left[\frac{\alpha L - U}{1 + U \tanh \frac{d}{L}} \right] \right.$$

$$\left. - \alpha L \right] (1 - R_2) P.$$

Equation 5.1 (b)

Equations 5.1 can now be used to gain some insight into the effect of the various materials parameters upon the quantum efficiency of this particular detector. For example, it is apparent that large P and small R_1 or R_2 are required for optimum sensitivity. The escape probability is dependent on photocathode activation, while the reflection coefficient R_1 can be reduced by use of antireflection coatings.[6] The layer directly on the detector also must serve as a passivating layer to reduce surface recombination velocity. Since interface II-III is the activated face, reflection coefficient R_2 cannot be adjusted.

The relationship between the quantum efficiency and the parameters L, d, and S expressed by Equations 5.1 does not lend itself to easy evaluation. It is possible to draw a few general conclusions by choosing typical values for the parameters. These results appear in Table 5.1 for the indicated values. The absorption coefficient chosen corresponds to III-V materials at wavelengths just short of the absorption edge. Qualitatively, the results in Table 5.1 show that large diffusion lengths are directly responsible for high efficiency, regardless of the value of surface recombination velocity. As the diffusion length becomes smaller than the thickness ($\alpha L \ll 1$), the efficiency drops rapidly since only those carriers generated

with n a diffusion length of the collecting surface contribute to the signal. At this limit:

$$\eta_T \approx \alpha L e^{-\alpha d} \qquad \text{and} \qquad \eta_R \approx \alpha L$$

independently of S, and those carriers generated near interface I-II which are affected by high recombination rates no longer contribute to the signal in any case.

TABLE 5.1 CALCULATED QUANTUM EFFICIENCY FROM EQUATION 5.1 (a)

$P = 1$, $R_1 = 0$, $\alpha d = 1$, $d = 1 \mu m$, $\tau = 1 \mu$ sec

L (μm)	η_T for ($S = 0$)	η_T for ($S = L/\tau$)	η_T for ($S \to \infty$)
10.0	.63	.60	.26
2.0	.58	.48	.25
0.5	.27	.23	.19
0.1	.04	.04	.04

For diffusion lengths greater than the sample thickness, high recombination rates reduce quantum efficiency due to carrier loss at the interface through which light is incident. This effect will be stronger at shorter wavelengths since the absorption coefficients are generally higher and photoelectron generation rates are highest close to the entrance surface.

For the photocathode discussed above, minority-carriers were generated in an undepleted part of the semiconductor and diffused to the vacuum surface to produce an output signal. Applications requiring detection of radiation modulated at high frequencies place a premium on the detector speed of response without significant loss of efficiency. Stated another way, the detector must have a wide frequency bandwidth. The solution of the time dependent diffusion equation shows that $L = L_o (1 + j\omega\tau)^{-\frac{1}{2}}$ must be used in Equations 5.1 where L_o is the actual diffusion length and L now becomes an effective diffusion length. For the simple case of small L_o, Equations 5.1 become:

$$\eta\ (\lambda,\ \omega) = \frac{\alpha\ L_o\ \exp\ (\alpha a - j\frac{\theta}{2})}{(1 + \omega^2 \tau^2)^{\frac{1}{4}}}$$

Equation 5.2

where $\tan\theta = \omega\tau$. The amplitude of the quantum efficiency decreases as $\omega^{-\frac{1}{2}}$ at higher frequencies, decreasing to 50 percent at $\omega_1 = 4/\tau$. For silicon τ can be several hundred μsec so that $\omega_1 \approx 4\,kHz$; in gallium arsenide, $\tau = 10$ nsec and $\omega_1 \approx 400$ MHz, implying that gallium arsenide would be a better detector of ruby laser light at $0.69\,\mu$m modulated at video frequencies ($\omega \approx 10$ MHz). While lifetime can be reduced by adding recombination centers, diffusion length L_o is reduced as well, giving a lower efficiency so that no net improvement would result.

An alternative approach for high-speed junction detectors is photon detection in the junction depletion region itself, using the field formed under reverse bias to sweep the carrier pairs out. The limiting time then becomes the transit time of the carriers through the depletion region. The electrons and holes reach a velocity limited by phonon scattering. The variation of signal power is specified by the variation of $[\ F'(\omega,\alpha)\ ]^2$ and is plotted in Figure 5.2. The quantity $F(\omega,\alpha)$ is called the signal reduction factor and acts much like the quantum efficiency to account for the fact that all the photons may not be absorbed within the field region and that the time for carriers to complete a transit of the field region may occupy an appreciable fraction of one cycle of the input waveform.

The insert in Figure 5.2 shows the time variation of signal current for an infinitely narrow pulse of carriers generated at the interface I-II of Figure 5.1. The current is constant during the drift of the carriers across d and then drops to zero. The width of the current pulse in time is the transit time, d/v. It is apparent that any process which tends to lengthen the current pulse will degrade the frequency response of the diode. Actual diodes may utilize a combination of drift in the field region and diffusion from the undepleted areas adjacent to it.

FIGURE 5.2

Signal Reduction Factor $F(\perp\alpha)^2$
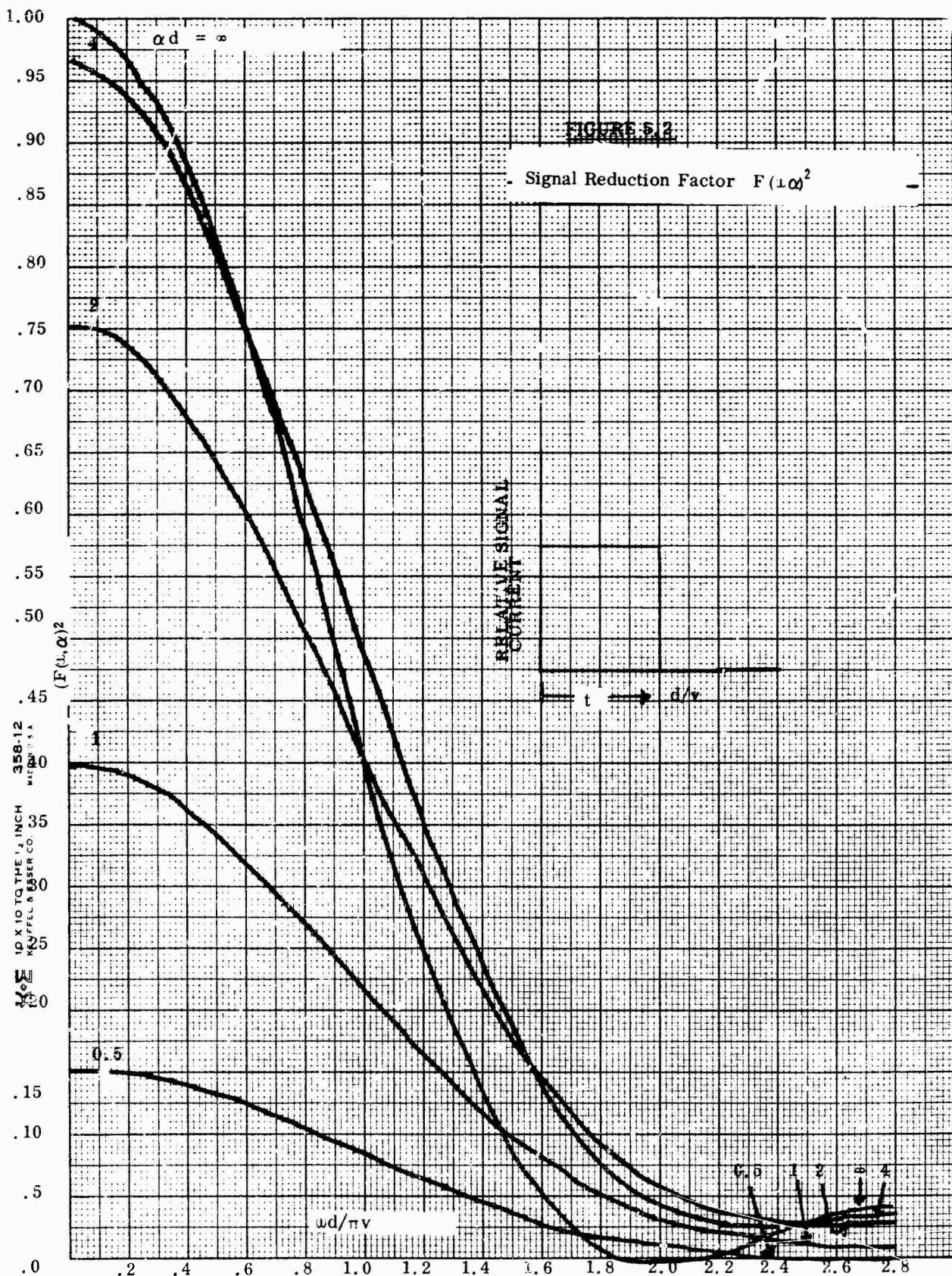
Considerable emphasis has been placed here on basic photodiode detection processes without a discussion of classical photoconductors. To a large extent, this is a reflection of the growing importance of photodiodes in detector systems for this spectral range. The photoconductor[8] is a slab of extrinsic (doped) material with ohmic contacts at both ends. Signal generation occurs when incident light reduces the dark resistance of the material, allowing increased current to flow when bias is applied. These devices frequently can be made to exhibit gain due to minority-carrier trapping at controlled defect sites. When this occurs, excess majority carrier current will flow until the trapped minority carriers are neutralized. For the most part, II-VI compounds such as ZnS, ZnSe, CdS, CdSe, and CdTe have been used as photoconductive detectors. Control of the doping level, trap type, and distribution is critical if reproducible results are to be obtained.

The gain mechanism itself provides a limitation on useful performance. Since the gain is achieved by a trapping process, changes in input light level will not be manifested until trapped carriers are ejected and swept out or neutralized. High gain, however, requires long trapping lifetimes so that these devices tend to have slow response times. This is particularly acute at low light levels. The dark current in photoconductors is predominantly due to majority carriers. Since this current sets the low-level threshold for detection, suppression of dark current can be achieved by reduction of the doping level or cooling, both of which reduce the number of majority carriers available for recombination with trapped minority carriers which increases trapping lifetimes. In reality, the behavior of trapping lifetime[8,9] with temperature or doping level may be considerably more complicated, depending on the energy level of the trap in the forbidden band and the capture cross sections for both types of carrier. In general, however, speed of response becomes an increasing problem as detection threshold is reduced.

A comparison between photoconductors and photodiodes shows that for the same material, the dark current from the photodiode tends to be smaller. In addition, photodiodes will have a shorter response time at low light levels although loading circuits must be taken into account as well. The loss of a gain mechanism in the detector in going from a photoconductor to a photodiode is compensated to an increasing extent by continued improvements in avalanche multiplication in photodiodes.

A brief discussion of the avalanche multiplication process is required to complete the description. When photodiodes are operated under high reverse biased conditions, controlled carrier multiplication can be initiated within the junction by the injection of photoelectrons (or holes) into the junction region. This multiplication takes the form of internal production of electron-hole pairs by the carriers accelerated by the junction field. Since secondaries may be swept out of the junction region before generating further pairs, the process does not go on indefinitely. At a critical field (a "breakdown" voltage, V_B), the incident electron and each secondary electron (hole) generate exactly one pair, producing a sustained breakdown in the junction. A detailed discussion of this process has been given by Chynoweth.[10]

If i is the total current, and i_o the incident current, the multiplication factor, M, is defined as:

$$M = \frac{i}{i_o},$$

Equation 5.3

and depends on voltage empirically (except for silicon) as:

$$M = \frac{1}{1-(\frac{V}{V_B})^n},$$

Equation 5.4

where n usually has a value between 3 and 6, depending upon the semiconductor materials,[11] doping profile, and exciting wavelength.

Avalanche multiplication often degrades the frequency response of a photo-diode due to the feedback effect of the multiplication process. If both electrons and holes cause ionization, the duration of a current pulse will increase with multiplication. In general, a distribution of ionization lengths and times exists, and the pulse will cut off only when all carriers are finally swept from the field region. The pulse has, in the meantime, increased in length.

Alternatively $[F(\omega, \alpha)]^2$ has been degraded and becomes $[F(\omega, \alpha, M)]^2$, a decreasing function of the avalanche gain, M. If the electron and hole ionization rates are equal, the gain bandwidth product of the avalanche photodiode will not improve over that of the high-frequency diodes. Furthermore, for equal ionization rates the signal-to-noise ratio decreases with increasing gain.

The case of unequal electron and hole ionization rates is somewhat different. The frequency response of the diode will degrade by a factor of two at most but a large increase in detector gain bandwidth product is possible. This is only true if the carrier with the largest ionization rate initiates the avalanche. The frequency dependence of the avalanche gain itself is absorbed into a factor $[M(\omega)]^2$ multiplying $[F(\omega, \alpha, M)]^2$. In principle, the signal-to-noise ratio is substantially independent of gain when the ionization coefficients are grossly disparate.

5.2.2 Performance Limitations

The photon-detection process for minority-carrier signal generation was discussed in the previous section. In this section, some of the limitations on signal levels detectable at the output are discussed. These limitations are imposed by both the detector and the radiation it intercepts; they take the form of "noise" currents (or voltages) at the output of the detector. The sources of noise currents are the uncorrelated, random arrival of photons at the detector or the random events occurring in carrier transport through the detector. These noise sources are not discussed in detail as more complete treatments are available[12-14] but the results are quoted to provide a complete view.

The underlying assumption regarding photodetectors with more than one noise source present is that no correlation exists between the noise sources, so that their respective noise "currents" may be added in quadrature. The four noise sources considered here are Johnson (thermal) noise, shot noise, 1/f noise, and avalanche multiplication noise. Bulk generation-recombination noise is frequently found in photoconductors and is generally equal in magnitude to the shot noise but does not contribute in junction devices. While all noise sources have a frequency dependence, particularly at high frequencies, the low-frequency case ($x < 1/\tau$) will be assumed here for simplicity.

- Johnson Noise - Solid-state detectors, photomultipliers, and vidicon camera tubes generally have associated with them a load resistor across which a signal voltage is developed by the device output current. While not part of the detector itself, the load resistor is frequently a limitation on the performance of the detector package. Further, in some detectors, series resistance in the detector itself may influence device performance. In both cases, random thermal motion of carriers through the material gives rise to fluctuations in the current. The mean square noise current is then given by:

$$\left(\overline{i_{JN}^2}\right) = \frac{4kT\,\Delta f}{R} \quad ,$$

Equation 5.5

where k is Boltzmann's constant, T is the absolute temperature, Δf is the measurement bandwidth, and R is the value of the load or series resistance.

Morton[15] has pointed out that a deliberate or parasitic capacitance, C, in a photodiode circuit may limit its performance as a photon counter. In conjunction with the diode load resistance, R, the bandwidth $\Delta f = 1/RC$ or $R = 1/C\Delta f$. In these terms, Equation (5.5) becomes:

$$\overline{\left(i_{JN}^2\right)} = 4e\left(\frac{kT}{e}C\right)\Delta f^2 ,$$

Equation 5.6

- Shot Noise - In solids it is possible for the density of carriers to fluctuate about the steady-state value. Such fluctuations occur in the emission of electrons by a cathode or the arrival of photons at the surface of the detector. In all cases, the mean square shot noise current associated with a current, I, is given by:

$$\overline{\left(i_{SN}^2\right)} = 2eI\Delta f ,$$

Equation 5.7

where e is the electron charge. The current, I, includes both signal and dark current.

Photons at a specific wavelength, λ, with the flux ϕ_o photons/cm^2 -sec, are converted into signal electrons with the efficiency $\eta(\lambda)$. Consequently, fluctuations in ϕ_o will be reproduced in the signal current but will correspond to the reduced arrival rate $\eta\phi_o$. The signal current used in Equation 5.6 for a detector of area A is then:

$$I = e\eta\phi_o A ,$$

Equation 5.8

Dark current in semiconductor diodes (including photocathodes) arises from either thermal generation across the gap or through impurity centers (traps) with energies located within the forbidden band. In p-n junctions, the generation-recombination process takes place primarily within the junction depletion region. The current due to bandgap generation outside the depletion region is given by:

$$I = e\left(\frac{D_n}{\tau_n}\right)^{\frac{1}{2}} \frac{n_i^2}{N_A} A ,$$

Equation 5.9

where contributions from the n-type side of the junction have been suppressed and the diode is assumed to be heavily reverse biased. D_n and τ_n are the diffusion constant and lifetime respectively of electrons in the p-type region, n_i the intrinsic carrier density, and N_A the aceptor doping density. The trap generation current is found from the expression:[16]

$$I_g = e \frac{n_i W}{\tau_e} A,$$

Equation 5.10

where W is the width of the depletion region. τ_e is the effective electron lifetime due to traps in the depletion layer and varies inversely with trap density.

It is important to note that generation-recombination current increases with the width of the depletion region and the inclusion of more trapping centers. Since the carrier densities are suppressed due to sweep-out by the field, only the generation process is significant with the trap alternately emitting electrons and holes as indicated above.

The shot noise current contributed by these processes is then given by:

$$\overline{\left(i_{SN}^2\right)} = 2e^2 A \left[\eta\Phi + \left(\frac{D_n}{\tau_n}\right)^{\frac{1}{2}} \frac{n_i^2}{N_A} + \frac{n_i W}{\tau_e}\right] \Delta f.$$

Equation 5.11

- i_f Noise - The surface of the detector material, particularly near a junction may contribute a separate noise current, one source of which is generation-recombination events due to surface states. The noise current can be represented by:

$$\overline{\left(i_f^2\right)} = \frac{BI^2 \Delta f}{f},$$

Equation 5.12

where B is an empirical constant. Suppression of this source
of noise is critically dependent on the passivation of the detector
surfaces and consequently is strongly related to the materials
technology available for a particular material.

- Avalanche Multiplication Noise – Current amplification by
  avalanche multiplication is an internal secondary "emission"
  process and as such is subject to fluctuations in the mean
  carrier gain per incident carrier, the multiplication factor
  M. This process then gives rise to an additional noise current

$$\left(\overline{i_{JN}^2}\right) = 2eIM^3 \Delta f.$$

Equation 5.13

When electron and hole ionization rates are related, $\alpha_p = k\alpha_n$,
McIntyre[18] has shown that

$$\left(\overline{i_n^2}\right) = 2eIM^3 \left[1 - (1-k)\left(\frac{M-1}{M}\right)^2\right] \Delta f,$$

Equation 5.14

for injected electron current.

A special case of the diode noise treatment is the negative af-
finity photocathode, which should exhibit no avalanche noise
since the fields are insufficient to support avalanche multiplica-
tion. It is doubtful if either thermal noise or 1/f noise would
be present in the photoemission. Consequently, the noise
current from this device will be the sum of contributions given
in Equation (5.12) from the photon flux and carrier generation
in the bulk and the surface band-bending (depletion) region.
The relative contributions to dark current and total noise cur-
rents in negative affinity photocathodes were treated by Bell,[18]
who concluded that generation currents from the band-bending

region and surface states would dominate the dark current.

As in the case of detectors in the far infrared, a figure of merit can be defined for these detectors. The ideal detector is limited in performance only by shot noise in the incoming photon signal. The signal-to-noise ratio can then be written as:

$$\frac{S}{N} = \frac{I_s^2}{2eI_s \Delta f} = \frac{\eta \Phi_0 A}{2 \Delta f} = \frac{\eta P_0 A}{2h\nu\Delta f},$$

where Equations (5.7) and (5.8) have been used and $P_0 = h\nu\Phi_0$ is the input power density with photon energy $h\nu$. The threshold power P_T is defined for $S/N = 1$ as:

$$P_T = \frac{2h\nu}{\eta A} \Delta f \text{ (watts/cm}^2\text{)} ,$$

from which the noise equivalent power (NEP) is given by:

$$NEP = \frac{P_T A}{(\Delta f)^{\frac{1}{2}}} = \frac{2h\nu}{\eta} (\Delta f)^{\frac{1}{2}} \text{ (watts/Hz}^{\frac{1}{2}}\text{)} ,$$

and the limiting detectivity D_L^* becomes

$$D_L^* = \frac{A^{\frac{1}{2}}}{NEP} = \frac{\eta}{2h\nu} \left(\frac{A}{\Delta f}\right)^{\frac{1}{2}} \text{(cm-Hz}^{\frac{1}{2}}\text{/watt)}.$$

For example, at $1eV(\approx 1.2\,\mu m)$, a detector with 100 percent quantum efficiency and an area of 1 cm^2 feeding a 1 Hz bandwidth has a $D_L^* = 3 \times 10^{18}$ cm-Hz$^{\frac{1}{2}}$/watt. Real detector efficiencies will be less than 100 percent due to reflection, absorption, and transport losses and will result in reduction in the measurable D^* even if other noise sources can be neglected. At wavelengths beyond $1.2\,\mu m$, the blackbody background becomes the limiting factor with a resultant decrease in D_L^*. Also as $\nu \to \infty$, $D_L^* \to 0$ as is apparent from the above definition.

The reader is advised that D_L^* defined here differs from that used in the infrared in that it is not independent of area and bandwidth.

Real detectors seldom have efficiencies approaching unity unless gain is present in the detector itself (photoconductors or avalanche diodes). A detector with 10 percent intrinsic efficiency (without gain) can have unity efficiency at its terminals if gain is present. However, in many applications (imaging, photon counting) such a detector has irretrievably lost 90 percent of the available information. For this type of detector, high quantum efficiency is imperative regardless of the current gain available or its location in the system.

From the discussion in 5.2.1, the material parameters limiting detector performance can easily be identified. The reflection and absorption coefficients are functions of the band structure, temperature, and, near the absorption edge, the impurity density. The reflection from the input surface can be minimized by an antireflection coating.

The parameters τ and μ in most semiconductors of practical interest are adversely affected by the defect density in the materials. The mobility is reduced by increased scattering from dislocations, grain boundaries, vacancies, and impurity centers as material quality is reduced. These same defects result in shorter carrier lifetimes by acting as recombination centers when they appear in the bulk of the material and as dark current generators when in a depletion layer.

The effect of surfaces is similar. Surface states arise in part, due to a discontinuity in the material resulting in local surface strain and accompanying defect states. Growth of a detector material onto a substrate has a similar effect if the mechanical properties (lattice parameters and thermal coefficients of expansion) do not properly match. Extra states can be added, due to interaction with the environment, by adsorption of or chemical reaction with foreign atoms.

Controlled treatment of surfaces with foreign substances (passivation) can reduce or compensate surface states. The surface can act as a sink for both minority and majority carriers and as a source of extraneous noise. In addition to pure chemical or material treatment, it is possible in junction devices to provide an encircling junction or contact that is independently biased to prevent surface leakage from reaching the output region. Similarly, if a passivation material is used, it is possible to deposit an encircling electrode on the passivator to further suppress leakage through bias control of the surface potential of the detector material at its interface with the passivator. Surface breakdown of avalanche diodes has been suppressed by diffusing an encircling junction (guard ring) contiguous with the detector junction but at a lower doping density so that surface fields are always much lower than in the bulk.

Dark current is a potentially major limitation for low-input-power levels and narrow-bandgap detectors if the output of the detector must be directly coupled to the amplifier or readout device. In this case, the operating temperature of the detector is reduced until an adequate ratio of signal to noise is obtained at the lowest input-power levels likely to be encountered, or other limitations are encountered. In depletion layer devices such as fast photodiodes or avalanche photodiodes, the dark current decreases as $kT/2$ due to the trap generation process and increases linearly with depletion layer width and the trap density. This implies that the temperature will have less effect on dark current than in the case of bulk generation, so that reduction of trap density is necessary to provide low dark currents. A simple numerical example will illustrate the magnitude of the difficulty involved. In a silicon diode at room temperature 10^{12} traps/cm^3 with energies at midgap will result in a dark current density of approximately 10 nanoamps/cm^2 for a depletion layer width of 10 μm. Lower trap densities than this strongly push the state of the art in the materials.

5.2.3 Illumination Sources

Sources of illumination can be classified simply as natural and artificial. The main natural sources are sunlight, moonlight, and airglow. The solar irradiance[19] at sea level is shown in Figure 5.3. The effect of atmospheric absorption bands is apparent when comparing the zero air mass curve with increasing thickness of atmosphere. Figure 5.4 compares a recent measurement[20] of moonlight with airglow radiance. The spectral band between 1.4 and 1.8 μm is due predominently to airglow, the differences in the figure being a result of differing level of cloud cover. The details of airglow excitation mechanisms are still not well understood and a considerable literature on the subject is developing.[21-23] It is generally agreed that the most intense infrared source is hydroxyl emission from 85-95 km altitude with supplementation from sodium at the same altitude, 5577 Å atomic oxygen emission from 100 km, and a higher altitude 6300 Å atomic oxygen emission. The aurora is a potential but highly unreliable source of radiation and is restricted to high latitudes.

Some idea of the relative integrated power levels available can be obtained from two comparisons. The first compares essentially the visible illumination levels of sunlight and moonlight. Clear sunlight at noon produces about 10^4 foot-candles at sea level compared to 10^{-2} foot-candles for full moon without overcast. The second comparison is between the power levels of clear moonlight and airglow integrated between 0.4 and 2.0 μm. Moonlight produces about 10^{-7} watts/cm^2-steradian while airglow provides about 10^{-8} watts/cm^2-steradian (the optical system has been factored out), both for diffuse reflectors aimed toward the zenith. The difference of one order of magnitude is due primarily to the visible outputs of the two sources. If the standard luminosity curve used to compare sunlight and moonlight were used here, the difference becomes a factor of 100. The large infrared content of the airglow is an important incentive for its efficient utilization in passive military systems.

P = 760 mm pressure
W = 2.0 pr. cm water vapor*
D = 300 dust particles/cm³
0.28 atmo – cm Ozone*
Q_λ (m=0) (Solar constant) = 1322 watts/m²

*Per unit of optical air mass.

Optical air mass	δ, deg
m = 1	0
m = 2	60.0
m = 3	70.5
m = 4	75.5
m = 5	78.5
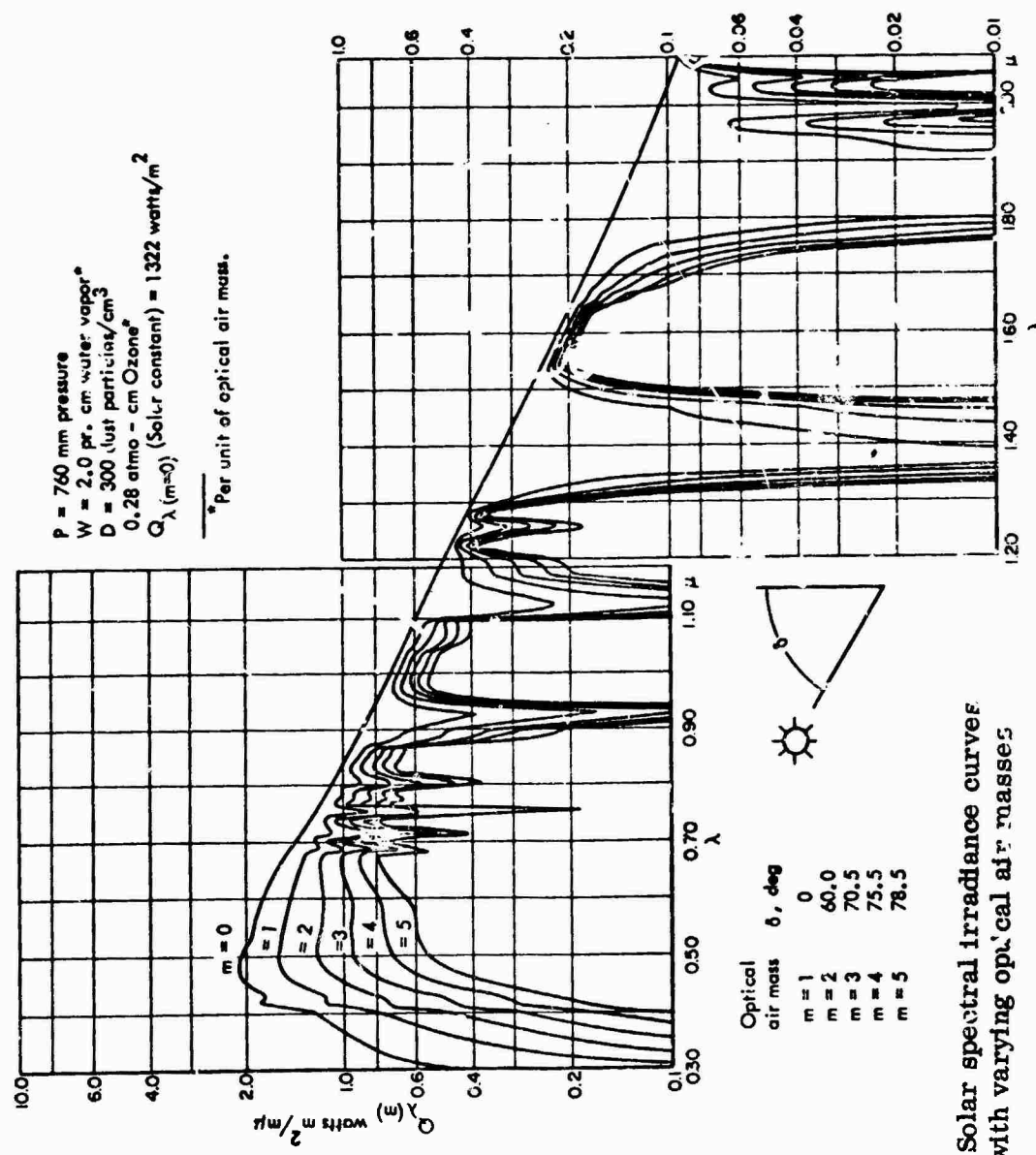
FIGURE 5.3 Solar spectral irradiance curves at sea level with varying optical air masses (19).
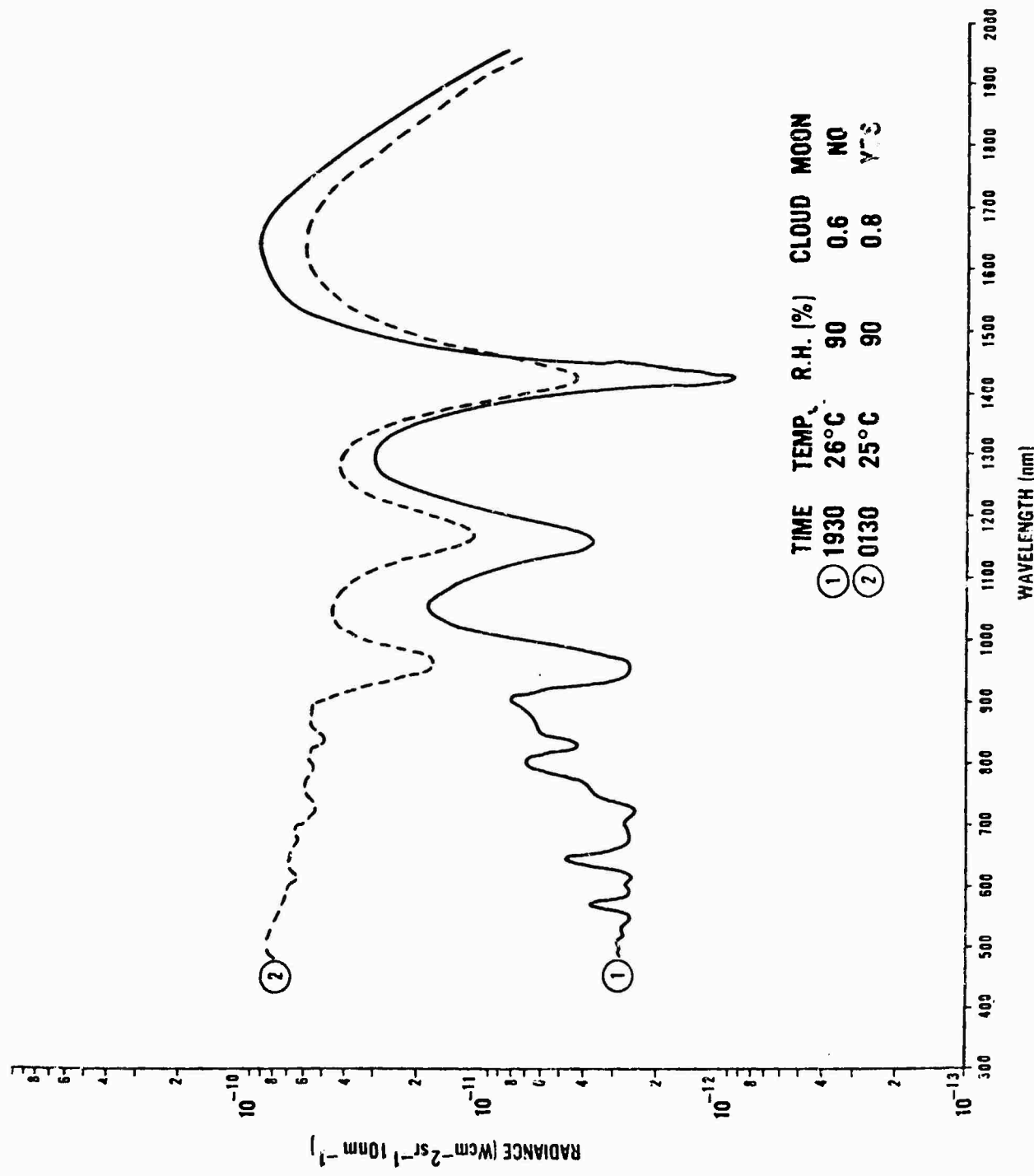
FIGURE 5.4 – Night sky spectra recorded at Rio Hato, Panama on June 14, 1968 (20)

Present sensor technology has no difficulty providing adequate detectors for sunlight. The only exception is in remote imaging (television) where small size and large dynamic range are still problematical. Under moonlight and airglow illumination, detectors are limited to wavelengths shorter than $1.1\,\mu$ m and waste a significant fraction of the available power. The low power levels particularly emphasize the critical signal-to-noise problems encountered.

Artificial illumination in military applications is available from a large variety of sources including hot engine exhaust gases, tungsten and xenon searchlights with and without infrared filters, a variety of increasingly important laser sources such as ruby, gallium aluminum-arsenide, gallium arsenide, and neodymium-doped YAG, flares, and tracers. With the exception of exhaust-gas detection, artificial sources are used to supplement natural illumination (active systems), to provide ranging data and target designation, or, potentially, to serve communication links. The quality of detector used in a specific application will depend on the size and power output of the illuminator available. In general, the trend in all cases is toward smaller illumination sources to reduce the illuminator power requirements and toward infrared output to insure covert operation, placing increasing demands on detector quality and spectral response. Searchlights, for example, are highly inefficient sources of infrared radiation and, despite wide deployment, will eventually be replaced by smaller, low-power laser illuminators such as gallium arsenide or Nd:YAG which, in addition, provide cheaply a ranging capability expensive or impractical with convention sources.

The lasers already mentioned above have narrow spectral lines with high power outputs in relatively narrow pulse widths. Typical data are given in Table 5.2 for several of the applicable lasers. The peak power corresponds to the tabulated pulse width and repetition rates.

TABLE 5.2

Laser Data in the 0.1 to 2.0 μm Range

Laser	Peak Wavelength λ_o (μm)	Peak Power P_p (Mwatts)	Pulse Width $\Delta\tau$ (nsec)	Rep. Rate R (P/sec)
Ruby	0.6943	1-1000	30	15
GaAℓAs	0.82-0.87	0.001	500	5000-10,000
GaAs	0.905	0.001	500	5000-10,000
Nd:YAG	1.063	10	30	20
Er:YAG	1.541	0.25	30	15

Radiation from both natural and artificial sources must pass through the atmosphere to and from the target. The radiation spectra in Figures 5.3 and 5.4 already contain atmospheric absorption which is responsible for the deep drops in power level. The atmospheric transmission data[24] over 5.5 km and 16.25 km path lengths are shown in Figure 5.5 but the details of the transmission bands will vary with relative humidity. Figure 5.6 shows transmission data[24] over a 300 meter path with identification of the major absorption bands.

104
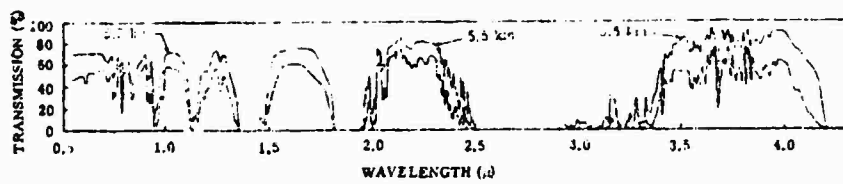
FIGURE 5.5 Atmospheric transmission at sea level over 5.5- and 16.25-km paths, 0.5 to 4.0 µ (24).
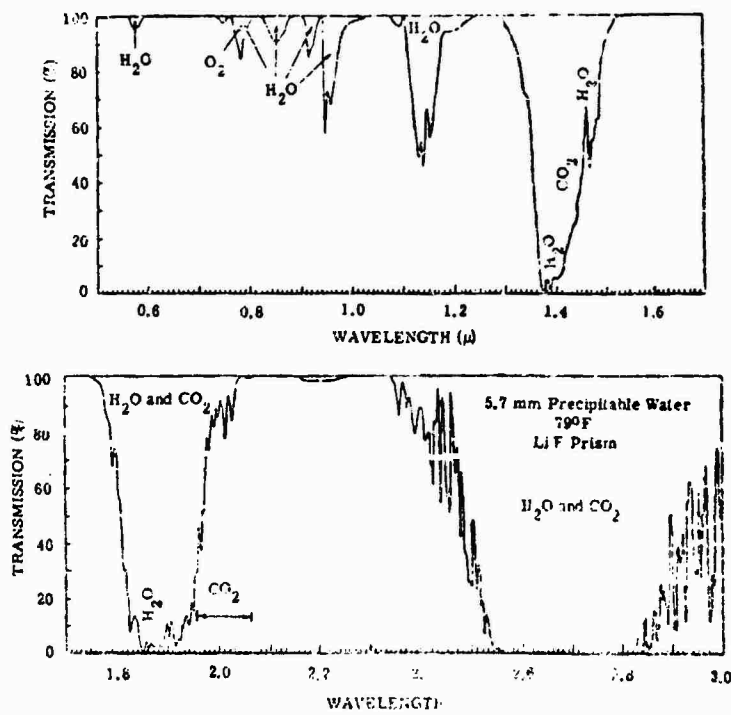
FIGURE 5.6 Atmospheric transmission at sea level over a 0.3-km path, 0.5 to 2.8 µ (24).

5.2.4 Imaging

The process of detection in semiconductor diode-like detectors, noise limitations, and the sources of radiation in the 0.1-2 μm range have been discussed. These factors are important where the gross level of input power or its change with time is sought. For an important class of detector devices the spatial distribution of radiation is needed as well. This imaging offers special problems for detector technology. The spatial intensity distribution must be reconstructed after processing by the detector and presented to the human eye-brain system, which, in turn, places special requirements on the character of the information it receives. The nature of these requirements is reviewed briefly here.

The detection and information-processing capabilities of the human eye-brain combination have been the subject of scientific and metaphysical investigation for centuries and a considerable literature has been accumulated on the subject. However, a complete understanding of the basic processes involved and the influences of physiological and psychological factors has yet to emerge. Further, the functions of pattern recognition and decision on a level-of-confidence basis are not as yet well defined in terms of information input requirements.

Imaging devices for very low input radiation require gain to produce a usable image, whether the devices are image intensifiers, television pickup tubes, or solid state, self-scanned arrays. The amount of gain required will depend upon either the brightness of the phosphor for a given current-voltage configuration of the image intensifier or the signal-to-noise ratio at the input to the video amplifier chain. These two cases require somewhat different treatment.

The image intensifier is a directly coupled device in the same sense as a DC amplifier. Aside from shot noise in the input radiation, threshold sensitivity and contrast are determined by the absolute dark current level. The detector surface (photocathode) is followed by an electron multiplier stage to provide area

current gain before final display on the output phosphor. The gain element, the phosphor, and connecting electron optics could conceivably contribute spatial and/or temporal image degradation, either as loss of modulation amplitude through distortion at high spatial frequencies or as smearing of image motion through a similar effect at high temporal frequencies. Further, the use of photon shot noise statistics in establishing image criteria has assumed that a photon to electron conversion event in the photocathode results in a corresponding output pulse at the phosphor, all such pulses having equal amplitudes. As a result, the image quality is independent of device gain so long as the mean display brightness is sufficient to give reasonable visual performance. In reality, both the gain and the phosphor conversion efficiency are statistical quantities since one input electron can produce a number of secondary electrons or photons. Consequently, the display pulses for single-photoelectron events will be distributed in amplitude as a result of convoluting the probability distributions for the gain and phosphor elements. Of these two processes, potentially the more serious is the gain distribution.

Television-type devices, on the other hand, convert the spatial image distribution into a time dependent electrical signal. If the dark current is uniform, the image degradation will result from intermediate and high-frequency electrical noise injected by the scanning mechanisms (beam shot noise in tubes or switching noise in solid state arrays), by shot noise from the dark current, and by Johnson noise in the load resistor. For camera tubes using image intensifier inputs, the corresponding limitations apply as well. Array devices will show a sharp drop in modulation transfer function[25] at and above spatial frequencies corresponding to twice the element spacing and, in addition, the noise mechanisms characteristic of single-element detectors are applicable here.

For all imaging devices, the uniformity of the material in terms of quantum efficiency, dark current, and noise generation is an additional consideration. Macroscopic non-uniformity leads to shading in the image which changes to blemishes and finally granularity as the spatial size of the variations in the relevant parameter

decreases. These characterizations are related to the degree of annoyance to the observer created by the non-uniformity and their resultant limitation may be due as much to psychological acceptance as to real performance limitations. This topic still requires considerable research but the scene being observed and conditions of observation bear heavily on the results.

5.3 Material and Device Technology

5.3.1 Bulk Material Preparation

Several stages of material treatment are involved between the raw materials and the final device. Each of these stages has an effect on the performance of the final device through the quality of the material as delivered to the next processing step down the line. A low defect density is necessary for good device performance. The term "defect" is used in its broadest sense to mean a deviation from perfect crystallinity; thus, it includes mechanical defects such as dislocations, unrelieved strain, grain boundaries, vacancies, and interstitials as well as the substitution of foreign elements for those of which the crystal is composed. Of course, a certain degree of imperfection cannot be removed (i.e., that due to the termination of the crystal lattice at the surface and that due to the introduction of controlled amounts of specific elements (doping) necessary for the performance of the device). Clearly, a worthwhile goal in all phases of materials processing is to reduce the incidental incorporation of impurities to the minimum. These stages of processing are discussed here.

The starting point for all device material is the collection of basic elements from which the final material is to be fabricated. These materials are available increasingly in purities on the order of parts per million and in some cases parts per billion total impurity concentration. Details of extraction, purification, and availability of the raw material are beyond the scope of this report and have not been identified as a major consideration for the device materials considered in this chapter.

A variety of techniques[26] have been developed for the growth of single crystals of many different materials. It is possible to classify these techniques into three major groupings:

- Growth from the melt
- Growth from the solution
- Growth from vapor phase

Each of these techniques presents a special situation for a given material or final device configuration and a single technique or combination of techniques is selected accordingly. In some cases, purification of the material may be possible particularly if a solid-liquid interface is involved. This would be due to higher solubility for a given impurity in the liquid than in the solid, a property characterized by the distribution or segregation coefficient[27,28] i.e., the ratio of solid to liquid concentration of impurity in equilibrium. This process can be used for doping as well if the solubility of the dopant in the solid is sufficiently large.

5.3.1.1 Growth from the Melt

Growth from the melt can take the form[26] of zone refining, normal freezing (Bridgman method), or crystal pulling (Czochralski method). In all three doping can be performed by dissolving the dopant in a predetermined quantity in the melt. This may have some disadvantage in terms of the uniformity of impurity concentration along the crystal due to both segregation and depletion of the dopant from the melt. Provision can be made in the normal freezing and crystal pulling techniques for supplemental addition of dopant to reduce this variatiion. In attempting to grow ternary alloys by any of these techniques, elementary atomic ratios and/or composition may vary along the length of the crystal through variations in melt concentration of one or more of the components. Again, provision may be made to offset this if large, uniform single crystals are desirable. However, trying to control doping, composition, and atomic ratios may be unnecessarily complicated so that a test procedure must be devised to select the desirable portions of the crystal. If large volumes of material with given characteristics are necessary, the cost of this procedure must be compared to the cost of a more complicated growth apparatus,

depending on the tolerance of the specifications on the material and the actual variations obtained. The possibility of performing supplemental doping during the growth process adds an additional flexibility in that by abruptly changing the dopant, it is possible to grow relatively abrupt junctions by these techniques. The abruptness of the junction is then limited by the rate of diffusion at the growth temperature of the new dopant into the region of the growth crystal adjacent to the growth interface. Out–diffusion of the original dopant from this region is not a factor since its concentration in the melt has not changed.

All three of these techniques may incorporate a gaseous ambient in the process to react with and/or remove possible contaminants or to provide an over-pressure if one of the crystal constituents has a large vapor pressure at the growth temperature. In any event, it is necessary to maintain high purity in the ambient gas to ensure low contamination from this source.

5.3.1.2 Growth from Solution

The solvent is usually a low-melting-point material which can be one of the constituents of the crystal. For example, gallium arsenide is frequently grown from a saturated solution of arsenic in molten gallium. This technique has some advantages over growth from a pure melt. For some materials, the vapor pressure of one or more constituents at the growth temperature for the stoichiometric melt composition may be prohibitively high or the resulting gas phase highly reactive with the growth apparatus. Growth from solution also may take place at temperatures appreciably below the melting point of the solute material if a suitable solvent can be found. Consequently, the problem of devising a high-pressure vessel for material growth can be avoided and the choice of crucible material made easier by this growth technique.

Solution growth of semiconductors, especially in the form of liquid phase epitaxy, has been used increasingly in recent years. It has been found particularly useful in growing III-V semiconductors, binary compounds and ternary alloys for

laser crystals, Gunn diodes, and photocathodes. In some cases, doping conditions not otherwise possible can be achieved. For example, certain laser diodes made from gallium arsenide use silicon, an amphoteric dopant, as both the p-type and n-type dopant, depending upon whether it occupies an arsenic or gallium site, respectively. Growth from the melt requires sufficiently high over-pressures of arsenic that silicon tends to be incorporated on gallium sites, producing an n-type material. In the liquid-phase growth of silicon-doped gallium arsenide, however, the significant excess of available gallium allows silicon to be incorporated onto arsenic sites to produce a p-type material.

The materials are normally heated by heater coils wrapped around the enclosing tube, which may be a closed or an open tube system. The solution is usually placed at one end, a short distance away from the substrate, and the whole structure including the furnace tipped to initiate growth by immersing the substrate in the molten solvent. To terminate growth, the system is simply tipped back to its original position.

The growth rate of the crystal from the seed is now limited not only by the dissipation of the heat of fusion from the interface but also by the diffusion of solute through the solvent to the growth interface as the solvent nearby becomes depleted. Several techniques have been devised to stir the solution and increase the growth rate but without marked success. The problem is further compounded by the necessary reduction in temperature of the melt to maintain the growth by driving the saturation concentration of the solute down as growth progresses. This has the effect of reducing convective stirring of the melt and enhancing the diffusion limit on the growth.

Thus far, the technique of homoepitaxial growth from the liquid phase has been discussed. It is possible to substitute as a seed crystal a material different from the material to be grown, a process known as heteroepitaxy. The conditions discussed above still apply, but nucleation and growth conditions may

be somewhat different on a foreign material. The added flexibility introduced makes possible the growth of materials for close confinement lasers and for high-sensitivity, semi-transparent photocathodes which require different optical properties in the substrate and film. Mutiple consecutive growths are possible by moving successive melts, confined in individual wells in a graphite block, across the substrate. If the solvent does not wet well to the growing layer, melt surface tension and the edge of the well will result in a clean surface, an important factor in maintaining purity and uniformity in successive growths. This technique is useful for low-contamination growth of diodes or transistors, growth of different materials or compositions for specific devices, or compositional grading from substrate to final film when good matching of mechanical properties, such as thermal coefficient of expansion or lattice parameter, is required.

Liquid-phase epitaxy has some inherent disadvantages which at this time appear more technological than fundamental. Films of about 1 to 2 μm, like those required for semi-transparent photocathodes, are difficult to grow uniformly by this technique. The dissolution and regrowth at the interface is uncontrolled for the most part and the final film thickness is unpredictable based on growth time alone. In addition, for sharp cut-off of layer growth at a specific thickness, it is necessary to remove the material from the melt and etch or scrape off the solvent that remains on the surface. In many cases this process leads to damage to the layer.* Finally, if improper nucleation occurs, or if contamination exists on the substrate to start with, it is possible that solvent islands will be included in the growing layer, resulting in gross non-uniformities and defects. Proper substrate cleaning to ensure uniform dissolution and regrowth become critical, particularly if protective oxides can form as is true with aluminum compounds and alloys.

---

*   Ideally, the solvent should wet the grown layer poorly across the surface so that removal from the melt is sufficient to guarantee the absence of solvent. Actually, defects and ingrown contamination will act as wetting agents, necessitating mechanical solvent removal.

5.3.1.3 Growth from the Vapor

Growth of detector materials from the vapor phase is used for metals, semiconductors, and insulators whether or not single-crystalline films are required. The material constituents are transported to the substrate in the vapor phase. Reaction between the components of the gas may take place in transit or at the substrate surface, or the final material may be simply transported intact from the source material and deposited out at the substrate. A carrier gas may be chemically neutral or react with the constituents and/or the substrate or growing film either deliberately or incidentally.

Vapor-phase growth can take place in closed tubes, a technique frequently used for II-VI compounds where both constituents have relatively high vapor pressures. A second more widely used approach to vapor-phase epitaxy, is open tube growth. The constituents of the deposit are passed over the substrate in vapor form with a carrier gas such as nitrogen, argon, or hydrogen; they react either on the substrate surface or in the vapor phase over the substrate; the undeposited residue is carried out the other end of the tube. Raw materials such as silicon, germanium, arsenic, phosphorus, sulfur, and selenium are generally introduced in vapor form as hydrides $(SiH_4, GeH_4, AsH_3, PH_3, H_2S, H_2Se)$ or chlorides $(SiCl_4, GeCl_4, AsCl_3, PCl_3)$. High-vapor-pressure metals such as zinc and cadmium may be simply heated or reacted with HCl gas to form the chlorides $ZnCl_2$ and $CdCl_2$, while the low-vapor-pressure metals, gallium and indium, must be reacted with HCl in such a way as to form the volatile monochlorides GaCl and InCl. Some materials are introduced as volatile, organic and organometallic compounds. A common example is the use of tetra-ethylorthosilicate (TEOS) to form SiO_2 from the vapor phase. For gallium, gallium trimethyl may be used. In these cases, the raw material is either a solid over which the carrier gas is passed while the solid is heated or a heated liquid through which the carrier gas is bubbled.

The open tube system where reaction takes place is commonly called a reactor. It is clear from the above discussion that considerable flexibility in the growth of different materials and/or doping compositions is possible with this technique. By appropriate design with sufficient inputs, complex lamellar structures can be fabricated without breaking seals. Control of flow rates, dilution, source and growth temperature, and the temperature gradient across the substrate leads to a high degree of reproducibility.

The nucleation properties of substrates during vapor phase growth are significantly different from those of liquid phase. No melting and regrowth occur at the substrate-grown interface so that substrate preparation is more critical than in the case of liquid-phase growth.

There are, of course, depositions and dopings that are extremely difficult or impossible with vapor-phase growth due to the thermodynamics of the growth processes. The example of silicon in gallium arsenide given in the discussion of liquid-phase growth is a good illustration.

Another example is the growth of alloys such as gallium indium arsenide. The formation rate of gallium monochloride is higher than that of indium monochloride so that transport of indium to the growth zone is inhibited. In addition, the growth rate of the indium compounds is slower at a given substrate temperature so that even with correct arrival rates (the metal sources can be kept at different temperatures to assure sufficient metal in the vapor) the composition of indium-rich alloys becomes more difficult to control closely as the indium content increases. This problem becomes increasingly difficult above an indium fraction of 20 percent. The same problem exists to a greater or lesser extent with all alloy systems, and growth conditions must be established accordingly, in many cases on a purely empirical basis.

5.3.1.4 Vacuum Evaporation

The commonest technique for the deposition of metal films is vacuum evaporation. Basically, the pure metal is heated in vacuum either indirectly by a coil wrapped around a crucible containing the metal charge or directly by means of an electron beam. The temperature of the charge is raised until the vapor pressure is sufficient for a reasonable rate of evaporation. Techniques have been devised to accurately monitor the rate of film deposition, the total film thickness, and the evaporation rate from the boat. The substrate can be heated, cooled, or kept at room temperature depending upon the desired film properties. In addition, masks can be used to produce accurate patterns of the deposit on the substrate.

Both insulators and semiconductors can be deposited by vacuum evaporation but decomposition of compounds is generally a problem. High-quality II-VI compounds have been prepared in thin film form by this method. In some cases, elaborate techniques have been developed to circumvent decomposition. The use of separate evaporation sources for the constituents of a compound semiconductor has been attempted for gallium arsenide, for example, including a separate source for the dopant. While the films are single crystalline and have a good appearance, photocathodes made from this material perform poorly in comparison with vapor- and liquid-phase gallium arsenide. Maintaining the required doping levels and reduction of structural defects appear to be the worst problems.

Except in the few cases noted above, vacuum evaporation has not proven successful in providing material of the quality necessary for high-performance detectors. The three techniques of growth from the melt, liquid-phase epitaxy, and vapor-phase epitaxy generally produce superior material, even in the cases where vacuum evaporation has been somewhat successful. The chief use of vacuum evaporation in the detector field is for deposition of contacts.

5.3.1.5 Sputtering

Reactive and cathodic sputtering have been used in the preparation of detector materials. Reactive sputtering takes place in an evacuated chamber that has been backfilled with one of the constituents in gaseous form. High voltage, either DC or at radio frequencies, is applied between two electrodes, one of which is the second constituent if the final material is a binary compound while the other is the substrate (the positive (for DC) terminal). A glow discharge is formed in the gas and the resultant ions bombard the cathode containing the evaporant, ejecting material on impact. Some reaction takes place at the cathode and on the way through the plasma to the substrate but most of the compound formation occurs on the substrate surface. Substrate heating can be used to enhance the growth of crystalline material. Cathodic sputtering is similar but uses a nonreactive gas, usually an inert gas like argon, and the cathode consists of the compound to be sputtered.

If the geometry of the chamber, power levels, and pressure are correct, sputtering from only the cathode will take place, even if RF is used. In order to clean the substrate surface, sputtering of the substrate may be performed, if the conditions are properly adjusted prior to film deposition.

In all sputtering operations it is important to carefully anneal the substrate after deposition to remove damage caused by the sputtering. The energy involved should be sufficiently low so that no significant implantation of the sputtered material into the substrate or grown layer occurs. The presence of the sputtering ambient gas in the film tends to degrade film quality unless the gas is one of the constituents. Sputtering holds some promise for making passivating insulator layers, but semiconductors deposited by these techniques have been inferior to those deposited by either liquid- or vapor-phase epitaxy.

5.3.2 Device Technology

The preceding section emphasized the preparation techniques used for detector materials. Several material-related topics important to detector performance must be discussed. The choice of substrate, particularly for compound semiconductors, determines in many respects the quality of the detector material. For many applications, junctions are required in the material and some discussion of their preparation is necessary. Both ohmic and rectifying contacts are necessary to apply bias and draw current from the device. Finally, much concern regarding passivation has been expressed; some of the problems associated with it need discussion.

5.3.2.1 Substrates

Germanium and silicon devices are generally made on or in the basic material. If thin layers are required for transmission-type devices, these materials can be easily thinned by either chemical or electrochemical means. Most work on II-VI compounds in the past has used either thick crystals or an evaporated thin film on a glass or quartz substrate. The evolving technology of III-V semiconductors, particularly the thin-film detectors such as photocathodes, has focused an increasing amount of attention on the interaction between a substrate and the film deposited thereon.

The best choice of substrate for any given semiconductor is obviously the material itself, as in the case of silicon and germanium. Thus, gallium arsenide would be the logical choice for a thin film of gallium arsenide and similarly gallium indium arsenide for gallium indium arsenide thin films. The substrate should be of sufficient size and thickness so that handling problems throughout the processing are minimized. Identical substrates clearly match the thermal expansion coefficient and lattice parameter of the thin film throughout the range of temperatures likely to be encountered.

Practical considerations are likely to require another substrate choice for a given device application. For example, semi-transparent photocathodes require a substrate optically transparent over some acceptable spectral band. The long wavelength limit of the band is set by the photoemissive threshold of the photocathode, which for NEA photocathodes corresponds to the bandgap of the active layer. If a semiconductor is used as the substrate (this appears to be technologically preferable at this time), the bandgap should be larger than that of the active layer in order to supply a usable sensitivity range. If this requirement is added to the conditions imposed by mechanical property matching, the available substrate choices are diminished. A further restriction is frequently imposed by the growth conditions such as temperature, nucleation, growth rate, and interdiffusion.

Another practical restriction on substrate choice is frequently the availability of wafers of sufficient size or indeed the availability of the material in wafer form at all. An example of this was encountered in the earlier stages of the development of the semi-transparent gallium arsenide photocathode. Gallium phosphide was selected as an obvious first choice for the substrate. Due to the unavailability of wafers of good optical and mechanical properties and particularly of a reasonable size, it was necessary to develop a technique for growing thick gallium phosphide layers onto gallium arsenide and then selectively etching away the gallium arsenide to provide a gallium phosphide substrate for the regrowth of a gallium arsenide active layer. This roundabout means of providing high-quality substrate wafers would be expensive for production devices; fortunately, high-quality substrate material is now becoming available.* The problem of providing a suitable substrate becomes more acute for the ternary alloys. In the case of gallium arsenide, substrates with better mechanical matching to the active layer would be preferred to those available but are unobtainable in a practical form. For both gallium arsenide and gallium phosphide,

---

* From Asarco Intermetallics Corporation and Atomergic Chemetals Company.

experience to date has shown that both the optical and mechanical properties of the substrate material depend strongly on the method of preparation. Boat-grown gallium arsenide, for example, is far better than pulled material as a substrate because of low dislocation density and low contamination level. The large investment required for the selection, development, and construction of production facilities for substrate-quality material has, to a large extent, inhibited the growth of this industrial capability, since such action must be based on the scanty information available on the growth of large crystals of III-V material. Desirable ternary alloys are not available in acceptable quality for use as substrates due to the greater complexity of the growth process. More fundamental investigation of the technology for the growth of a variety of single-crystal III-V materials in a form suitable for substrate use is crucial to the widespread application of these materials.

Logically, if III-V material could be grown in a high-quality, large crystalline size, the necessity of providing a compatible substrate (and possibly a complex one) would be obviated by applying the thinning approaches used for silicon and germanium. There are indications that this process can be used down to thickness of about 3-5 μm but the mechanical stability and etch uniformity of the III-V compounds do not appear to be as good as those of silicon and germanium. It is not clear at this point if the poor mechanical stability is an intrinsic property of the materials or a result of large internal stresses from the growth. This problem requires investigation, since, in principle, production costs for devices using III-V photocathodes could be lowered. In addition, a controlled etching technology must be developed for the III-V compounds that will allow the sort of layer uniformity available in silicon. An immediate application is in the area of transmission secondary electron multiplication (TSEM) dynodes where large dark currents and difficult activation for silicon dynodes make gallium arsenide extremely attractive if this type of technology can be developed. In this case, a substrate cannot be used, since the incoming primary electrons could not penetrate the substrate at the energy levels required in practical image tube designs (5-10 keV).

The thickness necessary for the thinned, self-supporting layer, whether used as a TSEM dynode or as photocathode, is determined by material properties such as diffusion length and surface recombination velocity on the input side as discussed in 5.2. Thus, improvements in these two parameters would allow the use of thicker films and relax the requirements on etched thickness and uniformity.

Finally, research on the mechanical and chemical properties of substrates prior to film growth should be part of any program to develop or improve the growth of thin detector films. The uniformity of the surface, presence of contamination such as oxides, and the dislocation density of the substrate material itself have a strong effect on the nucleation, growth, and hence final electronic properties and uniformity of the detector material. In addition, mobile contaminants on or in the substrate could be incorporated into the detector material and degrade performance. Chemical compatibility between the active layer and the substrate is an important consideration when chemical processing of either the substrate or the active layer is required subsequent to layer growth. For this purpose differential etching solutions must be developed specific to a given material. In general, the dynamics of chemical etching for III-V materials is inadequately understood for both this application and/or for the grosser thinning applications discussed above.

5.3.2.2 Junctions

For many device applications in this spectral range, it is necessary to be able to form p-n and p-i-n junctions in the detector material. The techniques applied most frequently to this process are direct growth, diffusion, and, more recently, ion implantation.

The direct growth of a junction in a material takes place either during the pulling of the crystal from the melt or by deposition of an epitaxial layer of opposite conductivity type from the substrate. The problems encountered in this process are similar to those found in the epitaxial growth of the basic material. Since this is usually a homoepitaxial growth, the substrate problem is not involved except that cleanliness and mechanical defects in the base material must be considered.

In some cases, the ideal junction may require an extremely thin overgrowth to avoid large dead-layer effects (e.g., growth of the p+ region at the top of a p^+-i-n^+ diode with an n^+ substrate). Vapor-phase epitaxy can generally produce mechanically and electronically uniform layers no thinner than 0.3 to 0.5 μm, while for liquid-phase epitaxy, this value becomes 0.8 to 1.0 μm. In addition, the growth temperature for a given material should be optimized to yield good material properties while suppressing interdiffusion of dopants. This process has presented no new problems for silicon, germanium, or gallium arsenide but, like the epitaxial growth of the base material itself, has not been extensively studied for other III-V binary compounds or ternary alloys.

The diffusion method[29] for forming junctions is very flexible in terms of allowed configurations and is very widely used. A diffusion barrier or mask, usually silicon dioxide, silicon nitride, or aluminum oxide, is first deposited onto the wafer of detector material and the desired pattern etched into the oxide by photolithography. In the actual diffusion, a vapor stream, evaporated film, or suitably doped glass may be used as the dopant source. When the diffusion parameters for a given dopant and host are known, the temperature and time then determine the depth of diffusion and the mean impurity concentration in the diffused region (taking the background doping into account). These parameters are the segregation or distribution coefficient, the diffusion coefficient, and the solid solubility limit. In addition diffusion depends on orientation, and this dependency must be known for a given material. The shape of the diffusion front is affected by dislocations and grain boundaries since diffusion rates increase along defects of this type. Strain may be induced in heating the material up to diffusion temperature or in cooling it down, thereby increasing the dislocation density. Further, for doping levels near the solid solubility limit, cooling may cause redistribution of the dopant at lower temperatures, where the normal solid solubility would be exceeded.

Diffusion coefficients for silicon and germanium are available for most of the normal dopants.[29-31] Similar data are available for gallium arsenide,[30-32] and to a lesser degree for gallium antimonide,[30] gallium phosphide,[30] and indium phosphide.[30] Segregation coefficients and solid solubilities can be found for silicon[29-31] and germanium[29] but have not been thoroughly studied in the III-V compounds. No work has yet been published on the ternary alloys.

The choices for diffusion masks are limited to the three insulators indicated above. Of these, silicon dioxide is used extensively in thermally grown form on silicon; silicon nitride, either vapor-phase grown or reactively sputtered, has been applied recently to some extent. For germanium, vapor-phase grown silicon dioxide has been used almost exclusively except for aluminum diffusion where reaction between the oxide and the aluminum takes place. In this case, aluminum oxide has occasionally been used. The lack of a general purpose diffusion mask has inhibited to some extent germanium planar technology; therefore, mesa devices are more popular. Both silicon dioxide and silicon nitride require temperatures of about 800° C to form high-quality layers. Although the materials can be formed at lower temperatures, the non-stoichiometric ratio of the resultant films leads to degraded performance. For gallium arsenide, reactively sputtered silicon nitride and vapor-grown aluminum oxide have been investigated but extensive work has not been done. Reaction temperatures of about 450° C seem to give good results. Silicon nitride and silicon dioxide react at temperatures well above the decomposition temperature of gallium arsenide. Work on other III-V compounds and ternary alloys for this spectral range, has not been reported.

Ion implantation as a technique for forming junctions is, to a great extent, in a developmental state. Extensive studies have been made on silicon devices.[33-34] In addition, some data[34] have been reported for germanium, silicon carbide, gallium arsenide, cadmium telluride, indium antimonide, cadmium sulfide, and silicon dioxide. The semiconductor is bombarded with high energy (30-250 keV) ions of dopant which either sputter material from the semiconductor surface or become

imbedded in the material. The implanted ions are stopped at a mean depth known as the penetration range, which is a function of the ion energy and the atomic numbers and masses of the ion and semiconductor. The semiconductor subsequently must be annealed to remove residual damage from the implantation region. Stable dislocation loops that form in spite of the annealing degrade device performance. The principal advantage of this technique for single-element detectors would be the capability of reducing the thickness of the degenerate dead layer to a few hundredths of a μm in thickness thereby improving the device efficiency. The potential of this technique for arrays is enhanced by the possibility of masking using a metal-oxide combination. The further development of high-resolution photoresist and electroresist techniques coupled with the small lateral spread and thickness of the implanted layer imply that very high-resolution arrays may be fabricable. This may have a particular application in diode array vidicons. Further work in this area is definitely needed, particularly on the III-V and II-VI compound systems.

Deviation from the stoichiometric atomic ratio of a compound can be used to produce junctions. Excess cadmium in cadmium telluride, for example, would result in tellurium vacancies or cadmium interstitials in the lattice, resulting in an n-type conductivity. Excess tellurium produces the opposite conductivity type. This deviation can be caused by heating the crystal appropriately in an over-pressure of one of the elements. Since the diffusion constants of the elemental constituents are usually well known, the junction depth as well as the doping density can be controlled. This technique is used extensively with those II-VI compounds that can assume either conductivity type.

5.3.2.3 Contacts

The formation of contacts to a detector material is a critical part of the device fabrication process. The category logically includes Schottky rectifying contacts and ohmic contacts. (Schottky contacts are discussed in 5.4.3.)

The ohmic contact, as the name implies, is ideally a pure resistance which forms part of the series resistance of a device. Ideally, the contact resistance is negligible in comparison with bulk resistance in the semiconductor. Since the contact is expected to carry current, a high degree of mechanical and thermal stability is usually necessary. The careful choice of contact material and the process used to apply the contact may not be neglected in material and device development program.

Several techniques have been developed for forming an ohmic contact, each of which has properties and advantages peculiar to itself, and the materials involved. The techniques most frequently used are diffusion alloying, wire bonding, and soldering, vacuum evaporation, plating, vapor-phase deposition, and sputtering.

Diffusion as a contact technique does not differ significantly from its use to form junctions. For contacts, the diffusant is the same as that of the base material but the concentration is made sufficiently high that the material loses its semiconductor character in the contact area. In addition, the surface concentration of impurity should remain sufficiently high to provide metallic behavior. Almost any means of applying a wire or lead-in pad to this region then results in a low-resistance contact, provided adequate care is used in post-diffusion cleaning steps. Like junction diffusion, controlled diffusion of contacts is limited by:

- Knowledge of the appropriate diffusion constants and solubility limits for a given material

- Insufficient solubility limits of appropriate dopants to provide a low resistance contact

- The undesirable necessity of performing an additional processing step which requires high temperatures

While the time involved can be relatively short, there is an opportunity for doping diffusion profiles to be disturbed, for introduction of strain and increased dislocation densities and for the introduction of higher levels of contamination, all three undesirable effects.

Alloy contacts involve the formation of a eutectic alloy between the contact material and the semiconductor. This technique is advantageous if the eutectic temperature is well below the diffusion or growth temperature used in fabrication of the device and if the resulting alloy has good mechanical properties. If pressure is used on the alloy, the temperature for achieving the eutectic may be somewhat reduced and a better contact area obtained. Upon cooling, the new alloy recrystallizes in a graded form, depending upon the solid solubilities of the materials. The eutectic temperature of a combination of the contact material and semiconductor must be known as well as the relative solid solubilities. The joint mechanical strength is related to the mechanical properties of the alloy interfaces, properties such as thermal expansion coefficient and lattice parameter. In some cases, large disparities in these properties cannot be accommodated across the interface and the contact peels off on cooling. A high degree of cleanliness, especially in terms of residual oxide, is required to assure good contact formation. Also, if dislocations are present at the interface, dissolution, diffusion, and regrowth will occur more rapidly along the defects leading to internal dendrite growth which may affect device performance, particularly for planar devices.

Wire bonding and soldering differ from alloying in that the contact wire or solder merely wets the semiconductor surface; alloy formation is not required. Wires are usually bonded by thermocompression, or by ultrasonic soldering, a form of thermocompression bonding accompanied by high frequency abrasion. The latter process may well be used when skin oxides are present on either the metal wire or the semiconductor. The correct wire must be chosen to wet a given semiconductor. The temperatures involved are generally well below both alloy and diffusion temperatures, a distinct advantage. Finally, the mechanical strength of the bond depends upon the degree to which wetting has occurred and upon the mechanical strength of the semiconductor under the contact area. Stress and damage introduced by the bond may result in poor mechanical strength. Similar arguments apply to soldering. When a flux is used to remove contamination, it should be either removable afterward or be chemically and thermally stable enough not to affect device performance later.

Deposition of metal contacts by vacuum evaporation (see 5.3.1.4) is frequently used for planar detector devices, particularly in arrays. The basic technique has already been described above. Contact areas may be defined by the use of masks but photolithography is much simpler and has inherently higher resolution. Aluminum, gold, gold-antimony and gold-indium alloys, indium, nickel-tin alloys, and molybdenum are the contact materials used most. Deposition of the metal onto the cleaned semiconductor in some cases is followed by an alloying step. Alternatively, a diffusion yielding degenerate (conducting) material is followed by deposition of the metal contact. Without either of these steps, deposition of the metal onto an n-type semiconductor usually gives a rectifying contact, particularly if the resistivity is high. The alloy or diffusion step thus provides an acceptable interface between the contact metal and semiconductor.

Plating has been used in some instances to provide ohmic contacts. The metal is present as an ion in a suitable electrolyte and is deposited onto the semiconductor upon application of a voltage. In some cases, a small amount of heating is required to "set" the contact. Nickel and copper contacts may be deposited in this way, particularly for large area contacts. The plating voltage, electrolyte pH and composition, and solution temperature are optimized for each semiconductor. Due to the possibility of contamination from the solution, this technique is not generally used for high-quality detector devices.

Vapor-phase deposition of metal contacts has been discussed above (see 5.3.1.3). Molybdenum, tungsten, and polycrystalline silicon are deposited by this technique when multilevel metallization (with insulator isolation of each layer) is to be utilized. Deposition is preceded by a diffusion step to supply the actual contact area. Photolithography is used to provide lead and contact definition. Organometallic, metal chloride, and metal hydride source materials supply the metal. While purity in the source materials is not critical for the metallization itself, contamination of the semiconductor may result from poor-quality metal sources.

This is a problem with the organo-metallic compounds for which the reaction temperatures are generally lower and for which a hydrogen or a forming gas (hydrogen-nitrogen mixture) reducing atmosphere can be used to retard surface oxide formation. Silicon contacts and leads have some advantage in multilayer steps since the isolating silicon dioxide can be grown directly rather than deposited. The series resistance of the leads may be higher than desirable unless doping and crystallite size are properly controlled. Again, cleanliness in the semiconductor area where contact is to be made is important. In addition, the range of temperature tolerated by the semiconductor must be considered in choosing this technique. Other metals such as aluminum and gold may be deposited by this method but vacuum evaporation is quicker and cheaper in these cases.

Radio frequency sputtering has not received a great deal of attention as yet for the deposition of contacts. Due to the penetrating power of the sputtered material, thin surface oxides and contamination may be unimportant. The wide variety of metals that can be sputtered allows a considerable selection of contact materials. If necessary, annealing at 400° C to 500°C is usually sufficient to remove residual damage to the semiconductor although imbedded argon or nitrogen from the sputtering environment may remain trapped. Aside from the obvious need to establish sputtering rates and annealing temperature, several questions must be answered before this technique can be more generally applied, particularly for planar devices. Sputter-deposition of metal layers on a passivating or masking oxide requires photolithographic steps to define the lead pattern. The fact that the metal penetrates the oxide to some extent means that the etching properties of the metal change as the interface between the two material is approached. In addition, the strain produced by the implantation may ex well into the insulator and change its passivating properties. High-purity metals can be used for the contact source materials; very pure gases can be used for the sputtering environment; thereby, contamination may be reduced to a very low level.

A systematic investigation of techniques and materials for forming ohmic contacts on a wide variety of semiconductors using any or all of the techniques described above has seldom been performed except in relation to specific device configurations as needed. As a result, the information on contacts is scattered, highly specialized, or proprietary. It would be extremely helpful in the development of devices using new materials or configurations to have the results of such an investigation at hand to remove some of the guesswork now involved. It could lead to important savings in making process choices.

5.4 Detector and Materials Status

5.4.1 Photocathodes

The photocathode is the detector material at the input side of photomultipliers and image intensifiers which converts photons to electrons and emits the electrons into vacuum (photoelectric emission or, commonly, photoemission). A large variety of spectral responses are available in photomultipliers,[36] but four have found the widest use due either to their efficiency or to the portion of the spectrum to which they are sensitive. Pertinent data on these are given in Table 5.3 and spectral response curves are plotted in Figure 5.7. Detailed spectral response at short wave lengths depends upon the window material. All four photocathode types have been in use for five years or more and in some cases the performance has improved as manufacturing technology was refined. A brief discussion of each follows (for more complete information see reference 37).

A new photocathode based on the NEA effect has recently appeared on the market in photomultiplier tubes and is also described in Table 5.3 and Figure 5.7. Since the NEA photocathode promises significant improvement in both absolute sensitivity and infrared response, a more detailed discussion is given of this photocathode. Image intensifiers for military applications generally use the multialkali photocathode with extended red response, although image converters with S-1 response have found application in connection with Nd:YAG lasers (1.06 μ m).

128

5.4.1.1 Ag-O-Cs(S-1)

The S-1 photocathode dates back 40 years and is the earliest semitrans-
parent photocathode to find commercial application. Since its application, few sig-
nificant improvements have been made in photocathode performance or understanding.
The S-1, in the current view, consists of nearly isolated islands of silver encapsula-
ted by a thin covering of cesium oxide. Characteristically of all four conventional
photocathodes, the material is processed in situ. Reproducibility depends upon the
development of a successful "recipe." * Generally, a layer of silver is deposited
onto the faceplate and oxidized by a glow discharge in oxygen. Cesium is then ap-
plied carefully to peak the sensitivity. The short wavelength peak (see Figure 5.7)
is believed due to photoexcitation of and emission from the cesium oxide while the
broad, longer wavelength peak results from photoemission of electrons generated
in the silver over the Ag-Cs_2O barrier; transport through the Cs_2O has negligible
attenuation. Attempts to substitute other metals for silver have been unrewarding,
as have attempts at metal combinations or use of elements other than cesium for
activation. Further, the island formation is critical to the sensitivity and island
size has been found to be important as well. In terms of structure and materials,
the S-1, as presently constituted, appears to be the optimum for this type of photo-
cathode.

The data presented in Table 5.3 and Figure 5.7 for the S-1 represent typi-
cal commercial data. Lumen sensitivity as high as 90 μa/lm can be obtained and
the response at 1.06 μm has reached 0.1 percent. The dark current ranges from
100 picoamperes/cm^2 to 100 femtoamperes/cm^2. The actual spectral responses and
dark currents of a random sample of S-1 photocathodes will vary due to unavoidable,
slight differences in processing. Attempts to improve device reproducibility have
been largely unsuccessful and the S-1 remains the oldest (and still poorly under-
stood) photocathode in active use with no real prospect of improvement. It is the
only commercial photocathode with substantial sensitivity beyond 0.9 μm and con-
sequently has proved valuable for neodymium laser systems using both photomulti-
pliers and image intensifiers. The low sensitivity and high dark current are serious

* "recipe" is used in this chapter to mean an empirical process.

TABLE 5.3

State-of-the-Art Photocathodes

Type	Designation*	Spectral Range (μm)■	Lumen Sensitivity (μa/lm)	Peak Response (ma/w) @ λ max (μm)	Dark Current, x10^{-15} a/cm$_2$
Ag–O–Cs	S–1 (ST)	0.3 – 1.1	30	2.8 @ 0.80	900
Cs–Te	Solar Blind (ST)	0.1 – 0.3	—	11.5 @ 0.20	n/a
K–Cs–Sb	Bialkali (ST)	0.3 – 0.7	85	97 @ 0.39	0.02
K–Na–Cs–Sb	Extended Red S–20 (ST)	0.3 – 0.9	250	45 @ 0.57	n/a
GaAs–Cs–O	NEA (O)	0.1 – 0.9	200**	35 @ 0.55	n/a

* ST = semitransparent
  O = opaque

** Laboratory values as high as 2000 have been recorded – (Private communication – W. E. Spicer)

■ Short wavelength limit is set by tube envelope absorption

n/a = data not available

130

FIGURE 5.7   Spectral Response at Selected Photocathodes (35)
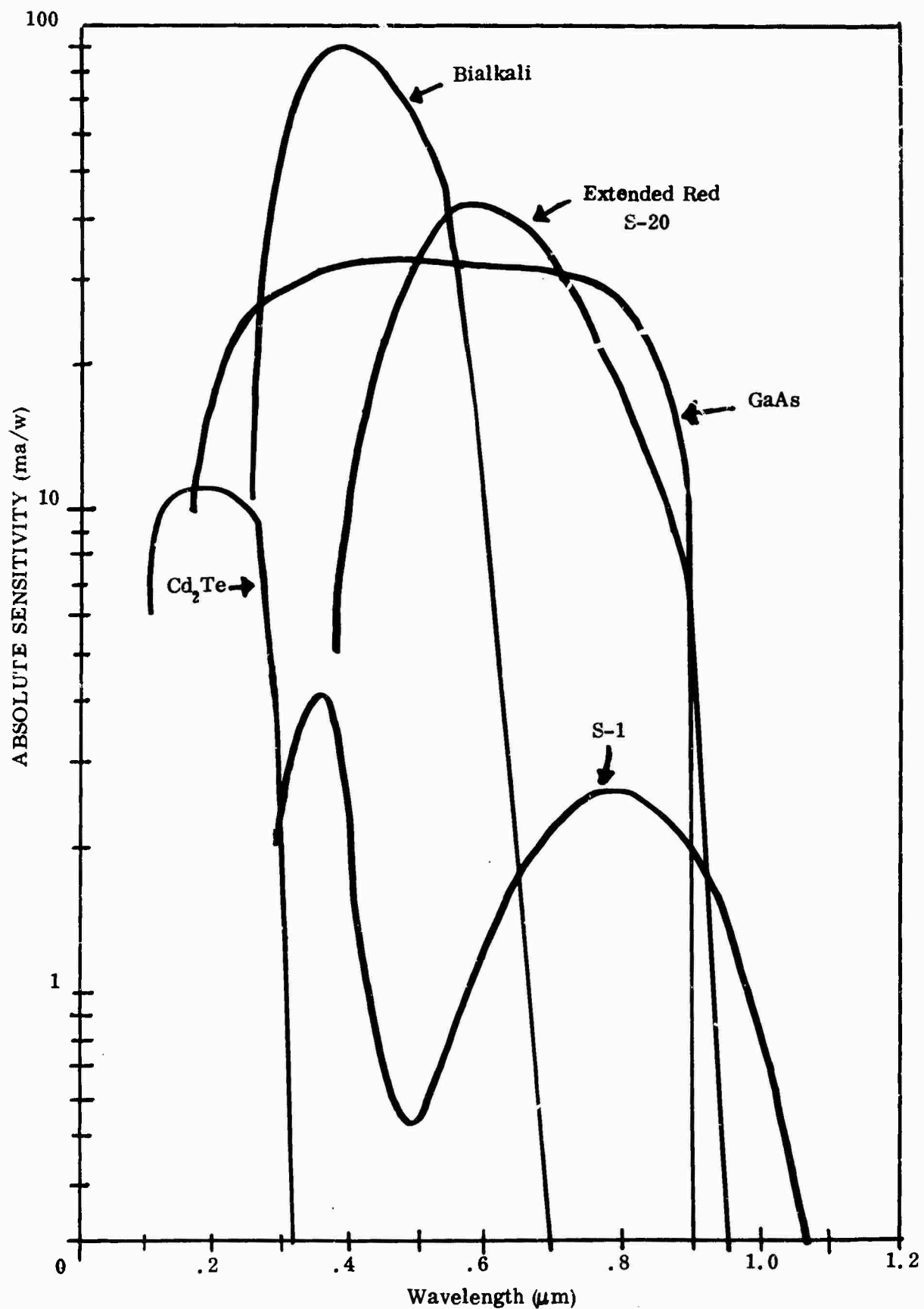
limitations to its usefulness and have prompted the search for a better alternative. In particular, its replacement by high sensitivity NEA photocathodes can be expected in the next few years.

5.4.1.2 Trialkali (S-20)

The trialkali or S-20 photocathode is used more widely in photomultipliers and image intensifiers than any other photocathode due to its broad spectral response, relative high sensitivity, and low dark current. The formula for the photocathode material is usually given as $Na_2KSb:Cs$; it is a cubic p-type semiconductor with nominally a 1.0 eV bandgap and a 0.35 eV electron affinity. The lumen sensitivity available commercially is typically 250 μa/lm as indicated in Table 5.3, but the application of computer-controlled processing is moving this value above the 300 μa/lm level in photomultipliers. Values of 400 to 500 μa/lm with significantly better red response ($\sim$ 50 ma/w @ 0.80 μm) than shown in Figure 5.7 have been obtained consistently in recent years in image intensifiers. It appears that values of about 550 μa/lm, which have been occasionally obtained, represent the best that can be expected with this photocathode; this is an opinion based on experience rather than analysis.

While a "recipe" is often necessary to success in processing a highly sensitive S-20, measurements during processing and considerable tolerance in the order and amount of the constituents deposited have allowed computer-controlled processing with a resultant high reproducibility in the manufacture of this photocathode. Wide variations in processing technique possibly and in use do, however, lead to a correspondingly wide variety of sensitivities and spectral responses, particularly in the long-wavelength portion of the response curves.

The empirical nature of the "recipe" is illustrated by the following typical process. Normally, antimony is deposited in situ to a predetermined thickness as determined by the optical transmission of the layer. Potassium followed by sodium is added to the layer at appropriate temperatures while monitoring the photoemission. Addition of the potassium produces initial photoresponse which is enhanced by

addition of sodium. Excess sodium decreases the response and its deposition is
stopped at this point. Alternating depositions of potassium and antimony are used
to restore the original maximum response. Finally, cesium and antimony are
alternated to optimize the response of the final photocathode. The temperature at
each of these steps is critical for proper diffusion, chemical reaction, and crystallite
growth.

Attempts to form the photocathode from single crystals and subsequently to acti-
vate them in vacuo have thus far been unsuccessful. It has been found that the
choice and cleanliness of window material has some effect on sensitivity, particularly
for the highest values; however, the photocathode will tolerate a wide range of con-
ditions if intermediate ($\sim 200\ \mu a/lm$) sensitivity is desired.

Opaque S-20 photocathodes on reflecting substrates can be made with
more than twice the sensitivity of semitransparent photocathodes, due to the ef-
fectively longer optical path in the material. Data from systematic studies of the
quantitative relationship between thickness and sensitivity for both semitransparent
and opaque photocathodes are hard to find since precise measurements of the photo-
cathode thickness are difficult to make in vacuum. There is some evidence that
the higher sensitivities obtained have been the result of slightly greater thickness
but the data are inconclusive.

5.4.1.3 Bialkali

While the term "bialkali" can in principle be applied to a variety of al-
kali metal combinations in an antimonide photocathode, like the term "multialkali"
applied to an S-20, it has come to mean specifically the K-Cs-Sb photocathode. The
bialkali photocathode is used primarily in photomultiplier tubes where high peak
spectral sensitivity and extremely low dark current are desirable and red response
is not important. As can be seen from Figure 5.7, this photocathode has a peak
sensitivity of about 100 ma/w, more than twice that of the S-20 at its peak value.
The high resistivity of the photocathode restricts its use to applications where small

photocurrents are drawn. The material is a cubic, p-type semiconductor with a 1.0 eV bandgap and an electron affinity of 1.1 eV. The composition is approximately K_2CsSb.

The bialkali photocathode is made by substantially the same technique as the S-20. It has been found experimentally that superficial oxidation of the photocathode after processing appreciably enhances the long-wavelength response due probably to a reduction in the electron affinity. This same effect has been observed for the earlier Cs_3Sb photocathode but a similar treatment of an S-20 will degrade the red response unless the initial sensitivity is very low. It does not appear, however, that this technique has been applied to production versions of the bialkali, probably for reasons of control. The treatment is used in the production of the new NEA photocathodes; the technique will probably be adopted eventually for bialkali processing as well.

5.4.1.4 CsTe (Solar Blind)

The Cs_2Te photocathode exhibits high sensitivity in the spectral range 0.14 μm to 0.35 μm and consequently is used where detection of ultraviolet radiation is desired without interference from sunlight.* While sufficient information is not available to fully characterize the material, the bandgap appears to be about 3.5 eV with an electron affinity on the order of 0.1 eV. The processing of the photocathode is similar to that of the alkali antimonides with tellurium substituting for antimony. The resistivity, however, is substantially higher and requires a thin ultraviolet transmitting coating on the substrate, usually a metal such as chromium, to allow useful current levels. The short wavelength threshold is determined by the substrate; sapphire was the substrate for the photocathode whose performance is plotted in Figure 5.7.

5.4.1.5 Negative Electron Affinity Photocathodes

Photocathodes such as the S-1 and S-20 as described above are thin-film compounds made and activated in situ. Due to the high surface barriers,

---

* Sunlight is strongly attenuated below 0.31 μm by ozone absorption in the upper atmosphere. See Figure 5.2.

photoelectrons must be hot relative to the lattice temperature in order to have suf-
ficient energy to escape the solid. Collisions reduce the energy of the photoelec-
trons, so that few are finally emitted into vacuum. Addition of oxygen, useful in
reducing the surface barrier of the S-9 (cesium antimonide) and bialkali photo-
cathodes, has been unsuccessful in the S-20 probably due to chemical reaction with
the material. Recent improvements in the S-20 are the result of some improve-
ment in material quality (5.4.1.2). However, no significant advance of the threshold
to longer wavelengths has occurred, although the efficiency at shorter wavelengths
has improved.

The NEA photocathode is an effort to achieve longer wavelength threshold
by using a better quality material and a reduced surface barrier. Schematic com-
parisons of the three types of photocathode are shown in Figure 5.8. It is apparent
from Figures 5.8 (a) and 5.8 (b) that the work function, Φ, will limit the long-wave-
length threshold. The gallium arsenide photocathode, however, has a lower work
function than the bandgap of the semiconductor so that near the threshold the ef-
ficiency is limited by absorption and transport in the semiconductor itself (See 5.2.1).
The band bending region accelerates the photoelectrons over the surface barrier.
While phonon emission may still reduce the escape probability, the width of the band
bending region can be reduced to a few mean free paths by increase of the bulk
doping density and, in principle, by decrease of the depth of band bending through
choice of crystallographic orientation.[37] Since recombination lifetime and hence
diffusion length decrease with increased doping density, a compromise between dif-
fusion length and the width of the band bending region is necessary to optimize the
efficiency.

The basic material, in this case gallium arsenide, is grown by vapor or
liquid-phase epitaxy onto a suitable substrate (see 5.3.1). For opaque GaAs photo-
cathodes, the obvious choice is bulk GaAs. The quality of the epitaxial layer in
terms of diffusion length and dislocation density is better than that of the substrate

(a) Metal Photocathode

(b) S-20 Photocathode

(c) GaAs NEA Photocathode
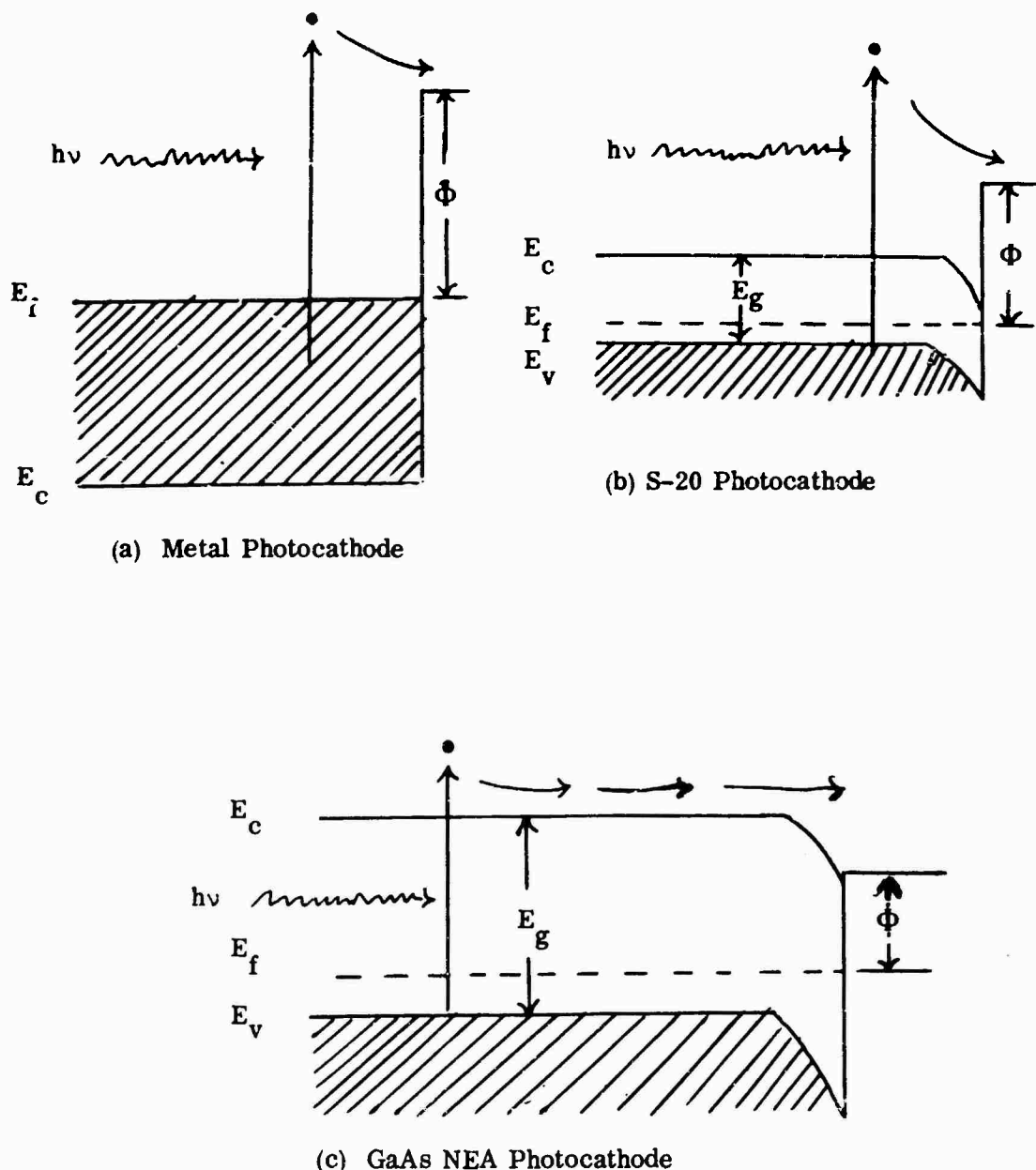
FIGURE 5.8 Models of Photoemissive Cathodes.

136

and growth conditions. Thin (1-2 μm) semitransparent layers can contain appreciable defect densities, particularly at the substrate/photocathode interface where high surface recombination velocity will result.

By the use of crystalline thin films one can adjust the bandgap of the detector. The semiconductor bandgap in Figure 5.8 (c) could be reduced theoretically from 1.4 eV for GaAs to a value $E_g = \phi$, resulting in improved infrared response. This reduction can be accomplished through the use of silicon (1.1 eV) or III-V ternary alloys such as gallium indium arsenide (GaInAs)*, gallium arsenide antimonide (GaAsSb), or indium arsenide phosphide (InAsP). The basic intermetallic compounds form substitutional alloy systems whose bandgaps are a function of the composition (Figure 5.9). Since work functions of about 1.0 eV or less have been observed with cesium oxide, a long wavelength threshold of 1.2 μm should be obtainable. Such photocathodes have been made successfully with GaInAs and InAsP in opaque form and to a limited extent in the semitransparent mode. It should be noted that the lattice parameter and thermal expansion coefficient are also functions of composition.

High-performance, semitransparent photoemitting III-V semiconductors were first made from GaAs layers grown by vapor epitaxy on GaP substrates. Residual strain in the GaAs layer due to the different lattice constants and thermal expansion coefficients of the two materials limited the diffusion length to about 1 μm. The introduction of ternary alloy transition layers such as GaAsP, GaInP, and GaAlAs between the GaP substrate and the GaAs photocathode layer has substantially reduced this problem. The best results so far were obtained using GaAlAs as the transition layer.

A tentative rule of thumb that has now emerged for both substrates and photocathode layers is that the greater the mismatch between the lattice constants of the component compounds, the greater is the residual strain in the final alloy.

---

* The correct form would be $Ga_x In_{1-x} As$ but the subscripts will be suppressed unless comparison is necessary.
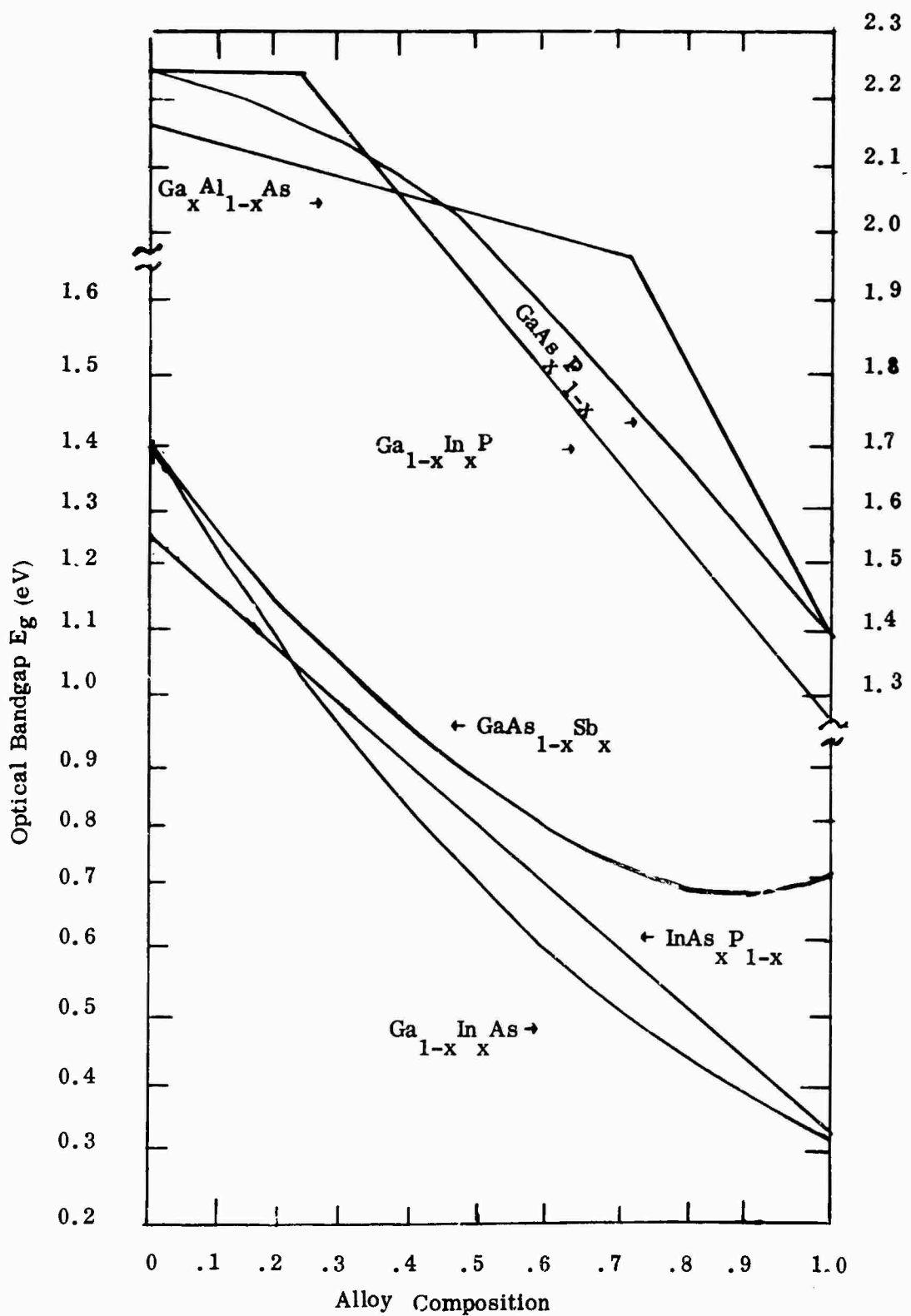
FIGURE 5.9 Bandgap variation of selected III-V alloy composition.

138

Thus, GaAlAs (0.4 percent compound mismatch) generally yields better results than GaInP (7 percent compound mismatch), although the lattice constant of the GaInP can theoretically be matched exactly to GaAs. GaAsP has a large compound mismatch (3.4 percent); there is no composition except pure GaAs which matches the photocathode layer exactly. GaAsP produces the poorest results. The smaller strain in InAsP photocathodes (3.1 percent compound mismatch) may be responsible for the fact that they have greater sensitivity than GaInAs photocathodes (6.7 percent compound mismatch), although factors such as mobility are probably also involved.

Considerable theoretical and experimental work is still necessary before a quantitative understanding of the III-V alloy systems is achieved. A particularly pressing problem is the choice of a suitable substrate for semitransparent InAsP photocathodes with high sensitivity at the $1.06\,\mu$m laser line and a broad spectral response. While a possible choice is AlAsSb, the large compound mismatch (8.2 percent) and the tendency for these aluminum compounds to oxidize quickly present problems in its use. An alternative approach is the quaternary alloy GaInAsP as the photosensitive layer. Since InAsP and GaInAs are both contained in this system, it should be possible to find a quaternary composition having high $1.06\,\mu$m sensitivity. Such an alloy should be sufficiently close to InAsP to retain its excellent transport properties, but sufficiently rich in gallium to allow use of the wider bandgap GaInP as a substrate. Preliminary work on this alloy has produced opaque efficiencies of 7.5 percent at $1.06\,\mu$m with low gallium concentrations. Much more research will be required to understand the quaternary system fully, particularly as to growth and transport properties.

A related problem important to image intensifiers, where large area uniformity is desirable, involves blemishes in the photocathode film. Blemishes can be defined as any structural or electronic defect leading to local reduction in detector sensitivity or local increase in dark current. For the photocathode systems thus far discussed, this problem is in some cases unimportant, and in other cases serious. In general, GaAs/GaInP and GaAs/GaAlAs photocathode/substrate combinations

have severe blemish problems, but GaAs/GaAsP does not. There are two very common sources of blemishes. Low density nucleation and solution inclusion (the latter peculiar to liquid-phase epitaxy) are one category. Both vary with substrate preparation, orientation, and growth conditions. A second category comprises high densities of dislocation-type defects. These affect the electrical properties and thermal etch rates of the films and result from strain in the substrate or at the photocathode/substrate interface. So far, there are no clear-cut fundamental arguments possible that allow rejection or acceptance of a particular material combination or process in terms of potentially blemish-free photocathode films.

Experience with the ternary alloys has shown that the model of Figure 5.8 (c) may be too simple to describe the photoresponse. Measurements of the spectral response of samples of GaInAs,[38] InAsP,[39] and GaAsSb[41] show that, as the bandgap of the semiconductor decreases, the photoelectron escape probability decreases as well. This effect is illustrated in Figure 5.10 for GaInAs and can be explained either in terms of a heterojunction[41] formed from thick (>3 ηm) cesium oxide activator layers on the semiconductor, or in terms of the increased effect of energy loss[38] as the magnitude of the NEA decreases, appropriate for monolayer quantities of cesium oxide. The depth of band bending will certainly influence this result, and it is in turn influenced by crystallographic orientation and/or surface states as well as the degree of surface coverage with cesium oxide. These effects have not been examined in detail, except for GaAs[42] and silicon, both of which show a definite dependence of photosensitivity on orientation. In the case of silicon, only the (100) surface can be activated to show NEA effects. More effort is required in this area before definitive conclusions can be drawn.

The opaque gallium arsenide (GaAs) photocathode is a relatively new addition to the inventory of commercial photocathodes. Published specifications give

140

FIGURE 5.10 Spectral responses of opaque GaInAs photocathodes with calculated escape probabilities.

No.	Eg (eV)	λo (μm)
● 1	1.39	0.89
△ 2	1.18	1.05
□ 3	1.13	1.10
✕ 4	1.08	1.15
○ 5	1.04	1.19
+ 6	0.96	1.29

Continuous curves give the Yield, Y; use left hand ordinates. Separated symbols are the surface escape probability, B; use right hand ordinates.

YIELD, Y (ELECTRONS/INCIDENT PHOTON)

SURFACE ESCAPE PROBABILITY, B

λ (μm)
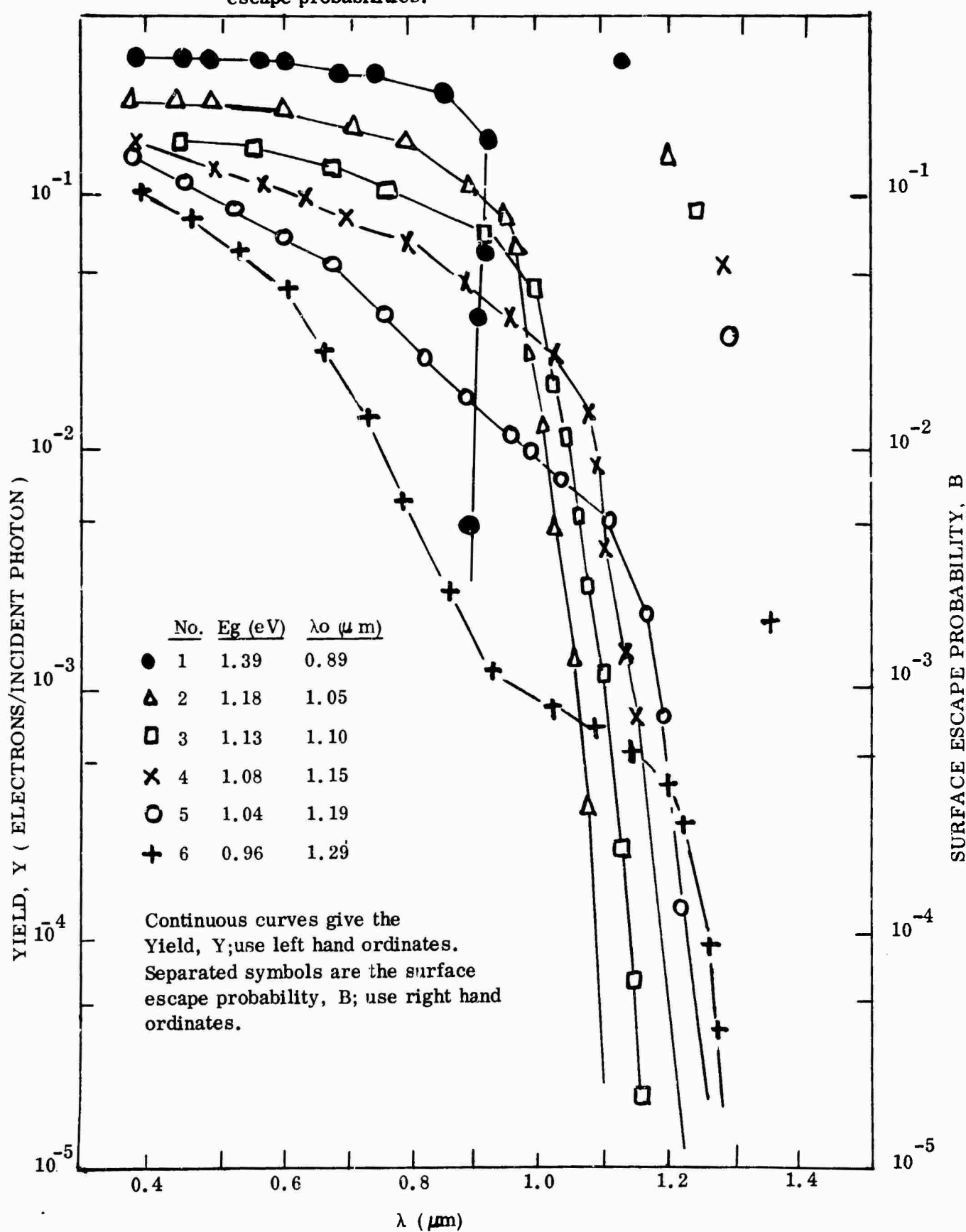
a sensitivity of about 200 $\mu a/lm$, but carefully selected photomultipliers can be obtained in the 600 to 700 $\mu a/lm$ range; rare tubes show 1000 $\mu a/lm$ sensitivity. This device is still in the product development stage but typical values of 1000 to 1200 $\mu a/lm$ may be practical in the long run. Laboratory experiments on these photocathodes have demonstrated sensitivities as high as 2000 $\mu a/lm$ and dark currents below 1 fa/cm^2. Research is continuing on the semitransparent GaAs photocathode but it will be some time before it is available in commercial tubes because of more complex materials problems.

At present, the NEA effect appears to hold considerable promise for improving both photomultiplier and image tube performance to a wavelength of 1.1 μm, by making use of ternary alloy materials. While it is difficult to give a single performance value characteristic of all ternary photocathodes, the response at 1.06 μm has military significance and provides a quantitative evaluation of the state of the art. The bandgap must be sufficiently low to give high absorption of 1.06 μm radiation, but high enough to provide a reasonable escape probability. The allowable bandgap is 1.19 eV $\pm \sim$ .03 eV. A quantum efficiency of 7 percent has been obtained on an opaque InAsP photocathode under these optimized conditions with a dark current of 10-100 fa/cm^2.

The activation techniques for III-V NEA photocathodes necessitate a heat cleaning step before introduction of the cesium and oxygen. After cooling to room temperature, successive applications of cesium and oxygen are made as required to obtain peak sensitivity. It is this step that leads to the thin or thick cesium oxide layers discussed above, particularly for the ternary alloys. If the heterojunction model is correct, a thick cesium oxide layer is required to reduce the work function sufficiently.[41] However, Fisher et al.[38] have found little difference between the amount of cesium and oxygen required to activate GaAs and the ternaries, a monolayer of Cs and Cs_2O, in that order, being sufficient. The different results may be a matter of overall cleanliness and material quality. In the worst case excess cesium oxide may be required for chemical cleaning of the surface.

Silicon is an obvious choice for an infrared-sensitive photocathode basic
material. The basic materials technology is well-understood due to decade-long
investments by industry. The development of the silicon vidicon has provided a
practical technology for making thin (5-7 μm), self-supported films. Opaque silicon
wafers have been successfully activated to 900 μ a/lm. Cleaning of the silicon is
more difficult than for the III-V photocathodes due to the strongly bonded oxide.
Dark current measurements on high-sensitivity opaque silicon photocathodes give
values of 0.01 to 5 nA/cm^2. The source of this high dark current, not observed in
III-V photocathodes of equivalent bandgap, is as yet unknown. High surface-state
densities and short minority-carrier lifetimes in the band-bending region, both a
result of the high temperature processing, are suspected.

The NEA effect also can be used in secondary emission dynodes. High-
gain secondary emission has been observed from both gallium phosphide and gallium
arsenide opaque dynodes and developed into practical photomultipliers with fewer
stages and, hence, faster pulse response than older versions. The noise factor is
improved as well. High gain has also been observed from silicon,[43] raising hopes
for a high gain transmission dynode for both image intensifiers and photomultipliers.
However, the presence of the large dark current in silicon makes it unsuitable for
either photocathode or transmission-dynode applications without cooling. This has
led to some preliminary work on thin, self-supporting GaAs dynodes as an alternative;
however, considerably more research in basic materials technology is required
before this device becomes practical. The lower processing temperature and dark
current make GaAs an attractive material which should be more compatible with
tube processing than silicon.

Preliminary measurements[44] on Zn-doped GaAs transmission dynodes
have shown some promise. Gains of about 20 at 5 keV have been obtained on 5 μm
thick, self-supported films with 2 μm diffusion lengths. The longer diffusion
lengths (up to 10 μm) possible with silicon or germanium-doped gallium arsenide
may allow thicker films to be used, permitting larger areas and less breakage in

manufacture. With improved processing it appears reasonable to expect gains of up to 100 at 5 keV primary electron energy from the GaAs films. It should be noted that these films also could satisfy the requirements for a high-performance semitransparent photocathode. The capability of forming thin, self-supported films of gallium arsenide thus assumes double importance.

The above discussion has been oriented primarily toward III-V binary compounds and ternary alloys. II-VI compounds, most notably CdTe and the CdHgTe alloy, are potentially applicable to photocathodes as well. No significant work, however, has been done in this area. The requirement for acceptor doping levels of 5×10^{18} cm^{-3} or greater and tube bakeout temperatures of 300° C or more excluded the II-VI compounds from consideration at an early stage. Consequently, almost nothing is known about the activation of these materials. While such studies should be performed for completeness if the appropriate material can be generated, the success and momentum gained with III-V materials would argue heavily against the cost-effectiveness of a substantial effort in II-VI NEA photocathodes. With the long wavelength limitiations of NEA photocathodes and the increasing work on field-assisted photocathodes (5.5.1) where the doping requirement can be relaxed, some consideration should be given to HgCdTe photocathode-type detectors for the 1 to 2 μm spectral range.

Possible ternary compound detector materials are discussed in Chapter 6 (6.3.3) as far-infrared-sensitive materials. Since ternary compounds with bandgaps falling in the 0.1 to 2 μm spectral range do exist, they should be examined as possible detector materials, particularly for the 1 to 2 μm region. However, new materials in this range face stiff competition from silicon and the rapidly evolving III-V compound technology.

NEA photocathodes provide an additional advantage important in image intensifier operation. The image tube design favored for man-portable systems, the wafer tube, consists of a plane-parallel configuration of photocathode, gain element (microchannel plate or transmission secondary electron multiplication (TSEM) dynode), and output phosphor. The spacing between the element pairs is

on the order of a millimeter. An accelerating field applied between the close-spaced element pairs focuses the electron image from one component to the next (proximity focusing). It is important that electrons be emitted from the photocathode or TSEM with as small a velocity component tangential to the direction of the field as possible so that little lateral spread in the electron image takes place in transit.

The S-20 photocathode commonly used in image intensifiers would be expected to have a wide energy distribution at all angles, because of the hot electron processes and the electron transport high in the conduction band of the material. In the NEA photocathodes, the photoelectrons enter the band-bending region thermalized, so that the mean energy will be~ kT. The field in the band-bending region will only accelerate normal to the emission surface so that even with some scattering the electron image approaching the emission surface can be expected to be well-collimated. If the surface is assumed to conserve transverse momentum the image will remain collimated on emission into vacuum. Recent measurements[45] of emission distributions indicate that the electron beam from a point source does in fact have a very narrow angular distribution, the shape being roughly gaussian with a half angle at half maximum of about 5°. The energy distribution has a half width at half maximum smaller than the resolution of the instrumentation (~ 0.1 eV) so that very high-resolution image tubes should be possible. Resolution measurements made on wafer diodes[46] (photocathode and phosphor only) with semitransparent photocathodes have failed to confirm this, but loss of resolution due to optical effects in the photocathode material may be dominating. Improvements in material quality may be expected to improve the resolution as well as the sensitivity of the NEA photocathode.

5.4.2 Gas-Filled Devices

A number of non-solid-state devices are available for detection in the ultraviolet which can operate in higher temperature environments than devices employing cesium. These include gas-filled devices in which the ultraviolet photon either ionizes the gas directly or produces photoelectrons (from a metallic

photocathode) which ionize the gas. If the configuration,gas pressure, and electric field are such that each initial electron or electron-ion pair gives rise to a specific average number of collected pairs, the output signal is proportional to the initial number of ultraviolet photons and the device is a proportional counter.

When the voltage across the device is increased and the multiplication factor goes up, the ultraviolet and visible photons generated during the multiplication process increase in number as well. Their number becomes sufficient to make the breakdown process regenerative, and the discharge travels the entire length of the anode wire. This is the mode of operation of the Geiger-Mueller counter and the output-signal amplitude is no longer a measure of the number of initial photons.

This type of device is simple in concept and design. Proportional detectors which operate on the gas ionization principle have reasonable quantum efficiencies over a limited spectral range. Typical quantum efficiency curves are shown in Figure 5.11 (a) for three gas /window combinations.[47] The long wavelength threshold is determined by the ionization energy of the gas while the window determines the short wavelength cutoff. With the fill gases shown, the detectors operate at unity gain. Addition of CO_2 to the NO or p-xylene allows operation in the gas multiplication mode to improve the sensitivity and dynamic range producing a gain /voltage curve such as that[47] in Figure 5.11 (b).

Available Geiger-Mueller counters use a metallic photocathode such as molybdenum with an argon-helium mixture to provide the ionization medium.[48] This device can be operated as a single photon counter at low count rates and has a moderate voltage requirement and a simple, rugged structure; thus it is widely used in spite of a relatively low quantum efficiency. The spectral response is generally broader than the gas-ionization type which is usually restricted to the vacuum ultra-violet. The noise source in the Geiger-Mueller tube comes principally from statistical fluctuations in the average output pulse rate.

146

FIGURE 5.11 Characteristics of gas ionization type UV detector devices.
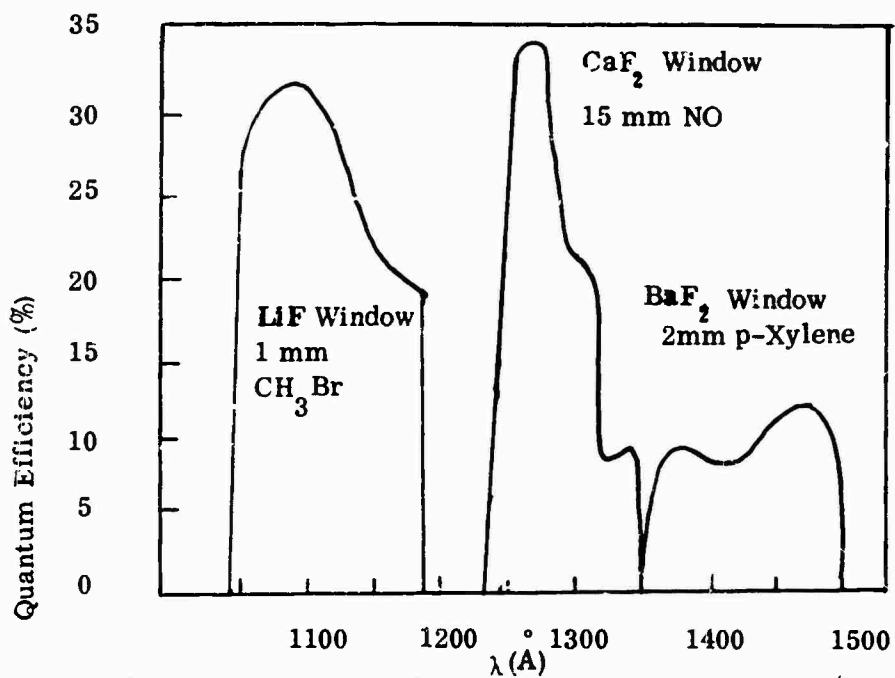
(a) Typical quantum efficiency curves for three fill-gas/window
combinations (47).
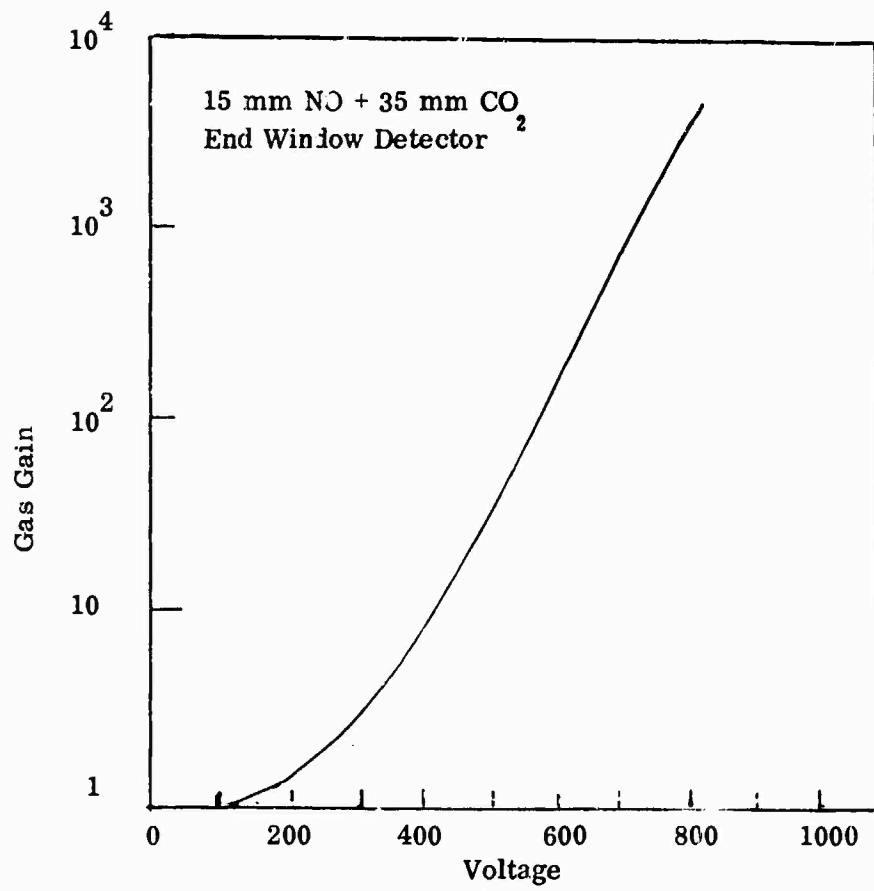
(b) Gain/voltage curve for NO/CO_2 gas ionization device (47).

5.4.3 Solid-State Detectors

Solid-state detector devices, single elements (point detectors) and arrays, constitute an important class of detector for the spectral range and can be expected to replace vacuum devices for many, if not all, applications over the next two decades. An increasing number of functions are being performed by hybrid solid state/vacuum devices where materials and techniques appropriate to solid state technology are being used in vacuum tubes. The outstanding examples of this are the NEA photocathode, already discussed, and the silicon diode array vidicon which is discussed in 5.4.4. This section treats solid state detectors such as non-avalanching photodiodes, avalanche photodiodes, and heterojunction photodiodes and some of the problems associated with imaging arrays of these devices.

5.4.3.1 Non-Avalanching Photodiodes - Phototransistors

There are two major types of this photodetector:

- The p-n junction photodiode.
- The surface-barrier (Schottky contact) photodiode.

A third type, the point-contact photodiode, is similar in many respects to the surface-barrier photodiode and is somewhat inferior to the other types of photodiode.

P-n junction photodiodes can be operated as either diffusion or depletion photodiodes (see Figure 5.12). In the former, the absorption takes place in the p-region, the carriers diffusing to the junction to be counted as signal. The p+ layer acts as a contact to the p-type region. The n+ layer is made sufficiently thin to minimize optical absorption and so contributes little to the photocurrent. The doping levels in the p+ and n+ layers are high to reduce series resistance. The p+ and n+ layers may be reversed; the p+ layer is then about $1000\overset{\circ}{A}$ in thickness and acts to reduce surface recombination. Diodes of this sort have little advantage over depletion photodiodes due to slow speed of response. They are available commercially and are used for sensing at relatively high light levels.

148
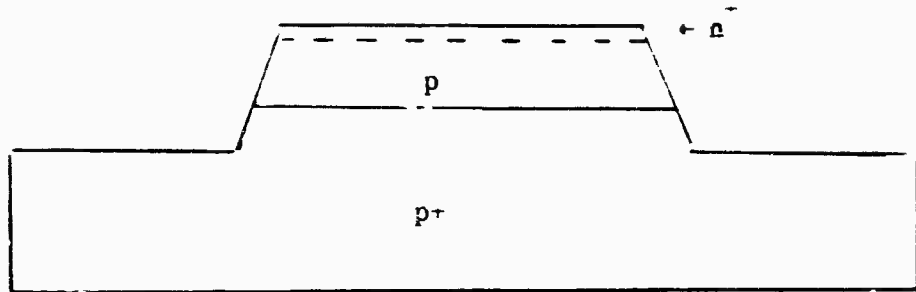
(a) Diffusion Photodiode
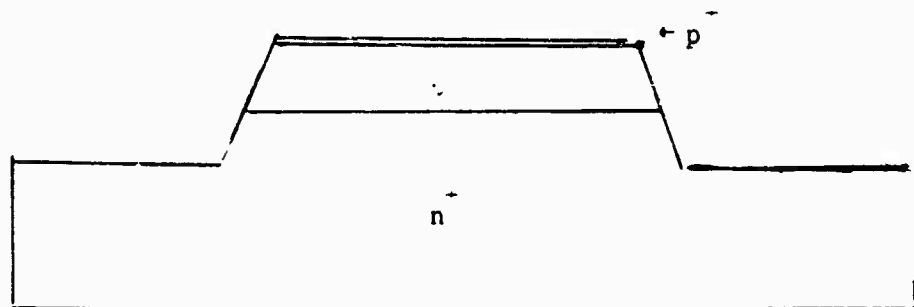
(b) Depletion Photodiode
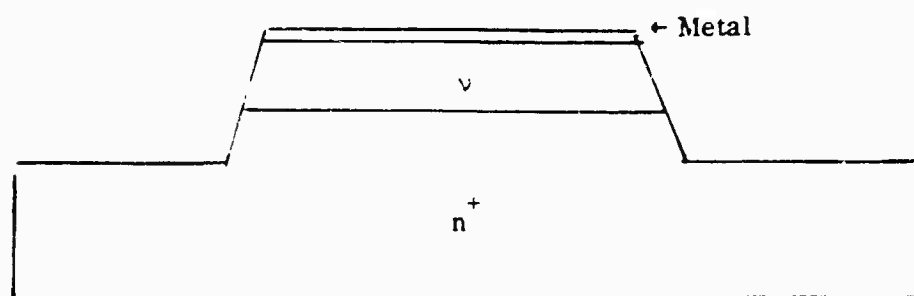
(c) Surface-Barrier (Schottky-Barrier) Photodiode

FIGURE 5.12   Schematic illustration of photodiode types using a mesa
form (unpassivated).

A sketch of a depletion or p-i-n photodiode is shown in Figure 5.12 (b). The p+ layer is made thin compared to an optical absorption length. The junction bias appears entirely across the intrinsic region which is many times the absorption length in thickness. The photogenerated carriers are rapidly swept out, providing response times on the order of d/v_D, where d is the width of the intrinsic (depletion) region and v_D is the limiting drift velocity. With $v_D = 10^7$ cm/sec and $d = 10 \mu m$, a bandwidth of $\Delta f \approx 10 GHz$ is possible.

Figure 5.13 shows representative spectral response for silicon and germanium photodiodes[49] for comparison. Figure 5.14 shows the relative spectral response for a planar silicon photodiode. Silicon devices of this type have room-temperature dark currents on the order of nA/cm^2 and cutoff frequencies of 5 to 25 GHz. Germanium devices have cutoff frequencies of about 2GHz, and the dark currents at room temperature are on the order of $\mu A/cm^2$. Peak D_λ^* for these devices have been measured between 10^{12} and 10^{13} cm-$Hz^{\frac{1}{2}}$/watt for silicon devices. D_λ^* is limited primarily by shot noise from the dark current which is, in turn, trap-generated in the depletion layer. The high level of device technology for contacts and passivation accompanied by the use of guard rings to block surface leakage eliminates extraneous $1/f$ noise sources. The value of D_λ^* for a germanium device is typically 10^{11} cm-$Hz^{\frac{1}{2}}$/ watt at room temperature, less than for silicon devices due to the higher dark current and poorer passivation.

The presence of copper as a generation center is responsible for a large fraction of the excess dark current in germanium devices. Further, the lack of a stable self-generating oxide has made passivation of germanium diodes difficult. Guard rings have not been used extensively but may improve performance as has been the case with silicon devices and avalanche diodes in silicon and germanium.

Figure 5.12 used the mesa configuration to illustrate various types of junction devices. The same forms are possible in planar configurations as well.
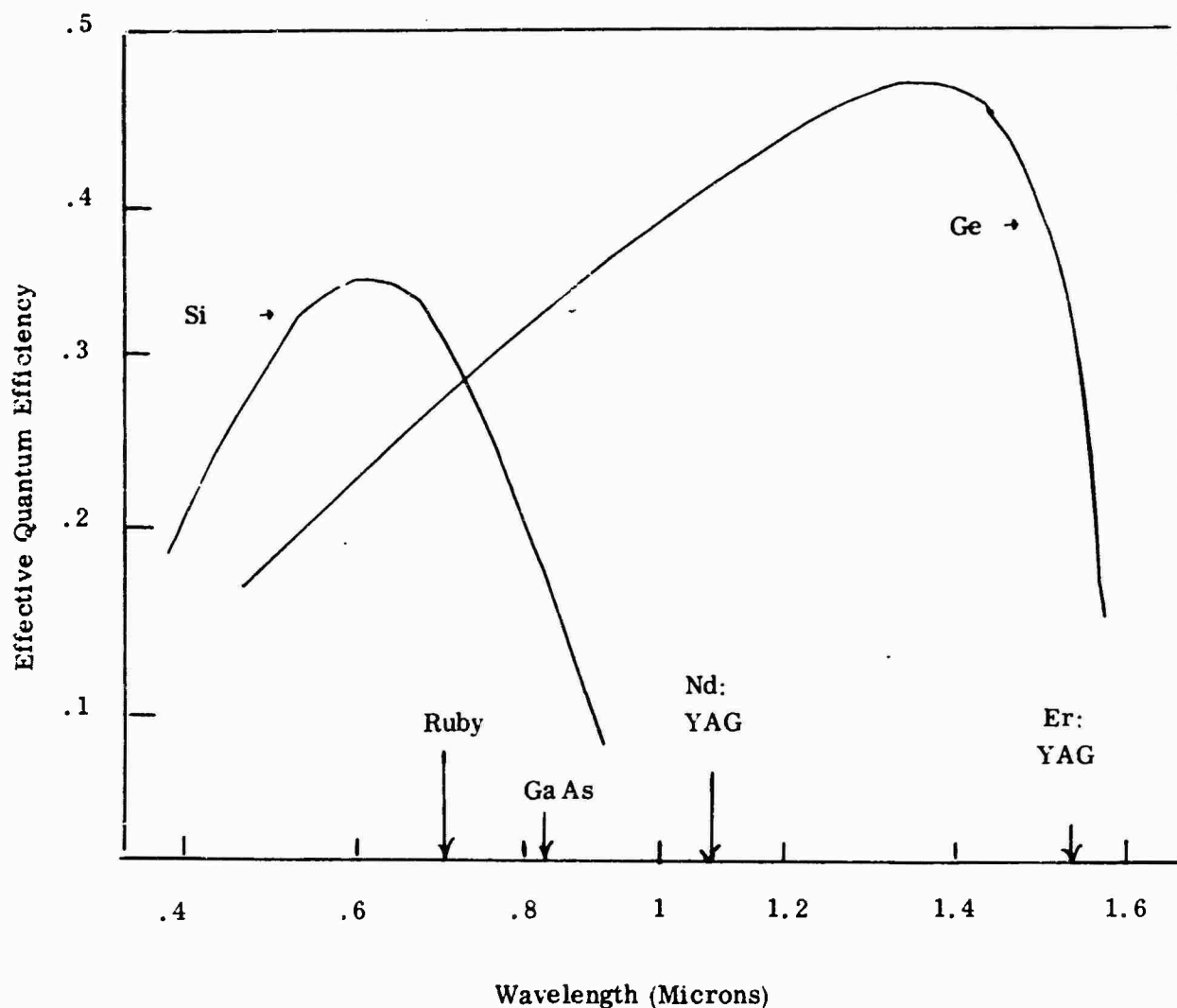
FIGURE 5.13   Effective spectral response curves for silicon and germanium
photodiodes (49).
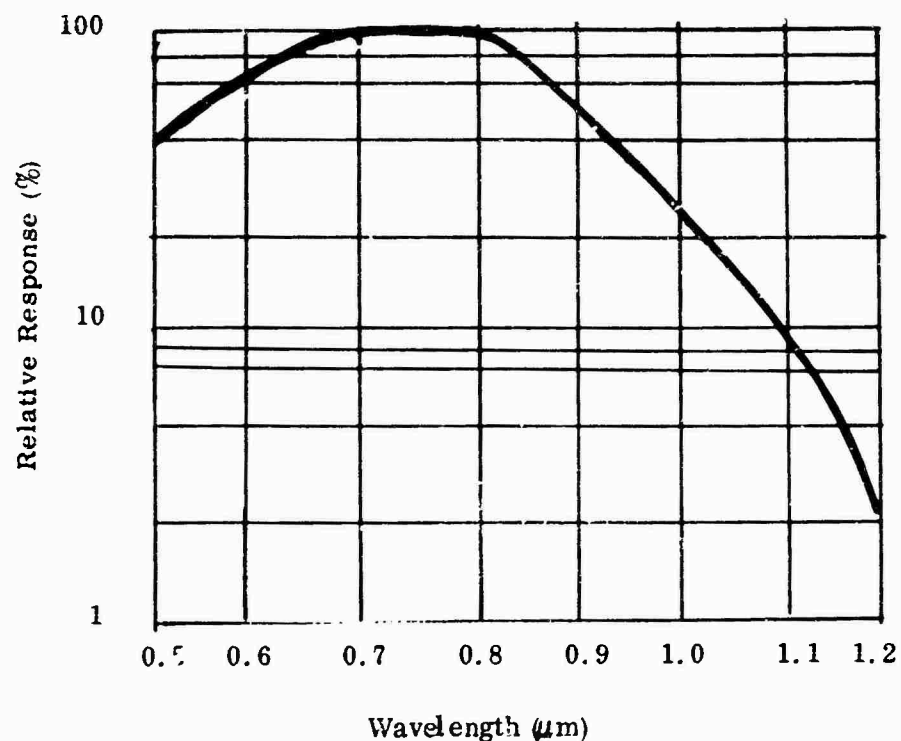
FIGURE 5.14 Relative response of a commercial high-speed silicon photodiode –
TI #LSX 900.

152

Diffusion and vapor-phase epitaxy are used almost exclusively to fabricate devices in either configuration. For single detector elements, mesa junctions can be formed by growing thick, high-quality intrinsic layers epitaxially onto degenerately doped substrates with (in most cases) better purity and crystalline perfection than the substrate material. The increasing use of oxide and epitaxy isolation techniques offers a possibility of simplifying the use of mesa diodes in arrays where multiple external contacts can be a problem.

Planar diodes are generally made by multiple diffusions using a number of sequential silicon oxide or nitride masks, depending on the configuration desired. They are well suited to arrays since metallization contacts to the array diodes are relatively easy to form. The masking material can then be used as the passivating layer.

Photodiodes of the surface or Schottky-barrier type are illustrated in Figure 5.12 (c). Photon absorption can take place in the metal layer for internal photoemission over the metal-semiconductor barrier. The threshold wavelength for this process is the height of this barrier while the efficiency is determined by the reflectance, hot electron scattering length, photon absorption length, and thickness of the metal. Since relatively small barrier heights can be obtained, thresholds into the far infrared are possible. Devices of this type are discussed in Chapter 6 (6.3.7).

When intrinsic absorption takes place in the semiconductor, the Schottky-barrier diode is operating like a p-n diode. However, reflection from and absorption in the metal will reduce the quantum efficiency across the response range unless anti-reflection coatings are used, and the metal is made very thin. The dark leakage current for the Schottky-barrier photodiode will be larger than its junction counterpart.[30] The relative spectral responses of silicon Schottky-barrier and p-n junction photodiodes are compared in Figure 5.15.
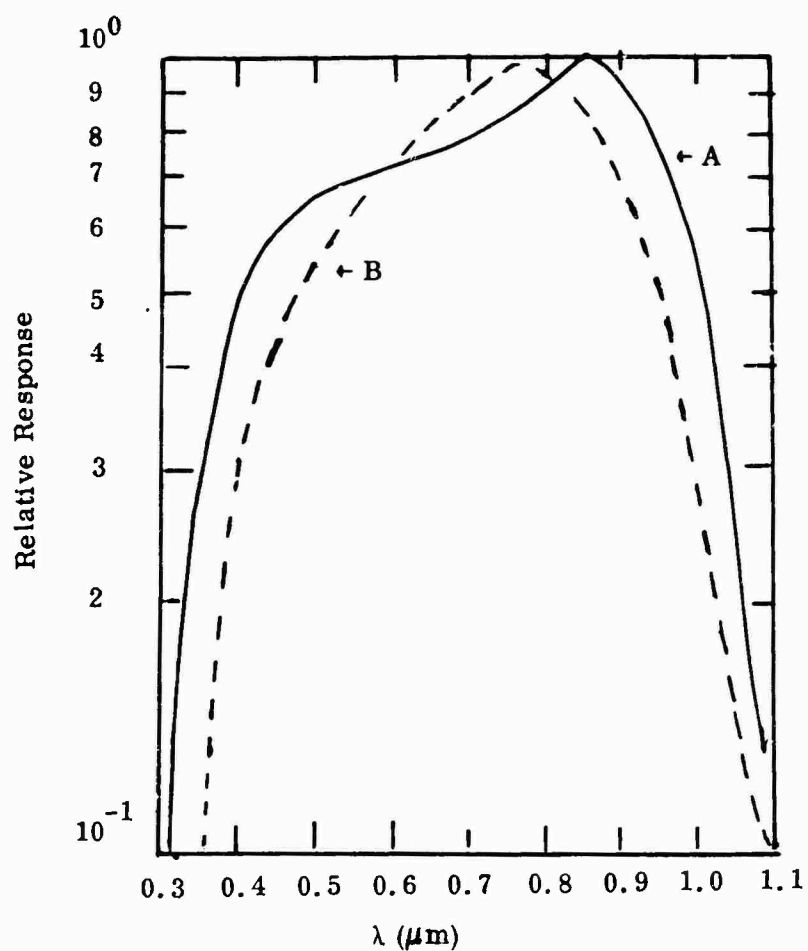
FIGURE 5.15   Comparison of spectral responses for Schottky-barrier (A) and
p-n junction (B) photodiodes in silicon.

Passivation and guard ring utilization in Schottky-barrier photodiodes are substantially the same as in the case of p-n junction devices. Lower processing temperatures can be used throughout, reducing the chance for contamination of the detector material. Several proprietary commercial techniques have been evolved. The metal may be deposited by evaporation, vapor-phase pyrolysis or plating. Residual oxides may result in a wide dispersion in the value of the barrier height and hence non-uniformities in dark current from element to element in an array.

The speed of response of surface-barrier diodes is substantially the same as that of p-n junctions, limited by the transit time in the depletion layer. Due to the larger dark current, the D^* of the Schottky diode is usually somewhat lower than that of a p-n junction at the same temperature.

None of the devices discussed thus far in this subsection exhibit internal signal gain. Gain is possible using the phototransistor with either diffused or Schottky-barrier collector contacts. Modifications of the basic form of a transistor to increase the effective collector area and reduce optical losses into the collector are required to convert a transistor into a phototransistor. The response of the device depends upon the illumination conditions. If excitation takes place in the collector-base junction, considerably greater gains can result than when the base alone is illuminated, since photocarriers are trapped in the base. This charge causes increased charge injection from the emitter until the trapped photocarriers are neutralized.

Commercial phototransistors are generally fabricated from silicon and germanium. Gains of several hundred have been realized and the basic technology is similar to that required for normal transistors. The sensitivities are as high as 600 amps/watt. The dark currents are relatively high, resulting in low D^* at low signal levels. The dynamic range is limited at the upper end by saturation effects so that linearity is limited to only a few decades of light intensity. The response time is typically 100 nanoseconds, corresponding to the trapped time. In some respects, the phototransistor is similar to a photoconductor and is not useful for low light level operation.

A variety of transistor type devices, including field-effect devices, can be converted to photon detectors. While photosensors have been made of all such devices, none has been developed for commercial or military markets. They show no advantage over the phototransistor or the avalanche diode and will not be discussed here.

Several attempts have been made to form photojunctions from dissimilar semiconductors, the so-called heterojunction photodiode.[50] The germanium/gallium arsenide diode is perhaps the most thoroughly studied. Difficulties arise in fabricating such a device. Unless extreme care is exercised in growing gallium arsenide onto germanium, interdiffusion will take place. If this can be surmounted by proper growth conditions, the difference (~ 0.1eV) in electron affinity between the two semiconductors results in a conduction band step which produces a barrier to electron flow from the germanium into the gallium arsenide. The effect of this barrier is reduced by the bias if some carrier heating takes place. Interface states, present at the junction, often provide an additional source of dark current and reduce charge stored at the interface.

Heterojunction photodiodes have yet to become practical since, as point detectors, they offer little advantage and require more expensive technology than homojunctions using germanium or silicon. Applications as field-assisted photo-cathodes will be discussed in 5.5.1; in this case heterojunctions offer some unique possibilities not achievable with homojunctions. (See 6.3.6 for a more detailed discussion of heterojunction photodetectors.)

5.4.3.2 Avalanching Photodiodes

The photodiode devices discussed have been, at best, unity gain devices. In 5.2.1, carrier avalanching was discussed as a means of providing internal gain in a diode. The basic configurations presented in Figure 5.12 and their planar counterparts are used, with some modification. To prevent surface breakdown across the junction under the high avalanche fields, guard rings are diffused around the junction perimeter at a doping level much lower than that of the highly doped contact but to a

greater depth. The surface field is then below the bulk value. An MOS guard ring can also be used to do this.

Avalanching requires material uniformity, particularly at the junction interfaces. Local deviations in the shape or composition of the interface may be caused by diffusion or growth along dislocations or other defects. Resulting variations in electric field and ionization coefficients produce fluctuations in the diode current. In regions with gains well above the mean, avalanche breakdown will occur at lower bias, producing microplasmas. Microplasmas may be initiated by both thermal and photoelectrons. The optimum operating voltage for the junction then depends on the mean gain desired and the maximum excess current noise that can be tolerated.

The technology required to make good avalanche diodes is essentially similar to that necessary for high-quality non-avalanching photodiodes. Silicon and germanium avalanche photodiodes have had extensive commercial development. Silicon avalanche photodiodes with breakdown voltages of 140 to 200 volts at room temperature (defined for 10 μA dark reverse current) have gains of 100 to 200 and quantum efficiencies in excess of 50 percent between 0.7 and 1.0 μm. Values of NEP are 10^{-12} w/Hz$^{\frac{1}{2}}$ at 1 GHz, with gain bandwidth products of about 100 GHz. Germanium devices at room temperature have breakdown voltages of 30 to 60 volts with gains of 20 to 50. The quantum efficiency is better than 50 percent between 0.8 and 1.6 μm. The gain bandwidth products are smaller than for silicon and the NEP larger; passivation of the semiconductor surface is a persistent problem.

Systems using lasers for target designation employ a square of four silicon avalanche diodes. Devices that are being specifically developed and produced for these systems perform somewhat better than those presently commercially available and are designed for low-gain, low-noise operation at relatively large biases. As a typical example, a matched quadrature set with an operating gain of 11 at 1875v would have an absolute responsivity in excess of 20 amperes/watt, a total leakage of 3 μA and an NEP less than 10^{-15} wHz$^{\frac{1}{2}}$ into a 30 to 50 MHz bandwidth (limited by noise in the

attached preamplifiers at large bandwidths) at a wavelength of $0.9\,\mu m$, with somewhat larger NEP values at $1.06\,\mu m$ due to the smaller quantum efficiency.

Single-element germanium devices for $1.54\,\mu m$ military laser systems appear to be virtually identical to their commercial counterparts. Avalanche diodes have been successfully fabricated from gallium arsenide and gallium phosphide but there appears to be little interest in their use as photodetectors and no commercial development for this purpose. While work is in progress on III-V ternary alloy avalanche photodiodes, reports of success (or failure) have not yet been published. It may be reasonably expected that the binary compounds, and even more so the ternary alloys, would present serious materials problems due to variations in composition and the possibilities of multiphase condensation (including growth of internal dendrites). Passivation is also important since deposited oxides must be used as with germanium.

Avalanche photodiodes can be made with Schottky contacts as with non-avalanching photodiodes. The NEP is somewhat higher than that achievable with grown or diffused junctions due to the higher dark current. The use of guard rings to suppress peripheral breakdown is identical to the technique used with junction diodes. As with non-avalanching Schottky-barrier photodiodes, an antireflection coating is required on the metal contact to improve the intrinsic conversion efficiency. See 6.3.7 of this report for further discussion.

5.4.3.3 Ultraviolet Detectors

The majority of the discussion of the status of solid-state detectors has centered on silicon and germanium devices because of their advanced technological base. These devices are primarily useful in the visible and near-infrared ranges. Below $0.4\,\mu m$, however, the quantum efficiencies of most solid state detectors drop rapidly. Surface recombination, dead contact layers, or absorption in passivating layers tend to reduce the ultraviolet sensitivity of these devices.

5.4.3.3.1 The II-VI Compounds

The best known and most widely studied materials providing useful ultra-
violet photoresponse are the Group II-VI compounds. These can be divided into two
subgroups: IIA-VIA compounds and IIB-VIA* compounds. The former group includes
the oxides, sulfides, selenides, and tellurides of boron, strontium, magnesium,
and calcium. Most of the members of this class have bandgaps greater than 3 eV
and will exhibit some photosensitivity in the ultraviolet. However, only small photo-
effects have been found in these materials as compared to their sister group (IIB-VIA)
and, consequently, have not been widely investigated.

In the IIB-VIA compounds, electrons are the majority contributors to the
photoconductivity.[51] The holes are rapidly captured at defect sites, where recombi-
nation with free electrons eventually occurs. The centers that give rise to high photo-
sensitivity are compensated acceptors. These have a capture cross-section for free
holes that is 10^4 to 10^6 times larger than their subsequent capture cross-section for
a free electron. These centers are associated with intrinsic crystal defects or de-
fect-impurity complexes. Many of the identifying characteristics of the particular
photoconductor depend directly on the location of the energy level of the sensitizing
centers. Such characteristics include the dependence of photocurrent on light intensity,
temperature dependence of photosensitivity, susceptibility to optical quenching, and
speed of response.

Among the Group IIB-VIA compounds are the well known photoconductors
CdS, ZnSe, CdSe, ZnTe, and CdTe which have their bandgap energies and peak sensi-
tivities in the visible part of the spectrum. These materials exhibit some photosensi-
tivity to ultraviolet radiation, but it is orders of magnitude less than their sensitivity
to visible radiation (Figure 5.16) and so they are not generally considered to be
ultraviolet photodetectors.

IIB elements are Zn, Cd, Hg.
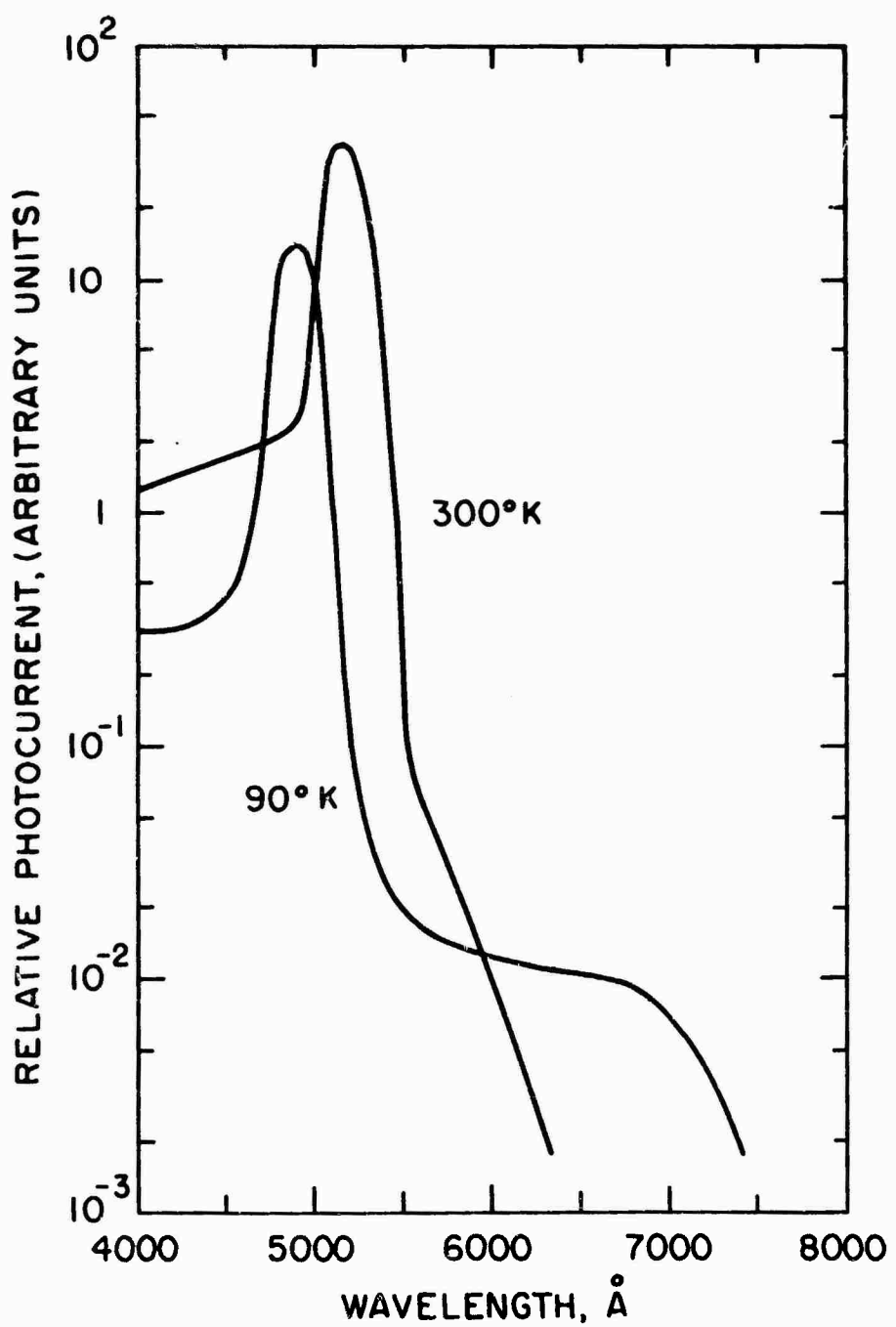
FIGURE 5.16 Spectral response of photoconductivity for a photosensitive pure CdS crystal (52)

Zinc sulfide is probably best known for its use as a luminescent phosphor. There is a commercial solid state ultraviolet detector which uses what is believed to be a ZnS powder as the photosensitive material. Because of the high degree of self-compensation in ZnS and its large bandgap (~ 3.7 eV), resistivities of 10^7 Ω-cm or greater are common in this material. This is advantageous since it permits the dc detection of low radiation levels.

ZnS exhibits a large photoconductivity effect which results from the long electron lifetime due to hole traps in the material. This same trapping phenomenon, however, results in a rather slow response time which varies from one to 10^{-3} sec depending on the intensity of the illumination source. The hole traps can generally be emptied by infrared illumination and hence ZnS exhibits an optical quenching effect.

Schottky barriers have been fabricated on ZnS[53] by evaporating thin layers of gold, chromium, or silver on the surface. The radiation is absorbed in the depletion layer. A Schottky-barrier photodetector has a maximum photogain of unity, but generally has a faster response than a bulk photoconductor. The spectral quantum efficiency for Schottky-barrier ZnS photodetectors is shown in Figure 5.17.

5.4.3.3.2 The Perovskites and Rutile

The perovskite transition metal oxides $SrTiO_3$, $BaTiO_3$, and $KTaO_3$ are best known for their ferroelectric and electro-optic effects. Recent investigations of photoeffects in these materials have produced evidence that this group of materials can be used to fabricate useful ultraviolet photodetectors.

Barium titanate is a clear insulating ferroelectric at room temperature and has a Curie point of 133° C. Heating the crystal in a hydrogen (reducing) atmosphere converts it to a bluish colored n-type semiconductor, presumably with oxygen vacancies. Farrell[54] finds that the magnitude and the spectral dependence of the photoconductivity depend on the defect states due to the oxygen vacancies.
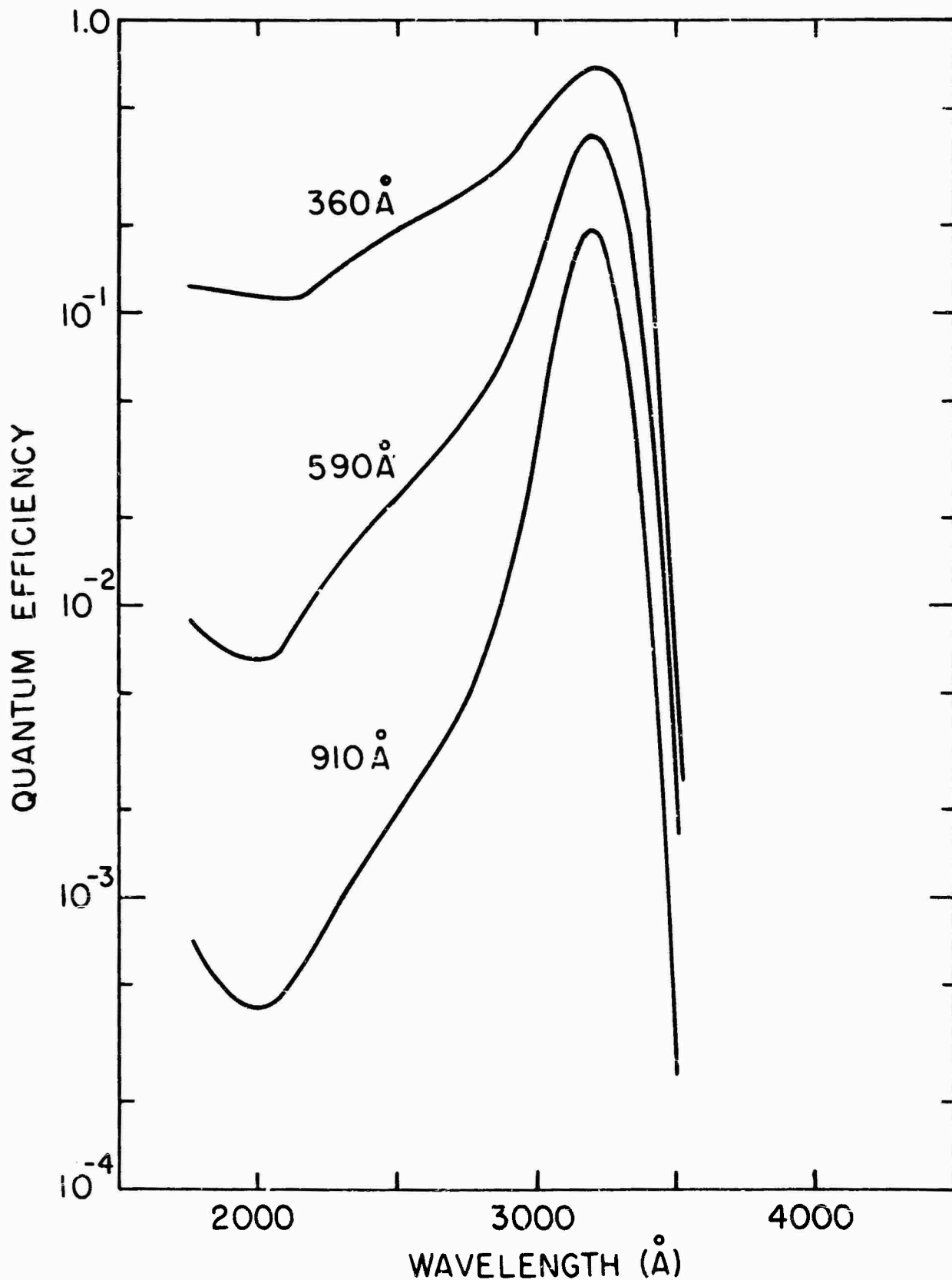
FIGURE 5.17 Measured spectral response of three silver-ZnS photodiodes with different silver thicknesses. (53)

Schottky-barrier photodiodes have been fabricated[55] on barium titanate by evaporating a 140 Å gold electrode onto a hydrogen reduced surface. The spectral dependence of the photogain is shown in Figure 5.18. Strontium titanate, another perovskite, has a bandgap of 3.2 to 3.4 eV. A. K. Ghosh[56] has studied photoluminescence and photoconductivity in insulating (10^{10} Ω-cm) samples of this material.

Recent investigations[57] of the photoproperties of the perovskite potassium tantalate show large photoeffects. Figure 5.19 shows the dependence on wavelength of the photogain for an insulating ($> 10^{14}$ Ω) sample of $KTaO_3$ having two metallic electrodes evaporated on the same surface. The rapid rise in the photosensitivity at ~ 3400 Å corresponds to the absorption edge. The photoproperties of the $KTaO_3$ photodetector depend markedly on the ambient surroundings. Investigations are still in progress to determine the nature of the mechanisms, in addition to photodesorption, which determine the photoeffects in $KTaO_3$.

Both photoconductivity and photovoltaic effects have been observed in titanium dioxide (rutile).[58] A Schottky barrier is formed when Ag is evaporated onto a rutile surface that has been reduced and then reoxidized. The proposed photomechanism is the standard separation of radiation induced electron-hole pairs in the barrier at the interface. Peak response (at 3150 Å) occurs at the wavelength for which the absorption coefficient is high enough for the excess carriers to be generated within a diffusion length of the barrier layer, but not so high that surface recombination effects reduce the responsitivity.

5.4.3.3.3 Metal Oxides

Many of the metal oxides have energy gaps greater than 3.0 eV. Zinc oxide has a bandgap of approximately 3.2 eV and is probably the most widely studied material in this class. The photodesorption of chemisorbed oxygen on the surface is the dominant[59, 60] photomechanism in ZnO.
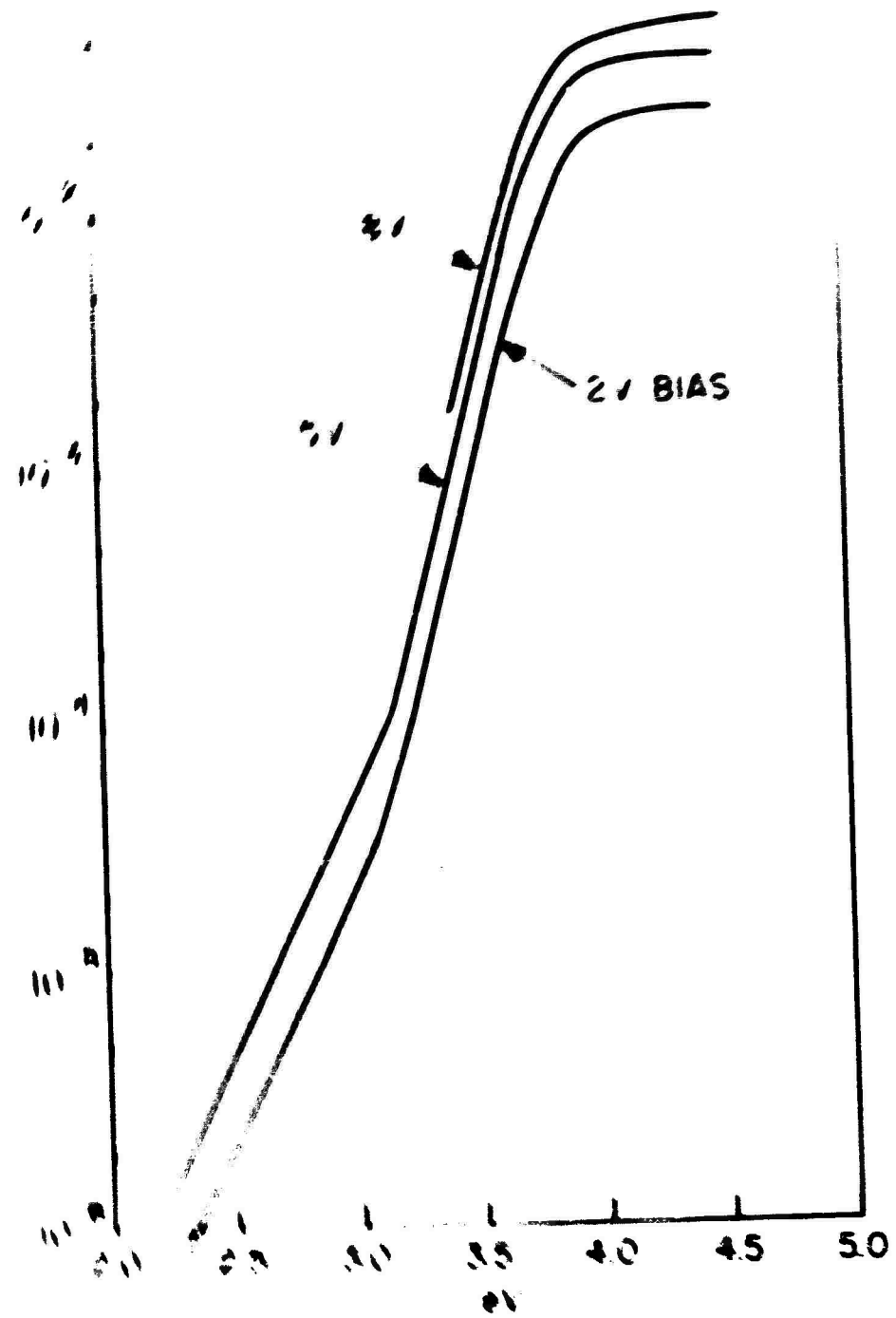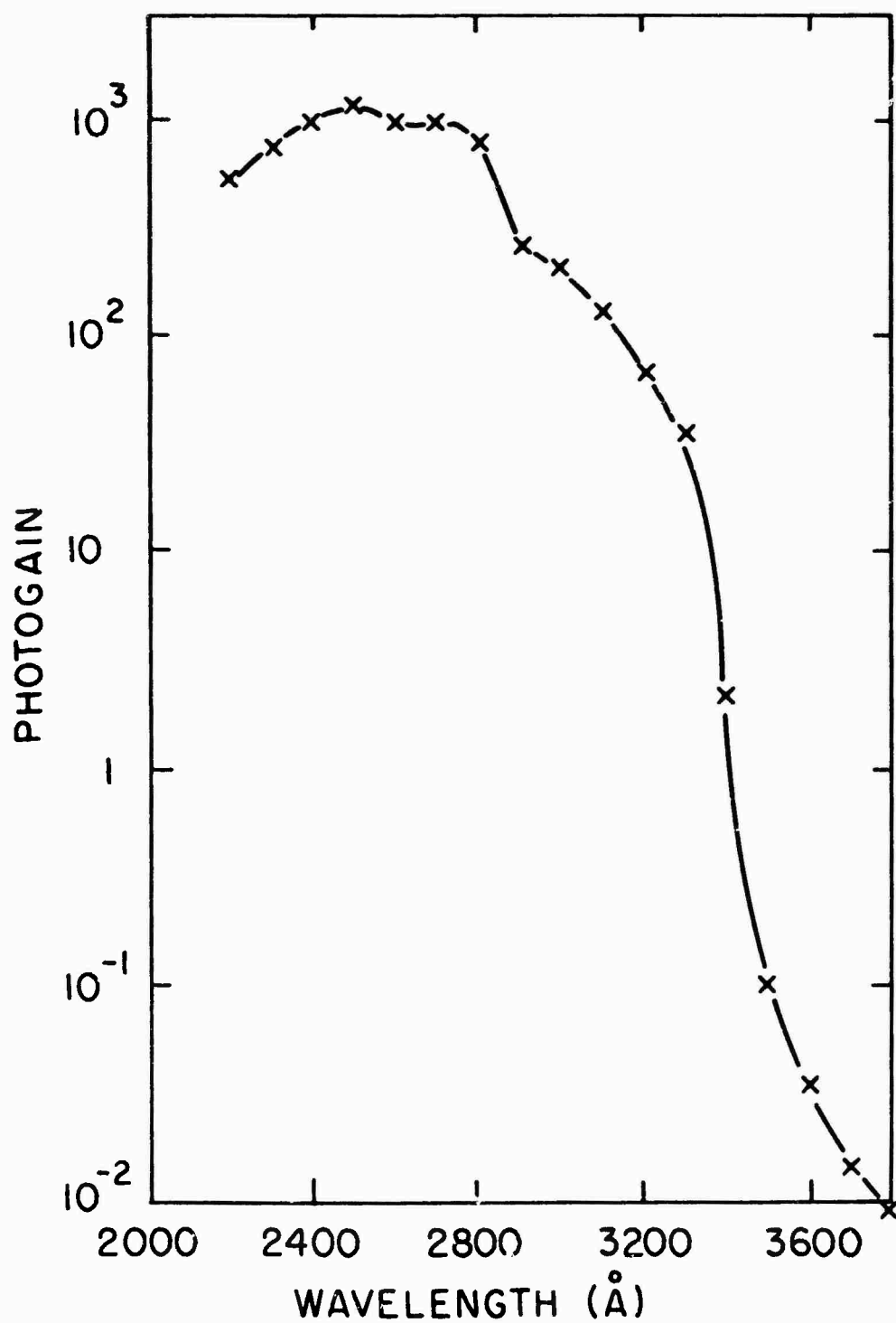
FIGURE 5.19   Photogain versus wavelength for KTaO$_3$ photodetector.(57)

When the sintered sample is irradiated by light near the fundamental absorption edge, electron-hole pairs are formed. A hole formed near the surface is pulled toward the surface where it recombines with an oxygen ion to form a neutral physically absorbed atom which is in equilibrium with the oxygen ambient. The hole mobility in zinc oxide is very small ں that only the holes formed in the barrier can contribute to the desorption. The electron member of the pair is in the conduction band where it enhances conductance. When the light is turned off the inverse process can occur. An occasional electron from the conduction band can surmount the potential barrier at the surface and then combine with an oxygen atom to form a chemisorbed oxygen ion.

Neville and Mead[61] have reported the characteristics of Au and Pd Schottky-barriers on ZnO. They reported the photoexcitation of carriers from the metal over the barrier but did not discuss excitation in the semiconductor depletion layer.

Photoconductivity has been observed in SnO_2[69] with a sharp peak in the photoresponse at the absorption band edge around 3700 $\overset{o}{A}$. The photomechanism in this material is very similar to that in ZnO.

5.4.3.3.4 The III-V Compounds

Most of the III-V compounds have energy gaps that are in the infrared or visible part of the spectrum. While they exhibit some sensitivity in the ultraviolet, their greatest sensitivities are at energies smaller than 3 eV, and generally they are not considered good ultraviolet detectors.

Richardson and Baertsch[63] have fabricated a Ag-GaAs Schottky-barrier ultraviolet detector. The incident radiation passed through the silver electrode into the depletion region of the semiconductor. Since silver has a narrow transmission window near 3225 $\overset{o}{A}$, it can be used to filter out the visible and longer wavelengths, making the device most sensitive in the ultraviolet part of the spectrum. In Figure 5.20 the spectral response of three Ag-GaAs photodiodes with different silver thicknesses are shown. Presumably this same technique could be used to fabricate ultraviolet detectors of material other than GaAs.
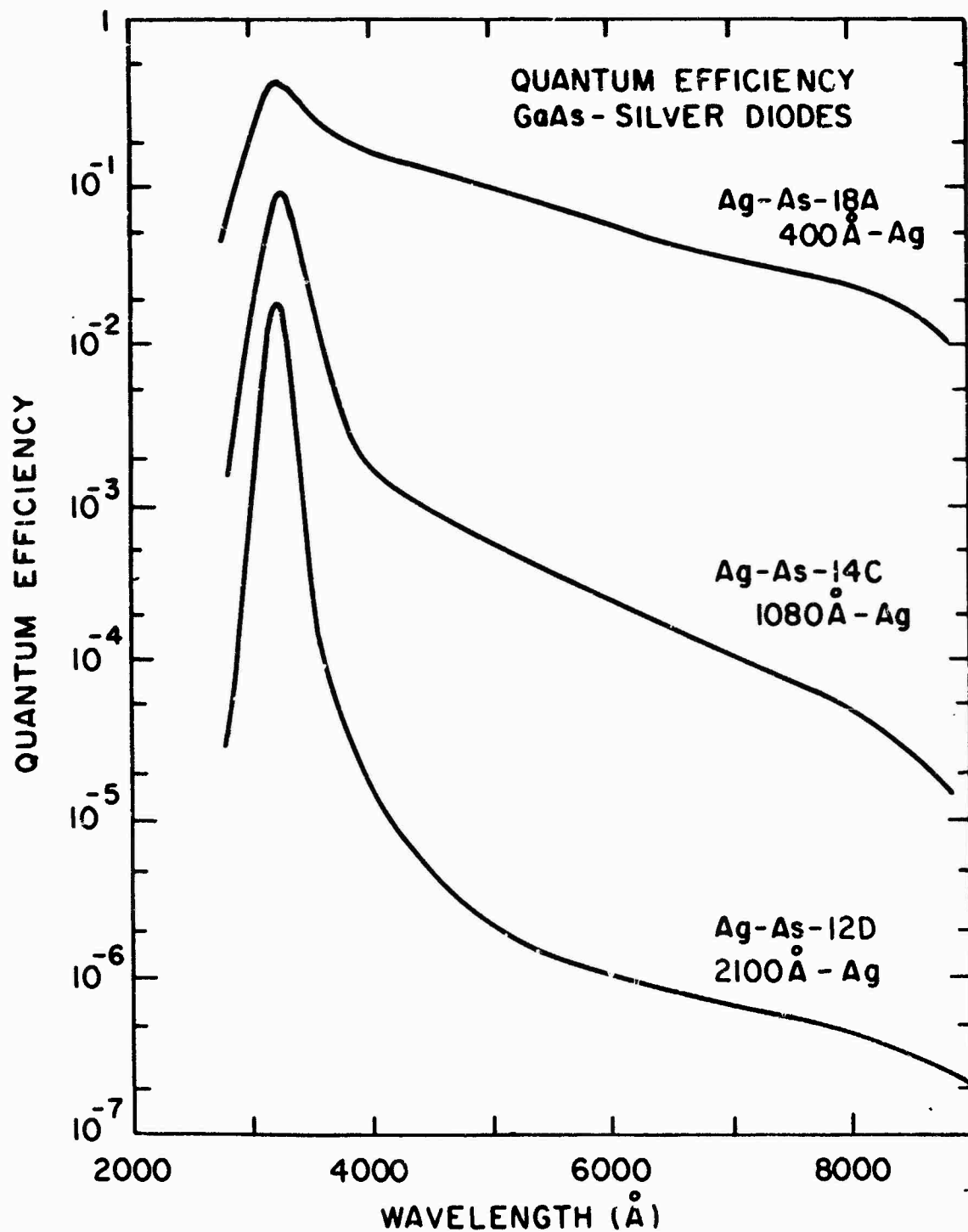
FIGURE 5.20   Spectral response of three Ag-GaAs photodiodes with different silver thickness. (63)

5.4.3.3.5 Group IV Compounds and Elements

P-n junctions fabricated in silicon carbide[64] have been utilized as ultra-violet detectors. SiC has a bandgap around 3.0 eV and hence has its peak response in the ultraviolet part of the spectrum and only a small response in the visible. SiC photodetectors can be operated at temperatures up to 500° C but SiC is a difficult material to work with.

Photoeffects have been observed in diamond,[65] but these effects are small.

Silicon diodes are well known infrared and visible detectors; they are also useful ultraviolet detectors.[66] The quantum efficiency of a Si photodetector is nearly constant in the ultraviolet range (see Figure 5.21) and in fact shows an increase in quantum efficiency as the incident photon energy is increased. They are sensitive to low energy light unless a suitable filter is used.

5.4.3.3.6 Organic Semiconductors (Aromatic Hydrocarbons)

Photosensitivity to the ultraviolet spectrum has been observed[67] in organic semiconductors. Intrinsic photoconduction has been observed in anthracene, benzene, naphthalene, biphenyl, and pyrene. The quantum yield for free-carrier production is low (10^{-4} to 10^{-2}) so that these materials are not very sensitive.

5.4.3.4 Solid-State Imaging

The detection and display of optical images with solid-state cameras has been a decade long goal for both commercial and military applications. The potential advantages of solid-state imaging systems are small size and weight and low-voltage operation. In addition, image processing could be integrated with the detector package.

Solid-state imaging can involve either parallel or serial image processing. In parallel processing, the information from all image elements is processed and displayed simultaneously, in a manner similar to an image intensifier. This type of system needs a frequency bandwidth of only 30 to 40 Hz, sufficiently faster than the eye to avoid image smear for moving targets.
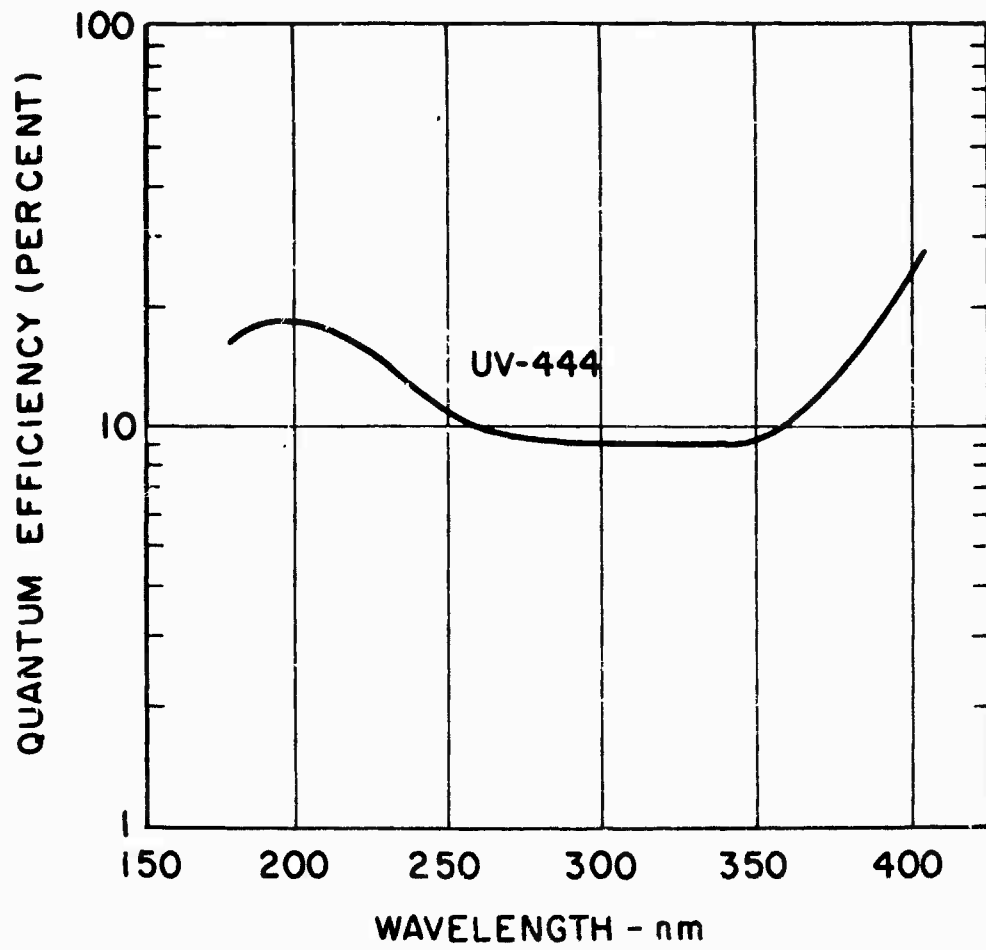
FIGURE 5.21   Photoresponse of typical EG &G UV-444 Si photodiode.

The best example of a serial processing system is a conventional television camera system. The image elements are interrogated sequentially and converted to a pure electrical signal. The bandwidth requirements are much higher for this type of system.

5.4.3.4.1 Parallel Processing Systems

The most popular example of this type of solid state imaging system is the photoconductor–electroluminescent (PC-EL) panel.[68] Basically, the device consists of a layer of electroluminescent phosphor deposited onto a substrate with a conductive coating. An opaque insulating layer is deposited onto the phosphor, followed by a high resistivity photoconductive layer. A conductive coating is then applied to the photoconductor to provide the second contact. The impedance of the photoconductor in the dark is made much larger than that of the electroluminescent layer by adjusting their relative thicknesses. The opaque layer is low impedance compared to the phosphor. Most of the voltage appears across the photoconductor and no output light is observed. If radiation to which the photoconductor is sensitive is imaged onto the panel, the impedance of the photoconductor drops in those areas being illuminated. A corresponding local increase in voltage drop occurs across the phosphor. This results in light emission.

The spectral response of this device is determined by the choice of photoconductor. For a visible input, cadmium sulfide is generally used. Panels sensitive to X-rays also have been made using cadmium sulfide. Zinc sulfide is used for the ultraviolet. In all cases, the useable illumination range is limited by the dark current in the photoconductor at low wavelengths and saturation of either the photoconductor or of the electroluminescent layer at the high wavelengths. Device gain is provided by the photoconductor through minority carrier trapping. The gain is proportional to the square of the photoconductor bias so that for low input levels, high overall biases are desirable. In practice, the allowable bias is limited by:

- Breakdown in the layers.
- By the increase in photoconductor dark current with increased bias.

A PC-EL panel, using cadmium selenide as the photoconductor can be made sensitive down to 10^{-8} w/cm^2 with moderate cooling and still achieve some response in the infrared. At this level, the gain required is so high that the response time becomes exceedingly slow. This is due to the fundamental limitation of the photoconductor's gain-bandwidth product, typically 1 to 10 MHz. At low illumination levels, the minority carrier lifetime increases; the device becomes too slow for practical use. As an ultraviolet detector, however, the integration and storage feature of the panel may be useful at low energy levels if detection of stationary images is desirable or if supplementary image tracking is possible. For X-ray applications, intensities are sufficiently high that response time is not a problem. Panel output for the same X-ray flux will be several hundred times higher than from standard X-ray phosphors.

Variations on the PC-EL theme have been tried over the years with about the same result as noted above at low input levels. Response times could be improved if diodes were used. An array of avalanche diodes would be required in order to make up for some of the lost photoconductive gain. The output phosphor necessarily must be DC activated. This would have lower efficiency than AC activation even at relatively high excitation levels. In principle, a matching array of electroluminescent diodes could be either grown onto the detector array or made separately and mated. The technology for this has not been developed. Even if it were successful, the output would not be bright enough for direct viewing. If the detector and display elements are both highly efficient, an avalanche gain of 10^6 or better is still required. This is well beyond the state of the art.

5.4.3.4.2 Serial Processing Systems

For this type of device the detection function can be treated separately from the display function. The majority of solid-state serially processed systems examined in the past have been mosaics of essentially discrete elements interconnected by XY-addressed power busses. For example, if there are 100 vertical and 100 horizontal lines and a full scan cycle (picture) is completed in 1/30 second, the vertical scan rate is 3kHz and the horizontal rate 300 kHz.

In the simplest case, the detector element is a photodiode connected across the intersection of a vertical and a horizontal line. The photodiode receives bias and is connected to the output load only when these lines are activated. Actually if the resistance-capacitance (RC) time constant of the biased photodiode is sufficiently high (in the dark) and the circuit impedance of the scan switches is high in the open state, the photodiode will maintain a bias charge between its terminals. Light impinging during this time will result in discharging the photodiode. The signal observed when the scan switches are closed is the recharge current. This second mode of operation is more sensitive since the signal integrated over a picture time is read, rather than the "instantaneous" value during the element "on" time.

Early work in serial processing was with thin-film photoconductor-diode detector elements and scanning circuits. Recent emphasis has been on the application of monolithic integrated circuit technology to silicon imaging arrays. This approach has introduced a variety of problems and complicated device schemes.[70] Some of the problems are:

- Photoconductive or photovoltaic crosstalk between elements
- Insertion of switching transients into the readout line through parasitic capacitances
- Difficulty in achieving full picture storage time
- The small amounts of charge to be read out in high-density arrays

Most problems are due to array design and layout, to processing limitations or to the inherent properties of integrated circuit technology. It is, in fact, the nature of these problems that makes the surface charge-coupled approach so attractive for future solid state imaging devices.

The requirements for detector materials with extended infrared response are basically the same as those for good single element photodiodes: high-quality basic material (defect free), low trap density, and, for compounds and alloys, good composition control and stoichiometry. In addition, controllable diffusion and growth characteristics, surface passivation technology, and large area (~ 1 cm^2 or better)

172

uniformity are necessary for arrays. Since the passivating layer is frequently used as the diffusion mas' 'n making planar devices, low permeability of the layer to diffusants at the diffusion temperature is necessary. SiO_2 is generally used for passivating germanium and the III-V compounds since it can be deposited at relatively low temperatures. Its use as a diffusion mask in germanium is limited since it reacts with aluminum, the most popular p-type dopant for germanium, at the diffusion temperature. Attempts to use silicon nitride and aluminum oxide as mask/passivating layer have been reported but are only marginally successful. Decreasing commercial interest in germanium devices due to the dominance of silicon planar technology makes military support critical when germanium is needed for military detector applications. In the case of the III-V compounds, the technology is still in an early stage of evolution. but military interest and support has been significant in the progress made to date.

Special mention should be made of the uniformity problem for imaging arrays. Non-uniformities in dark current and shorted or leaky elements in the array give a fixed pattern noise in the output. Non-uniformity of sensitivity caused by variations in doping or composition also will produce a fixed pattern noise. However, a number of completely shorted elements scattered over the array may be cosmetically objectionable but tolerable for a military system where cost is a consideration.

5.4.4 Television Camera Tubes

Imaging systems using currently available television camera tubes are extremely sensitive and versatile. They present an image of acceptable quality over a wide range of scene illumination intensities. At moderate light levels, photoconductive targets are used with low light level performance, primarily limited by preamplifier noise. Operation at lower light levels consequently requires gain before the storage target. This is most frequently accomplished by use of electron-bombardment gain in a suitably chosen target. Photon-to-electron conversion then is performed by a photocathode at the tube input. If sufficient target gain and photocathode sensitivity are not available, an additional stage of image intensification is required in front of the camera tube. At these light levels, resolution is limited by shot noise in the converted input image.

Several types of storage targets are in use, the most recent being the silicon diode array target. A brief discussion of the interaction between the readout mechanism and the target provides some perspective on the problem associated with this type of device; the diode-array target with vidicon scanning is used as the example.

The use of silicon planar technology in the silicon diode-array target[71] has been the key to its rapid, successful development. The basic target structure has p-type islands diffused into high-resistivity n-type silicon through an SiO_2 diffusion mask. Metal or semiconductor contact pads are deposited and delineated by etching. A high-resistivity semiconductor such as antimony trisulfide is frequently used in place of the pads to form a resistive "sea."

The target diodes are biased by the electron beam that scans the side with the p-type islands. The n-type substrate is held at a positive bias with respect to the cathode of the scanning electron gun. Electrons landing on the target charge the diode capacitances to cathode potential, at which point the electron beam is repelled. Photons or electrons falling on the target (from the opposite side) generate holes in the n-type material. These holes reach the junction and discharge the junction bias. The scanning beam replaces the lost charge on the next scan, generating a video signal in the target load circuit.

The quantum efficiency of the target can be as high as 80 percent if anti-reflection-passivation coatings are used. In the electron bombardment mode of operation, gains reach values over 1000 above 7kV accelerating voltage. At voltages below 2kV, the gain drops faster than the voltage due to surface recombination at the input side of the target. Treatment of this surface (passivation, a shallow n^+ layer) can reduce this effect. The drop off in gain has some advantage when automatic gain control is used.

Target dark current is typically about 10 nA at 10 volts of target bias. The number of shorted or dead diodes is usually below 50 for the entire scanned area of several hundred thousand diodes. This is an excellent rate; many targets are fabricated with fewer than 10 defects. The diode-array target resists pattern burn-in caused in other targets by input overloads. A remaining problem for engineering design is the "blooming" that occurs with large input levels that are fairly localized. The diodes under the high level image are rapidly discharged, and holes then generated go instead to adjacent diodes.

With the exception of dark current, defect density, and blooming the silicon diode-array target is operating almost as well as can be expected. Improvements in resolution can come about by:

- Increasing the packing density of diodes (a problem in photo-lithography or the application of electroresist techniques)

- Reducing beam diameter

- Increasing the size of the target

Reduction in beam diameter, however, is limited by defocusing, due to space charge effects in the beam for constant beam current. Extensive improvements in low light level camera tubes can be achieved through incorporation of photocathodes with higher sensitivity, particularly in the infrared, such as the III-V photocathodes discussed in 5.4.1. Size and weight could be reduced by using a transmission secondary electron multiplication dynode in place of the additional image intensifier stage now used. Incorporation of a cold cathode electron source with a narrow electron energy spread could improve the signal handling at high input levels. Target degradation now occurs as a result of damage to the oxide mask by soft X-rays generated when the electron beam strikes the grid of the electron gun facing the target. Targets with a resistive "sea" are less susceptible since X-rays are absorbed in the coating material. Damage in this material accumulates, however, and leads eventually to the same result.

The silicon diode array vidicon used as a photon sensor is sensitive to a power level of about 10^{-8} w/cm^2 on the target, limited primarily by video preamplifier noise in a 10 MHz bar width. This threshold level is too high for imaging under airglow conditions with any reasonable optical system. Schottky diode arrays[72] generally have higher dark currents. Diffused phototransistor arrays[73] have major problems: dark current, gain variations, and defect density are higher than in diode-array targets due to the more sophisticated target processing required. Target gain as high as 70 from transistor action has been demonstrated without insertion of additional noise. If gains of 50 could be achieved uniformly in a high-density array, the additional stage of intensification could be removed from the intensified diode-array vidicon. However, the sensitivity would still be insufficient for detection of reflected airglow radiation, an important military application.

The diode-array target concept can be extended to other infrared-sensitive materials if the appropriate technology is developed. Sone work has been done with germanium[74] and indium arsenide.[75] A germanium target would have the correct spectral response to intercept a large portion of the airglow spectrum but insufficient sensitivity to provide good signal to noise ratio. A gain of 50 would be necessary. The technological problems of a transistor-type germanium target are far greater than with silicon targets, where much work remains to be done. Target cooling would be required to reduce dark current to an acceptable level.

The spectral response of indium arsenide makes it a potential candidate as a target for the 3 to 5 μm band of thermal radiation; vidicons for this spectral band are discussed in Chapter 6. The materials and device technology required for the III-V compounds are basically the same as for single element detectors, with the additional requirement of large area uniformity. Gallium antimonide is a logical choice for use in an airglow detector but the difficulties in achieving acceptable control over doping levels and passivation have limited its use. The ternary III-V alloys can be expected to have problems in compositional control, as well as problems in doping and passivation, for devices of the required area.

5.5. Detectors under Study

5.5.1 Field-Assisted Photocathodes

The photocathodes discussed thus far have depended either on sufficient photoelectron energy to provide the photoemission or, in the case of NEA photocathodes, on a combination of natural internal field and low work function for high-efficiency photoelectric emission. Potentially available materials cannot be used for response beyond 1.1 μm due to the surface restrictions. An alternative method of getting infrared response is field-assisted photoemission (FAPE). Here an applied electric field assists the emission of a photoelectron initially insufficiently excited to surmount the surface barrier. The electron may be accelerated in a high field region and/or the barrier may be lowered by the field. In principle, the long wavelength threshold of a field-assisted photoemitter is limited only by the bandgap absorption of the bulk material. In most cases, the concept can be successfully demonstrated but limitations in technology or fundamental processes have so far precluded reduction to practice, particularly for imaging devices.

The field-assisted photocathode in semitransparent form can be characterized by the internal quantum efficiency (see 5.2.1) and the independent escape probability. The escape probability for a FAPE device is a function of the applied bias and it is affected by the several layers of materials that may be present.

5.5.1.1 External Field Enhancement

External field-assisted photoemissive devices have been made. At externally applied fields less than 10^6 volts/cm, Schottky lowering of the barrier provides improved response, particularly at the long wavelength threshold. This has been observed for both regular and NEA photocathodes using fields of about 10^4 volts/cm. At higher field-strength, extraneous emission from other parts of the tube structure is seen.

The silicon diode array vidicon used as a photon sensor is sensitive to a power level of about 10^{-8} w/cm^2 on the target, limited primarily by video preamplifier noise in a 10 MHz bandwidth. This threshold level is too high for imaging under airglow conditions with any reasonable optical system. Schottky diode arrays[72] generally have higher dark currents. Diffused phototransistor arrays[73] have major problems: dark current, gain variations, and defect density are higher than in diode-array targets due to the more sophisticated target processing required. Target gain as high as 70 from transistor action has been demonstrated without insertion of additional noise. If gains of 50 could be achieved uniformly in a high-density array, the additional stage of intensification could be removed from the intensified diode-array vidicon. However, the sensitivity would still be insufficient for detection of reflected airglow radiation, an important military application.

The diode-array target concept can be extended to other infrared-sensitive materials if the appropriate technology is developed. Sone work has been done with germanium[74] and indium arsenide.[75] A germanium target would have the correct spectral response to intercept a large portion of the airglow spectrum but insufficient sensitivity to provide good signal to noise ratio. A gain of 50 would be necessary. The technological problems of a transistor-type germanium target are far greater than with silicon targets, where much work remains to be done. Target cooling would be required to reduce dark current to an acceptable level.

The spectral response of indium arsenide makes it a potential candidate as a target for the 3 to 5 μm band of thermal radiation; vidicons for this spectral band are discussed in Chapter 6. The materials and device technology required for the III-V compounds are basically the same as for single element detectors, with the additional requirement of large area uniformity. Gallium antimonide is a logical choice for use in an airglow detector but the difficulties in achieving acceptable control over doping levels and passivation have limited its use. The ternary III-V alloys can be expected to have problems in compositional control, as well as problems in doping and passivation, for devices of the required area.

The region above 10^6 volts/cm has been thus far restricted to point emitters, using material such as Ge,[76-80] Si,[77-80] and GaAs.[81] The results indicate photoconductive control of the emission current, and high dark currents are usually present. Response from extrinsic absorption extends the spectral sensitivity beyond the intrinsic threshold. While this approach may be practical for photomultipliers, large area photocathodes for image intensifiers would require a matrix design. A point emitter matrix may be obtained by etching the pattern using an oxide mask so that the etch undercuts the oxide.

The lower threshold of such a device will be limited by the dark resistance of the semiconductor. In the photoconductor controlled mode of operation, the best results would be obtained with intrinsic material. While photoconductive gain is possible, the response time would then suffer. This technique should not be discarded, however, until more thorough studies have been made.

5.5.1.2 Schottky Diode

Reverse-biased, metal to p-type semiconductor Schottky contacts are also used. This approach is similar to the NEA effect, except that the surface layer is more metallic. For the Schottky contact, photoelectron energy losses in the depletion layer and contact metal drastically reduce the quantum efficiency unless both are sufficiently thin. The depletion layer must be thick enough, on the other hand, to suppress hole tunneling under bias and the metal contact thick enough to remain an equipotential under current loading. In principle, it is possible to obtain band edge response with this structure at longer wavelengths than the work function of the metal (activated with cesium or cesium oxide). In practice, this has been observed at low quantum efficiencies for Si-Al:Cs diodes.[82]

The detector material for this device can be chosen from a wide variety of p-type materials. The basic materials technology developed for NEA photocathodes (see 5.4.1.5) can be extended, with the use of narrower bandgap materials and the additional requirement that a bias be applied to the surface.

An importan' criterion for the metal contact material is the height of the potential barrier between it and the p-type semiconductor. Elementary theory requires that the metal work function be smaller than tha: of the semiconductor if a positive hole barrier is to be achieved. Measured values[83] of Schottky-barrier heights on p-type semiconductors indicate a stronger dependence on the properties of the interface than on the work function difference, even when the latter is nearly 1 eV.

It is clear that extensive additional work is needed to characterize the metal-semiconductor contact, in spite of the large amount of effort that has already been expended. This is particularly true in the case of the III-V alloy system that would be of interest for this photocathode. Natural choices of metallic layers are the alkaline and alkaline earth metals, singly or in combination, that could serve also for low work function activation. The sheet resistance of the layer is also important. A systematic study of these metals on GaAs and eventually on GaInAs layers should be of value. Low energy electron diffraction and Auger spectroscopy can be used to establish the surface conditions and the species present in the contact. The surface cleaning techniques that have been successful for NEA photocathodes should naturally be used here as well. In analogy with the S-1 photocathode, silver is a potential candidate for the contact metal.

5.5.1.3 P-n Junction

Band edge photoemission has been observed from both Si[84,85] and Ge[86,87] reverse-biased p-n junction, but with low quantum efficiency. Emission occurred only from the neighborhood of the junction intersection with the surface. Attempts to produce sufficiently shallow layers for emission through the n-layer (or p-substrate) have been unsuccessful so far. Alternatively, a design must be developed that yields a large junction area at the surface with a large fraction of the p-type surface exposed. Activation with cesium oxide produces both a low surface work function and a bent band region under the surface. These can be utilized to increase the escape

probability with applied bias. While the conductivity of the n-type region should be high to maintain a uniform surface potential, the doping density could be reduced if a metallic layer could be deposited on top of any n-type material exposed on the semiconductor to provide high conductivity. Since the semiconductor must undergo a heat treatment before activation, the choice of material for the metallic layer must be made with this processing step in mind.

In order to develop the p-n junction photocathode, activation studies should be made with chosen metal and metal oxide layers on Ge and III-V materials with differing bandgaps and orientations. Since junction formation is necessary, the appropriate technology must be developed for the material and configuration selected.

5.5.1.4 Photon-Induced Tunnel Emitter

Electron tunneling in solids also could be used to provide field-assisted photoemission.[88] Photon-induced tunnel emission is basically a minority carrier process. The theory for minority carrier tunneling has been developed for metal-insulator-semiconductor (MIS) diodes.[89] In the tunnel emitter the metal is replaced by an appropriate emitter layer, and the quantum efficiency derived for the MIS diode is multiplied by the transfer efficiency of the emitter layer to yield the device efficiency. The semiconductor is p-type and biased negatively with respect to the emitter layer.

Tests have been conducted on emitter structures[89] which used silicon as the detector, silicon nitride or aluminum oxide as the insulator, and gallium phosphide treated with cesium for the emitter layer. The feasibility of the basic concept was successfully demonstrated; but, the transfer efficiency of the gallium phosphide was generally less than 0.1 percent. The best transfer efficiency achieved was 6 percent but reproducibility was poor.

The basic structure lends itself well to planar techniques. Since the insulators in the structures in the preceding paragraph were amorphous, the gallium phosphide was generally polycrystalline, leading to poor emitter efficiency. Recent results[90] on a thin-film emitter layer consisting of cesium oxide-treated silver have shown that transfer efficiencies of 10 percent are reproducibly achievable and values as high as 20 percent have been observed.

Several materials problems require further work in connection with this device. Little has been done on the deposition of thin (50 to 500 Å) insulators onto semiconductors for use as tunneling barriers. The growth of the appropriate insulator must be compatible with the semiconductor in terms of thermal, environmental, and mechanical properties. Thus far, thermal oxidation (SiO_2 on Si) and vapor-phase growth (Al_2O_3 and Si_3N_4 on Si) have been used successfully, while other techniques such as vacuum evaporation and radio frequency sputtering have been unsuccessful. The basic criteria to use in choosing an insulator are the dielectric field strength ($> 10^6$ V/cm) and the barrier height (preferable < 2 eV). In addition, the dark current and efficiency of this type of device are strongly influenced by interface states at the semiconductor-insulator boundary. Pinhole defects in the insulator must be avoided; variations in thickness of the insulator as large as 10 percent can be tolerated, because the device is operated under conditions of saturation of the photocurrent as a function of bias.

The emitter layer also offers problems. In the case of thin semiconductors such as cesium-treated gallium phosphide or cesium oxide-treated gallium arsenide layers, it is unlikely that single crystalline layers can be obtained. While vapor-phase deposition has not yet been attempted, the nucleation of these materials on amorphous substrates is poor and controlled growth of the necessary thin layers, (1000 to 2000 Å) difficult.

5.5.1.5 Double Heterojunction Photocathode

This device[91] is basically a three-layer structure similar to the tunnel emitter except that the insulator is replaced by a high-resistivity, wide-bandgap semiconductor. Two structures were proposed: p-Ge/ν-GaAlAs/p-GaAs and p-Ge/ν-ZnSe/p-GaAs. If ternary III-V alloys are substituted for the germanium, a variety of additional combinations are possible. It is the purpose of the wide-bandgap semiconductor to block hole current from the gallium arsenide to the germanium when bias is applied such that the germanium has the most negative potential. The materials must be chosen so that: the electron affinity differences are small (to avoid electron barriers at the heterojunction interfaces) and the mechanical properties of the materials match (to suppress interface state formation at the junctions).

The double heterojunction approach has the potential advantage that it can utilize the developing technology for thin-film III-V compounds and ternary alloys. However, all three layers require efficient transport of the minority carriers. In the absence of interface barriers and recombination sites, the quantum efficiency can be factored into the product of: the internal efficiency of the germanium detector, the transfer efficiency of the middle semiconductor layer, and emission efficiency of the gallium arsenide emitter layer when activated with cesium oxide. Long diffusion lengths are required. Considering the known difficulties of providing a single thin-film semiconductor with a long diffusion length and a high degree of uniformity, this approach may be beyond the state of the art at this time, but it has sufficient potential to warrant some research effort.

The problem of interface barriers and states has been encountered to some degree in all of the previous work on heterojunction devices. In addition, interdiffusion between the two constituents of a heterojunction can occur and may be confused with a barrier, or high recombination state density, since doping inversion and consequent homojunction formation could result. Clearly, considerable skill and technique are called for in this device fabrication process.

As a final point, the heat treatment currently required to activate gallium arsenide is near its decomposition temperature of about 610° C. This heating process could significantly disturb the junctions in the material. For this application, therefore, a lower temperature technique must be developed to clean and activate the gallium arsenide emitter layer. This would also benefit III-V NEA photocathode processing.

5.5.2 Charge-Coupled Devices (CCD)

Solid state devices for image pickup and processing components were discussed above. As indicated, high resolution implies high packing densities for the sensitive elements. Under these conditions, the detectors are connected by the scanning circuits to the bias lines and switching transients are introduced as noise into the video signal at low signal levels by the capacitative coupling between elements at high densities. In addition, sophisticated arrays require a large number of diffusion and oxidation steps which degrade the quality of the detector material.

A new technique known as surface charge coupling[92] has been proposed to circumvent these problems. The device is an extension of MOS transistor technology on silicon to the area imaging problem. In its simplest form, a two-dimensional array of pads is deposited onto a uniformly oxidized silicon wafer forming an array of MOS capacitors. When bias of the proper polarity is applied to one pad with the remainder held at zero bias, the semiconductor surface under the biased pad will become depleted, forming a potential well. Minority carriers, generated either optically or thermally, will collect in the well until the saturation level is reached. This charge may be transferred to an adjacent pad by setting its bias greater than or equal to the level of the original pad and dropping the bias of the first pad to zero. By this means, the original charge can be transported across the wafer to an output sensor. (More information on design configurations and considerations can be found in References 93.)

The bulk material for these devices functions as the detector with charge processing taking place along one particular surface. The requirements for the bulk material are similar to those of other detectors previously discussed. At the processing surface, the passivation requirements are far more stringent and the choice of passivating gate oxide more critical if distortion-free image reproduction at low input levels is to be achieved. The signal can be extracted at the end of the transfer chain by coupling through an integrated field-effect transistor with a gate capacitance on the order of 10^{-15} farads so that kTC noise (the Johnson noise equivalent for a capacitative load) is negligibly small. The capacitative coupling means that the DC level of dark current is suppressed but spatial variations and shot noise must still be considered in relation to the image signal.

Fast interface states at the semiconductor-insulator boundary and slow states in the oxide play a dominant role in determining the performance of a CCD. Passively, these states act as recombination centers, reducing device efficiency; actively, they are a source of dark current and reduce the device integration time. In addition, the slow oxide states may store charge during the integration cycle which is slowly and randomly released during read-out transfer. This effect may result in a phenomenon similar to streaking in conventional TV systems. For an overall low level signal, an additional noise component is introduced due to the random absorption and reemission during transfer. Further, the width of a video signal pulse is ideally determined by the drift/diffusion time of charge from one gate site to the next but may be lengthened by emission from slow oxide states, thus reducing the transfer efficiency of the device and as a result its resolution.

Effective CCD units have, as yet, only been made with silicon due to its advanced technology and in particular the availability of SiO_2 as high-quality passivating gate oxide.

184

The situation with regard to other potential detector materials is worse due to the lack of a passivating gate material of sufficient quality for this device. The objectives of current research on silicon are to improve the resolution by going to larger array densities at high transfer efficiencies and rates and to suppress noise due to the slow states in order to provide a practical solid state camera at or below airglow illumination levels. The next logical step is to extend this technique to suitable narrow-bandgap semiconductors to detect radiation over the near-infrared portion of the airglow band and, in particular, to sense far-infrared thermal images in the 2 to $14\,\mu$m range.

The far-infrared (FIR) application places slightly different requirements on the CCD than low level airglow detection. The storage mechanism of the CCD has an upper limit on stored charge density related to the oxide capacitance and the bias. An incoming signal exceeding this saturation charge over an integration time will be lost and at high input levels the charge stored becomes a sublinear function of the input so that contrast is lost before saturation is reached. This is an intrinsic property of the mechanism and operating conditions of the device even if suitable materials can be obtained. Since FIR images are superimposed on a large radiation background and are low contrast images to begin with, this situation would be intolerable, shot noise effects aside. The potential solution to this problem is restriction of the spectral response of the detector material by appropriate selection of the bandgap. Further, the transfer technique allows passage of small, differential charges by a suitable choice of transfer gate bias, allowing some suppression of background level in addition to the capacitative output load. Shot noise in the background radiation then determines the sensitivity of the device. The potential advantage of this technique for the FIR is the projected low system cost in comparison with mechanically scanned systems.

Two general approaches are possible for both airglow and FIR sensor arrays. First, the narrow bandgap semiconductor can be used for a separate, photosensor mosaic which is then interfaced with a silicon storage and transfer array for signal

processing. The approach has the advantage of using available silicon technology for the transfer device and separating out the problems of the detector material. The interface between the two arrays would require advanced techniques. Second, a monolithic structure would be constructed directly on the detector material itself. A research program on this approach requires a large side effort on the development of MIS technology for suitable narrow-bandgap materials such as germanium, gallium-indium arsenide, indium arsenide, and indium antimonide. The achievement of low densities of both fast and slow interface states is the most important factor. For FIR devices, the slow state effects may be less important since transfer lines of 200 to 300 may be adequate and transfer efficiencies of 80 to 90 percent acceptable.

The long range-promise of this technique is chiefly in small, cheap, highly sensitive image detectors for both near- and far-infrared military applications and as such it should receive considerable attention. Since silicon technology is so far in advance, the results of this work will have an important bearing on the eventual feasibility of devices developed from other detector materials. The outcome of the silicon work should thus be used as a guide for the development of new CCD materials technology, keeping in mind the compromises that may be implied by a specific device application.

5.6 Conclusions and Recommendations

In the earlier parts of this chapter, we have attempted to develop a picture of the status of relevant materials and device technology for radiation detectors in the 0.1 to 2.0 μm spectral range. In the conclusions drawn here, the detector applications have been divided into those involving imaging and those which are not imaging detectors. Priorities in the range 1 (high), 2 (moderate) and 3 (low) have been assigned within each of the two groups.

5.6.1 Imaging Detectors

The use of imaging devices in military systems is primarily oriented toward low light level detection and recognition of targets where illumination is a combination of night airglow and varying levels of moonlight. While searchlights and lasers may be used as well, the observer is most secure when using ambient radiation reflected from the scene.

The performance of state of the art imaging systems under these conditions is limited to quarter moonlight by the low sensitivity to airglow of the multalkali

photocathodes used by these systems as detector surfaces. The limitation is imposed by the shot noise in the photocurrent, resulting in poor resolution and hence short effective operating ranges as illumination intensity is reduced. The poor airglow conversion efficiency of multialkali photocathodes is due to the poor response of these photocathodes to the infrared airglow spectrum from 0.9 to 1.8 μm where a hundred times more radiation is available. A photocathode with a peak efficiency of 10 percent (equivalent to a multialkali in its sensitive range) in this spectral range crudely means achieving the same operating range as current image intensifiers but at 100 times lower light level, assuming the system resolution is better than the shot noise limit at this light level.

A practical trade-off occurs as detector response is extended further into the near infrared. Cooling usually will be required to maintain signal contrast which would otherwise be reduced by uniform dark current levels, reducing the effective operating range. The cooling, however, adds to the weight and power requirements of the system and should be minimized. When selection of a material and detector approach is made for development of a component, whether photocathode or solid state detector, the ultimate cooling needs of the detector, desired performance levels, and system constraints must be considered.

5.6.1.1 Conclusion on GaAs Photocathodes

The semitransparent, negative electron affinity photocathodes have shown considerable promise under laboratory conditions. The use of single-crystal materials for both active detector layer and substrate have been advantageous in the development of these photocathodes, together with a relatively simple activation process. This has introduced the twin problems of finding a substrate material compatible with a given photocathode layer and of developing techniques for depositing uniform, strain-free layers over practical areas.

Substrates have been found for the GaAs photocathode with a high degree of compatibility, notably GaAlAs and GaInP. In most cases, these have been grown previously onto thick GaP wafers. This photocathode is well along in the R&D cycle

including investigation of its imaging properties in simple image intensifier tubes. The most significant materials problems remaining are the uniformity of the photo-cathode since hillock formation during growth or activation indicate insufficient nucleation density and residual strain in the GaAs layer due to substrate preparation and growth conditions. Techniques have recently been demonstrated for eliminating the GaP starting wafer, including sealing the GaAs with a passivating layer, such as GaAlAs, directly onto a glass faceplate or of etch-thinning the GaAs by either chemical or electrochemical means. The etch-thinned wafers with a thin passivating layer have good potential for use as a relatively high gain (100 at 5kV primary energy) transmission electron multiplier dynode.

Recommendation (Priority 1)

Continued materials research on the GaAs photocathode is recommended because of its intrinsic worth as a high performance photocathode and because the information fallout from this material has helped guide work on more complicated photocathode layers. Specific studies should include investigations of preparation techniques for GaAlAs and GaInP substrate and substrate surfaces including uniformity of resistivity and optical transmission and the growth parameters of GaAs on these substrates by vapor- and liquid-phase epitaxy. Techniques for sealing GaAs to glass faceplates and of etch-thinning GaAs wafers should be investigated to eliminate the expensive GaP substrate and reduce photocathode costs.

5.6.1.2 Conclusion on the Alloy GaInAsP and Quaternary Alloys Useful at 1.1 μm

The quaternary alloy GaInAsP appears, from recent preliminary data, to offer a useful alternative to InAsP and GaInAs as a NEA photocathode sensitive to 1.1 μm. Within this alloy system, it is theoretically possible to find a composition that will retain much of the good transport properties of InAsP. The increasing gallium content makes GaInP a suitable substrate whose bandgap increases correspondingly, producing, in effect, a wider spectral sensitivity band. The activation process is not expected to differ from that of the corresponding ternary alloys. The results of stability studies on these ternary alloys can be expected to be applicable to the quaternary system as well.

Recommendation (Priority 1)

A study of the growth and transport properties of the quaternary alloy GaInAsP should be supported over the range of compositions from InAsP to GaInAsP and corresponding to a bandgap of 1.1 eV. Work on other quaternary alloys which may also operate in this range should be supported.

5.6.1.3 Conclusion on Ternary III-V Compound Alloys

NEA photocathodes sensitive at $1.06\,\mu m$ use the ternary III-V alloys, $InAs_x P_{1-x}$ and $Ga_x In_{1-x} As$ where $x \approx 0.15$, as the active layer with the InAsP producing the best results. The substrates which have proved effective for semitransparent operation are InP and GaAs, respectively, but the spectral band over which the resulting photocathode is sensitive becomes severely limited, particularly for InAsP on InP. For applications where narrow-band response is desired to discriminate against all but laser radiation, these photocathodes are superior. At present, the only obvious broad-band substrate for InAsP is $AlAs_x Sb_{1-x}$, $x \approx 0.5$. This alloy tends to oxidize in air but it may be possible to grow the alloy onto GaAlAs with Ga:Al = 1:1 followed by InAsP using multiple-well liquid epitaxy. For GaInAs, the alloy $Ga_x In_{1-x} P$ with $x \approx 0.6$ could be used as the substrate, but it can be anticipated that nucleation problems encountered in growing GaAs onto GaInP will be found to occur in the growth of GaInAs onto this substrate until more information is available on the surface chemistry and growth dynamics related to this substrate material.

These photocathodes in both semitransparent and opaque operation and in both laboratory and tube environments show considerable decay in performance with time, originally thought due to a greater sensitivity to ambient contamination than GaAs photocathodes due to the narrow band gap. Some evidence exists, however, for insufficient cleanliness of the film surface before activation with subsequent nucleation of the Cs:O layer about the contaminant. Increasing care in cleaning has produced positive results but the data are not conclusive. While the character of the Cs:O layer is fairly well understood for GaAs and Si NEA photocathodes, such is not the case with the ternary alloy photocathodes.

<u>Recommendations</u> (Priority 1)

(a) The alloy AlAsSb should be investigated as a broad-band substrate for InAsP to improve the airglow efficiency of the NEA photocathode. The stability of this photo-cathode should be investigated more thoroughly with particular emphasis on the impact that small levels of surface and ambient contaminants have on the sensitizing Cs:O layer. This work should be complemented with more definitive studies of the character of the Cs:O layer and the nature of the activation process itself for the InAsP photo-cathode.

(b) Studies of GaInP as a substrate for the GaInAs NEA photocathode should be supported with emphasis on the substrate surface chemistry and the growth dynamics of the GaInAs layer. The stability of the activation process, the effects of surface and ambient contamination, and the character of the sensitizing layer should be investigated to reduce this photocathode to a practical device.

5.6.1.4 Conclusion on Silicon Charge-Coupled Devices

Within the past few years, silicon charge-coupled devices have developed into the most promising approach to solid state imaging available at this time. The basic feasibility of this approach has been demonstrated for small numbers of image elements and for correspondingly low scan rates. These devices demand considerably more from silicon MOS technology, however, than MOSFET devices since the acceptable surface state density is lower. The surface states constitute an additional noise source which masks the others present, particularly those states with lifetimes near the inverse of the line scan frequency and they reduce the transfer efficiencies that can be achieved. Unless this limitation can be removed, either array densities will remain small or scan rates must be reduced to maintain transfer efficiency; in either case, image resolution and acceptability will be sacrificed.

<u>Recommendations</u> (Priority 1)

(a) Support is recommended for development of high-efficiency, high-density silicon charge-coupled devices for imaging at standard video rates and with element numbers of at least 500 x 500.

(b) Until the feasibility of the silicon charge-coupled device is demonstrated for this application, similar programs on other detector materials are likely to prove wasteful and are not recommended. The superiority of silicon MOS technology makes it a useful guide to the problems of and, potentially, the solution to later development programs on other materials once the surface properties of these materials are better understood.

5.6.1.5 Conclusion on Materials for Field Assisted Photocathodes

The Cs:O sensitizing layer does not appear capable of producing practical sensitivities beyond 1.1 or 1.2μm. It is possible, in principle, to obtain photoemission beyond this limit by applying a bias to the sample, a process known as field-assisted photoemission. As a result the sample configuration becomes more complicated than is the case with NEA photocathodes. While several approaches to this problem have been proposed, insufficient work has been done to support a strong choice of any specific approach. The techniques discussed in 5.5.1 have perhaps the highest probability of success, especially in light of the materials and sensitization technology developed for NEA photocathodes. The common feature of these approaches provide a basis for several recommendations applicable to all.

The prime candidates for the detector material in the 1 to 2μm range are Ge, GaSb, GaInAs, and InAsP. For transmission applications, the basic requirements noted for NEA photocathodes (5.4.1.5) are expected to apply here: a thin, single crystalline p-type detector film either self-supporting or deposited onto a mechanically compatible substrate, transparent over as wide an optical band as possible. Subsequent processes or materials would then use and be designed around this material. With the exception of Ge and the ternaries with bandgaps in excess of 1.1 eV, this type of work has not been done for these materials. Ge can be etch-thinned to produce appropriate thin films; but, it would be an expedient material only because the absorption coefficient is lower and the intrinsic carrier density is higher than the III-V materials with equivalent bandgap. Wide bandgap substrates for GaSb and $InAs_xP_{1-x}$ with $x \approx 0.6$ will be difficult to find due to the large lattice constants.

For $Ga_x In_{1-x} As$ with $x \approx 0.4$, the ternary alloy $InAs_x P_{1-x}$ with $x \approx 0.1$ is a possible substrate. The GaInAs bandgap would be then ~ 0.68 eV compared to a substrate bandgap of 1.25 eV. The substrate preparation and the growth and doping parameters of the active layer for all of these materials requires considerable investigation based on experience with the relatively simple GaAs system. Electrochemical thinning is a possibility for Ge and GaSb. Finally, the minority carrier transport properties of these materials in thin film form will require study, particularly as to the diffusion length and surface recombination velocity. Active layer thickness of 5 to 10 μm is required to optimize response and resolution.

Recommendation (Priority 1)

Research on detector materials for field-assisted photocathodes in the 1 to 2 μm region should be supported. The prime candidates for the active detector layer are Ge, GaSb, GaInAs, and InAsP. The key areas of investigation should include substrate selection and preparation, growth and doping parameters for the active layer and transport properties within the active layer.

5.6.1.6 Conclusion on Heterojunction Diodes

One of the recent suggestions for a field-assisted photocathode involves the growth of two consecutive heterojunctions, both of which are active parts of the device. Previous experiences with heterojunctions have been less than satisfactory. Strain due to mechanical mismatches between the constituent materials, induced depletion layers at the interface due to interdiffusion during growth, and conduction band barriers due to electron affinity differences between the materials cause low transfer efficiency across the interface, high-carrier recombination velocity at the interface, and excess dark current generation as a result of the internal cathodic action of the interface. Recent results with liquid-phase and close-spaced vapor-phase epitaxial growth appear promising toward solving these problems. In the liquid-phase case, etch-back and regrowth at the interface may allow rapid, strain-relieving compositional gradients without a significant loss of carrier mobility or lifetime. The quantum efficiency of sample diodes at varying illumination intensities

and measurements of the capacitance versus bias would indicate surface state saturation effects if charge is stored at the interface since the transfer efficiency then increases with intensity due to a lower surface recombination velocity.

Recommendation (Priority 2)

It is recommended that studies of the growth and electrical characteristics of heterojunction diodes be supported. The narrow-band p-type semiconductor should be chosen as the detector material for radiation out to $2\,\mu m$. Carrier transport across the diode, interface states, and quantum efficiency should be investigated for appropriate combinations of materials. Similar studies should be supported on double heterojunction samples.

5.6.1.7 Conclusion on Insulator Materials

Thin insulator films for tunneling photocathodes offer unique problems in materials technology. The basic requirements are high dielectric field strength, thickness in the 100 to 500 Å range, low barrier height for electron tunneling but high barrier height for hole tunneling, uniformity within 10 percent with no pinholes and minimal interface state density at the semiconductor/insulator interface. Examples of possible insulators are Si_3N_4 and Al_2O_3. Deposition techniques include vapor-phase deposition, with either surface pyrolysis or plasma reaction, radio frequency reactive or anodic sputtering, and thermal oxidation or anodization from solution where self-generated oxides are feasible.

Deposition techniques and process parameters such as temperature must be chosen to be compatible with semiconductor stability and with low trapped insulator charge. With the exception of the barrier height requirement and the lower thickness values, these problems are the same as those encountered in the deposition and properties of passivating and gate insulators. This allows some economy by establishing common programs.

Recommendation (Priority 2)

A study of insulator materials suitable for tunneling barriers should be supported in connection with field-assisted photocathode applications. Insulator properties such as dielectric field strength, barrier height, uniformity, and interface state density at the semiconductor/insulator boundary should be evaluated. It is recommended that available deposition methods be studied for a given semiconductor and insulator combination in order to develop the most cost-effective deposition technique compatible with low interface state densities including fixed charge in the insulator, semiconductor thermal stability, and insulator uniformity.

5.6.1.8 Conclusion on "Conventional" Photocathode Materials

Conventional photocathodes like the S-20 bialkali, cesium telluride, or S-1 have reached a point in their developmental life cycle where improvements are being made slowly as a result of adjustments to manufacturing processes rather than through improvements in understanding of materials or physical phenomena. This is in spite of considerable time, effort, and money expended on research. The primary reason for this is that research samples have been consistently of poorer quality than commercial samples since the quality is completely dependent upon the proprietary manufacturing process. In addition, the variation in spectral response among the poorer quality samples invalidates any but the most imprecise conclusions. The difficulty in obtaining basic materials data adds to the problem; there is no basis leading to hope for a better understanding of these materials or useful predictions concerning the ultimate sensitivity that can be achieved through their use.

Recommendation (Priority 3)

Further research on the conventional S-series and similar photocathodes is not recommended. A modest effort to understand the improved S-20 photocathode could be justified if knowledge of basic materials properties becomes available.

5.6.1.9 Conclusion on Silicon Photocathodes and Electron Multipliers

Silicon has been studied as both a photocathode and as an electron multiplier. While good activation has been achieved, the presence of dark currents in the 10^{-9} to 10^{-10} amp/cm^2 range preclude its use in either application. Attempts to suppress this dark current, which appears to be surface-generated, have proved unsuccessful.

Recommendation (Priority 3)

Further work on silicon photocathodes or electron multipliers is to be discouraged, unless there is evidence that the dark current problem can be solved.

5.6.1.10 Conclusion on GaAsSb Alloys as NEA Photocathodes

An arsenic-rich composition of the ternary alloy GaAsSb was studied as an NEA photocathode. No significant sensitivity was achieved.

This result was ascribed to either reaction between the cesium and the antimony in the alloy or the dominating role played by surface states in pinning the Fermi level at the surface. Work on this material was discontinued.

Recommendation (Priority 3)

In view of the progress made with other materials for NEA photocathodes sensitive to 1.1 μm and the results of previous work with GaAsSb, no further work on this material for this application is recommended.

5.6.1.11 Conclusion on II-VI Compounds and Alloys for NEA Photocathodes

The II-VI compounds, in particular HgCdTe, have been largely ignored in the development of NEA photocathodes. Virtually nothing is known of their activation properties or if they can be doped to the levels required for NEA activation in the bandgap ranges necessary. There is no substantive evidence to indicate they can be competitive with III-V alloys for this application.

Recommendation (Priority 3)

Work on the ternary alloy HgCdTe should be carried on at a low level pending successful development of a ternary III-V alloy NEA photocathode for use as an airglow detector.

5.6.1.12 Conclusion on Ternary Diamond-Like Compounds for NEA Photocathodes

The ternary compounds of the form $A^{II}B^{IV}C_2^{V}$ (see 6.3.3) show some potential advantage over ternary alloys due to less need to control composition precisely as a result of the formation of a true compound. So little is known about these materials that their application as NEA photocathodes does not appear warranted at this time.

Recommendation (Priority 3)

No work is recommended on the ternary diamond-like compounds for NEA photocathode applications.

5.6.1.13 Conclusion on HgCdTe Alloys for Detectors in the 1 to 2 μm Range

The II-VI ternary alloy $Hg_xCd_{1-x}Te$ with $x \approx 0.4$ is a potential detector material for the 1 to 2 μm range. The lattice constant (≈ 6.46 Å) of the alloy is larger than most of the III-V and II-VI compounds but is within 0.3 percent of the CdTe lattice constant which is, therefore, the most likely choice for a wide-bandgap substrate. Liquid-phase epitaxy is a reasonable choice of growth technique if a solvent can be found. A study of the growth and doping parameters is then required, as well as a study of the stability of the alloy during subsequent thermal processing. It is uncertain whether the alloy can be activated with the low work function surface required by field-assisted devices. In some cases, such as the tunnel emitter, where low p-doping is acceptable and processing temperatures can be sufficiently low, the HgCdTe alloy may be acceptable if an appropriate insulator can be found. The transport properties of the alloy should be studied to determine minority carrier diffusion lengths; the efficiency of simple diodes and surface recombination phenomena at the substrate/semiconductor and semiconductor/insulator interfaces should be investigated.

Recommendation (Priority 3)

The HgCdTe alloy composition appropriate to a threshold wavelength of 1.7 μm should be studied. The use of CdTe as a transparent substrate is recommended. Coincident investigation of the growth parameters, maximum practical doping levels, thermal stability, and transport properties should be supported.

5.6.1.14 Conclusion on Ternary Semiconductors for Detectors in 1 to 2 μm Range

At least two ternary compounds exist with cutoffs between 1 and 2 μm: ZnGeAs$_2$ (E_g = 0.85 eV) and ZnSnAs$_2$ (E_g = 0.65 eV). The relative simplicity of the compounds makes them interesting detectors in this spectral region. Before they are considered in comparison with the materials already discussed, more detailed information about bulk metallurgy, optical parameters, and carrier transport is required. Such information includes the effect of self-compensation on conductivity type and doping levels, the values of the absorption and reflection coefficients, and the minority carrier diffusion lengths. These compounds should lend themselves to liquid phase epitaxial growth with a suitable choice of substrate, particularly since thick layers can be used for these studies, although bulk single crystal techniques probably would be simpler.

Recommendation (Priority 3)

Support of research on the metallurgical and electronic properties of bulk single crystalline ternary compounds, including but not limited to ZnGeAs$_2$ and ZnSnAs$_2$, is recommended. This work should precede thin-film studies for detector applications to determine if these compounds have a decided advantage over more conventional materials.

5.6.1.15 Conclusion on MOS Technology for Promising Materials Other Than Silicon

While CCD development programs are not recommended for materials other than silicon, the development of a more general MOS technology for detectors in the 1 to 2 μm range is necessary. The problems of insulators for tunnel emitter photocathodes have already been discussed (5.6.1.7). To this must be added the passivation of detector surfaces for materials other than silicon, diffusion masks, and, of course,

possible application to CCD imaging arrays. While it is probable that a single insulator may not satisfy the requirements of all applications, combinations of insulators, metals, and semiconductors, applied simultaneously or sequentially, should be able to solve most problems eventually.

Recommendation (Priority 3)

Support of work on MOS technology for detector materials such as Ge, GaSb, GaInAs, InAsP, InAs, InSb, PbSnTe, and HgCdTe is recommended. Tunneling barriers, diffusion masking, surface passivation, and surface charge storage and transfer are applications requiring this work. Previous work in this area represents only a small part of detector device development and consequently receives little attention. Because of the potential impact on imaging devices for both the near- and far-infrared, a well organized program specifically on MOS problems using the detector materials discussed above should be given attention.

5.6.1.16 Conclusion on Photoconductive-Electroluminescent Imaging Panels

Solid-state imaging panels have been studied with considerable thoroughness. Threshold sensitivities of 10^{-8} watts/cm^2 are the best that have been achieved at the cost of a sacrifice in response time. While new configurations are possible with incorporation of avalanche diodes and planar technology, current performance estimates are well below a level sufficient to justify support of this work. In addition, no substantial improvements in the display end of the panel have been forthcoming. Competition on the other hand, from small scanning arrays has been increasing with the additional prospect of both in-line and off-line signal processing.

Recommendation (Priority 3)

No further work on solid-state imaging panels (photoconductive-electroluminescent) is recommended at this time.

5.6.1.17 Conclusion on Materials for Diode Array Vidicon Targets

The silicon diode array vidicon target is not a sufficiently sensitive detector for airglow levels. Substitution of a detector material with sensitivity out to near 2 μm is not feasible even with substantial improvements in preamplifier input equivalent noise levels and use of the cold cathode electron beam source. At best, the small changes in stored charge will produce long response times and noise limited pictures. Competition from the more sensitive, lighter, smaller, potentially less expensive, self-scanned charge-coupled devices may make most conventional gun-scanned devices obsolete both as image sensors and for electron gain and charge storage devices.

Recommendation (Priority 3)

No further support is recommended for diode array vidicon targets.

5.6.1.18 Conclusion on "Conventional" Solid-State Imaging Arrays

Solid-state imaging arrays using bus line switching from shift registers have grown more complicated (and expensive) as lower threshold sensitivities are sought. Silicon, cadmium sulfide, and germanium devices have been studied but switching noise is a persistent problem at low input levels. In addition, the large number of image elements, particularly for high-density arrays, requires considerable space and a large number of interconnections; this adds to the complexity and expense. Charge-coupled devices are considerably more attractive.

Recommendation (Priority 3)

Further work on conventional solid-state imaging arrays is not recommended.

5.6.2 Non-Imaging Detectors

The principal military applications for non-imaging detectors in the 0.1 to 2 μm range include laser communication and target designation in the near infrared and flame monitoring and star tracking in the ultraviolet. Because these applications place specific requirements on the devices, each will receive separate treatment.

The laser lines currently of greatest interest in this spectral range are the ruby line at 0.69 μm and the Nd:YAG line at 1.06 μm. The 1.06 μm line is used chiefly for target designation and tracking. The ruby line is of interest for communications. Nd lasers are being investigated for this purpose as well since detectors with improved sensitivity are becoming available. The visual security at 1.06 μm is also better. The possibility of eye damage from high-power lasers at these wavelengths has generated interest in the eye-safe band from 1.4 to 1.6 μm. Atmospheric absorption between 1.4 to 1.5 μm limits the useful width of this band. Because of the inefficiency of the Er-doped YAG and glass lasers which operate in this band, and the present lack of adequate detectors for this band, the use of this spectral band is severely limited. Semiconductor injection lasers are possible, in principle, but peak power outputs are smaller than for optically pumped lasers in spite of better device efficiencies. Large arrays of laser diodes have been built to provide higher output powers but the 6° beam spread in the individual diodes limits the effective power that can be delivered to the target; this is not a problem with optically pumped lasers.

5.6.2.1 Conclusion on Compound Semiconductors for Avalanche Diodes to Operate at 1.06 μm

Research work on InAsP/InP has shown that good internal quantum efficiency can be obtained at 1.06 μm because of the large absorption coefficient and the band edge can be tailored to take advantage of the better absorption above the band edge. The narrow range of spectral sensitivity due to the substrate absorption implies that a high degree of extraneous radiation can be rejected as well. Avalanche diodes using this material combination with light entering through the substrate side are potential replacements for silicon devices. The improvement in quantum efficiency is potentially a factor of 3. In addition, the large differences in carrier mobilities and, possibly, in ionization coefficients tend to make carrier multiplication a single carrier process, reducing multiplication noise. The smaller intrinsic carrier densities in these compounds, compared to silicon, result in smaller bulk dark current. The important areas where work is required are diode formation, passivation, and characteristics. Careful consideration of the width of the depletion region is required since carrier

lifetimes are shorter in InAsP than in silicon. An analysis of the problem would indicate the maximum width tolerable from this standpoint while the lower limit will be set by the depletion capacitance that may adversely effect the frequency bandwidth.

The InAsP/InP combination has been used as an example for this application. The same arguments can be applied to other III-V combinations such as GaInAs/GaAs and GaAsSb/GaAs. Similarly, the II-VI combination HgCdTe/CdTe is a possibility. The spectral bandwidth of these combinations is fairly wide but can be narrowed by going to double layers with appropriately different compositions.

Recommendation (Priority 2)

It is recommended that a design analysis be performed to determine the feasibility and expected performance of avalanche diodes made from combinations of alloy and compound in the III-V or II-VI group, for use in 1.06 μm laser tracking applications. Comparison with silicon for this purpose should be made, and systems advantages should be considered. In order to provide a meaningful data base, work on selected alloy materials should be supported to supply values for carrier mobilities, lifetimes, ionization coefficients, and leakage current levels. Examples of possible material combinations are InAsP/InP and HgCdTe/CdTe. This work should use the best current materials technology to fabricate, passivate and test avalanche diodes using the materials selected. Such a program should precede and guide any decision on a more substantial effort to develop practical devices.

5.6.2.2 Conclusion on Compound Semiconductors for Avalanche Diodes to Operate in the 1.4 to 1.6 μm Region

The arguments for laser tracking systems using alloy avalanche diodes for the 1.4 to 1.6 μm range are basically the same vis-a-vis germanium as those for alloy diodes for 1.06 μm discussed in 5.6.2.1 (and compared with silicon).

Recommendation (Priority 2)

It is recommended that a performance analysis for III-V and II-VI alloy avalanche diodes similar to that recommended in 5.6.2.1 for 1.06 μm detectors be performed for the 1.4 to 1.6 μm eye safe laser region.

5.6.2.3 Conclusion on Germanium Avalanche Diodes

Single-element avalanche diodes have been built using germanium. These are sensitive to both the 1.06 μm and the 1.54 μm laser lines. Normal bulk generated current and excessive leakage of current due to generation through impurities in the depletion region and surface states limit the effectiveness of these devices. While cooling would improve performance, the excess current from the depletion layer is better addressed by more effective pre- and in-process exclusion of copper which has a high diffusion coefficient and solubility in germanium. Improvements in passivation technique are required to suppress surface dark current. Since cooling would still be required due to bulk current, to match the performance of silicon devices at 1.06 μm the improvement in sensitivity at this wavelength does not warrant replacement of silicon devices with germanium versions. The germanium avalanche diode, however, is a viable candidate for 1.54 μm lasers.

Recommendation (Priority 2)

Work on germanium avalanche diode for detection in the eyesafe region (1.4 to 1.5 μm) should be supported and intensified if a final system decision is made to shift laser tracking operations into that wavelength range. Exclusion of copper contamination from the starting material and during processing and development of an adequate passivation technique should receive primary emphasis in any work on device technology. Sensitivity to 1.06 μm radiation should not be used to justify such work on germanium avalanche diodes and such an application is not recommended.

5.6.2.4 Conclusion on GaP for Detectors for Star Tracking

Detectors for star tracking applications in satellite orientation and guidance have the same requirement as laser tracking detectors. The radiation source to be

detected is rich in short wavelengths; thus, wider bandgap materials can be used.
In principle, this means lower dark currents and consequently smaller detectable
power levels. Two promising options are available for this function:

- The photocathode-silicon avalanche diode combination using
  the efficient bialkali photocathode

- Avalanche diodes using a detector material such as GaP

No recommendations will be made on the former option since the problems are basically
in device development.

An avalanche diode detector could potentially take, without loss of sensi-
tivity, a wider range of environmental extremes in terms of temperature and ac-
celeration than a vacuum device. GaP and III-V compounds with similar bandgaps
are likely selections for the detector material. As with all materials other than
silicon, however, device technology is the principal limitation. In this respect,
the chief areas requiring technological development are growth of the junction ma-
terials and passivating the junction surface including the diffusion of guard rings.
With regard to materials growth, GaP is in an advantageous position in comparison
with other available wide-bandgap III-V compounds due to past work on this material
for light-emitting diode applications. The problems of passivation and diffusion mask-
ing require a considerable effort. GaP suffers from the disadvantage of low, nearly
equal carrier mobilities and short lifetimes; these may lead to high multiplication
noise in the diode. Since GaP is an indirect bandgap material, the short lifetimes
may be the result of high defect densities.

Recommendation (Priority 2)

It is recommended that the materials technology be developed for GaP ava-
lanche diodes for star tracking applications. Study areas should include the growth
of high-purity materials and the development of passivation and diffusion materials
and technology. Coincident studies of device parameters such as carrier mobilities,
lifetimes, and ionization coefficients should be made. Performance parameters of
avalanche diodes such as quantum efficiency, leakage current, and multiplication
gain and noise should be measured.

5.6.2.5 Conclusion on AlP and AlAs for Star Tracking Applications

Two other III-V compounds are potential candidates for star tracking devices: AlP and AlAs. These materials have nearly the same bandgaps as GaP but available information indicates that they possess larger carrier mobilities with some asymmetry in favor of electrons. The materials technology for these compounds is not as advanced as that of GaP so that other parameters are ill-defined. The tendency of the aluminium compounds to oxidize implies that a specialized device technology must be developed to avoid exposure of the material to humid ambients.

Recommendation (Priority 2)

The III-V compounds AlP and AlAs should be investigated as potential competitors to GaP for star tracking systems. Chief study areas should include materials growth and purity control as well as passivation and diffusion materials and techniques. Parameters of importance to device design such as carrier mobilities, lifetimes, and ionization coefficients should be measured. Avalanche diodes performance parameters such as quantum efficiency, dark current, and avalanche gain and noise should be studied. Techniques to protect the surfaces of these materials from humid ambients should be devised.

5.6.2.6 Conclusion on Silicon for Avalanche Diodes

The detector package for the 1.06 μm laser tracking function consists of four detectors arranged in quadrature. The kev characteristics are high sensitivity at the laser line, fast speed of response, low dark current, and low noise internal gain. Silicon avalanche diodes have become the best choice and silicon quad detector heads are undergoing prototype production. These devices were discussed in 5.4.3.2. Product development in production can be expected to improve these values somewhat but the basic technology exists.

Recommendation (Priority 3)

No further work on the basic materials technology for silicon avalanche diodes is recommended.

204

5.6.2.7 Conclusion on Materials for Laser Detectors in Communication Systems

The requirements for laser detectors in communications systems are basically the same as those for laser tracking except that only single elements are required and the width of the frequency bandwidth is more critical. Silicon avalanche diodes cover a sufficiently broad spectral bandwidth to be used as detectors for both ruby and Nd:YAG systems. Special photomultipliers using deflection demodulation just behind the photocathode can use S-20 photocathodes for the ruby line and InAsP at 1.06 μm. In view of the above discussion of laser tracking systems, no separate recommendations will be made here.

5.6.2.8 Conclusion on Solid-State Ultraviolet Detector Materials

Choosing a suitable material for a solid-state ultraviolet device is difficult. A bandgap of 4 eV is required to prevent detection of solar radiation. Indirect bandgap materials and Schottky-barrier diodes with thresholds at 3 eV may be suitable if these devices are inefficient at wavelengths greater than 0.3 μ. Examples of such materials are SiC, AlP, barium titanate, and potassium tantalate. More effort in terms of both materials and device technology is required on the properties of these materials.

Recommendation (Priority 3)

It is recommended that an experimental investigation of wide-bandgap semiconductors such as SiC, AlP, barium titanate, and potassium tantalate be initiated to develop a detector for ultraviolet in high temperature environments. Growth techniques, dopants, contact materials, and passivation should be examined for junction devices using these materials. The efficiency and dark current of simple diodes should be measured to temperatures up to 500° C. Material selection should be based on device stability at these temperatures as well as on levels of performance.

5.6.2.9 Conclusion on Materials for Schottky Diode Detectors

Schottky diodes using internal photoemission over the interface barrier have operated successfully in both avalanche and nonavalanching modes. The semiconductor generally has been silicon, and response beyond the absorption edge has been achieved. For response to radiation up to wavelengths of about $2\,\mu$ m, germanium and III-V p-n junctions with appropriate bandgaps offer greater potential as detectors, based on their higher quantum efficiency and lower dark current, than silicon Schottky diodes. For applications where cost and availability are primary considerations, the silicon Schottky diodes may compete successfully with germanium junction devices.

Recommendation (Priority 3)

No further research support is recommended for Schottky diode detectors for the 0.1 to $2\,\mu$m range. Where necessary, the available technology may be used.

5.6.2.10 Conclusion on Vacuum and Gas-Filled Devices for Ultraviolet Detectors

Devices to detect and monitor high-temperature flames must be blind to solar radiation, resist high-temperature ambients, and provide high sensitivity and fast response. Vacuum and gas-filled devices do not satisfy the high-temperature requirement and should not be considered for this application.

Recommendation

Further work on vacuum and gas-filled devices for ultraviolet detectors in flame detection and monitoring is not recommended.

5.7 References

1. R. L. Bell and W. E. Spicer, Proc. IEEE $\underline{58}$ 1788 (1970).

2. M. H. Crowell and E. F. Labuda, Bell Syst. Tech. J. $\underline{48}$, 1481 (1969).

3. H. Melchior and W. T. Lynch, IEEE Trans. Elect. Dev. $\underline{ED-13}$, 829 (1966).

4. L. Altman, Electronics, June 1971, p. 50; W. S. Boyle and G. E. Smith, IEEE Spectrum, July 1971, p. 18.

5. J. P. McKelvey, Solid State and Semiconductor Physics, Chapter 10. Harper and Row, New York, 1966.

6. J. T. Cox and G. Hass, Physics of Thin Films, Vol. 2, pp. 239-304, Academic Press, New York, 1964.

7. L. K. Anderson, "Photodiode Detection", Optical Masers Symposium, Brooklyn Polytechnic Institute, April 16-18, 1963.

8. R. H. Bube, Photoconductivity of Solids, Wiley & Sons, New York, 1960.

9. J. S. Blakemore, Semiconductor Statistics, pergamon Press, New York, 1962.

10. A. G. Chynoweth, Semiconductors and Semimetals, ed. by R. K. Willardson and A. C. Beer, Vol. 4, Chapter 4, Academic Press, New York, 1968.

11. S. M. Sze and G. Gibbons, Appl. Phys. Lett. $\underline{8}$, 111 (1966).

12. K. M. van Vliet and J. R. Fassett, Fluctuation Phenomena in Solids, ed. by R. E. Burgess, Chapter VII, Academic Press, New York, 1965.

13. P. W. Kruse, L. D. McGlauchlin, and R. B. McQuiston, Elements of Infrared Technology, pp. 251-259, Wiley & Sons, New York, 1963.

14. S. M. Sze, Physics of Semiconductor Devices, pp. 678-680, Wiley & Sons, New York 1969.

15. G. A. Morton, Appl. Optics $\underline{7}$, 1 (1969).

16. A. S. Grove, Physics and Technology of Semiconductor Devices, pp. 173-175, Wiley & Sons, New York, 1967.

17. R. J. McIntyre, IEEE Trans. Elect. Dev. $\underline{ED-13}$, 164 (1966).

18. R. L. Bell, Solid State Elect. $\underline{12}$, 475 (1969).

19. S. L. Valley, USAFCRL Handbook of Geophysics and Space Environments, McGraw-Hill, New York, 1965.

20. M. L. Vatsia, K. Stich, and D. Dunlap, "Night-Sky Radiance from 450 nm to 2000 nm" (to be published).

21. J. W. Chamberlain, Physics of the Aurora and Airglow, Academic Press, New York, 1961.

22. F. E. Roach, "The Nightglow," Advances in Electronics and Electron Physics, 18, ed. by L. Marton, Academic Press, New York, 1963.

23. Aurora and Airglow, ed. by B. M. McCormac, Reinhold, New York 1967.

24. H. W. Yates and J. H. Taylor, NRL Report 5453, U. S. Naval Research Laboratory, June 1960, AD 240 188.

25. Applied Optics and Optical Engineering, Vol. II The Detection of Light and Infrared Radiation, by R. Kingslake, Academic Press, New York, 1965

26. Semiconductors, ed. by N. B. Hannay, New York, 1959.

27. American Institute of Physics Handbook, 2nd Ed., pp. 9-55, McGraw Hill, 1963

28. O. Madelung, Physics of III-V Compounds, Wiley & Sons, New York, 1964.

29. B. I. Boltaks, Diffusion in Semiconductors, Academic Press, New York, 1963.

30. S. M. Sze, Physics of Semiconductor Devices, Wiley & Sons, New York, 1969.

31. A. S. Grove, Physics and Technology of Semiconductor Devices, pp. 35-83, Wiley & Sons, New York, 1967.

32. M. Neuberger, III-V Semiconducting Compounds, Vol. 2, Handbook of Electronic Materials, IFI/Plenum, New York, 1971.

33. J. Gibbons, Proc. IEEE 56, 295 (1968).

34. O. Marsh, G. Shifrin, R. Baron, R. Wilson, and G. Brewer, Ion Implantation Doping Techniques, Technical Report AFAL-TR, 68-281, October 1968, AD 843471.

35. RCA Chart: "Typical Photocathode Spectral Response Characteristics," RCA Electronic Components, Harrison, New Jersey; ITT Chart: "Typical Absolute Spectral Response Characteristics of Photoemissive Devices," ITT Electron Tube Div., Fort Wayne, Indiana.

36. A. H. Sommer, Photoemissive Materials, Wiley & Sons, New York, 1968.

208

37. K. R. Crowe and J. L. Gumnick, Appl. Phys. Letters 11, 249 (1967).

38. D. G. Fisher, R. E. Enstrom, and B. F. Williams, Appl. Phys. Letters 18, 371 (1971).

39. L. W. James. G. A. Antypas, J. J. Vebbing, T. O. Yep, and R. L. Bell, J. Appl. Phys. 42, 580 (1971).

40. G. A. Antypas and L. W. James, J. Appl. Phys. 41, 2165 (1970).

41. J. J. Uebbing and L. W. James, J. Appl. Phys. 41, 4505 (1970).

42. L. W. James, G. A. Antypas, J. Edgecume, R. L. Moos and R. L. Bell, J. Appl. Phys. 42, 4976 (1971).

43. R. U. Martinelli, Appl. Phys. Lett. 17, 313 (1970).

44. W. Gutierrez, D. Pommerrenig and S. Holt (to be published).

45. J. H. Pollard (to be published).

46. A. J. Kennedy and L. V. Caldwell (to be published).

47. G. R. Carruthers, Optical Spectra, Jan. 1971, p. 36.

48. H. H. Glascock, Jr., and H. F. Webster, IEEE Trans. Elect. Dev. ED-18, 330 (1971).

49. H. Melchior and W. T. Lynch, IEEE Trans. Elect. Dev. ED-13, 829 (1966).

50. R. L. Anderson, Solid State Elect. 5, 341 (1962); W. G. Oldham and A. G. Milnes, Solid State Elect. 7, 153 (1964).

51. R. H. Bube, Physics and Chemistry of II-VI Compounds, ed. by Aven and Prener, Wiley & Sons, New York, 1967.

52. R. H. Bube, RCA Rev. 20, 564 (1969).

53. J. R. Richardson and R. D. Baertsch, Solid State Elect. 12, 393 (1969).

54. R. Farrell, Proc. Third Int. Conf. on Photoconductivity, ed. by E. M. Pell, p. 123.   Pergamon Press, New York 1969.

55. D. E. Sawyer, Appl. Phys. Letters 13, 392 (1968).

56. A. K. Ghosh, Proc. Third Int. Conf. on Photoconductivity, ed. by E. M. Pell, p. 99, Permagon Press, New York, 1969.

57. P. Chapman, P. Petersen, and O. Tufte (unpublished).

58. R. Keezer, J. Modar, and D. Brown, J. Appl. Phys. 35, 1866, 1868 (1964).

59. S. Morrison, Adv. in Catalysis VII, 259 (1955).

60. D. Melnick, J. Chem. Phys. 26, 1136 (1957).

61. R. Neville and C. Mead, J. Appl. Phys. 41, 3795 (1970).

62. R. Cunningham, J. Marton, and J. Schlesinger, J. Appl. Phys. 40, 4664 (1969)

63. R. Baertsch, and J. Richardson, J. Appl. Phys. 40, 229 (1969).

64. R. Cambell, Tech. Report AF APL-TR-68-148.

65. E. Mitchell, J. Phys. Chem. Solids 8, 444 (1959).

66. A. Tuzzolino, Rev. Sci. Instr. 35, 1332 (1964).

67. G. Castro, IBM Res. and Dev. 15, 27 (1971)

68. R. Orthuber and L. Ullery, J. Opt. Soc. Am. 44, 297 (1954); B. Kazan and F. Nicoll, J. Opt. Soc. Am. 47, 887 (1957).

69. P. Weimer, G. Sadasiv, J. Meyer, L. Meray-Horvath, and W. Pike, Proc. IEEE 55, 1591 (1967).

70. W. List, IEEE Trans. Elect. Dev. ED-15, 256 (1968).

71. M. Crowell, T. Buck, E. Labuda, J. Dalton, and E. Walsh, Bell Syst. Tech. J. 46, 491 (1967).

72. P. Wenland, IEEE Trans. Elect. Dev. ED-14, 285 (1967).

73. R. Madden, D. Kiewit, and C. Crowell, IEEE Trans. Elect. Dev. ED-18, 1043 (1971).

74. D. Boone, E. Harp, and M. Whatley, Germanium Optical Mosaic Sensors, Final Technical Report, Contract No. DAAKO2-68-C-0113, September, 1969. M. Poleshunk and A. Milch, Research and Development of Low-Light-Level/ Near IR Camera Tube With Solid-State Array Target, Seventh Quarterly Report, Contract No. DAAB07-69-C-0263, April, 1971.

75. C. Kim and W. Davern, IEEE Trans. Elect. Dev. ED-18, 1062 (1971).

76. J. R. Arthur, J. Appl. Phys. 36, 3221 (1965).

77. P. G. Borzyak, A. F. Yatsenko, L. S. Miroshnichenko, Phys. Stat. Sol. 14, 403 (1966).

78. T. M. Lifshitz and A. L. Musatov, J. E. T. P. Pism. Red. 3, 134 (1966) (Russian).

79. I. L. Sokolovokaya, V. C. Ivanov, G. N. Fursey, Phys. Stat. Sol. 21, 789 (1967).

80. P. G. Borzyak, V. F Bihar, A. F. Yatsenko, Ukrainian J. Phys. 13, 868 (1968) (Russian).

81. Z. P. Boot, A. E. Krabtsob, A. G. Yatsenko, Ukrainian J. Phys. 14, 1568 (1969) (Russian).

82. K. Miyaji, "Studies of Infrared Image Converters," Contract No. DA-92-557-FEC-38337, Report No. J-255-3, 1966.

83. C. Mead, Solid-State Elect. 9, 1023 (1966); S. Sze, Physics of Semiconductor Devices, pp 397-399, Wiley & Sons, New York, 1969.

84. R. Simon and W. Spicer, Phys. Rev. 119, 621 (1960).

85. P. Thornton and D. Northrop, Solid State Elect. 8, 437 (1965).

86. R. Simon and W. Spicer, J. Appl. Phys. 31, 1505 (1960).

87. I.Davis and P. Thornton, Appl. Phys. Lett. 10, 249 (1967).

88. D. Fisher and W. Harty, "Fabrication and Study of Photoconductor-Tunneling Electron Emitter," Report No. 6, Contract No. DA44-009-AMC-1176 (T), December 1969.

89. C. Thomas, "Minority Carrier Tunneling Effects in Silicon MIS Diodes," University Microfilms, Ann Arbor, Mich., December, 1969.

90. B. Miller (to be published)

91. A. Milnes and D. Feucht, Appl. Phys. Lett. 19, 383 (1971).

92. W. Boyle and G. Smith, Bell Syst. Tech. J. 49, 587 (1970).

93. W. Engeler, J. Tiemann, and R. Baertsch, Appl. Phys. Lett. 17, 469 (1970). L. Altman, "The New Concept for Memory and Imaging: Charge Coupling," Electronics, June 21, 1971, p. 50; G. Amelio, W. Bertram, Jr. and M. Tompsett, IEEE Trans. Elect. Dev. ED-18, 986 (1971).

DETECTORS FOR RADIATION OF WAVELENGTHS FROM 2 μm TO 200 μm

6.1 Introduction

The development of semiconductors for infrared photon detectors has pro-
ceeded in several readily defined stages. During and immediately following World
War II, attention centered upon the lead chalcogenide photoconductors including PbS,
PbSe, and PbTe, in the form of polycrystalline photoconductive thin films. Of these,
PbS still finds application for high-performance detectors in the near infrared for
ground-to-air and air-to-air missiles and in spaceborne arrays for missile-plume
detection. PbSe is employed in a similar manner and is also useful for thermal im-
aging applications.

During the 1950s detectors using the photoconductivity of extrinsic Ge were
developed. These involved Ge:Cu, Ge:Cd, Ge:Zn, and, most important, Ge:Hg. The
exigencies of Vietnam caused great emphasis on reconnaissance techniques, include
thermal mapping systems and forward looking infrared systems (FLIR), and Ge:Hg
was found to be suitable for such systems operating in the 8 to 14 μm spectral interval.
Real time imagery systems were developed based upon linear arrays of approximately
300 elements. The high cost of such systems was due, in part, to the need for opera-
ting at about 20° to 30° K and for the associated sophisticated multiplex switching
systems.

Ge:Hg and the other extrinsic Ge semiconductors also are presently employed
in cold background space detection systems, where extremely high detectivities are
required.

During the past five years there has been considerable interest in extrinsic
Si for long wavelength infrared applications. The advantages of extrinsic Si over ex-
trinsic Ge include a higher density of impurity atoms which means that the detector
absorption length is about 100 μm rather than 1 mm, an important consideration in
arrays. Furthermore, Si is the preferred material for integrated circuits so that

detector, preamplifier and multiplex switch can be prepared in the same chip. On the other hand, the impurity ionization energies in Si tend to be shallow, so that the useful spectral ranges are generally greater than $20 \mu m$.

During the 1950s, investigations of the III-V semiconductors began. Foremost among these for infrared applications has been InSb which was seen as a single-crystal competitor to thin-film PbSe for 3 to $5 \mu m$ thermal mapping and missile guidance applications. Both photoconductive and diffused junction photovoltaic InSb detectors were developed. These exhibited BLIP limited detectivities (see 3.3.1.1) when operated at 77° K against a room-temperature background. Applications of cooled InSb detectors now include missile-plume detection at $4.3 \mu m$. InAs photo-voltaic detectors and phototransistors find similar applications, including $2.7 \mu m$ plume detection.

About 1960 a need for a 0.1 eV gap semiconductor to be employed as an intrinsic 8 to $14 \mu m$ detector was recognized. Since no existing elemental or binary compound semiconductor met this requirement, work began on the alloy semiconductor $Hg_{1-x}Cd_xTe$ (written HgCdTe). In principle, it was possible to tailor the energy gap to any value between 0 and 1.4 eV by controlling the composition. Investigations focused on $Hg_{0.8}Cd_{0.2}Te$, and in about 1965 the first BLIP limited detectors were produced. At present HgCdTe is one of the most useful infrared detectors. Multi-element arrays of $Hg_{0.80}Cd_{0.20}Te$ compete with Ge:Hg for thermal mapping applications. $Hg_{0.56}Cd_{0.44}Te$ finds application as a detector for $2.7 \mu m$ plume radiation, a need also currently served by InAs and PbS. $Hg_{0.71}Cd_{0.29}Te$ finds application as a $4.3 \mu m$ plume detector, competing with InSb and PbSe. $Hg_{0.82}Cd_{0.18}Te$ competes with Ge:Cu, Ge:Cd, and Ge:Hg in cold-background applications.

Other alloy semiconductors useful in infrared detection are PbSnSe and PbSnTe. Their development began after that of HgCdTe and, therefore fewer applications have been made. Of these, PbSnTe is the better, being of principal importance when operated in the photovoltaic mode. Because the largest energy gap in PbSnTe is about 0.3 eV, the spectral interval of principal interest is 8 to $14 \mu m$.

What of the future? It can be argued that since BLIP-limited alloys are available for use in all the spectral intervals of military importance, there is little incentive to develop new materials. There is an element of truth to this; yet there is a counter argument. The trend in military systems is toward high-density multi-element arrays containing very large numbers of elements. Some applications within the decade may require about 10^5 elements of .001" dimensions. Each element must be nearly BLIP limited; there must be very little variation from element to element in the responsivity, resistance and response time. At the same time, the cost per element must be very low to make the system economically feasible.

Cost can be reduced in two ways: First, an intensive campaign can be waged to drive down the cost through development of manufacturing procedures leading to large, uniform crystals. Second, new materials of the proper energy gaps can be developed in which uniformity is theoretically much less of a problem.

Consider the latter approach. There is a class of semiconductors known as the ternary diamond-like compounds whose members are numerous. Although extensively exploited in the Soviet Union, they have received little attention in the United States. It seems reasonable that several will be found to have energy gaps of about 0.1 eV, causing them to be responsive in the 8 to 14 μm spectral interval. Being true compounds rather than alloys, their preparation would be relatively free of certain compositional problems associated with the alloys. It may well be that their spatial uniformity could be achieved at less cost than that of the alloys. Because the list of the diamond-like ternaries is so extensive, it is likely that compounds with energy gaps at nearly any desired spectral interval from the visible throughout the infrared could be synthesized. Accordingly, the diamond-like ternaries are promising candidates for exploitation as detectors in the 1970s.

214

Although high-performance photon detectors are clearly the most important class of infrared detector, applications do exist for thermal detectors. Thermistor bolometers have long served as detectors of radiation from objects at room temperature; they are particularly utilized in spacecraft horizon sensors and planetary sensors. Of more recent interest are evaporated thermopile arrays made from Bi and Sb employed in a similar manner. The pyroelectric is the most promising thermal detector. Its detection mechanism is based on the time rate of change of the temperature due to the radiation falling on a ferroelectric crystal. The commonly used ferroelectric for this application is triglycine sulfate; other materials such as $SrBaNbO_3$ and lanthanum-doped led zirconate titanate are promising candidates. Applications of the pyroelectric detector include arrays employed for imaging; a pyroelectric vidicon is under development. Recently the pyromagnetic effect in ferromagnetic materials has been studied as a detection mechanism.

One of the most interesting topics in modern optics has been the rise of new detection modes for laser radiation. Among these is the optical heterodyne technique, that can be employed in principle with any photoconductor or photodiode. Also included is the metal-oxide-metal diode with a 10^{-14} sec response time and the use of nonlinear optical crystals for parametric upconversion. Proper exploitation of these novel modes may well require the development of new materials.

Attention also should be paid to the general topic of infrared imaging systems of both the direct view and indirect view types. Some of the approaches, e.g., the far-infrared vidicon, have been explored for more than a decade; others, one of the most promising being the pyroelectric vidicon, are of more recent origin.

In this chapter these topics will be developed in greater detail. The state of the art will be reviewed in tabular and graphic form in the remainder of this section. Certain criteria which materials should meet to be useful in infrared detection will be examined. The many materials now available or under development will be reviewed, with emphasis on those applicable to photoconductive and photovoltaic operation. Finally, conclusions and recommendations will be presented concerning research on pertinent infrared materials.

6.1.1 Detector State of the Art

Figure 6.1 and Table 6.1 illustrate the unclassified state of the art of the most important photon and thermal detectors in the 2 to 200 μm range as of January 1972.
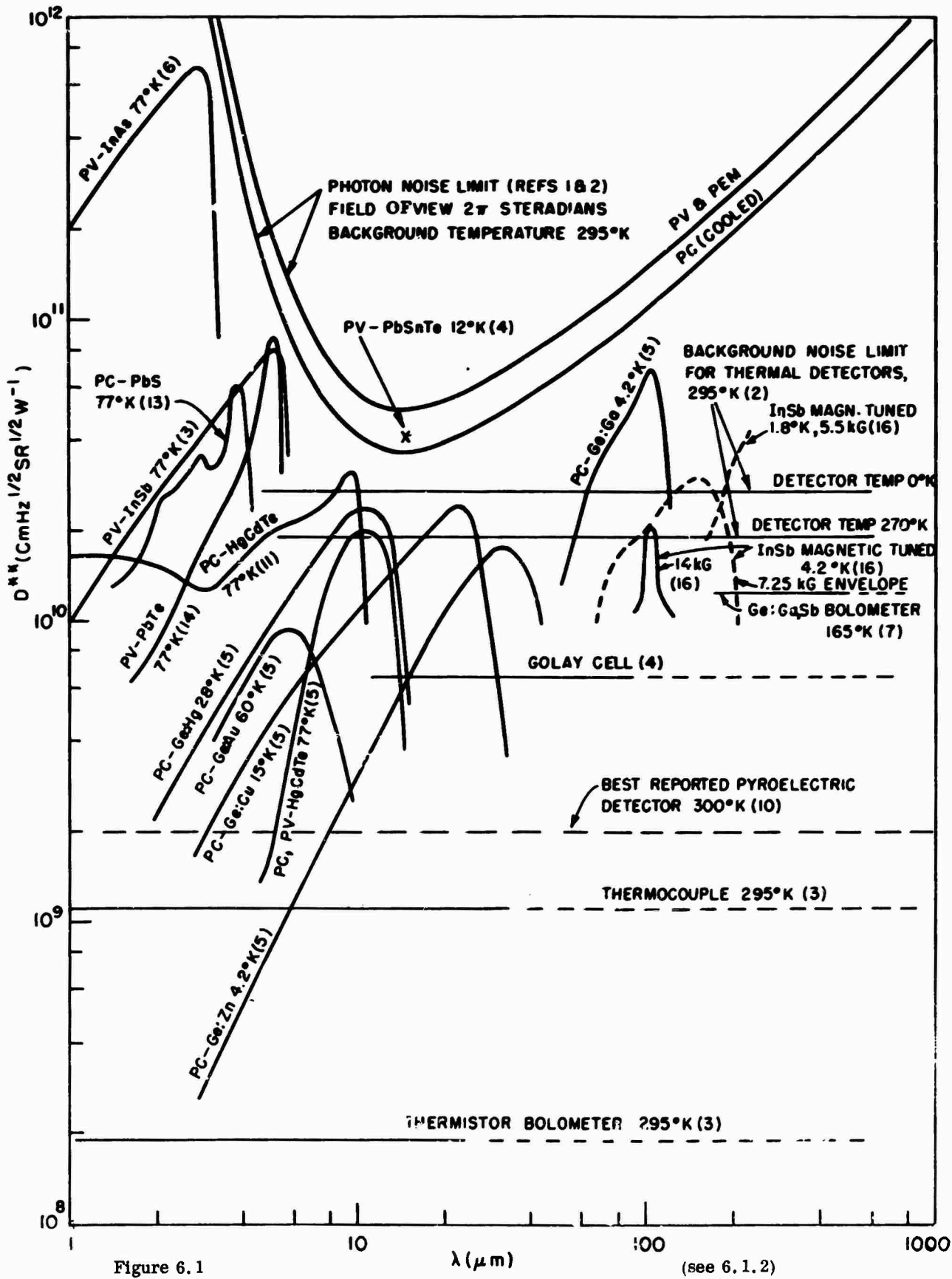
Figure 6.1

(see 6.1.2)

State of the Art Infrared Detectors 2 to 200 μm (Unclassified) Excluding Polycrystalline Devices

Material	Operating Mode	Max. Temp. for BLIP (°K)	Test Temp. (°K)	Peak Wavelength λ_m (μm)	$D^{**}_{\lambda m}$ cmHz$^{\frac{1}{2}}$ sr$^{\frac{1}{2}}$ w^{-1}	Approx. Response Time (seconds)	Reference(s)	Additional Notes
ATGS	pyroelectric	-	300	-	2×10^9	$> 1 \times 10^{-1}$	(10)	
Ge:Ga(Sb) Bolometer		-	1.65	-	1.22×10^{10}	-	(7)	optimum modulation Freq. 200-500Hz
Thermistor Bolometer		-	295	-	1.98×10^8	$1 \times 10^{-3} - 5 \times 10^{-3}$	(3)	
Thermocouple		-	295	-	1.1×10^9	$1.3 \times 10^{-5} - 3 \times 10^{-5}$	(3)(4)	
InSb	hot electron	-	4.2	tunable 60 to 200μm	3×10^{10}	$2 \times 10^{-7} - 5 \times 10^{-7}$	(16)	60° field of view assumed for calc. of D^{**}
Ge:B	PC	-	4.2	108	4.6×10^{10}	1×10^{-8}	(15)	field of view assumed r ume (0.75 sr) as Ref. (8) for calc. of D^{**}
Ge:Ga	PC	-	4.2	104	6.8×10^{10}	4×10^{-8}	(8)	
Ge:Cu	PC	17	4.2	23	$2 \times 10^{10} - 4 \times 10^{10}$	$3 \times 10^{-9} - 1 \times 10^{-8}$	(5)(6)(17)(21)	
Ge:Cu(Sb)	PC	17	4.2	23	2×10^{10}	$<2.2 \times 10^{-9}$	(6)(24)	
$Pb_{1-x}Sn_xTe$	PV	-	12	16	4×10^{10}	$1 \times 10^{-8} - 1 \times 10^{-7}$	(4)	$x = 0.17-0.20$
	PC, PV	-	4.2	14	1.7×10^{10}	1.2×10^{-6}	(4)(5)	
			77	10	3×10^8	1.5×10^{-8}	(29)	

See 6.1.2

TABLE 6.1

TABLE 6.1 (continued)

Material	Operating Mode	Max. Temp. for BLIP (°K)	Test Temp. (°K)	Peak Wavelength λ_m (μm)	$D^{**}_{\lambda_m}$ cmHz$^{\frac{1}{2}}$sr$^{\frac{1}{2}}$w^{-1}	Approx. Response Time (seconds)	Reference(s)	Additional Notes
Hg Cd Te 1-x x	PC, PV	-	77	12	1×10^{10} - 6×10^{10}	$<2 \times 10^{-7}$ - 4×10^{-6}	(4)(6)(9) (25)(26) (27)(28)	x = 0.2
	PC	-	77	9.6	3.1×10^{10}	8×10^{-7}	(11)	
Ge:Hg(Sb)	PC	35	4.2	11	1.8×10^{10}	3×10^{-10} - 2×10^{-9}	(5)(6)	
Ge:Hg	PC	35	4.2	11	7×10^{9} - 4×10^{10}	1×10^{-9} - 3×10^{-8}	(5)(6)(17) (9)(20)	
		-	27.	10.5	4×10^{10}	-	(23)	
Ge:Au	PC	60	77	6	3×10^{9} - 1×10^{10}	3×10^{-8}	(3)(6)(17) (19)(20)	
Ge:Au(Sb)	PC	60	77	6	8×10^{9}	1.6×10^{-9}	(5)(6)	
InSb	PC, PV	110	77	5.3	6×10^{10} - 1×10^{11}	5×10^{-6}	(4)(6) (17)(18)	
	PV	-	77	4.9	1×10^{11}	$<2 \times 10^{-8}$	(12)	
PbTe	PV	-	77	5	8.7×10^{10}	2.5×10^{-8}	(14)	
PbS	PC	-	77	3.8	6×10^{10}	3.2×10^{-5}	(13)	
InAs	PV	-	77	2.8	7×10^{11}	5×10^{-7}	(5)(6)	

See 6.1.2

6.1.2 References for Figure 6.1 and Table 6.1

1. Jacobs, S. F. and Sargent M., Photon Noise Limited D* for Low Temperature Backgrounds and Long Wavelength, Infrared Physics 10, 233-235 (1970).

2. Kruse, P. W., McGlauchlin, L. D. and McQuistan, R. B., Elements of Infrared Technology, Wiley, New York (1969).

3. Hudson R., Infrared Engineering, Wiley, New York (1969).

4. Beer, A., and Willardson, R., Semiconductors and Semimetals, Volume 5. Infrared Detectors, Academic Press, New York (1970).

5. Melchior H., Fisher, M. B., and Arams, F. R., Photodetectors for Optical Communication Systems, Proc. IEEE 58, 1466-1486 (1970).

6. Manufacturer's Data from SBRC, T. I., Honeywell, Philco-Ford, Raytheon.

7. Zwerdling, S., Smith, R. A., and Therjault, P. P., A Fast High-Responsivity Bolometer Detector for the Very-Far Infrared, Infrared Physics 8, 271-336 (1968).

8. Moore, W. J., and Shenker, J., A High-Detectivity Gallium-Doped Germanium Detector for the 40-120 μ Region, Infrared Physics 5, 96-106 (1965).

9. Cohen-Solal, G., and Riant, Y., Epitaxial (Cd Hg) Te Infrared Photovoltaic Detectors, Appl. Phys. Letters 19, 436-437 (1971).

10. Lock, P. J., Doped Triglycine Sulphate for Pyroelectric Applications, Appl. Phys. Letters 19, 390-391 (1971).

11. Eisenman, W. L., Naugle, A. B., and Merriam, J. O., Properties of Photodetectors (78th Report (Unclassified)), December 1968, Naval Weapons Center, Corona Laboratories, Corona, California.

12. Foyt, A. G., Lindley, W. T., and Donnelly, J. P., n-p Junction Photodetectors in InSb Fabricated by Proton Bombardment, Appl. Phys. Letters 16, 335-337 (1970).

13. Schoolar, R. B., Epitaxial Lead Sulphide Photovoltaic Cells and Photoconductive Films, Appl. Phys. Letters 16, 446-449 (1970).

14. Donnelly, J. P., Harman, T. C., and Foyt, A. G., n-p Junction Photovoltaic Detectors in PbTe Produced by Proton Bombardment, Appl. Phys. Letters 18, 259 (1971).

15. Shenker, H., Moore, W. J., and Swiggard, E. M., Infrared Photo-conductive Characteristics of Boron-Doped Germanium, J. Appl. Phys. 35, 2965-2970 (1964).

16. Putley, E. H., Indium Antimonide Submillimeter Photoconductive Detectors, Applied Optics 4, 649-659 (1965).

17. Levinstein, H., Extrinsic Detectors, Appl. Optics 4, 639-647 (1965).

18. Morton, F. D., and King, R. E. J., Photoconductive Indium Antimonide Detectors, Appl. Optics 4, 659-663 (1965).

19. Johnson, L. and Levinstein, H., Infrared Properties of Gold in Germanium, Phys. Rev. 117, 1191-1203 (1960).

20. Beyen, W., et.al., Cooled Photoconductive Infrared Detectors, J. Opt. Soc. Am, 49, 686-692 (159).

21. Bode, D., and Graham, H., Comparison of Performance of Copper-Doped Germanium and Mercury-Doped Germanium Detectors, Infrared Phys., 3, 129-137 (1963).

22. Borrello, S. R., and Levinstein, H., Preparation and Properties of Mercury-Doped Germanium, J. Appl. Phys., 33, 2947-2950 (1962).

23. Darviot, Y., et. al., Metallurgy and Physical Properties of Mercury-Doped Germanium Related to the Performance of the Infrared Detector, Infrared Phys. 7, 1-10 (1967).

24. Yardley, J. T., and Moore, C. B., Response Times of Ge:Cu Infrared Detectors, Appl. Phys. Letters, 7, 311-312 (1965).

25. Schlickman, J., Mercury Cadmium Telluride Intrinsic Photodetectors, Proc. Electroopt. Syst. Conf., Industr. Sci. Conf. Mgmt., Inc., (Chicago, Ill.), 289-309 (September 1969).

26. Kruse, P. W., Photon Effects in $Hg_{1-x}Cd_xTe$, Appl. Optics $\underline{4}$, 687-692 (1965).

27. Bartlett, B., et.al., Background Limited Photoconductive HgCdTe Detectors for Use in the 8 to 14 μm Atmospheric Window, Infrared Physics, $\underline{9}$, 35-36 (1969).

28. Mocker, H., A 10.6μm Optical Heterodyne Communcation System, Appl. Optics $\underline{8}$, 677-684 (1969)

29. Melngailis, I., and Harman, T. C., Photoconductivity in Single-Crystal $Pb_{1-x}Sn_xTe$, Appl. Phys. Letters, $\underline{13}$, 180-183 (1968).

6.2 Limitations to the Performance of Infrared Detectors

It is important to realize what limits the performance of a given material in a given detection mode. The development of a new infrared detecting material, or the improvement of a known one, generally requires an extensive crystal-growth and purification program. Purification to the degree required for high-performance detectors is an arduous, time consuming and expensive process. A definite goal is necessary to avoid needless effort.

As was pointed out in Chapter 3, there exist certain limits to the performance of electromagnetic radiation detection devices. These limits can be characterized as fundamental, environmental, and technological (material). It is these limits which serve as the goal for a new detector development program. The application of this generalized concept to infrared radiation detectors is the subject of this section. For convenience, the limitations are classified as:

- Fundamental and environmental.
- Technological (material).

6.2.1 Fundamental and Environmental Limitations

The principal fundamental limit, which is also an environmental one, is the photon noise (BLIP, or background limit, see 3.3.1). The most common type of background is that of the earth, whose emission approximates that of a 295°K blackbody.

222

In general, most modern infrared photon detectors that operate at wavelengths greater than about 5 μm are background limited in a "wide open" (2π ster) field of view. For narrow field of view, achieved with cooled apertures, the D_λ^{*+} value of the background limit rises, and the practical performance of many detectors also rises. until eventually some form of internal noise dominates. At this point, the detector is no longer background limited.

The other fundamental limit, the signal fluctuation limit (see 3.4.1) does not usually limit the performance of infrared detectors. For wavelengths longer than about 2 μm, the signal fluctuation limit is far less restricting than the 295° K background fluctuation limit. This is, of course, a generalization; in certain instances involving cold space backgrounds or very narrow angular fields of view, the signal fluctuation limit may dominate.

The 295° K BLIP limit is in general the dominant one, and Figure 6.2 illustrates the dependence of that limit upon wavelength and field of view. The values shown are for the cooled photoconductive mode, which is the most common one. The D_λ^* values for the cooled, photovoltaic mode are a factor of $\sqrt{2}$ higher.

6.2.2 Material and Technology Limitations

Although there are several classes of infrared detection mechanism (Chapter 3), only photon detection will be considered here. This is the most important class; most of the new materials of interest in detection research are semiconductors used in this mode.

Perhaps the first choice that must be made in any detector development program is between the photoconductive and the photovoltaic effect. The usual choice is photoconductivity, since it affords the possibility of an internal gain mechanism whereby more than one electron can pass through the external circuit for each photon absorbed in the material. The short circuit signal current, i_s, of an infrared detector is given by:
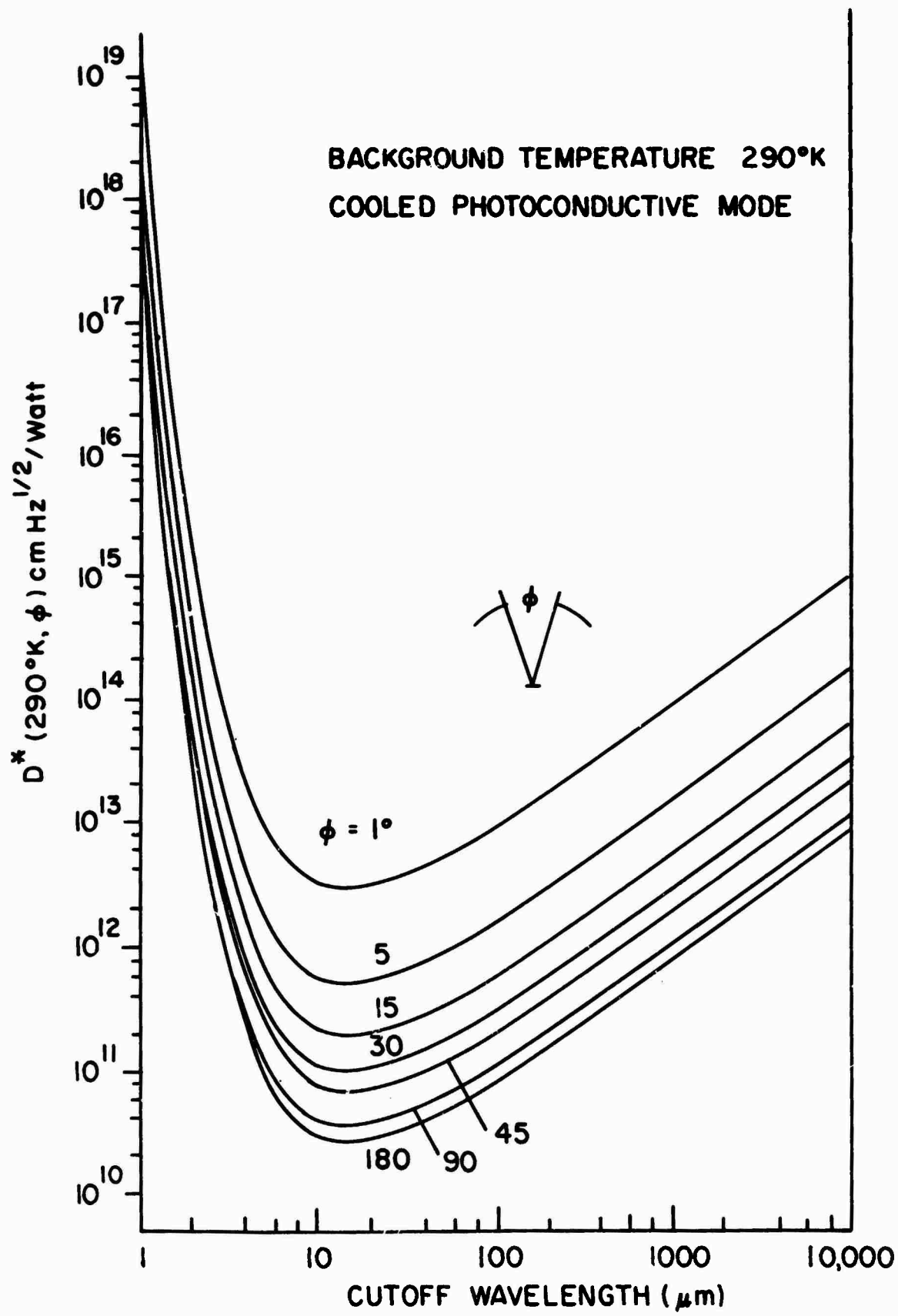

$+D_\lambda^*$ = Detectivity figure of merit.

Figure 6.2

Dependence of BLIP limit on wavelength and field of view.

$$i_s = \eta e N G$$

where η is the quantum efficiency, e is the electronic charge, N is the number of photons absorbed per unit time, and G is the gain. For a photoconductor it can be readily shown that:

$$G = \frac{\tau}{t_r} = \frac{\mu \tau V}{\ell^2} ,$$

where τ is the majority carrier lifetime, t_r is the majority carrier transit time, V is the applied voltage, and ℓ is the distance between electrodes. For small detectors and attainable values of μ, τ, and V, gains in the thousands are possible. However, a limit to the gain is imposed by the maximum value of V which can be applied before breakdown or excessive heating occurs. Another limit is established by sweepout of the minority carriers, a subject too detailed to discuss here. [1]

In the conventional photovoltaic detector, the value of G is unity; thus, the signal, or responsivity is usually less in that mode than in photoconductivity. Carrier avalanche can be used to provide an internal gain, which, in practice, may be as high as 100. [2] Although the avalanche photoeffect (see 5.4.3.2) offers promise as a solid state analogue of the photomultiplier, it has not been exploited to any marked extent as an infrared detector.

Another major consideration is the ease of preparation of the material. To prepare a high-performance infrared photoconductor generally requires a rigorous material purification program, to the point where the concentration of unwanted impurities is usually no greater than 10^{15} cm^{-3}, and frequently must be one or two orders of magnitude less. However, photovoltaic detectors usually have impurity concentrations in the 10^{17} - 10^{18} cm^{-3} range; this means a greatly eased purification problem. Balanced against this is the need to prepare either a p-n junction or a Schottky barrier; in general, the junction has the higher efficiency and is, therefore, the more desirable. In some materials, e.g., PbSnTe, it has not been found possible to purify sufficiently for photoconduction so that only photovoltaic operation is feasible. Unwanted impurities include not only foreign atoms but also stoichiometric

defects. In some materials, e.g., InSb, stoichiometric defects pose no discernible problem. In others, such as $Hg_{0.8}Cd_{0.2}Te$, it is their concentration, rather than that of foreign atoms that establishes the limit to the purity.

Some semiconductors can be prepared either n-type or p-type, but not both. This problem is serious in wide-gap semiconductors, e.g., CdS and ZnS; it is not generally encountered in the semiconductors useful for infrared detection.

In principle, the intrinsic photoconductor is preferred over the extrinsic because of the large optical absorption coefficient (allowing a thinner detector) and less stringent cooling requirements. The fabrication of multi-element arrays is easier in intrinsic material, and optical crosstalk is reduced. On the other hand, extrinsic detectors offer two advantages: the wide range of excitation energies (long wavelength limits) available and, in the case of Si, compatibility with integrated circuits. Only two extrinsic semiconductors are of practical interest, Ge and Si; current interest concerns Si.

Semiconductors have either direct or indirect bandgaps, according to whether the maximum of the valence band energy does or does not coincide in momentum space with the minimum of the conduction band energy. Direct gap semiconductors are, in general, preferred in intrinsic mode use; their optical absorption coefficient is greater, allowing thinner samples, and their free-carrier lifetime tends to be shorter allowing a superior frequency response.

The basic problem of modern detector materials technology centers about crystal growth and purification. Elements and stable compounds can be purified by zone refining, but decomposing solids and alloy semiconductors often cannot. Single-crystal growth from the melt is usually preferred to vapor-phase growth because of the ease of preparing centimeter-size crystals. Epitaxy, especially from the liquid phase, is of increasing importance in preparing large uniform areas of semiconductor materials suitable for arrays; however, the choice of a suitable substrate upon which to grow the epitaxial layer is often difficult.

6.3 Photon Detectors

In photon detectors, the incident photon produces a free hole and a bound electron, a free electron and and a bound hole, or a free hole-electron pair. Although the Dember and photoelectromagnetic effects are also internal photoelectric effects, only the photoconductive and photovoltaic modes have been used extensively in detectors. The detector materials are semiconductors. They can be divided into elemental, binary compound, and ternary compound semiconductors, semiconducting alloys, and amorphous materials. Only the extrinsic photo-effect is of importance for infrared detection in the elements, and only the intrinsic photo-effect is of importance in the compound and alloys.

6.3.1 Intrinsic Binary Compound Semiconductors

6.3.1.1 PbS, PbSe, and PbTe (Lead Chalcogenides)

6.3.1.1.1 Introduction

The compounds PbS, PbSe, and PbTe are small-bandgap semiconductors widely used as infrared detectors. The first lead chalcogenide detector dates back to 1904 when Bose obtained the first patent for an infrared detector utilizing the photovoltaic effect in natural PbS crystals.[3] Later attempts to develop sensitive photoconductive films of the lead chalcogenides used vacuum evaporated and chemically deposited polycrystalline films. Most of this work was performed secretly during the war years and was not published until after 1945. Extensive reviews of this early work were presented by Smith,[4] Moss,[5] and Cashman.[6]

The technology associated with the formation of polycrystalline films advanced greatly as a result of development of surface passivation techniques. Complex high-density arrays were developed that provided high spatial resolution and high detectivity with moderately rapid response. These developments have been reviewed by Bode.[7]

The most recent advances in polycrystalline film technology involve complex mosaic structures of detectors coupled to integrated circuits. However, the detector characteristics of polycrystalline films have shown little improvement over the past decade. This has led to a search for new detectors with higher detectivities and more rapid response times.

Epitaxially grown single-crystal films of the lead compounds show considerable promise for applications as infrared detectors with the desired characteristics. Photoconductive as well as photovoltaic detectors with high detectivities and fast response have been prepared from these films. The purpose of this section is to summarize the properties of these newer materials with emphasis on their device applications. No discussion of the properties of polycrystalline films is included, since this work has been so thoroughly reviewed.[4-8]

6.3.1.1.2 Current Understanding of Detector-Related Properties, Film Preparation, and Quality

Epitaxial films of the lead chalcogenide semiconductors have been grown on a variety of substrates using several different techniques. Chemical deposition has been used to grow PbS epitaxially on Ge, Si, CdS, and GaAs.[9] The heterojunctions formed between the films and substrates have many interesting and sometimes unusual characteristics. Liquid-phase epitaxy has been used to grow thick PbTe and PbSnTe epitaxial layers on PbTe substrates.[10] This technique generally yields n-type layers and can be used to form planar p-n junctions.

Most of the work on films prepared by chemical deposition and liquid epitaxy has been on the rectification characteristics of junctions between the films and substrates. Relatively little is known about the properites of the films per se other than their crystallographic orientation and, in some cases, their carrier density.

Vacuum evaporation onto heated, single-crystal substrates has been the most widely used method for epitaxy of the lead compounds. High-quality films of PbS, PbSe, and PbTe have been grown on a variety of substrates including NaCl, KCl, CaF_2, BaF_2, PbS, and mica.[11] This method has been highly successful because the lead compounds and alloys sublime at temperatures far below their melting points. This reduces dissociation of the evaporant and results in nearly stoichiometric films. Recently, a new method of vacuum evaporation under near-equilibrium conditions has been developed for growing high-quality PbS films of controlled stoichiometry.[12] This technique can be used to grow n- and p-type PbS film varying in carrier density from 1×10^{17} to 3×10^{18} cm^{-3} and in thickness from 1 to 75 μm.

Extensive studies have been conducted on the crystallographic, electrical-transport, optical, and magneto-optical properties of epitaxial lead chalcogenide films prepared by vacuum evaporation.[11] The studies have established that these films are single crystal with essentially the same properties as high-quality bulk crystals.[13]

Band Structure

The band structures of the lead chalcogenides (see Table 6.2) are reasonably well understood.[14] They are small-bandgap semiconductors having conduction and valence band extrema located at the L points in crystal momentum space. The constant-energy surfaces are four prolate ellipsoids elongated along the < 111 > directions; the elongation is strongest in the PbTe and weakest in the PbS. As a result of their large static dielectric constants, the impurity levels are very close to the band edges.

Extensive studies of the epitaxial lead chalcogenide films have established that they have the same band structure as bulk crystals. However, the energy gap may be slightly smaller at low temperatures due to differential contraction between the film and the substrate. Removing the film from the substrate and mounting it on a more suitable support alleviates this strain effect.[15] An alternate solution is to grow the films on a substrate having approximately the same thermal expansion coefficient as the film.

TABLE 6.2

Band Structure Parameters of PbS, PbSe, and PbTe

(m_o is the free electron mass and ϵ_o is the permittivity of free space)

Compound	Temperature (°K)	E_g (ev)[*]	m_e/m_o[**]	m_h/m_o[**]	ϵ/ϵ_o[**]
PbS	77	0.307	0.087	0.083	184
	300	0.41	-	-	172
PbSe	77	0.176	0.047	0.041	227
	300	0.27	-	-	206
PbTe	77	0.217	0.034	0.032	428
	300	0.31	-	-	380

[*] Reference 11 and 14.

[**] Reference 13.

Carrier Density and Transport Phenomena

The electrical properties of the lead chalcogenides are governed by lattice defects and impurities. It has been shown that each lead vacancy produces one free hole in the valence band and each chalcogen vacancy contributes one free electron in the conduction band. Impurity atoms also can alter the carrier density of the lead compounds. For example, Bi and O act as n-type and P-type dopants, respectively. The carrier density depends weakly on temperature down to very low temperatures because of the large static dielectric constants and the resulting very small impurity ionization energies.

Free-carrier mobilities in lead compound single crystal epitaxial films are very similar in magnitude and temperature dependence to values reported for high-quality bulk crystals.[11] Mobilities of the purest films exhibit a $T^{-5/2}$ temperature dependence from 300° K to very low temperatures and then the mobility levels off due to residual scattering. This residual scattering has been attributed to excess compensating vacancies and can be reduced by annealing the films at 350° C for 20 to 100 hours.[16] Post-deposition annealing may be an important step in obtaining device-quality materials since removal of excess defects may also increase excess carrier lifetimes.

There are few measured values of carrier lifetime in epitaxial films in the literature. Schoolar[17] has reported values as long as 32 μ sec in epitaxial PbS at 77° K, and Schoolar and Lowney[15] have reported values of 0.7 μ sec in epitaxial PbSe at 77° K. These values agree with estimates of the radiative lifetimes, τ_R, of these semiconductors.

An important fundamental property of a material is its intrinsic carrier density, n_i. Calculated values of n_i are presented in Table 6.3 together with other transport parameters of the lead salts at 77° K and 300° K.

TABLE 6.3

Transport Parameters of PbS, PbSe, and PbTe

(μ_e and μ_h are the electron and hole mobilities, respectively)

Compound	Temperature ($^{\circ}$K)	N_i(cm^{-3})	μ_n* (cm^{2}v^{-1}sec^{-1})	μ_h* (cm^{2}v^{-1}sec^{-1})	τ_R** (Sec)
PbS	77	6×10^5	11000	15000	-
	300	2×10^{15}	600	700	2.1×10^{-5}
PbSe	77	2×10^6	16500	13700	-
	300	3×10^{16}	1200	1000	7.5×10^{-7}
PbTe	77	4×10^6	31600	21600	-
	300	1.5×10^{16}	1800	900	8.7×10^{-7}

* Reference 20.

** Reference 13.

Optical Properties

Detailed studies of the optical properties of PbS epitaxial films have established that their optical absorption and dispersion characteristics are the same as high-quality single crystals.[19] The variation of the absorption coefficients of PbS, PbSe, and PbTe with photon energy is shown in Figure 6.3.[20] The absorption coefficients at energies above the energy gap are quite large because the lead compounds are direct gap semiconductors with large densities of states. The absorption at energies below the energy gap (not shown) is dominated by free-carrier and lattice vibrations.

The dispersion of the lead chalcogenides has been determined from optical studies of epitaxial films.[21] Figure 6.4 shows the variation of the refractive index with photon energy. The data presented in Figures 6.3 and 6.4 can be used to predict such important devices parameters as the quantum efficiency of detectors and the resonance modes and the gain of lead salt lasers.

6.3.1.1.3 State of the Art of Detector Development

Photoconductive Detectors

Photoconductive infrared detectors have been prepared from epitaxial films of PbS,[17] PbSe,[15] and PbTe[18] having carrier densities in the low 10^{17} cm^{-3} range. These detectors have little sensitivity at room temperature; however when cooled to 77° K, the PbS and PbTe epitaxial films are nearly as sensitive as the sensitized polycrystalline films of these compounds.

The response times of the epitaxial PbS[17] and PbSe[15] films have been reported to be 32 and 0.2 μsec, respectively. These values are two to three orders of magnitude faster than the polycrystalline film detectors.
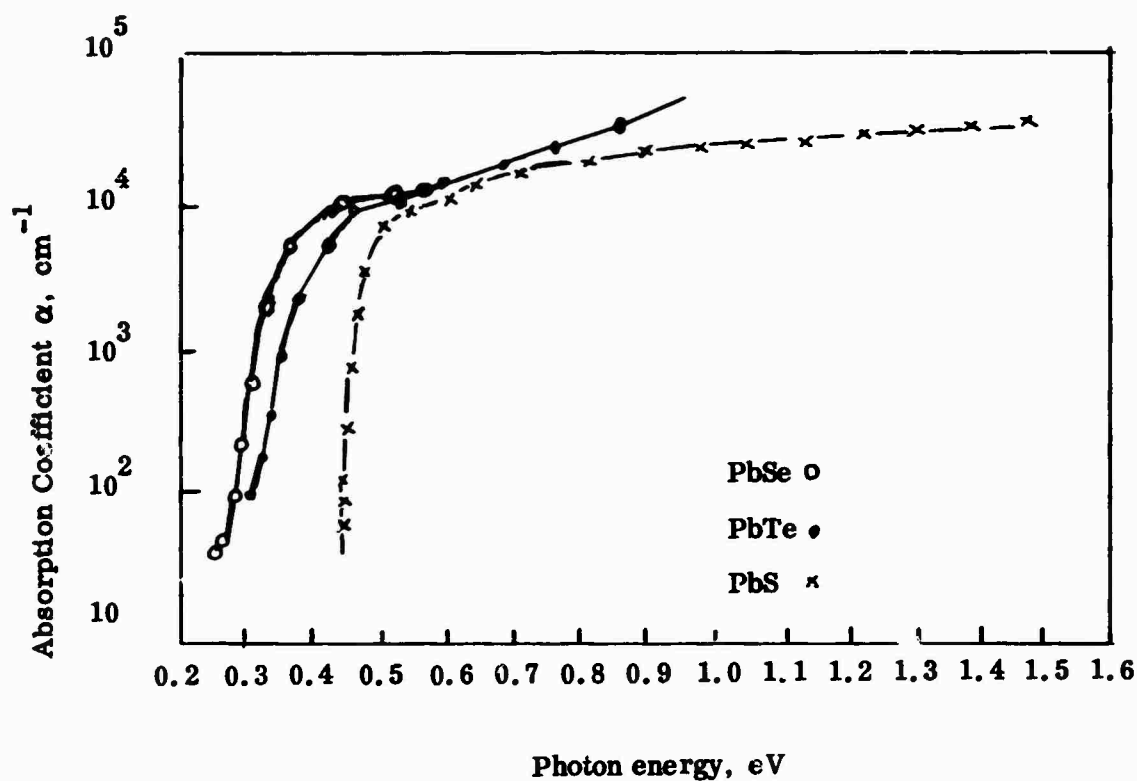
FIGURE 6.3 The optical absorption spectra of PbS, PbSe and PbTe at 300°K (after Scanlon[20]).
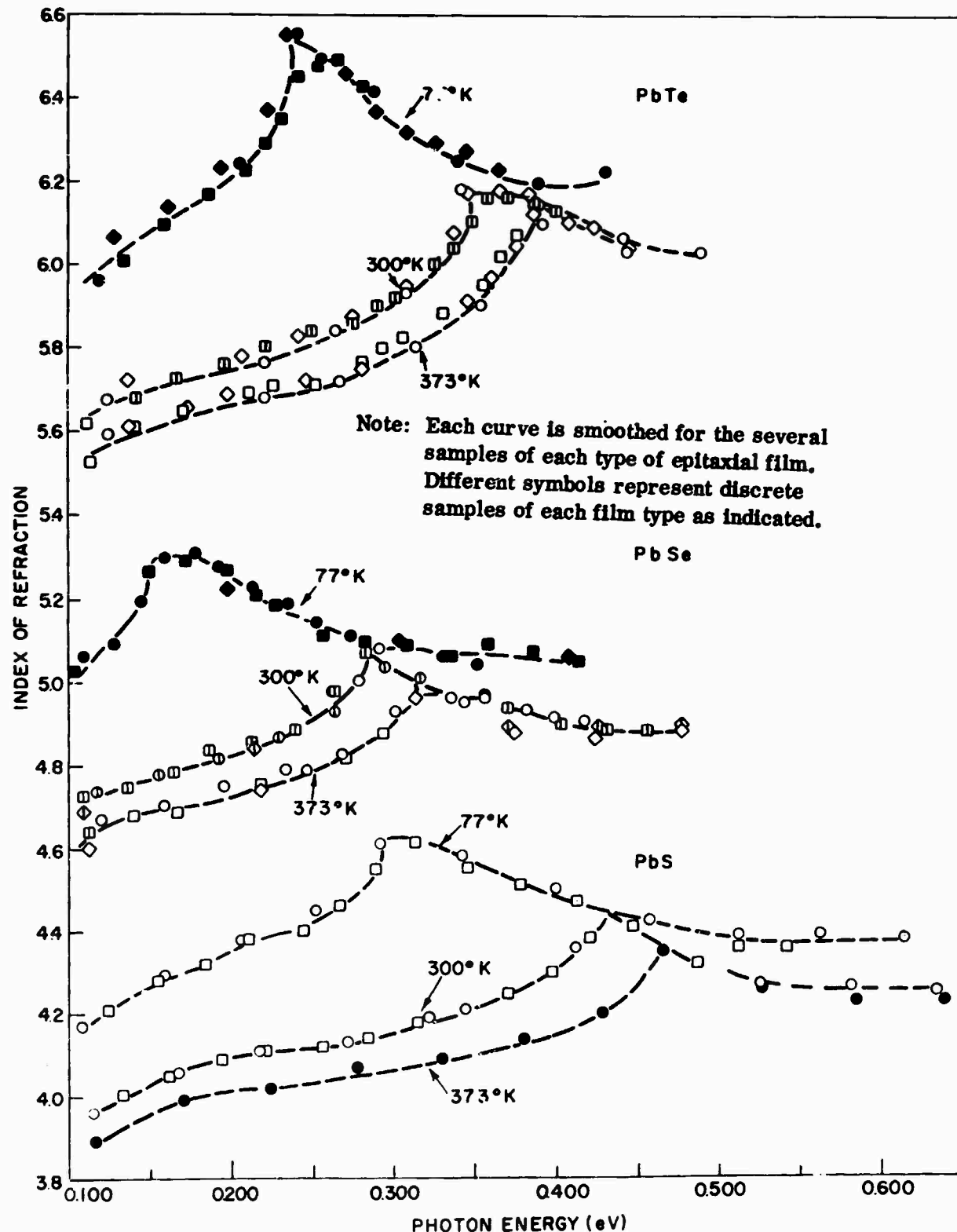
FIGURE 6.4 Variation of the refractive index of
epitaxial PbS, PbSe, and PbTe with
photon energy (after Zemel, et al[21])

A major problem in these detectors is the high carrier density. A recent study has shown that peak detectivities of 10^{12} cm(Hz)$^{\frac{1}{2}}$W^{-1} can be achieved for epitaxial PbS photoconductors operating at 190° K, provided the carrier density can be reduced to 2 x 10^{15} cm.$^{-3}$ [12] Such low carrier densities in the lead salts will require improved control of the stoichiometric composition and purity of these materials.

Junction Devices

Photovoltaic infrared detectors have been prepared from epitaxial lead salt films by several techniques. P-n junction detectors have been made by growing p-type layers of PbS on n-type substrates.[17] Heterojunction devices also have been made by growing PbS on other single-crystal substrates.[9] Although photovoltaic responses of these structures have been investigated, such detector parameters as spectral detectivities have not been reported.

Proton bombardment has been used to form p-n junction-type detectors in bulk PbTe crystals.[22] These devices have peak spectral detectivities in the 10^{12} cm(Hz)$^{\frac{1}{2}}$W^{-1} range. Preliminary results indicate that proton bombardment also can be used to form p-n junctions in epitaxial films; however, the infrared detection characteristics of these devices are not yet known.[23]

Schottky-barrier photodiodes with high detectivities have been prepared from epitaxial PbS[12] and PbTe.[24] The technique also has produced current injection lasers on bulk PbTe crystals.[25] The detectors were made by evaporating indium and lead rectifying contacts on p-type PbS and PbTe films, respectively. The detector films had carrier densities of 10^{17} cm^{-3}. Peak detectivities are very high, especially in the case of PbTe which was measured under reduced background conditions. Response times of the PbS detectors are reported to be 8 μ sec, two orders of magnitude faster than that of the polycrystalline film detectors.

The ultimate potential of these Schottky-barrier photodiodes is not yet known, and their major limitations have not been elucidated. It appears that they may offer superiority in both peak detectivity and speed of response over the poly-crystalline film detectors and the epitaxial film photoconductors.

6.3.1.1.4 Discussion

Basic Research

The band structure of epitaxial lead chalcogenide films is reasonably well understood. However, there are other areas where our basic understanding of these materials is inadequate for applied research to proceed rapidly.

- Epitaxy - A comprehensive study of epitaxial growth should be conducted with emphasis placed on:
  - Nucleation and growth on polished substrates.
  - Control of stoichiometry and purity.
  - Relationship of defect structure to growth conditions.
  - Influence of post-deposition annealing.

- Transport Phenomena - The following mechanisms should be determined and correlated with conditions of epitaxy, purity, and defect structure:
  - Majority and minority carrier scattering.
  - Energy of donor and acceptor levels.
  - Excess carrier lifetime and recombination rate.

- External Influences - Changes in the properties of the lead salts resulting from external influences should be better understood. The most important external influences are:
  - Proton bombardment and ion implantation.
  - Electric fields.
  - Ambients and dissimilar solids at surfaces and interfaces, respectively.

Applied Research

The applied research on epitaxial films should emphasize studies of several types of junctions and barriers. Research on these devices could lead to improved infrared detectors, infrared emitters (and lasers), and infrared field-effect modulators. The following devices should be studied:

- Schottky barriers, metal-semiconductor p-n junctions.
- Proton-bombarded and ion-implantated p-n junctions.
- Epitaxially grown p-n junctions (on polished substrates).
- Epitaxially grown heterojunctions (on polished substrates).

6.3.1.2 InSb and InAs

6.3.1.2.1 Introduction

It should be noted that infrared detector sensitivity depends directly on free-carrier lifetime, regardless of the mode of detection. In the past, emphasis in detector material preparation development had been placed on reduction of impurity concentration and other defects such as deviation from stoichiometric proportions. The idea was to reduce the free-carrier concentration associated with such defects and thus effect an increase in detector responsivity and lower noise. Purification of InSb and InAs has achieved excess carrier densities in the 10^{12} and 10^{15} cm^{-3} ranges, respectively;[26] however, detectors made of material with at least an order of magnitude higher free carrier density had the same sensitivity as those made of the best material.

Measurements and analyses made during the past several years show the limiting parameter to be free-carrier lifetime.[27] There is a sensitivity-speed relationship for any detector and the sensitivity is a direct function of lifetime. The upper limits on lifetime are Auger and radiative recombination mechanisms at the higher temperatures and Shockley-Read recombination at low temperatures.[27,28] Minority carrier trapping can be used to obtain higher detector sensitivity, i.e., provide longer effective lifetime because of longer response time or trapping time, at the cost of greatly increased cooling.

The Shockley-Read recombination center usually is associated with non-ionized defects and is, therefore, not readily apparent in "pure" material. Sometimes the temperature dependence of majority carrier mobility indicates the presence of these centers. Because significant detector improvement will require a large reduction in Shockley-Read center density, it will be necessary to identify these defects and devise growth and anneal methods that result in fewer such defects.

Defects which may be introduced during crystal growth and/or detector preparation include crystal deformities such as Frenkel defects, dislocations, slippage, and polycrystalline nucleated regions. The presence of nonionized bulk crystal defects in densities exceeding $10^{15} cm^{-3}$ is inferred from recent detector development data. The photovoltaic detector's sensitivity is limited by its depletion current, a direct result of short carrier lifetime. The phototransistor takes advantage of trapping that is thermally limited by the activation energy of the defect center.

6.3.1.2.2 Preparation of InSb

InSb received a great deal of attention during the early work with III-V compound semiconductors. Crystal growth from the melt by controlled freezing was the first technique applied to InSb and is still considered to be the best for achieving high purity and high carrier mobility. Using high-purity starting materials, palladium-purified hydrogen gas ambient, ultra-high purity quartz boats and crucibles, and extended zone refining, crystals with excess carrier densities as low as $10^{12} cm^{-3}$ have been grown.[26] Although growth of InSb from the melt by Czochralski pulling or horizontal zone melting has produced the best crystals from the standpoint of purity and crystalline perfection, this technique often results in a non-uniform distribution of dopant across the diameter of the crystal.[29]

Unlike most of the other III-V compounds, no satisfactory vapor-phase deposition process has been reported for InSb. Evaporation techniques which use high-purity precompounded InSb as source material have been explored for preparing thin polycrystalline films; these have electrical properties greatly inferior to the bulk single-crystal material.

More recently, liquid-phase epitaxy has emerged as an important and useful method for preparing thin epitaxial layers of high-purity compound semiconductors. Melngailis and Calawa have grown thick layers of InSb from indium rich solutions at temperatures as low as 300° C.[30] Using p-type (zinc-doped) substrates and tellurium-doped, indium-rich melts, they were able to prepare p-n junctions from which injection lasers were fabricated. This low-temperature solution growth technique obviously resulted in an improved crystal structure since this was the only method of preparation that provided thin layers transparent to the radiation generated at the p-n junction.

6.3.1.2.3 Preparation of InAs

The preparation and purification of high-quality single-crystal material is a much more formidable task for InAs than for InSb. Although extremely high purity indium can be readily obtained, the purification of arsenic is much more difficult. Many impurities normally associated with arsenic such as sulfur and tellurium, are easily volatilized and are difficult to remove completely from arsenic in the fractional sublimation process used for its purification.

The most satisfactory method for Czochralski pulling of InAs is that described by Gremmelmaier; the InAs charge and pulling apparatus are totally sealed inside a quartz chamber and the seed withdrawal mechanism is activated by means of magnetic coupling.[31] Single crystals prepared in this way exhibit excess carrier concentration in the range 1 to 3 x 10^{16} cm^{-3} and electron mobility of 3.0 x 10^4 cm^2/V-sec at 300° K.

Effer used vacuum-baked indium and high-purity arsenic to produce single-crystal InAs with excess electron concentration of 8×10^{15} cm^{-3} and electron mobility of 7.5×10^4 cm^2/V-sec, at 77° K. This material was prepared by horizontal zone refining in quartz boats.[32]

Although melt grown InAs is not the equal of InSb with respect to purity, InAs can be rather easily prepared by chemical vapor-phase epitaxial deposition, using HCl and temperatures chosen to favor indium monochloride formation as an intermediate step.[33]

Both InAs and GaAs substrates have been used. Higher quality material was formed when InAs substrates were used. Excess carrier concentrations in the 3 to 7×10^{15} cm^{-3} range with mobilities as high as 1.1×10^5 cm^2/V-sec at 77° K have been reported.[34] When deposited on semi-insulating GaAs, the mobilities at 77° K were generally a factor of two lower.[35] Presumably this degradation is due to lattice defects induced at the substrate-epitaxial layer interface as a result of the nearly 7 percent difference in lattice constant between InAs and GaAs.

With few exceptions little work has been reported concerning the preparation and properties of pure InAs by liquid-phase epitaxy from indium-rich solutions.[36] Most of the work involving solution growth from indium has been concerned with the preparation of the III-V alloys such as GaInAs,[37] and InAsSb.[38] The relatively low- efficiency InAs lasers prepared by solution-growth techniques were only made functional by subjecting the material to heat treatment following epitaxial growth. This again suggests a lattice defect which introduces a non-radiative recombination center and which annealing helps to remove. Perhaps what is necessary is a low-temperature growth technique in which the rate of crystallization can be held to a carefully controlled low value.

6.3.2 <u>Intrinsic Alloy Semiconductors</u>

6.3.2.1 <u>HgCdTe</u>

6.3.2.1.1 <u>Introduction</u>

The pseudo-binary alloy system $Hg_{1-x}Cd_xTe$ has been developed during the last decade into a very useful material for high-performance intrinsic infrared photon detectors.[39] Both photoconductive and photovoltaic detectors of BLIP limited performance have been made. The continuous variability of the energy gap with alloy composition permits the design of an alloy detector optimized at any wavelength throughout most of the infrared spectrum. $Hg_{1-x}Cd_xTe$ alloys are "well-behaved" semiconductors, whose basic properties are understood and can be controlled in large measure to achieved desired detector performance. These alloys crystallize in the zincblende structure.

6.3.2.1.2 <u>Electronic Energy Band Structure</u>

Cadmium telluride is a semiconductor with an energy gap of $E_g = 1.6\,eV$ (at $0°\,K$), whereas mercury telluride is a semimetal which can be considered to have a "negative" energy gap (band overlap) of about $0.3\,eV$ (at $0°\,K$). In the alloy system $Hg_{1-x}Cd_xTe$, the energy bands vary linearly with x at least in the region $0 < x < 0.3$, so that for $x > 0.15$, the alloy is a semiconductor. The semiconductor side of the alloy system is useful for intrinsic infrared photon detectors. In these alloys the electron effective mass is much smaller than the hole effective mass, the conduction band is non-parabolic, and the valence band has two branches that are degenerate at the edge.

The long-wavelength cutoff, λ_{co}, of detector photoresponse is related to the energy gap by:

$$\lambda_{co} = \frac{hc}{E_g} ,$$

and λ_{co} varies with x as shown in Figure 6.5.[40,41] These are the basic $Hg_{1-x}Cd_xTe$ "material design" curves for infrared detectors. Thus, the composition and operating temperatures of $Hg_{1-x}Cd_xTe$ can be selected to give a detector with optimum response between 0.8 μm and very long wavelengths, covering nearly all the infrared spectrum.

6.3.2.1.3 Crystal Preparation

Single crystals of $Hg_{1-x}Cd_xTe$ for use in infrared detectors are usually prepared by solidification from the melt. Crystal preparation is based on knowledge of the phase diagram of the alloy system.[39,42] The purified elements are melted and mixed together in proper proportion to form the desired alloy. The resultant charge is solidified under controlled conditions of shape, temperature, and pressure to achieve a single crystal. A rapid quench is used to inhibit segregation of the constituents. The crystal may then be annealed at high temperature to eliminate any dendritic structure and to acquire the desired composition based on the phase diagram. Crystals prepared in this manner generally yield alloy compositional uniformity to within 0.002 mole fraction over distances of 1 cm.

Single-crystal films have also been deposited epitaxially from the vapor phase;[41] however, the resultant material usually has not been as suitable for detectors as the melt-grown crystals.

6.3.2.1.4 Semiconducting Properties

Carrier concentrations, carrier mobilities, the behavior of doping impurities, and recombination lifetimes are some of the semiconducting properties that must be known when using HgCdTe in an infrared detector. Typical of HgCdTe crystals are some measurements made for n- and p-type samples of $Hg_{0.8}Cd_{0.2}Te$. N-type samples have a net carrier concentration of about $10^{15} cm^{-3}$. Excess interstitial mercury atoms are believed to act as singly ionized donors with a very small ionization energy. The electron mobility is about $10^5 cm^2/volt-sec$ at low temperatures. This high mobility implies that the donors are largely uncompensated. Similar results are also found in samples of higher x.
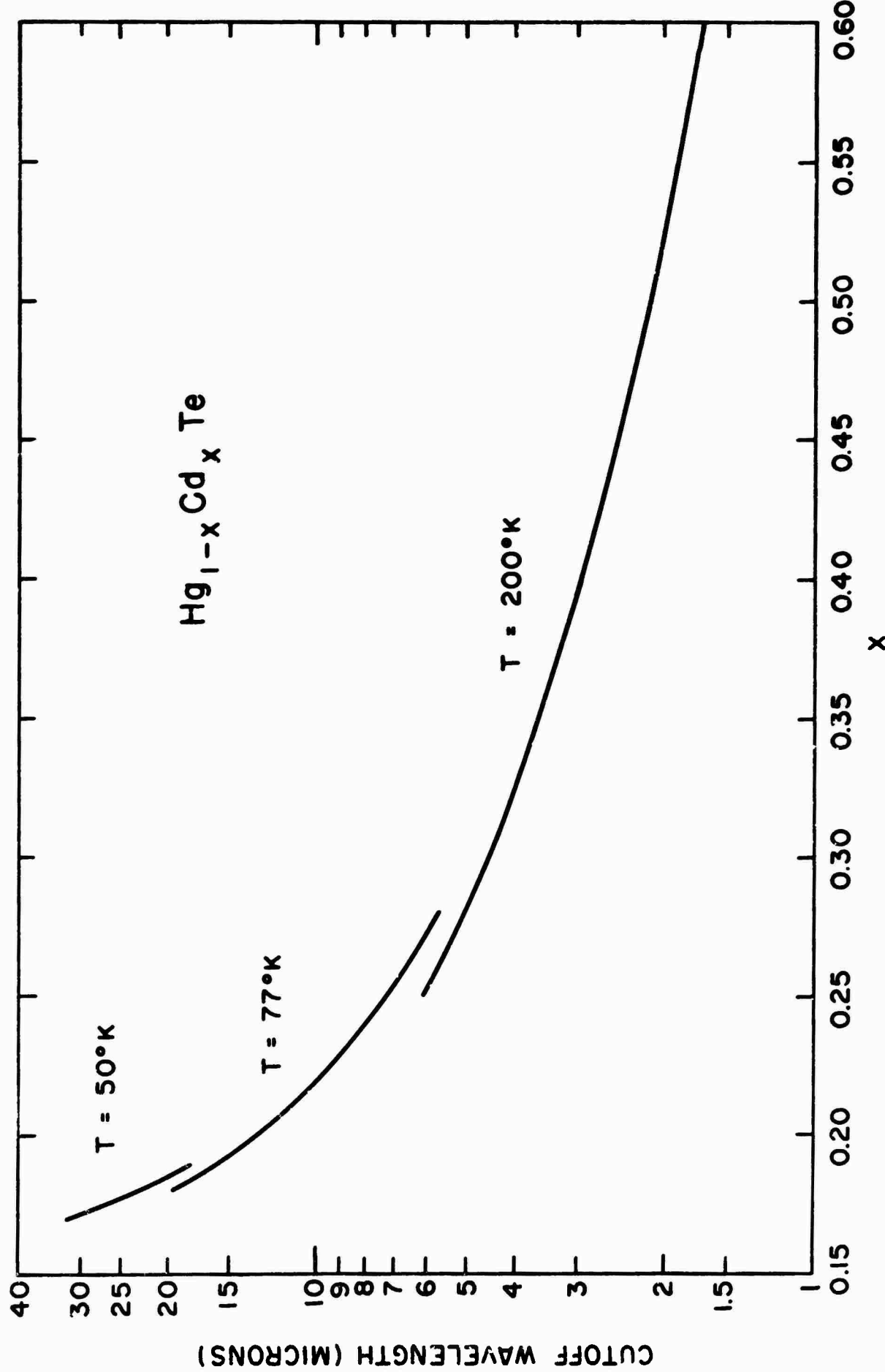
FIGURE 6.5 Long-wavelength cutoff of photo-response λ_{co} vs x for $Hg_{1-x}Cd_xTe$ at three common temperatures of detector operation.

244

P-type samples have higher extrinsic carrier concentrations (about $5 \times 10^{16} cm^{-3}$ or higher). The hole mobility is much lower than the electron mobility in a comparable n-type sample; the electron/hole mobility ratio is greater than 10. The higher mobility ratio implies that high photoconductive gain* is possible in photoconductive detectors made of n-type material even without minority carrier trapping.

Relatively little is known experimentally about the properties and effects of impurities in $Hg_{1-x}Cd_xTe$. Gold acts as an acceptor, but its energy level is unknown. Indium is a shallow donor.

Excess carrier lifetimes in $Hg_{1-x}Cd_xTe$ are governed by various recombination and trapping mechanisms, depending upon temperature and carrier concentration. At very low temperatures, trapping effects often are observed. In the vicinity of liquid nitrogen temperature the lifetime is usually controlled by Shockley-Read recombination[28] in pure material; typical lifetime values lie between 0.1 and 1 μ sec. Near room temperature, Auger or direct-radiative recombination[27] dominates.

6.3.2.1.5 Devices

Infrared detectors have been made of $Hg_{1-x}Cd_xTe$ having photoresponse maxima from about 1 to 35 μm. These devices include both photoconductive and photovoltaic detectors; the photoconductive is the more common mode.

The detectors are made either singly or in arrays. Indium is generally used as the electrical contact material on a photoconductive detector. The photovoltaic detectors are basically p-n junctions, made by:

- Diffusion of excess Hg into a surface layer of a p-type crystal
- Diffusion of gold into an n-type crystal
- Proton bombardment of a p-type crystal to convert a surface layer to n-type[44]

---

* Reference 8, Chapter 5

$Hg_{1-x}Cd_xTe$ detectors have achieved BLIP limited performance in the 8 to 14 μm range at ~77° K, under the conventional conditions of background radiation. Photoconductive detectors have shown very high values of D* at liquid helium temperatures in very weak background radiation.

6.3.2.2 PbSnSe and PbSnTe

6.3.2.2.1 Introduction

The semiconducting alloys $Pb_{1-x}Sn_xSe$ (0 ≤ x < 0.4) and $Pb_{1-x}Sn_xTe$ (0 ≤ x ≤ 1) are of interest for infrared detector applications for several important reasons. Of major significance is the fact that the unusual behavior of the valence-conduction bands makes it possible to tune optical devices over wide ranges of wave-length in the near and far infrared. Homogeneous single crystals can be prepared with relative ease, both in bulk and epitaxial film forms. Another important characteristic is that carrier concentrations can be controlled over a wide range by simple heat treatment procedures. Finally, good photovoltaic detectors can be fabricated by diffusion, proton bombardment, and Schottky barrier techniques.

The following comments refer to $Pb_{1-x}Sn_xTe$. A discussion of $Pb_{1-x}Sn_xSe$ would be analogous.

6.3.2.2.2 Band Structure

The $Pb_{1-x}Sn_xTe$ alloys are semiconductors having a NaCl crystal structure with valence and conduction bands centered at the L points in the Brillouin zone. The upper part of Figure 6.6 shows the dependence of the energy gap on composition at 300° K. As the composition varies from pure PbTe to Pure SnTe, there is an inversion of the conduction and valence bands.[46] The electron states of L_6 symmetry which originally formed the conduction band in PbTe become the valence band states in SnTe and vice versa.

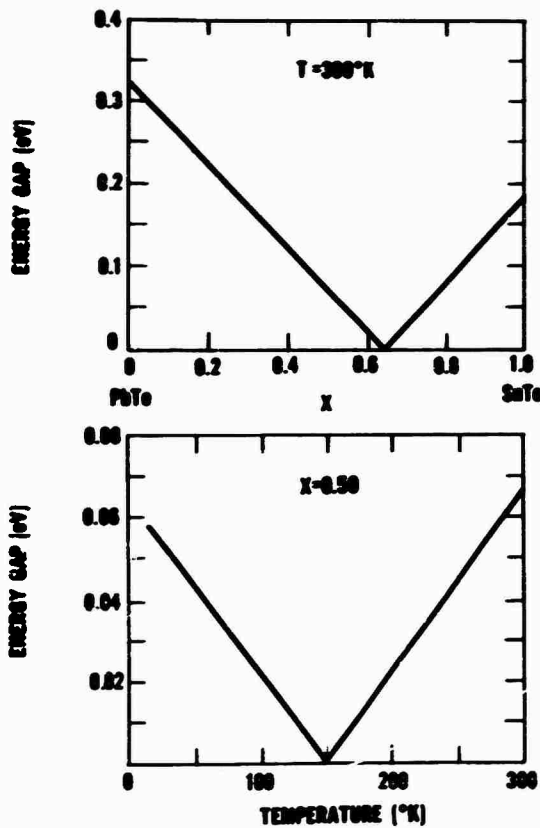FIGURE 6.6   The upper part of the figure shows a typical variation

of the energy gap for $Pb_{1-x}Sn_xTe$ with composition for

a fixed temperature. The lower portion shows a typical

variation of the energy gap with temperature for a fixed

alloy fraction.

The bandgap depends not only upon the composition, but also upon temperature, as shown in the lower part of Figure 6.6 for $x = 0.5$. Note the similarity of the variations of the energy gap with temperature and composition. It is thus possible to selectively "tune" the cutoff wavelength of an infrared detector by varying either the composition or the operating temperature. However, because doping causes a shift of absorption edge toward shorter wavelengths (Burstein shift), it is extremely important to lower the carrier concentration as much as possible. This allows one to achieve the maximum range of "tuneability" for a photoconductive device. For example, Figure 6.7 illustrates the range of optical tuneability as a function of the carrier concentration for $Pb_{0.5}Sn_{0.5}Te$ between $0°$ K and $300°$ K. From the figure it is evident that the tuneability range is greatly extended as the carrier concentration is lowered.

High carrier mobility improves device performance by reduction of Johnson noise. Fortunately, the effective masses of both the holes and electrons in $Pb_{1-x}Sn_xTe$ are believed to be small.[47] In the narrow gap region both masses are extremely small and should lead to unusually high mobilities for both carriers. This is in contrast to the $Hg_xCd_{1-x}Te$ system, for which only the electrons possess a light mass and associated high carrier mobility. Furthermore, the light masses of $Pb_{1-x}Sn_xTe$ lead to low intrinsic carrier concentrations and to correspondingly low minority carrier concentrations. Thus $Pb_{1-x}Sn_xTe$ detectors have the potential for operating at relatively high temperatures.

6.3.2.2.3 Crystal Preparation Techniques

Bulk

High quality-bulk crystals of $Pb_{1-x}Sn_xTe$ and $Pb_{1-x}Sn_xSe$ have been produced by the Bridgman[48], Czochralski[49], and vapor-growth methods.[50] Of these three techniques, vapor growth appears to produce the highest quality crystals.
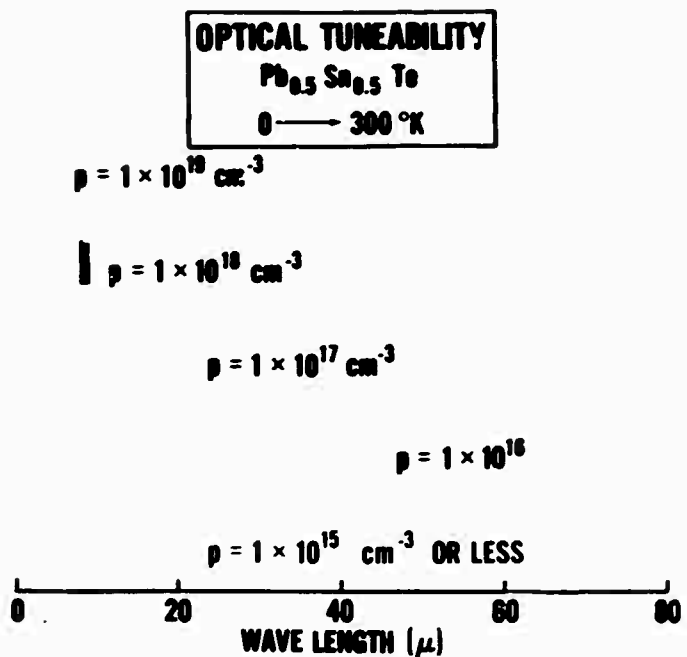
FIGURE 6.7   Range of photoconductive detector tuneability corresponding

to $Pb_{0.5}Sn_{0.5}Te$ and temperature range of 0° K to 300° K

for various carrier concentrations.

For example, vapor-grown crystals of $Pb_{0.83}Sn_{0.17}Te$ have been heat-treated to give free-electron mobilities in excess of $8 \times 10^6 cm^2/V\text{-sec}$.[51] In addition, most of the successful lasers and photovoltaic detectors which have been produced thus far have been made from vapor-grown materials.[52]

Films

Epitaxial films of $Pb_{1-x}Sn_xTe$ and $Pb_{1-x}Sn_xSe$ have been grown on a variety of substrates using three different growth techniques:

- Evaporating the parent binary compounds from two separate sources.[53]
- Evaporating the desired alloy from a single source.[54]
- A recent quasi-equilibrium evaporation technique which has been developed and has produced high-quality epitaxial films of $Pb_{1-x}Sn_xTe$ with thicknesses up to $400 \mu m$[55].

Each of these three methods produces strained films due to the differential thermal expansion between the substrate and film. A recently developed "parting-layer" technique shows considerable promise of alleviating the strain problem.[56] For $Pb_{1-x}Sn_xTe$ alloy, a very thin layer of NaCl is deposited onto a carefully prepared surface of high-quality single crystal PbTe. The PbSnTe alloy is subsequently deposited on the NaCl. Because of the very close match between the thermal coefficients of PbTe and $Pb_{1-x}Sn_xTe$ and the thinness of the NaCl layer, the film remains relatively unstrained during deposition and cool down. In addition, the NaCl permits easy separation of the film from the PbTe substrate. It is believed that a combination of this parting layer technique with the quasi-equilibrium technique has considerable promise for producing high-quality, thick,unstrained, free films.

6.3.2.2.4 Carrier Concentration Control

Lead and tin combine with tellurium and selenium to form the binary compounds PbTe, SnTe, PbSe, and SnSe. The composition range over which the compound (e.g., PbTe) can exist as a solid single phase is very narrow, usually represented in a phase diagram as a single line at 50 atomic percent Te, the stoichiometric

composition. In reality, however, this single line is a region of finite width; the deviations from stoichiometry which are possible lead to free carriers in the material. Excess Pb contributes electrons to the conduction band, while excess Te contributes holes to the valence band. It is thus necessary to control the deviation from stoichiometry. This is usually accomplished by annealing the as-grown material in the presence of a metal- or chalcogenide-rich powder in a closed tube under vacuum and at a specific temperature.[57] This serves to shift the composition of the sample toward either the metal or chalcogenide boundary of the solidus field, respectively. The resulting carrier concentration will depend upon the annealing temperature since it is this temperature that determines how close the solidus boundary is to the stoichiometric composition. The lowest carrier concentrations accompany annealing at the temperature for which the solidus boundary crosses the stoichiometric line. As SnTe is added to PbTe, the solidus field shifts toward excess Te, and the temperature at which the solidus boundary crosses the stoichiometric line moves progressively to lower temperatures. Therefore, as one alloys more SnTe with PbTe it becomes necessary to anneal at lower and lower temperatures to obtain the lowest possible carrier concentrations. There is a practical limit to the lowest temperature at which annealing may be carried out since the rate of the diffusion process involved in the equilibration is a function of the temperature. As one lowers the temperature the time required to reach equilibrium finally becomes the limiting practical factor. It is estimated that one could anneal thin films of $Pb_{1-x}Sn_xTe$ to the stoichiometric composition for alloy fractions in the range $0 \leq x \leq 0.4$. Alloys of greater Sn content on the other hand, would have to be annealed at temperatures that are too low to allow the process to reach equilibrium in reasonable time.

Foreign impurities are believed to control carrier concentrations below $10^{17} cm^{-3}$. Unfortunately, insufficient research effort has been directed towards identifying and controlling foreign impurities in these materials. While the compounds usually are synthesized from starting materials which are 99.9999 percent pure, it has been shown that this leads to an impurity concentration of about

10^{17} cm^{-3}.[58] This estimate is consistent with the result of mass spectrographic analysis.[59] The mobility in the lead chalcogenides tends to decrease as the carrier concentration is lowered below 1×10^{17} cm^{-3}, indicating strong compensation.[60] It is believed that impurity concentrations several orders of magnitude lower than 1×10^{17} cm^{-3} will be required for high-performance photoconductive devices.

6.3.2.2.5 Device Fabrication and Limitations

Because of the difficulties involved in reducing impurity concentrations in these materials, considerable effort has been directed toward p-n junction device development. By so doing the foreign impurity problem has been somewhat circumvented.

Several techniques have been successfully used to make p-n junctions. The first was simply to diffuse an n-type layer into a p-type sample.[52] A more recent method is to bombard the surface of a p-type sample with protons and convert the surface to n-type.[61] Further, Schottky barriers have been successfully formed on both n- and p-type samples of $Pb_{1-x}Sn_xTe$ for $x < 0.3$.[62] The results of these various techniques have yielded photovoltaic detectors with D* as high as 10^{12} cm Hz$^{\frac{1}{2}}$/W.[61] Although the behavior of these photovoltaic detectors is impressive, there is prospect of still further improvements in the performance and ease of fabrication when foreign impurity concentrations are reduced.

6.3.2.3 InAs-InSb Alloys

6.3.2.3.1 Introduction

In solid solutions of the intermetallic semiconducting III-V compounds InSb and InAs, the energy gap, E_g, and carrier effective masses both exhibit well defined minima as a function of alloy composition. Coderre and Woolley[63] found for $InAs_xSb_{1-x}$ a minimum value of 0.17 eV for E_g at $T = 0°$ K, for $x = 0.4$. Their results are plotted

in Figure 6.8. Although Kudman and Ekstrom[64] found a minimum value of 0.195 eV for x = 0.1, optical absorption studies agree with the Coderre and Woolley result[65,66]. Potential applications of these alloys include spontaneous and stimulated radiation sources, infrared detectors with variable response peaks in the spectral range between $\sim 3\,\mu m$ and $\sim 9\,\mu m$ in wavelength, spin-flip Raman lasers, and high efficiency galvanomagnetic devices.

6.3.2.3.2 Preparation and Properties of InAsSb Films

The equilibrium phase diagram of the pseudobinary InAsSb system consists of widely separated liquidus and solidus curves, which lead to a variation in the ratio of InAs to InSb as the alloy solidifies. There are two contradictory requirements for single-crystal growth. Rapid solidification is needed to overcome compositional inhomogeneities, but it usually leads to nucleation of multiple crystallites and high defect densities. Slow cooling in near thermodynamic equilbrium conditions also is needed to grow crystallographically well-ordered crystals.

Epitaxial growth of $InAs_{0.5}Sb_{0.5}$ films by flash evaporation onto single-crystal Ge and on fused quartz substrates was investigated by Mueller and Richards[67]. Neither optical nor electrical measurements were made on these films.

Liquid-phase epitaxy was used by Stringfellow and Greene to grow 80 to 100 μm-thick epitaxial $InAs_xSb_{1-x}$ layers on single-crystal InAs substrates for $0.65 < x < 1$ and on InSb substrates for $0 < x < 0.11$.[68] The optical absorption edge of the films appears to be quite steep; the room-temperature composition dependence of E_g is in good agreement with previous bulk measurements[66]. However, the electron mobility in these films is poor: at 300° K, it was only 2.7×10^4 cm^2/V-sec for x = 0.3, while 8.5×10^4 cm^2/V-sec was expected for single crystalline material. Kudman and Ekstrom obtained an electron mobility of 7.96×10^4 cm^2/V-sec on bulk material with x = 0.315, in agreement with theoretical expectations.[64]
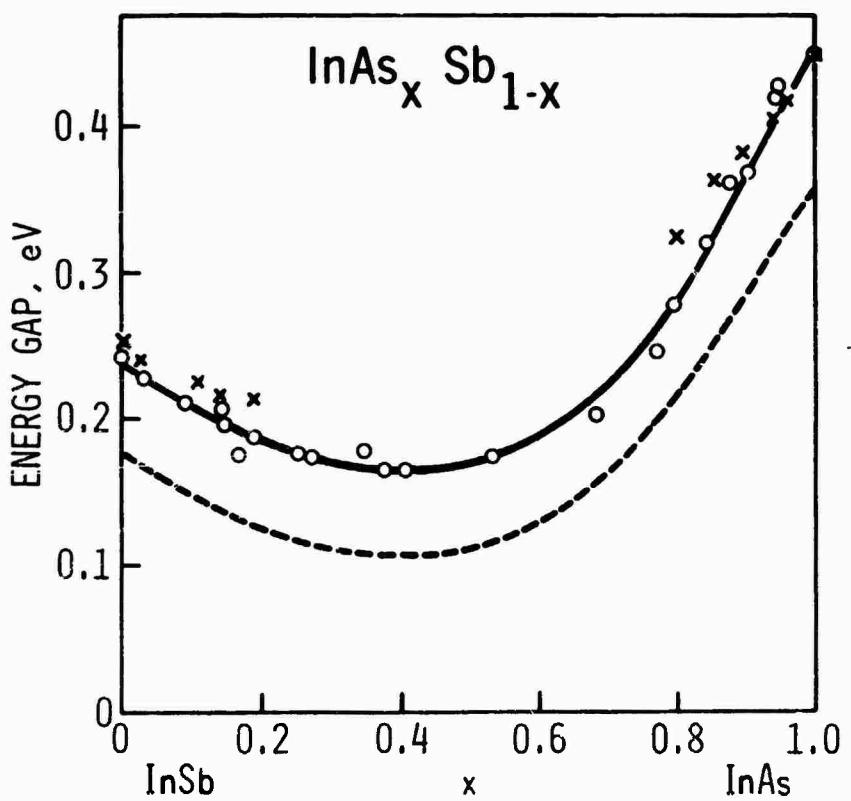
FIGURE 6.8   Dependence of Energy Gap on alloying   in $InAs_xSb_{1-x}$.
The solid curve is for $T = 0°K$; the dashed curve
is for room temperature (53).

Wieder has prepared $InAs_x Sb_{1-x}$ films by the flash-evaporation of variable ratio mixtures of fine-mesh powdered InSb and InAs on single-crystal semi-insulating GaAs substrates.[69] Although the films had strong preferential crystallographic orientations, they were microcrystalline which is thought to reduce electron mobility. Annealing these films in hydrogen at temperatures below the melting point for 10 days induced an order of magnitude increase in the size of the crystallites, and some rise in electron mobility. The electron mobility was still low, however, being $\sim 10^4 cm^2/V$-sec at room temperature, with an electron density of $\sim 2 \times 10^{17} cm^{-3}$. This density is an order of magnitude higher than in films grown by liquid-phase epitaxy.

Electron beam microzone crystallization cannot be used directly in the $InAs_x Sb_{1-x}$ films deposited on GaAs substrates because of the relatively high thermal conductivity of GaAs which prevents the establishment of a narrow liquid zone in the films. It can be used to recrystallize flash-evaporated $InAs_x Sb_{1-x}$ films deposited on glass substrates, for $x \leq 0.3$. Efforts to make $x > 0.3$ resulted in films deposited in two phases, one nearly pure InSb, the other with $x \geq 0.7$. Electron beam microzone crystallization improves the electrical and galvanomagnetic properties of the $InAs_x Sb_{1-x}$ films. Electron densities are decreased by more than one order of magnitude and electron mobilities are increased by two orders of magnitude over their corresponding values prior to recrystallization. Although mobilities are higher than those of epitaxially flash-evaporated films with the same fractional arsenic content, they are well below bulk values.

The energy gaps of these films were determined from transport measurements and from photoconductive and photovoltaic measurements, such as those shown in Figure 6.9.[70] The data on the $InAs_x Sb_{1-x}$ films is in better agreement with that measured on bulk crystals by Woolley and his co-workers[63, 65, 66] than with the data reported by Kudman and Ekstrom.[64]
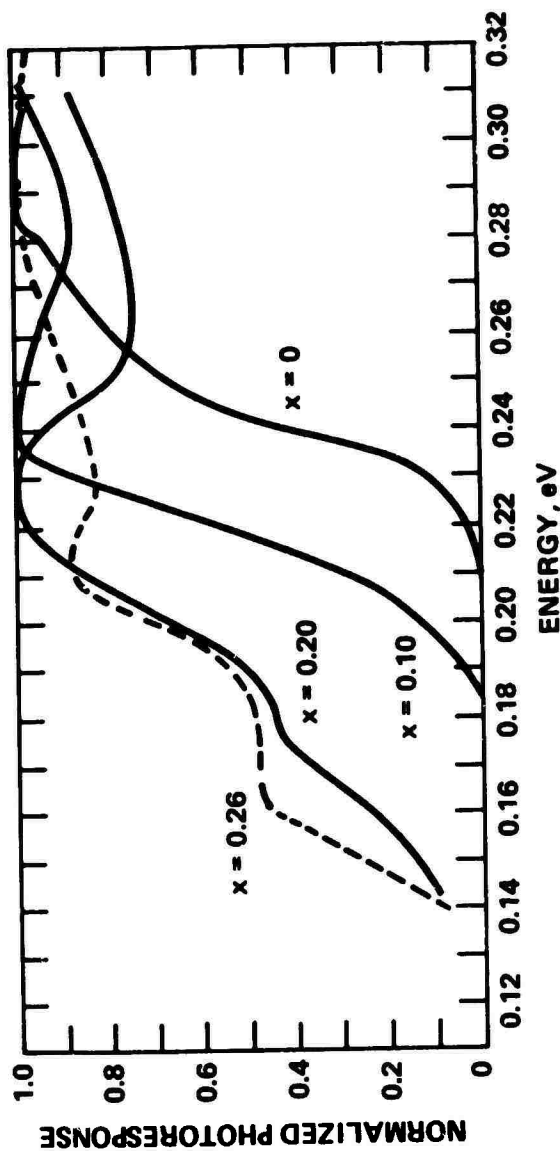
FIGURE 6.9 Photoresponse of electron-beam recrystallized InAs$_x$Sb$_{1-x}$ films at T = 77 K (70).

6.3.2.3.3 Discussion

The evidence presented here provides support for the monotonic decrease in E_g with increasing As concentration for $0 < x < 0.3$. The electron beam micro-zone crystallization technique has provided $InAs_x Sb_{1-x}$ solid solution alloy films grown on chemically inert insulating substrates. Only polycrystalline films with $x < 0.3$ have been synthesized thus far. Chemical disproportionation transport reactions and liquid-phase epitaxy might be more suitable processes for device-quality materials.

There are many unresolved issues. Among them are the following:

- Is it possible to grow homogeneous single-crystal layers and bulk crystals in the vicinity of the minimum bandgap without phase segregation?

- Is it possible to reduce the residual impurity concentrations to $10^{15} cm^{-3}$?

- What causes the minimum in $E_g(x)$?

- What are the charge carrier scattering processes in these alloys?

- How and why does the effective mass of the carriers depend on composition?

Extensive optical and magneto-optical investigations are required in order to determine the effective masses of the charge carriers and the energy dispersion of the complex index of refraction. Preliminary investigations of donor doping of epitaxial layers have been made.[68] It would be desirable to extend these to include a variety of donors and acceptors and to investigate the formation of p-n junctions suitable for detector applications.

It is recommended that basic research in thin films of InAsSb be supported, with particular emphasis on the concentration range where the forbidden energy gap is a minimum. This program should include evaluation of methods for preparing single-crystal films of approximately 1 cm area sufficiently uniform for use in high-density arrays. Studies of the electrical and optical properties of the films

should be made, and their suitability for use as both photoconductive and photovoltaic detectors should be explored.

6.3.2.4 PbTe - GeTe Alloys

6.3.2.4.1 Introduction

Alloys of PbTe and GeTe show promise as infrared detector materials for use in the 3 to 5 μm wavelength atmospheric transmission window. This alloy system is also being developed for infrared-emitting diode lasers. Unlike most other alloy systems which have been investigated for these applications, PbTe and GeTe have different crystal structures at room temperature; the rock salt crystal structure characteristic of PbTe is stable only if the GeTe content in the alloy is kept less than about 6 percent. One of the distinctive properties of the $Pb_{1-x}Ge_xTe$ alloy system is a transition to a ferroelectric state at cryogenic temperatures. This transition provides an unusual opportunity to investigate the effects of ferroelectricity on the properties of infrared detectors.

The preparation of PbTe was discussed in 6.3.1.1. Its melting point is 917° C and it crystallizes into the cubic rock salt crystal structure. The melting point of GeTe is 724° C. At room temperature, GeTe is a ferroelectric with a trigonal crystal structure analogous to bismuth. Above about 400° C, GeTe transforms to the cubic rock salt crystal structure. The phase diagram of the $Pb_{1-x}Ge_xTe$ alloy shows that above 570° C PbTe and GeTe form a fully miscible alloy with the rock salt crystal structure.[71] Below 570° C a miscibility gap appears which causes separation into two stable phases. PbTe rich alloys cannot stably contain more than about 6 percent GeTe without eventual exsolution into two phases. Single-phase crystals with more GeTe can be obtained by rapid quenching, but the stability of these samples decreases with increasing GeTe content. The results reported on infrared detectors and lasers are all on material containing less than 6 percent GeTe. These crystals were grown by vapor transport.

$Pb_{1-x}Ge_xTe$ also undergoes a ferroelectric phase transition similar to that reported for GeTe.[71] In GeTe, the Curie temperature for the ferroelectric transition depends critically on whether the sample is Ge-rich or Te-rich. For metal-rich $Pb_{1-x}Ge_xTe$, the phase transformation occurs at room temperature for x = 0.18, at 77° K for x near 0.025 at 0° K for x near 0.01. Studies of capacitance as a function of temperature for PbGeTe p-n junctions have shown that the capacitance goes through a maximum near the Curie temperature.[72] The magnitude and temperature dependence of the capacitance maximum depends critically on bias voltage.

Vapor-transport-grown $Pb_{1-x}Ge_xTe$ is usually p-type. It can be converted to n-type by annealing at a reduced temperature. With a shorter anneal, a p-n junction can be formed in $Pb_{1-x}Ge_xTe$; p-n junctions can also be formed by impurity diffusion.

Diode lasers also have been developed using $Pb_{1-x}Ge_xTe$.[73] They cover the wavelength range between 4.5 μm and 6.0 μm. PbGeTe diode lasers are wavelength tuneable with bias current. They can be used for monitoring atmospheric pollutants as well as in heterodyne infrared detection systems. These diode lasers are operated near 5° and 77° K temperature. A suprise in this work is the reversal in the temperature dependence of the band gap for x > 0.028. This is correlated with the ferroelectric transition for this composition. More recent results indicate that the temperature dependence of bandgap between 5° and 77° K is unexpectedly small in the ferroelectric phase.[74]

6.3.2.4.2 Infrared Detectors

As yet, very limited data are available on $Pb_{1-x}Ge_xTe$ infrared detectors. Data for x = 0.03 have been reported in the classified literature for photovoltaic infrared detectors fabricated by antimony diffusion into p-type material.[75] The test temperatures (> 77° K) in this study placed the material in the paraelectric phase rather than the ferroelectric phase. Responsivities and detectivities approaching the theoretical limit were obtained. As expected, the RC time constant of the detectors was much greater than 1 μ sec depending on the temperature and background used. The long time constant can be a problem in some applications. The long wavelength cut-off for infrared

detection for $x = 0.03$ $Pb_{1-x}Ge_xTe$ was $5.0\,\mu m$, $4.6\,\mu m$ and $4.2\,\mu m$ for temperatures of $77°\,K$, $140°\,K$ and $195°\,K$, respectively.

Photoconductive detectors could be developed using single crystal $Pb_{1-x}Ge_xTe$ annealed to low carrier concentration. Studies of photoconductivity in other single-crystal lead chalcogenide compounds have shown that they make inferior detectors. This is due in part to the very high purity required for good photoconductive detectors and to the fact that the similarity in electron and hole effective masses in the lead chalcogenides reduces photo-conductive gain.

Much of the emphasis in recent years on infrared detectors for the 3 to $5\,\mu m$ spectral range has centered on increasing the operating temperature of the detector. One operating temperature goal for $5\,\mu m$ cut-off detectors is $170°\,K$. The wavelength cut-off for PbTe at $170°\,K$ is $4.86\,\mu m$. To obtain $5.0\,\mu m$ cut-off at $170°\,K$, $Pb_{.982}Sn_{.018}Te$ (see 6.3.2.2) must be used rather than PbGeTe. Although it is usual to design the detector to cover as much of the 3 to $5\,\mu m$ spectrum as possible, there are specialized applications which call for wavelength cut-offs between 4 and $5\,\mu m$. The addition of 6 percent GeTe to PbTe decreases the wavelength cut-off at $77°\,K$ from $5.9\,\mu m$ (PbTe) to $4.2\,\mu m$. Thus, appreciable wavelength shifts may be obtained with small additions of GeTe.

6.3.2.4.3 Discussion

Considerable interest has been generated in materials for infrared charge-coupled detectors for image scanning; this interest stems from the success of visible and near-infrared image scanning using silicon. One of the problems in the application of this concept to the infrared is that the large background signal rapidly bleeds off the charge stored on the detectors between consecutive scans. In this case, the large dielectric con-stant of PbGeTe could provide an advantage in that more charge is stored for a given voltage bias and the RC time constant matches the scan times under consideration. For this ap-plication the surface properties of PbGeTe need to be investigated. Various insulator-passivation layers should be examined with MIS structures to see if the surface potential can be modulated. Schottky barrier infrared detectors as well as p-n junction detectors could be particularly useful in conjunction with silicon-CCD multiplexers in electronically-scanned image sensors.

The role of the ferroelectric transition on detector performance needs to be clarified. To obtain large dielectric constants, the paraelectric state just above the Curie temperature may be preferable. The rapid variation of the dielectric constant with temperature, the variation of the dielectric constant with electric field, the variation of Curie temperature with stoichiometry and electric field, and the presence of a remanent polarization below the Curie temperature all provide new variables on infrared detector performance and may provide new useful detector characteristics.

6.3.3 Ternary Diamond-Like Semiconductors

6.3.3.1 Introduction

Those elements and compounds that have proven to be of the greatest importance in semiconductor and electro-optic device applications have been the diamond-like materials. These include the elements Si and Ge and binary compounds of the form $A^{III}C^{V}$ and $A^{II}C^{VI}$. The atoms in all these substances have tetrahedral coordination with an average of four valence electrons per atom giving them the diamond-like structure. The next stage in complexity are the ternary diamond-like compounds, which are close analogs of the binary compounds with respect to their crystal structure and chemical bonding.

The ternaries can be considered to be formed from the binaries by replacement of either the anion or cation by elements from other groups in the periodic table in such a way as to yield the same average number of electrons per atom. Examples of this are the $A^{II}B^{IV}C_2^{V}$ compounds which are ternary equivalents of the $A^{III}C^{V}$ compounds. Here the A^{III} atoms from two molecules are replaced by an A^{II} and B^{IV} atom yielding an average of three electrons per cation. Similarly, the $A^{I}B^{III}C_2^{VI}$ compounds are ternary analogs to the $A^{II}C^{VI}$ compounds.

Although there is a large body of Soviet literature regarding the ternary diamond-like semiconductors, these materials have not been studied in detail in the United States. The basic reference to them, the monograph by Berger and Prochukhan, classifies in detail those ternaries that have the tetrahedral coordination characteristics

of the diamond and zinc-blend lattice structure.[76]   These authors have identified a total of 30 classes of ternary diamond-like compounds which should exist. Five of these are two-anion type compounds; the others are two-cation type compounds. The majority of the work has been devoted to the two-cation type compounds and of the twenty five possible compounds, the only ones that have been studied to any degree are the following:

$$A^{II}_B{}^{IV}C^V_2 \qquad A^I_B{}^{III}C^{VI}_2 \qquad A^I_{B_2}{}^{IV}C^V_3$$

$$A^1_2{}_B{}^{IV}C^{VI}_3 \qquad A^I_3{}_B{}^VC_4{}^{VI}$$
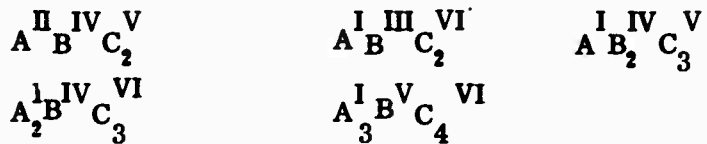
Simply identifying the classes of ternary compounds that are possible is only part of the problem. An equally important consideration is the ability to predict which compounds in a given class can or should exist. There appears to be no positive method for doing this; however, Goryunova and Berger and Prochukhan have postulated a rule that has thus far proven valid.[77,76]   Since the phase diagrams of the ternary compounds where tetrahedral phases can form have not been investigated, they have been able to judge the possibility of chemical interaction by examining the phase diagrams of the binary systems. They postulate that the formation of a ternary tetrahedral phase in the system A-B-C is governed by the chemical interaction in the A-C and B-C systems in a two-cation phase and in the A-B and A-C systems in a two-anion phase. Essentially their postulate says that the ternary compound A-B-C (e.g., $A^{II}_B{}^{IV}C^V_2$) will form if binary compounds of the system A-C and B-C exist. The fundamental basis of the postulate is uncertain, but all of the compounds formed to date satisfy this condition.

6.3.3.2 $A^{II}_B{}^{IV}C^V_2$ Ternary Compound Semiconductors

Of the several classes of ternary diamond-like semiconductors the $A^{II}_B{}^{IV}C^V_2$ has received the greatest attention.[78]   A large number of papers have appeared in the Soviet literature describing their synthesis, electrical, photoelectric, and luminescent behavior. The bulk comes from the laboratory of N. A. Goryunova in Leningrad.[79,80]

Berger and Prochukhan[76] point out that $A^{II}B^{IV}C_2^V$ compounds are ternary analogs of the III-V semiconducting compounds, and thus are expected to have similar properties. From this point of view, inclusion of these ternaries is an expansion of the limited list of III-V compounds.

The $A^{II}B^{IV}C_2^V$ compounds that have been synthesized to date include all of the possible combinations of Zn, Cd, Si, Ge, Sn, P, and As. In addition, there has been a very limited amount of work on $BeSiN_2$, $MgGeP_2$, and $ZnSnSb_2$.

From their position in the periodic table, it is to be expected that the Zn compounds have wider bandgaps than the Cd, the Si wider than the Ge, which in turn are wider than the Sn, and the P wider than the As. This is generally true. With the exceptions of $BeSiN_2$ and $MgGeP_2$ no work has been done on the N, Mg, or Be compounds. It is to be expected that the Be compounds would have wider gaps than the Mg compounds, the Mg compounds wider than the Zn compounds, and the N ores wider than the P compounds. Except for $ZnSnSb_2$, almost no work has been reported on the Sb compounds. These are expected to have smaller gaps than the As compounds. There are no reports of the Hg compounds, which should have smaller gaps than those of Cd. The absence of these ternaries may be partially explained by the Goryonova-Berger postulate regarding the need for the existence of the corresponding binary phases.

6.3.3.2.1 Crystal Structure

The $A^{II}B^{IV}C_2^V$ compounds crystallize in the chalcopyrite, wurtzite, or sphalerite structures all of which exhibit tetrahedral coordination. $BeSiN_2$ is the only one having the wurtzite structure. $ZnSnP_2$ is the only one exhibiting the sphalerite structure at all temperatures below the melting point. The other compounds exhibit the chalcopyrite structure at room temperature. Six of the compounds, $ZnGeP_2$, $ZnSnP_2$, $ZnGeAs_2$, $ZnSnAs_2$, $CdGeAs_2$, and $CdSnAs_2$ exhibit the sphalerite structure above a transition temperature. The remainder of the 12 listed above exhibit chalcopyrite structure at all temperatures below the melting point. It should be noted that $CdGeAs_2$ and $CdGeP_2$ can also exist in the amorphous (glassy) state.

6.3.3.2.2 Band Structure

Studies of the band structure of the $A^{II}B^{IV}C_2^V$ compounds have been summarized by Borshchevskii, et al.[78,81-83] In general, the band structure is similar to that of the III-V compounds. Karavaev, Poplavnoi, and Chaldyshev predict a negative differential resistance (Gunn effect) in some of the ternaries.[83] For example, calculations show that $ZnGeAs_2$ should have subsidiary minima 0.3 eV above the center-zone conduction band minimum. A similar situation is predicted for $ZnSiP_2$.[83]

6.3.3.2.3 Properties of the $A^{II}B^{IV}C_2^V$ Ternaries

Some of the important properties of 13 $A^{II}B^{IV}C_2^V$ ternaries are listed in Table 6.4. The compounds are arranged in order of descending energy gap. The listing of more than one value of a parameter indicates disagreement in the literature. Note the trend toward decreasing microhardness and melting point with decreasing energy gap, although the dependence is not perfectly monotonic.

6.3.3.3 $A_2^I B^{IV} C_3^{VI}$ Ternary Compound Semiconductors

This class of compound is one of the ternary equivalents to the $A^{II}C^{VI}$ binary semiconductors. The list of $A_2^I B^{IV} C_3^{VI}$ compounds that have been synthesized to date includes almost all combinations of Cu and Ag as the Group I element, Si, Ge, and Sn as the Group IV element, and S, Se, and Te as the Group VI element. No compounds of this class have been synthesized containing either Pb or Au.

The important properties of the known $A_2^I B^{IV} C_3^{VI}$ compounds are given in Table 6.5. The compounds are listed in order of decreasing energy gap wherever possible. There is no clear-cut trend in the energy gap as a function of increasing atomic number of either the chalcogenide or the Group IV element. The energy gap, however, does appear to decrease as the Group I element changes from Cu to Ag.

TABLE 6.4

Properties of the $A^{II}B^{IV}C_2^V$ Ternary Semiconductors

Compound	Energy Gap 300°K (eV)	1.24/E$_g$ (μm)	Electron Effective Mass Ratio Theory	Electron Effective Mass Ratio Experiment	T Melt (Deg C)	Microhardness (kg/mm²)	Density X-ray	Density Pycnometric	Structure	Transition Point, Chalcopyrite-Sphalerite (Deg C)	Other Transitions in Solid State	Lattice Parameters a (Å)	Lattice Parameters c (Å)
BaSiN₂							3.24	3.12	Wurtzite				
ZnSiP₂	2.3 2.13 1.99	0.54	0.096	0.08	1370	1100 ± 100	3.39	3.35	Chalcopyrite			5.400	10.441
CdSiP₂	2.25	0.55	0.092		<1200		3.998	3.97	Chalcopyrite			5.678	10.431
ZnGeP₂	2.25 2.2	0.565			1020 1025	980 ± 80 690	4.175		Chalcopyrite-Sphalerite	952		5.466	10.722
ZnSiAs₂	2.10 1.76 1.64	0.59 0.76	0.071		1038 1096	920 ± 20 590	4.72	4.69	Chalcopyrite			5.606 5.59	10.890 10.8
CdGeP₂	1.8	0.69			776 800	850 ± 70 460	4.483		Chalcopyrite Amorphous			5.741	10.775
CdSiAs₂	1.62(?)	0.77(?)							Chalcopyrite				
ZnSnP₂	1.46	0.85				650			Chalcopyrite Sphalerite	Depends upon cooling rate			
CdSnP₂	1.5 1.22	0.83 1.01							Chalcopyrite				
ZnGeAs₂	0.85	1.46	0.038	0.04(?)	850	680 ± 10	5.325	5.29	Chalcopyrite Sphalerite	812		5.67	11.2
ZnSnAs₂	0.65	1.9	0.029	0.029	775	455 ± 10 460	5.533	5.53	Chalcopyrite Sphalerite	645,635 700,669	575 583	>5.8515	11.703
CdGeAs₂	0.53	2.34	0.020	0.027	665 670	471 ± 10 490	5.612	5.60	Chalcopyrite Sphalerite Amorphous	630,621 632		5.9427 5.94	11.2172 11.2
CdSnAs₂	0.26	4.78		0.020	593 ± 2 596 ± 2	395 ± 5	5.716	5.66	Chalcopyrite Sphalerite	567 587			

TABLE 6.5

Properties of the $A_2^I B^{IV} C_3^{VI}$ Compounds

Compound	Energy Gap (300°K) eV	T_{Melt} (°C)	Microhardness (kg/mm²)	Density gm/cm³	Structure	Lattice Parameters (Å) a	c
Cu_2SiS_3		925		3.81	<u>Wurtzite (High T)</u> <u>Hexagonal (Low T)</u>	3.684	6.004
Cu_2SiSe_3							
Cu_2SiTe_3				3.63	Cubic or Tetragonal	5.290	10.156
Cu_2GeTe_3		492 to 595	295	5.59	Cubic (High T) Tetragonal (Low T)	5.956	11.852
Cu_2SnTe_3	1.1	410	210	6.51	Cubi	6.047	
Cu_2GeSe_3	(.6, 0.94)	760 to 788	391	5.57	Cubic (High T) Tetragonal (Low T)	5.595 5.55	10.564
Ag_2GeSe_3	0.9	540					
Ag_2SnSe_3	(0.7, 0.81)	490					
Cu_2SnS_3	(0.59, 0.91)	839 to 874	283	5.02	Cubic	5.445 5.43	
Cu_2SnSe_3	0.7 (0.5, 0.66)	685 to 698	256	5.94	Cubic	5.696 5.68	
Cu_2GeS_2	0.53	933 to 956	464	4.46	Cubic (High T Tetragonal (Low T)	5.326 5.30	10.438
Ag_2SnS_3	0.5						
Ag_2GeS_3	0.3						
Ag_2GeTe_3	0.25	330					
Ag_2SnTe_3	0.08	315					

6.3.3.3.1 Crystal Structure

The crystal structure of a number of $Cu_2B^{IV}C_3^{VI}$ compounds have been studied by Goryunova and Sokolova[84] and Palatnik et al.[85] They found that when B^{IV} was Si or Ge, the compound crystallized in a cubic structure but then underwent a low-temperature phase change to a tetragonal structure. When Sn was the B^{IV} element, there was no apparent low-temperature phase change. Investigations of Ag_2SnSe_3 and Ag_2SnS_3 were unable to identify the crystal structures in these compounds, and work by Goryunova et al showed a two-phase structure in Ag_2SnTe_3, part of which was the sphalerite structure.[86]

6.3.3.2 Band Structure

Insufficient data are available to determine the band structure of these compounds. The different values of energy gap show the uncertainty with which it is known. Measurements by Kaharakhorin and Petrov have indicated that the Cu and Ag selenides of Ge and Sn have an indirect gap.[87] The values they obtained for the thermal and optical gaps are written as a bracketed pair in Table 6.5. Whether the tellurides have a direct or indirect gap is unknown.

6.3.3.3.3 Preparation and Properties of the $A_2^I B^{IV} C_3^{VI}$ Compounds

The compounds of this class are grown by the direct fusion of the individual elements in sealed quartz ampoules, and zone leveling has been used for purification after growth.[88] The melting points of the compounds are relatively low and the constituents are of relatively low volatility. These considerations favor reproducible simplified crystal growth. The maximum reported melting point of 925° C occurs for Cu_2GeS_3. The Ag compounds have low melting points; 310°C is reported for Ag_2SnTe.[89] Such low melting points may not be desirable since room-temperature annealing might occur, altering the supposed properties of the compound.

6.3.3.4 $A^I B^{III} C_2^{VI}$ Ternary Compound Semiconductors

The $A^I B^{III} C_2^{VI}$ compounds are another of the ternary analogs of the $A^{II} C^{VI}$ binary compounds. The $A^I B^{III} C_2^{VI}$ compounds synthesized to date include all possible

combinations of Cu and Ag as the Group I element, Al, Ga, In, and Tl as the Group III element, and S, Se, and Te as the Group VI element. Some important properties of this group are shown in Table 6.6.

Members of this class of compounds usually have relatively wide bandgaps. There is a trend toward smaller bandgap as the element from each group increase in atomic number. Theoretical calculations of the energy gap by Matare suggest forbidden gaps ranging from 2.5 eV in $CuAlS_2$ to 0.1 eV in $AgTlTe_2$.[90]

6.3.3.4.1 Crystal Structure

Generally, the crystals have a chalcopyrite structure. The only exception reported is $AgInS_2$, which has both wurtzite and chalcopyrite modifications.

6.3.3.4.2 Band Structure

Very little is known about the band structure of this class of compound. The energy gaps shown as a pair of numbers in Table 6.6 are, again, the thermal and optical gaps. Recent studies of Tell and co-workers have expanded our knowledge of gaps and carrier mobilities.[91] A large fraction of the compounds appear to be indirect gap materials; $CuInS_2$ and $CuGaSe_2$ are direct.[91]

6.3.3.4.3 Preparation and Properties

Compounds in this class have been produced both by direct reaction of the components and by reaction of the binary compounds. No particular problems are reported in the literature concerning the growth of these compounds. Zone leveling and Bridgman growth have been used to produce material, but the preparation of large single-crystal ingots has not been reported. Transport measurements and annealing studies on some compounds have been reported.[91]

The Ag compounds generally have lower melting points than the corresponding Cu compounds; by analogy, the melting point of Au compounds may be expected to still be lower.

Properties of the $A^I B^{III} C_2^{VI}$ Ternary Semiconductors

Compound	Energy Gap (300°K) (eV)	T_{MELT} (°C)	Micro-Hardness (kg/mm²)	Density (gm/cm²)	Structure	Lattice Parameters a (Å)	c (Å)
AgGaSe₂	1.82	883,850	450	5.71	Chalcopyrite	5.97	10.8
CuGaSe₂	1.68	861,1040	430	5.45	"	5.60	10.9
CuAlS₂	3.46	∼1200		3.45	"	5.31	10.4
CuGaS₂	2.40			4.29	"	5.34	10.4
CuInS₂	1.53			4.71	"	5.51	11.0
AgAlS₂	2.7			3.93	"	5.69	10.2
AgGaS₂	2.7			4.58	"	5.74	10.2
AgInS₂	1.87			4.97 / 4.83	Chalcopyrite / Wurtzite	5.18 / 4.12	11.1 / 6.67
AgInSe₂	1.24	780,773	230	5.80	Chalcopyrite	6.09	11.6
CuAlSe₂	2.7	1000		4.69	"	5.60	10.90
CuInSe₂	0.96	980,990	260	5.65	"	5.77	11.5
CuGaTe₂	.82, 1.0	872	360	5.87	"	5.99	11.9
AgGaTe₂	.52, 1.1	714,720	180	5.96	"	6.28	11.9
AgInTe₂	.52, .93	650,692	190	6.08	"	6.40	12.5
CuAlTe₂	.88	890		5.47	"	6.16	12.3
CuTlSe₂	.72, 1.07	405	120	7.08	"	5.96	11.78
AgAlSe₂	.70	950		4.99	"		
AgAlTe₂	.56, .93	729,680	190	6.15	"		
CuTlS₂	1.	375	100	6.07	"	5.95	10.7
AgTlS₂		290	140	7.08	"	6.29	11.8
CuTlTe₂					"	5.58	11.1
AgTlTe₂					"	5.83	11.6
CuInTe₂	0.67, 0.95	778,791	190	6.00	"	6.17	12.3
AgIlSe₂	0.72	328	120				

6.3.3.5 Other Ternary Compounds

The other ternary two-cation compounds considered here are the $A_3^I B^V C_4^{VI}$ and the $A^I B_2^{IV} C_3^V$ compounds, but only a limited amount of information regarding these compounds is available. Very few of the remaining diamond-like compounds, namely the single-cation compounds have been synthesized. Properties known for a few of the $A_3^I B^V C_4^{VI}$ group are given in Table 6.7.

TABLE 6.7

$A_3^I B^V C_4^{VI}$ Compounds Synthesized to date.

Compound	Melting Temp. (°C)	Energy Gap Thermal Optical (eV)
$Cu_3 AsS_4$	655	0.8 , 1.48
$Cu_3 SbS_4$	555	
$Cu_3 AsSe_4$		0.76, 0.88
$Cu_3 SbSe_4$	425	0.42, 0.31

6.3.3.6 Discussion

The ternary diamond-like semiconductors are an important new class of compound semiconductors of potentially great importance as photodetectors. Indeed, photoeffects have been explored in several of the wide gap compounds including $ZnSiP_2$[92, 93] $ZnGeP_2$[94, 95], $CdGeP_2$[94], and $ZnSiAs_2$[96]. It is logical to assume that intrinsic photoconductivity and junction photoeffects will be observable in most, if not all, of the compounds. Depending on how easily they can be purified, some of the compounds may eventually find application as high-performance infrared detectors. The ability to synthesize a new material with a desired energy gap was the impetus behind the development of the alloy semiconductors HgCdTe, PbSnTe and PbSnSe. The numerous ternaries offer a choice of nearly any energy gap by selection of the appropriate compound. The compositional nonuniformity problem of the alloys should be absent in the ternary compounds, a significant advantage particularly in large arrays.

6.3.4 Extrinsic Semiconductors

6.3.4.1 Germanium

Impurity-activated germanium detectors have been available since the early 1950s. Their long wavelength threshold is determined by the impurity that may be added to germanium either during crystal growth or by diffusion after crystal growth. The ionization energy of the usual impurity atom is considerably less than for germanium atoms, thus producing a long wavelength threshold at longer wavelengths than for pure germanium. Thus, while Ge responds to about $1.8\ \mu m$, Ge with Au responds to about $8\ \mu m$, with Hg to about $13\ \mu m$, with Cd to about $25\ \mu m$, Cu to $28\ \mu m$, Zn to $40\ \mu m$ and B to beyond $100\ \mu m$.

These detectors were developed at a time when no single element or compound with response beyond $7\ \mu m$ were available. The recent development of HgCdTe and PbSnTe alloys, whose intrinsic response may be tailored to specific requirements, has reduced the need for those impurity-activated Ge detectors with threshold wavelengths less than $20\ \mu m$. This applies particularly to Ge:Au and Ge:Hg.

Impurity-activated detectors have a serious disadvantage with respect to intrinsic detectors, because they require more cooling to achieve background limited detectivity, when used under normal background conditions. Under reduced background conditions cooling requirements for both types may be quite similar, however. Since the response is determined by the number of absorbing centers and since usually no more than $10^{16}\ cm^{-3}$ impurities may be added to the Ge lattice without affecting the crystal quality, impurity-activated Ge crystals must be made considerably thicker than intrinsic detectors. In certain production programs this may not be desirable.

One of the real advantages of impurity-activated detectors over intrinsic detectors is the manner in which the speed of response may be controlled. This is accomplished by varying the density of compensating impurities. Time constants have been varied by this technique by at least three orders of magnitude, from the microsecond to the nanosecond range.

Other properties of impurity-activated detectors may be of importance. These detectors are unusually stable. They may be stored in a vacuum even at elevated temperatures for a number of years without degradation. The material may be prepared and stockpiled in single-crystal form to be used for detectors and arrays as the need arises. Detector material prepared by conventional techniques is usually uniform; variation among array elements produced from the same slice is usually due to nonuniformities in contacting techniques. It is not clear at this time if similar characteristics may be achieved with the intrinsic alloys (HgCdTe and PbSnTe). Difficulties experienced with the alloys in the above mentioned areas may require a continued production program of impurity-activated Ge for certain applications. Beyond about 20 μm, the alloy detectors are not now competitive with impurity-activated Ge.

6.3.4.1.1 Discussion

It is quite clear that a research and development effort in impurity-activated Ge must be continued. This effort should be aimed in several directions:

- Preparation of germanium with greater purity and fewer imperfections.
- Improved contacting techniques and surface studies
- Elucidating the role of impurity pairing
- A study of recombination processes and trapping

The properties of the detectors eventually produced depend greatly on the starting material. The one impurity that proves most harmful is Cu except, of course, in Ge:Cu detectors where it is intentionally added. It may be present in the starting material or enter during crystal growth. Every effort must be made to reduce Cu impurities to levels below those where they might adversely affect detector characteristics.

No extensive study has been performed to determine the presence of other undesirable impurities and their effects. These impurities may act as trapping centers or may extend the long wavelength threshold beyond the desired value, thereby requiring additional detector cooling. A concerted effort should be made to improve

the quality of Ge. Efforts are now underway to produce high-quality Ge for use in nuclear radiation detectors (see Chapter 4). The same effort and care should be expended to produce Ge for use in infrared detectors.

Surface properties and behavior of contacts must be better understood in order to predict detector behavior. This is especially important when detectors are used under reduced background conditions and when detector elements are to be stored for a considerable time.

The distribution of impurities and the pairing of impurities with others have significant effect on material behavior. Thus, the pairing of a deep impurity with Li produces a new series of impurity levels and therefore a whole series of new detector possibilities. It is not clear at this point if these new levels have technological significance or if they merely provide us with a better understanding of Ge behavior. Such understanding is required since it would be desirable to predict how Ge with selected impurities might be expected to behave under a variety of operating and environmental conditions and, thus, determine its suitability for a particular application. A better understanding of material behavior would also aid in explaining various effects as they are observed (multiple time constants, for example) and help in eliminating them if they are undesirable. There should, furthermore, be a detailed evaluation of extrinsic detectors in a nuclear environment, when the device is exposed to sudden bursts and when it is maintained in such an environment for extended periods of time.

6.3.4.2 Silicon

6.3.4.2.1 Advantages of Extrinsic Si Phodetectors

The development of germanium transistors in the 1950s and the concurrent perfection and "impurity" control obtained in single-crystal germanium set the stage for the early development of infrared detectors based on germanium. Although silicon dominated the transistor field, the quality of germanium detectors was so advanced that, until recently, there was little motivation to return to silicon. Nevertheless,

there are some significant advantages available with silicon detectors. These include better radiation hardness, greater choices of spectral and temperature ranges of operation as well as the potential application of monolithic silicon technology with its clear advantages for arrays of uniform quality and reduced costs. In addition to these advantages, recent work has demonstrated that Si:As detectors can be prepared with superior performance in regard to yield, detectivity, and quantum efficiency than any germanium infrared detector.

The advantages that accrue to silicon detectors can be traced to the character of the "impurities" that are used to provide the infrared sensitivity. In germanium the "impurities" are "deep" with limited solubility ($\sim 10^{16} cm^{-3}$). They (Cd, Hg, Te) are introduced by growing the crystal under several atmospheres of pressure of the "impurities" which results in nonuniform impurity distributions and poor crystal perfection. For Ge:Cu the copper is introduced by diffusion followed by a quench which also has detrimental effects on the crystal homogeneity and perfection.

For silicon the useful "impurities" are from the III and V columns of the periodic table. The ionization energies and corresponding long wavelength limits of the "impurities" are given in Table 6.8[97].

TABLE 6.8

Ionization energies E_i and long wavelength

limits λ_c of impurities in Si.

	E_i (eV)	λ_c (μm)		E_i (eV)	λ_c (μm)
Si:P	0.045	27.6	Si:B	0.04385	28.2
Si:As	0.0537	23.1	Si:Al	0.0685	18.2
Si:Sb	0.043	28.8	Si:Ga	0.0723	17.2
Si:Bi	0.0706	17.6	Si:In	0.1551	8.0

The impurities (also called "dopants") can be introduced in high concentrations. It is possible, using precision crystal growing techniques, to obtain excellent doping homogeneity, crystal perfection, and stringent control of residual impurities. Higher yields of detectors can be obtained by using silicon rather than germanium. Because the extrinsic absorption coefficient is greater in silicon than in germanium and because higher impurity concentrations can be used in silicon, it is possible to use silicon elements which are thinner. While germanium detectors must be 1 to 3 mm thick, excellent silicon detectors 0.1 mm thick have been obtained, and detectors as thin as 0.025 mm may be possible.

Photolithography, etching, and other compatible microelectronic processes for use in processing arrays of silicon detectors may be used for thin detectors. This provides a large potential advantage in the continuing quest to provide high-performance arrays of large numbers of elements at minimum cost. The ability to utilize thin elements also provides a significant advantage in a nuclear radiation environment since the interaction is a function of thickness. With germanium and silicon detectors of equal original performance, tests have demonstrated that the post-irradiation performance of the silicon detector is less degraded than that of the germanium detector.

Detector arrays require load resistors and preamplifiers for each channel. At low backgrounds when the detector resistance is very high, a high load resistance is used and a field effect transistor or metal oxide semiconductor field effect transistor preamplifier is used. The present state of the art in array fabrication is that of discrete component assembly--detectors, load resistors, and metal oxide semiconductor field effect transistors wired together in a conventional fashion. This is a tedious and expensive assembly process requiring great skill. Use of silicon detector material offers an opportunity for low-cost device production in the area of array integration; with the detectors and metal oxide semiconductor field effect transistors made of silicon, the development of a monolithic integrated array of detectors and preamplifiers after the fashion of large-scale integration (LSI) appears feasible. No other

detector material but silicon offers any realistic near-term promise of monolithic integration with electronic components.

6.3.4.2.2 Discussion

Since existing silicon detectors have performance equal or superior to germanium detectors and since s'.icon detectors have special advantages over germanium detectors with regard to nuclear radiation hardness and low-cost array potential, it is expected that the following work would be important:

- Studies of the parameters limiting detector thickness and the realization of high-performance "thinned" detectors
- Development of methods to fabricate silicon detectors using microelectron techniques
- Development of methods to integrate detectors, load resistors, and preamplifiers on a common substrate using compatible microelectronic techniques

6.3.5 Amorphous Materials

6.3.5.1 Introduction

Amorphous materials are glassy solids that possess no long-rang order in the arrangement of atoms. Some of these substances exhibit "semico.iducting behavior". This class of materials, the amorphous semiconductor, has been recently reviewed.[98]

Electrical conductivity is a fundamental property of a semiconductor. In general, the electrical conductivity of amorphous semiconductors is an exponential function of temperature (as in the case of an intrinsic crystalline semiconductor) with an activation energy corresponding roughly to the spectral position of both the optical absorption edge and the onset of photoconductivity. The magnitude of the conductivity, however, can be very low relative to crystalline semiconductors. Hall and drift mobilities are typically orders of magnitude lower for material in the amorphous state.

276

Photoconductivity is common in amorphous materials, having long been known to exist in S, Se, Te, Sb, Ge, Si, As_2S_3, and the vast group of systems of P, As, S, Se, Te, and Tl.[99] With the renewed activity in amorphous materials resulting from the development of Ovshinsky switches, the list of amorphous photoconductors is growing rapidly.[100] Most, if not all, are limited to sensitivity in the visible and near infrared. Moss has reported photosensitivity in amorphous antimony to 16 μm in the infrared but could not determine whether the effect was photoconductive or bolometric in nature.[101] Middle-infrared bolometric photosensitivity has recently been observed in evaporated amorphous films of Ge-Pb-Sn-Te deposited on glass,[102] and in hot-pressed films of $Tl_2SeAs_2Te_3$ and $Ge_{10}As_{20}Te_{70}$.[103]

It should be noted that an expected important property of amorphous material is resistance to radiation damage.

6.3.5.2 State of the Art

The understanding of amorphous semiconductors, in general, is in a very primitive state relative to that of single-crystal materials. Energy band structure models are being proposed, modified, and correlated with structure models. Familiar phrases such as dangling bonds, impurity effects, molecular rings and chains are frequently used. New phrases such as the ideal amorphous structure amorphons (a basic building block of atoms), and percolation theory are appearing in the literature.

The impetus behind the current surge of activity in amorphous semiconductors is the discovery of threshold and memory switching in these materials.[106] The physical basis of switching behavior is still a controversial subject.[104] Likewise, little is known about the effects of impurities, alloy homogeneity, crystallization, surface effects, trap states, etc. New models are being introduced such as the postulation of a recombination gap to explain some experimental results on radiative recombination in amorphous $2As_2Te_3 \cdot As_2Se_3$.[105,106]

Reproducibility of results is a problem. Different results are found for the "same" material made in different ways or even in the same way but at different times. This is associated with lack of knowledge of structure and compositional parameters. Little is known about the physical and chemical structure of amorphous materials or about their dependence on preparation techniques.[98]

Most of the amorphous detectors studied have been laboratory models, the photosensitivity being used as a means of determining fundamental properties. Exceptions are amorphous selenium employed in xerography and possibly some amorphous photoconductors in TV camera tubes. Most of the latter are not truly amorphous but have a rather fibrous-like or microcrystalline-like structure.

The available data characterizing amorphous photoconductors in terms of detectivity are limited. The highest reported value of D^*_λ is 2×10^{11} cm/W-sec$^{\frac{1}{2}}$ at room temperature for vitreous Bi-Se films.[107] Response times for these films range from 0.3 to 3 msec. The value of D^*_λ peaks in the near infrared at $\sim 1\,\mu m$ wavelength.

6.3.5.3 Discussion

Amorphous semiconductors could be an important element in future infrared technology since they have some rather desirable characteristics as far as detectors are concerned. They appear to be highly resistant to radiation damage, cheap and easy to fabricate, can be made in bulk or large-area-evaporated-film form, are optically homogeneous, have high electrical resistance and impurity insensitive electrical conductivity, show continuous variation of properties (e.g. spectral response) with alloying, and are rather durable. Such properties would imply the feasibility of a variety of infrared detectors: single elements, arrays, optical switches, image tubes requiring large area film detectors, and possibly even multi-color infrared image tubes.[108]

To achieve these goals much needs to be done and many problems need solving. First, a better understanding of the physical and chemical structure of amorphous materials, and the relationship of this structure to preparation techniques must be developed. Understanding the effects of impurities, amorphous stability and crystallization should all be a part of this endeavor to understand the physical and chemical structure. Second, new amorphous materials and alloys that will extend the photosensitivity farther out into the infrared should be sought. Third, a better understanding must be developed of electrical transport and energy band structure: the density-of-states at low energies, trap levels, band mobility edges. Before any intensive effort on arrays is launched, evidence of single-element detectors with high detectivity should have been demonstrated.

6.3.6 Heterojunction Photodetectors

The term heterojunction is sometimes taken broadly to mean the intimate contact between any of the six possible combinations of metals, insulators and semiconductors. The heterojunction is defined as the junction between two different semiconductors which form a single-crystal lattice. The heterojunction semiconductor device dates back to theoretical consideration in 1950.[109] Virtually no experimental work was done until after Kroemer's theoretical application of a heterojunction in a transistor.[110] He predicted increased emitter injection efficiency resulting from a wider gap heterojunction emitter.

Substantial experimental investigations were begun with the work of Ruth et al on the epitaxial deposition of Ge on GaAs in 1960.[111] Wolf proposed the application[112] to solar cells, where high efficiencies were anticipated. In a "high efficiency" heterojunction solar cell, the material on one side of the junction has a large absorption coefficient for the radiation of interest and the other side (facing the incident radiation) is essentially transparent to the incoming radiation. Most of the radiation is absorbed very close to the junction, therefore; the charge carriers are collected more efficiently.

The failure to produce experimentally either a really useful wide-gap emitter transistor or a high-efficiency solar cell is due to several causes. The first involves the difficulty of making a truly abrupt junction. Since most semiconductors must be prepared at high temperature there is almost always some interpenetration of one material into another. This problem can be minimized in some cases by appropriate selection of growth techniques. If the two materials are not in an isolectronic sequence in the periodic table then severe doping can result.[113] In fact one might well wird up with a homojunction on each side of the heterojunction. Even for isoelectronic materials, lattice mismatch results in unpaired bonds at the heterojunction interface that can act as generation-recombination centers or can serve to create extraneous energy barriers. Oldham[114] and Oldham and Milnes[115] have shown the importance of interface states that result from lattice mismatch in Ge-Si heterojunctions. Additional problems result from the discontinuity in electron affinity and effective mass at the heterojunction.[116]

A variety of photoeffects have been measured in heterojunctions made with many combinations of materials. Ge-GaAs heterojunctions have been investigated the most intensively.[117] An n-Ge, p-GaAs device capable of responding to 1.06 μm laser radiation modulated at 2.78 GHz has been reported by Kruse and Schulze.[118] Infrared up-conversion in three-junction devices, including one Ge-GaAs heterojunction, was reported by Kruse et al.[119] Other heterojunction material combinations include Ge-Si,[114, 115] Ge-GaP,[120] Si-GaP,[121] GaAs-InP,[122] Ge-ZnSe,[123, 124] and ZnSe-ZnTe.[125] The Proceedings of the International Conference on the Physics and Chemistry of Semiconductor Heterojunction and Layer Structures provides an execellent recent collection of work representing the state of the art in a wide variety of material combinations.[126]

As a photodetector the heterojunction still promises high detection efficiency because the radiation can be absorbed most heavily in the narrower energy gap material immediately adjacent to the junction. This "window" effect further reduces the effect of recombination centers resulting from states on the surface.

Substantially more will have to be learned about the energy band structure that results at the interface of different semiconducting materials. The effect of interface states that results from lattice mismatch also must be better understood. In addition, progress must be made in materials preparation to minimize the interpenetration of the two materials if abrupt junctions are desired. This last point is essential if the two materials contain elements that are electronically active in each other. These tasks are indeed formidable. It is doubtful whether the resulting heterojunction photodetectors would be sufficiently better than those made by conventional homojunction techniques to justify the effort.

6.3.7 Metal-Semiconductor (Schottky-barrier) Detectors

Schottky-barrier photodetectors may be divided into two classes: intrinsic detectors where photogeneration of carriers takes place in the semiconductor and "hot-electron" detectors where photogeneration takes place in the metal. Intrinsic detectors are directly analogous to conventional p-n junctions in operation; the Schottky contact serves only to provide an internal energy barrier for charge carriers. Schottky structures are used in conventional materials such as silicon where they are found to have low 1/f noise and superior short wavelength sensitivity relative to p-n junction structures. The latter property follows directly from the fact that the barrier is very close to the detector surface ($< 200\text{Å}$). They are also used in materials where p-n junction fabrication is difficult, because of inability to dope both n- and p-type or because of degradation under high-temperature processing conditions.

The hot-electron Schottky-barrier detector operates by internal photoemission as shown in Figure 6.10. Incident light passes through the semiconductor to the metal Schottky electrode where it is absorbed, resulting in an excited electron that can be collected at the internal barrier. The energy of the internal barrier, ψ_{ms}, is determined by the particular semiconductor, the metal, and whether the semiconductor is p-type or n-type. Values of ψ_{ms} ranging from zero to the energy gap of the semiconductor have been reported. The long wavelength cut-off of these devices is determined by ψ_{ms} and, in principle, the photoresponse can be extended to
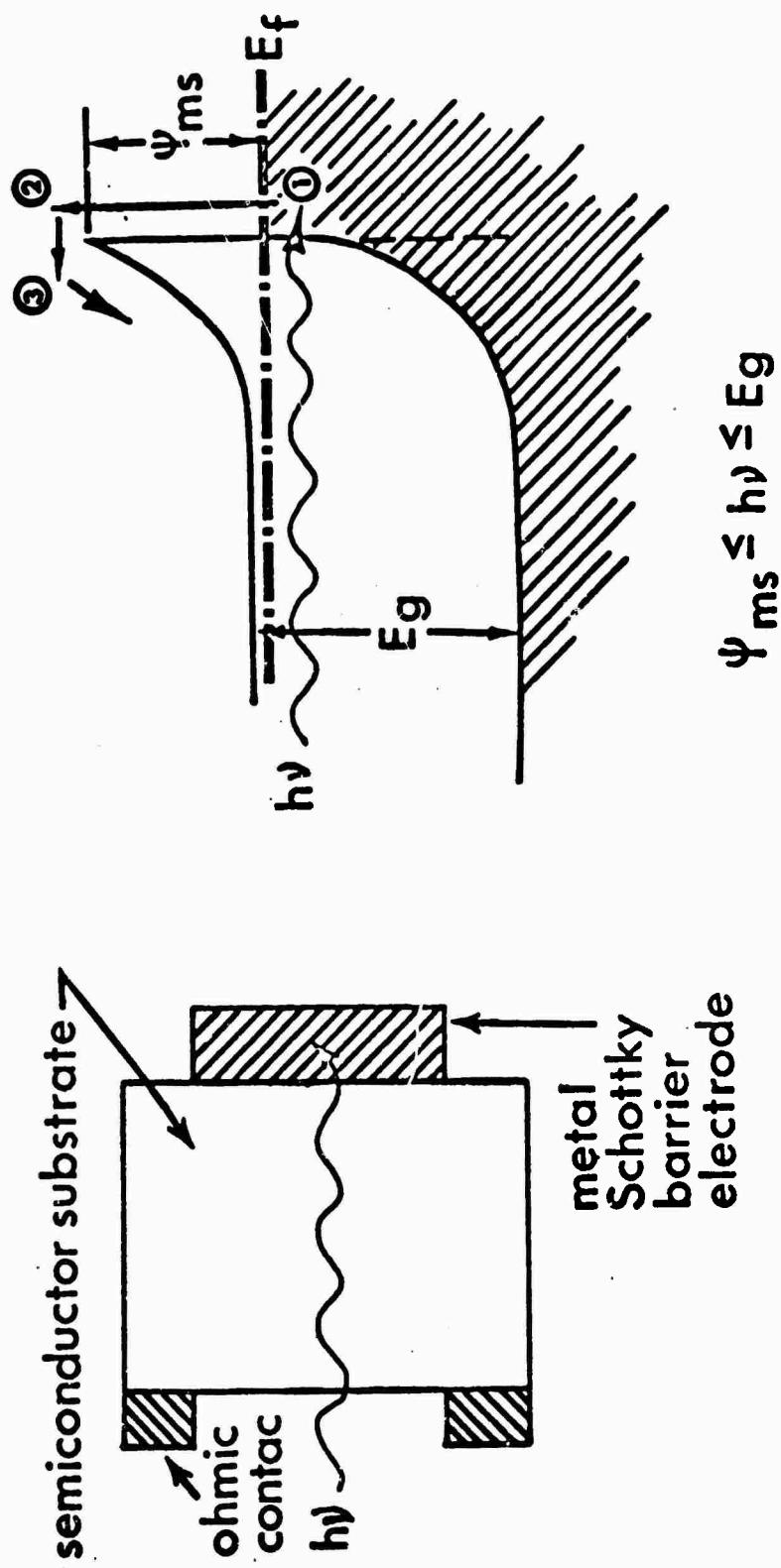
FIGURE 6.10   Internal photoemission.

arbitrarily long wavelengths. In practice, the long wavelength cut-off is limited for most semiconductors. Cut-off wavelengths of the order of 4 to 10 μm have been reported for silicon and germanium devices respectively.[127]

The absorption efficiency of the metal layer may be about 50 percent but the condition of conservation of momentum during barrier transition leads to practical quantum efficiencies of the order of 0.1 to 1 percent despite enhancement of the collection process by phonon scattering of excited electrons.[128] Details of the transport and collection process are given by Vickers and others.[129, 130, 131] It should be noted that the internal emission process leads to majority-carrier injection, so that these devices have very high frequency capabilities with risetimes of 10^{-11} sec considered possible. In addition, Shepherd, et al have reported the operation of hot-electron photodiodes in an avalanche multiplication mode with current gains in excess of 200.[132] If the Schottky contact is very thin, illumination from the metal side results in a combination of intrinsic and hot-electron photoresponses. The resulting photoresponse for a silicon Schottky barrier is shown in Figure 6.11 for a high internal barrier electrode (Pd-n) and a low internal barrier electrode (Au-p).

6.4 Thermal Detectors

The second major category of detection materials are those operating in the thermal mode, where the temperature rise caused by the signal radiation falling on the material causes a change in some readily measured property. Of the four mechanisms of principal interest, two of them, bolometers and thermopiles, have been used for many years. Because very little room appears to exist for improvement in materials for use in these modes, they will not be discussed here. The other two modes, the pyroelectric and pyromagnetic, have assumed increasing importance recently. Of these, the pyroelectric appears at present to be the most important. Materials suitable for use in pyroelectric and pyromagnetic detectors are discussed below; application to the pyroelectric vidicon will be found in 6.6.2.
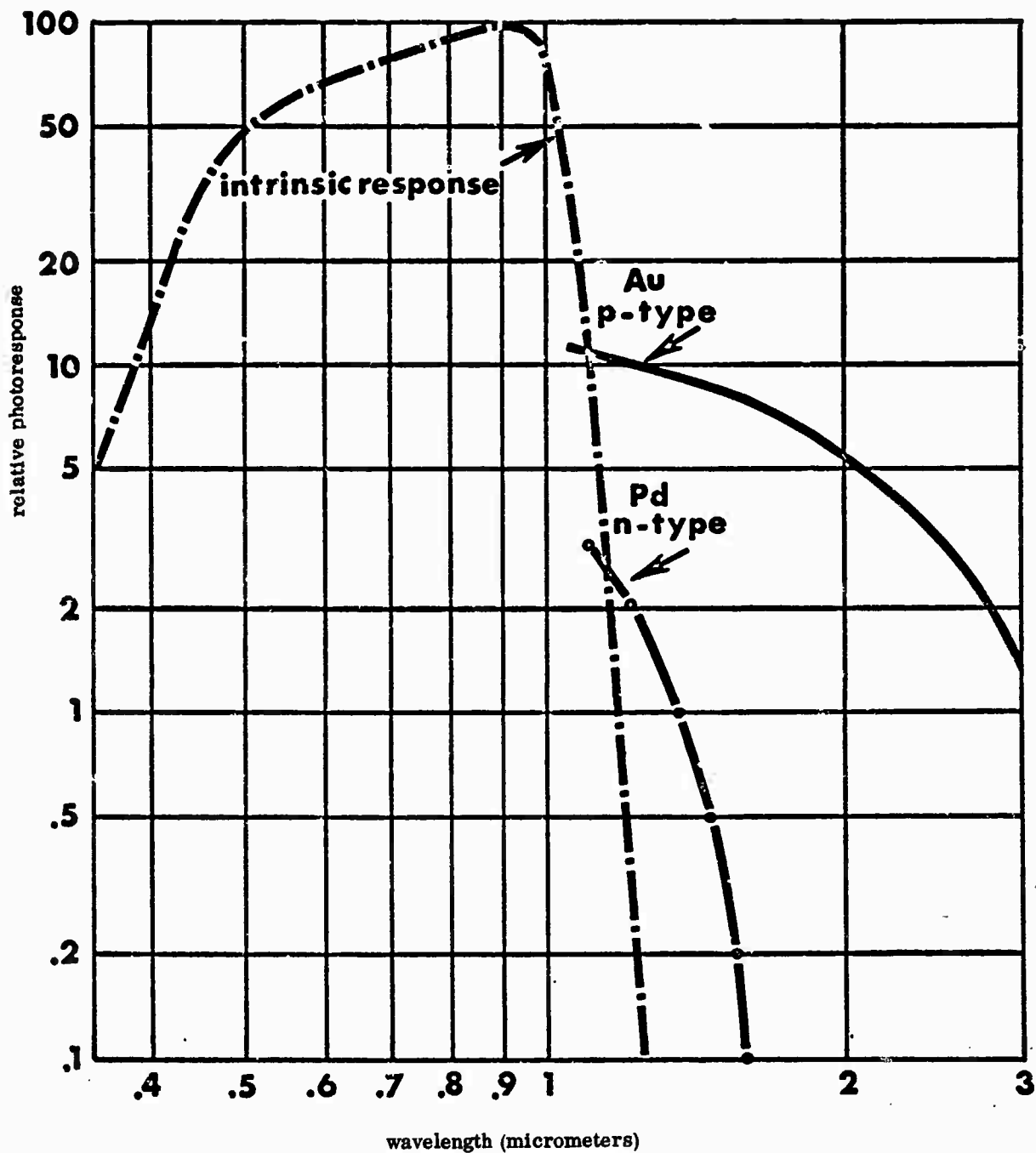
FIGURE 6.11 Extended hot-electron photoresponse.

6.4.1 Pyroelectric Detectors

While the basic pyroelectric effect has been known for a long time, effective modern pyroelectric detectors have been developed in this country and in England during the past five years,[133, 134] The pyroelectric detector employs a temperature-sensitive ferroelectric crystal, such as triglycine sulfate, which has two parallel electrodes deposited on it making it into a parallel plate capacitor. As the temperature of the polarized crystal is changed, a charge is generated in the pyroelectric detector. When employed in the voltage mode, the responsivity and the noise both decrease as a function of frequency and the D* of the detector stays nearly constant up to quite high frequencies.

The theory of operation and of noise generation in the pyroelectric detector were discussed in detail by Astheimer.[134, 135] Pyroelectric detectors are particularly advantageous in wide bandwidth systems where their performance at both low and high frequencies is superior.

Pyroelectric detectors can be conveniently formed into linear arrays with associated preamplifier arrays for use in two-dimensional scanning systems. The current practical limit in the size of array elements is of the order of 0.25 x 0.25 mm. Below this area, for the current material and thickness limitations, the capacitance becomes small compared with the stray capacitance of the associated circuitry. For small elemental area detectors or arrays, materials of higher dielectric constant would be particularly valuable. Examples are SBN and PLZT.[136, 137]

The responsivity of pyroelectric detectors above the thermal time constant is determined by the ratio of the pyroelectric coefficient to the dielectric constant of the detector material and the thermal capacity per unit volume of the detector material. To date this has been found to be optimum for triglycine sulfate just below its Curie point which occurs at 47° C and for triglycine fluoberyllate just below its Curie point of 73° C.[138]

To the extent that the pyroelectric detector is an ideal capacitor, it is free of electrical noise and, therefore, would be limited only by temperature noise, which is the fluctuation of detector temperature through radiation exchange with its surrounding. In practice, at intermediate to higher frequencies the detector is generally limited by Johnson noise associated with the dielectric loss in the ferroelectric crystal. At low and very high frequencies, the limiting noise is usually that of the field-effect transistor preamplifier. Considerable progress has been made in improving the ferroelectric materials being used, in methods of attaching electrodes free of contact resistance, in minimizing electrical leakage around the detector, and in obtaining field-effect transistors with lower electrical noise characteristics.

The improvement in detectivity in pyroelectric detectors obtained during the last five years has been about an order of magnitude. The best pyroelectric detectors being made in the United States and in England now approach a D* of 2×10^9 cm $Hz^{\frac{1}{2}} W^{-1}$, and the average detectors are within a factor of four of this value.[139] The best detectors are now about a factor of ten away from the ideal thermal radiation noise limited performance.[139] There appears to be no reason why considerable progress toward reaching this fundamental limit of thermal detector performance at about 20° C could not be made over the next few years. Recent studies of polyvinylfluoride film pyroelectric detectors are also of interest.[140]

Ferroelectric materials should be investigated to find those having: (a) a better ratio of pyroelectric coefficient to dielectric constant, (b) greater thermal capacity per unit volume, and (c) higher Curie temperature. Material research is complicated by the wide variation of the dielectric properties of the material with temperature with the state of polarization of the crystal, with the previous thermal history, and with poling method employed. Several materials currently being investigated such as TGFB,[138] deuterated TGS, alanine-doped TGS,[139] SBN,[136] and PLZT[137] show considerable promise in this direction. Crystal growth needs to be perfected to obtain uniform crystals with minimum dielectric loss and methods of attaching leads need to be improved to avoid resistance loss in the lead attachment.

It appears that considerable improvement in the characteristic of pyro-electric infrared detectors could be achieved with moderate research support. Because of the importance of pyroelectric detectors, not only as elemental detectors at low frequencies, but also as laser heterodyne receivers[141] and in the pyroelectric vidicon (see 6.6.2), a strong and vigorous materials research program is recommended.

6.4.2 Pyromagnetic Detectors

Although the pyromagnetic effect has been known for some time, its use as a radiation detector has been demonstrated only recently[142,143]. Pyromagnetism is a thermally induced change in the magnetic state of a material; the pyromagnetic effect is observed as a voltage induced in a coil linking to the detector material when it is exposed to time-varying radiation. This pyromagnetic voltage depends on the rate of change of the temperature in a manner similar to that of the pyroelectric detector.

For frequencies greater than the reciprocal of the thermal time constant, the responsivity depends on the ratio of the pyromagnetic coefficient to the thermal capacity per unit volume of the detector material. Because of its low impedance, the pyromagnetic detector is inherently suitable for fast radiation detection. The responsivity for this wide-band mode of operation is directly proportional to the pyromagnetic coefficient and is highest at the magnetic transition. It has been suggested that operation at the critical temperature will enhance this effect[143]. Pyromagnetic coefficients for many magnetic materials have been determined[143]. Among them, the coefficient of MnAs is the highest with a value of 0.60 Wb-m^{-2}K^{-1} at 315° K. However, gadolinium having a pyromagnetic coefficient of 0.05 Wb-m^{-2}K^{-1} at 293° K has been found to make the best detector. For wide band application, a responsivity of about 20 mV/W has been demonstrated with Gd.

Although the basic noise mechanism has been assumed to be thermal noise, this may not be correct. Since random switching of magnetic domains occurs at the critical temperature, critical fluctuations should be a fundamental noise source. Although some theoretical work has been done in this area, experimental results are virtually non-existent and deserve some research effort.

Because of the lack of knowledge about causes of noise in these detectors, the thermal noise assumption has been adopted for determination of the detector performance. Under this case, the best pyromagnetic detector made of gadolinium has an NEP (see 3.4) of 10^{-8} W/Hz$^{\frac{1}{2}}$ [143]. This is equivalent to a detectivity of about $D^* = 3 \times 10^7$ cm(Hz)$^{\frac{1}{2}}$/W for the experimental device, a value comparable to that of pyroelectric detectors at high frequencies. Research is needed to characterize the pyromagnetic materials at the room temperature of detector application rather than at the critical temperature.

In summary, the pyromagnetic detectors feature low impedance and inherently fast response, constant responsitivity over a wide range of frequencies, ruggedness and an abundance of magnetic materials from which to select detector elements. Their potential disadvantages are the low responsivity, an undetermined noise mechanism, and the greater complexity of manufacture than that for pyroelectric detectors.

A research effort on pyromagnetic detectors should be supported, with the principal objective of clearly distinguishing those areas where these detectors are superior to pyroelectric ones.

6.5. Infrared Detectors for Laser Sources

6.5.1 Introduction

Most infrared detectors are capable of responding over a fairly wide portion of the infrared spectrum. This is important for detection of thermal targets, where high sensitivity can be obtained by collecting thermal radiation over a broad

spectral bandwidth and detecting it with a broad-band detector. For instance, a good detector for a near room-temperature target is expected to have a broad-band response over at least a sizeable portion of the 8 to 12 μm window which contains the energy distribution peak of room-temperature thermal radiation.

With the advent of lasers, a variety of new applications have become possible in which the signal to be received is either in the form of a monochromatic laser signal, or consists of incoherent radiation distributed over a narrow band width (corresponding to, say $Q = (\lambda/\Delta\lambda) \sim 10^4$). In all these cases, considerable improvement in detection sensitivity can be obtained by limiting the response of an otherwise broadband detector to within a narrow wavelength region around the signal wavelength. Accordingly, these applications require modes of detection considerably different from those used for a thermal target and their material requirements are different.

Applications of lasers in the infrared are relatively recent. In some applications, the detection modes and their material requirements are now fairly well understood (e.g. laser radars and laser illuminators). In these cases, a program for material developments can now be outlined with some detail. However, a host of potentially important military and civilian applications exists where exploratory research efforts are badly needed before the required detection modes and the corresponding material needs are completely understood. An example is the possibility of developing a narrow-band superheterodyne radiometer that can be tuned over a wide portion of the infrared (and the far-infrared) spectrum. Such a radiometer can be applied to the detection of infrared (and far-infrared) spectral emission lines from a hot gas where the radiation in each line is distributed over a narrow bandwidth (corresponding to a Q of about 10^3 or 10^4)*. An important potential application of such a radiometer is remote-point sampling and spectroscopic chemical analysis of a distant target, quite possibly a hot gas plume. The theoretical sensitivity of a superheterodyne radiometer is very high. Because of this, it is potentially applicable in important astrophysical studies including exploration of the sun's corona

---

* $Q = \dfrac{f}{\Delta f}$

in the far-infrared and infrared. The latter may be useful in solar flare studies and the prediction of the subsequent communication blackout. A rapidly tunable infrared radiometer can also be used in intelligence collection. The civilian applications include basic spectroscopic studies in the mid- and far-infrared and in monitoring air pollution, for example, by remote point sampling of a smoke stack[144].

The above example is cited specifically to illustrate a general need for a broadly defined detector research and development program for laser application including massive exploratory research of potentially important possibilities. Modes of detection and their corresponding material needs are discussed below.

6.5.2 Infrared Superheterodyne Receivers and Other Applications of High-Speed Detectors

Infrared and far-infrared superheterodyne receivers have been reported and demonstrated.[145-148] The receiver's detection system consists of a frequency mixing element and an intense laser local oscillator at a frequency close to that of the signal to be received. The signal and the local oscillator frequencies are mixed in the frequency mixing element and the subsequent beat note is observed by means of a postamplifier at the beat frequency with a specified band width. For a receiver limited by local oscillator noise, the minimum detectable signal at infrared frequencies is given by $2 h\nu \Delta f/\eta$ where $h\nu$ is the quantum energy, Δf is the postamplifier band width, and η is the quantum efficiency of the mixing element. In one experiment, this minimum detectable signal was approached to within a factor of ten at $10 \mu m$ using a CO_2 laser local oscillator.[145] The frequency mixing element was Ge:Cu (copper atomic concentration of about $7 \times 10^{15} cm^{-3}$). Compensation by donors provided a free hole lifetime of about 2×10^{-9} sec at $4°$ K. (The free hole lifetime determines the speed of the detector response).

Since the local oscillator is an integral part of the detection system, consideration of material needs should include the frequency mixing element as well as the laser local oscillator. Although a number of existing lasers can be used adequately as the local oscillators for some applications, there are some important applications for which the necessary laser local oscillators are not readily available.

But the development of materials for infrared lasers has received considerable attention for reasons not necessarily related to the detector applications. Development of materials for laser local oscillators should, therefore, emphasize those lasers required in detectors which have not been considered seriously in the existing laser development program (see below).

In an application such as Doppler laser radar, the frequency of the return signal may be shifted from that of the transmitter laser by tens of MHz and more.[146, 149] In principle, even a detector with a relatively slow response time may be used for frequency mixing if part of the transmitter laser output is shifted in frequency close to that of the return signal and used as the local oscillator. However, it is generally advantageous to use a sufficiently fast detector element so that the frequency mixing is done directly in the tens of MHz region. There are other potential applications of superheterodyne receivers in which the signals to be received may differ from those of the available laser local osciallators by more than thousands of MHz (see below). For these reasons, development of materials for fast response frequency mixing elements is badly needed. This is particularly so for the 8 to 12 μm atmospheric window and also in the 5 μm region where, at discrete wavelength intervals between the water vapor absorption lines, the atmosphere is found to be highly transparent.[150] There are good lasers available for practical applications in both of these regions and, with further developments in the rapidly growing fields of infrared and far-infrared lasers, other wavelength regions are expected to become of importance. This is expected to create additional demands for high-speed detectors, both in the near-infrared and at wavelengths longer than 10 μm.

It may be useful to note that in some applications, the ultimate sensitivity obtainable from superheterodyne receivers may not be necessary. Furthermore, in cases where sufficiently large local oscillator power is available, a mixing element with relatively low detectivity may be used adequately. Accordingly, while high detectivity is a very desirable feature, it may not be an ultimate requirement in some applications.

Infrared (and far-infrared) detectors with ultra-high speeds are of importance in a variety of applications other than the superheterodyne receivers. In recent years, subnanosecond pulses of radiation in the near-infrared have been generated. Mode-locked pulses of tens of picoseconds duration should be available soon in the 5 and 10 μm regions. Laser-triggered nuclear fusion is a currently pursued application for these. High-speed infrared detectors with subnanosecond response time may, in principle, be used to observe and determine the pulse width. This will undoubtedly play an important part in the development of generators of short duration infrared radiation pulses.

In addition to high speed, many laser applications require a fairly large detector area with a large field of view and good light-gathering capability.[151] It is also desirable that the detector have a high detectivity and, ideally, it should be capable of room-temperature operation. Lastly, the detector's impedance should be sufficiently low to yield a reduced RC value necessary for high speed; but the impedance should not be so low that matching to the post-intermediate frequency-amplifier becomes a major practical problem. In practice, these requirements are not necessarily compatible with one another. For example, unless the detector's impedance can be chosen appropriately, a large surface area may have to be balanced against the need for high speed.

There are also some applications where large area detectors are needed without a requirement for ultra-high speed. In these cases, a speed of response in the tens of KHz may be sufficient.

Current developments of thermal detectors are often directed towards fabrication of small elements for use in mosaics. As a result, detector elements with sufficiently large surface areas useful in many laser applications are not generally available.

6.5.2.1 Conventional High-Speed Infrared Detectors

Most existing infrared solid state detectors are theoretically capable of high-speed performance. But much additional material research and special detector fabrications are needed to achieve the ultimate high-speed potential of these detectors. These detectors have previously been discussed in this chapter in considerable detail. Here an indication of the state of the art will be given with brief comments on some existing high-speed detectors in the 10 μm region.

Ge:Cu with free hole carrier lifetime of approximately 10^{-12} sec has been fabricated.[145] This lifetime sets the theoretical upper limit to the speed of response. In practice, there are difficulties in packaging the detector element with sufficiently low RC* loading to utilize the full potential of the high-speed limit. Ge:Cu at 4° K has a speed of response of about 1300 MHz at 10 μm.[152] Photovoltaic HgCdTe diodes at 77° K had a speed of response above 1 GHz.[153] In these experiments, the measurements were done by heterodyning in the element the outputs of two lasers, one a fixed frequency laser and the other a tuneable laser. These high-speed detectors are not readily available. The material purity and homogeneity in the p-r junction are problems requiring further development.

At shorter wavelengths, there are a large variety of detectors potentially capable of ultra-high speed operation. The problems are the same: they require further development and are not readily available.

6.5.2.2 Metal-Metal Oxide-Metal Infrared Tunneling Diode

A room-temperature frequency mixing element has been developed and demonstrated to respond to radiation throughout the infrared and far-infrared region with an experimentally verified frequency response limit of about 10^{14} Hz.[154, 155]

---

* Contribution to time constant due to resistance and capacitance.

The frequency mixing element consists of a metal-metal oxide-metal point contact electron tunneling diode which is used at an infrared frequency as a lumped circuit element much the same as an ordinary rectifier or frequency mixer diode is used at radio frequencies. The infrared radiation is coupled to the diode by means of a thin wire antenna which is contacted to a metal base covered by an oxide layer several $\overset{\circ}{A}$ thick. An alternating voltage at the infrared frequency is developed across the oxide layer, giving rise to an alternating tunneling current flowing through the thin oxide layer. Because of the nonlinear voltage-current characteristic, this alternating current has a distorted wave form, with an average rectified dc value and high order harmonics. The high speed of response of this diode has enabled frequency mixing of two infrared lasers at frequencies differing by more than several octaves. This enabled construction of a frequency multiplier chain capable of comparing the frequency of a near-infrared laser with that of a microwave clock.[154-156]

The development of the infrared metal-metal oxide-metal diode is still in an early state. The detailed behavior of the diode and the role of materials parameters in its operation are not completely understood. For example, diodes made by contacting tungsten with two different types of nickel reproducibly give different results. In fact, tungsten used to contact different sites in a given piece of metal also gives different results. This may be due to differences in the work functions of different sites in the same metal caused by inhomogeneity in the impurity distribution. Controlled experiments, include studies of clean surfaces under high vacuum, are needed to determine optimum conditions of operation and the criteria for materials.

Point contact metal-semiconductor diodes also have been demonstrated to respond to the infrared frequencies, but at 10 μm the speed of response is in the range of hundreds of GHz. Since the carrier lifetime is expected to limit the high frequency response, highly doped semiconductors (obtained, e.g., by ion implantation) may prove useful for improvement of the infrared detectivity and the speed of response.

The existing methods of coupling radiation to the infrared metal-oxide-metal diodes have a considerable amount of insertion loss. Performance limited by local oscillator noise has not yet been demonstrated. In preliminary experiments at 10 μm with a room temperature detector, a minimum detectable signal of about 10^{-13} watts at 1 Hz bandwidth is obtained.[148] The infrared rectification of the same diode leads to video detection at 10 μm of about 2×10^{-9} watts at 1 Hz bandwidth.

It may be possible to improve the coupling of the incident infrared radiation to the diode by optical techniques and considerably reduce the amount of insertion loss. Microcircuitry fabrication techniques could, in principle, be used to deposit on an appropriate substrate a metal-oxide-metal infrared diode consisting of a thin antenna of specified length, permanently contacted at its tip to a metal layer with a controlled thickness of dielectric in between. Such a method, combined with the recently developed art of integrated optics, may provide new methods of enhancing the coupling of the radiation to the diode. Furthermore, depositing the diode on a substrate would enable realization of an array of metal-oxide-metal diodes with numerous interesting properties.

Despite all the promising indications, however, there is some probability that these detectors may end up as highly specialized devices, not useful for general field operation. There is a great need for more exploratory work before the systems application capabilities and limitations of the metal-oxide-metal infrared tunnelling diodes are completely comprehended.

Theoretical analysis of electron tunneling between electrodes separated by a thin insulating film was performed by Sommerfeld and Bethe for low and high values of applied dc voltages.[157] Other treatments of the subject appeared in the early 1960s and un adaptation of these to the metal-oxide-metal diode has been summarized[158] in a recent publication.[159] But a great deal of additional theoretical study, coupled with detailed experiment, is needed before the actual mechanisms occurring in the diode can be thoroughly understood.

6.5.2.3 Tuneable Far-Infrared and Infrared Radiometer

A tuneable far-infrared and infrared radiometer has a variety of potential applications, such as remote point sampling and spectroscopic chemical analysis of a distant target (possibly observations on rocket and stack plumes). There are two alternate methods, each of which requires considerable material development.

The first method is based on a superheterodyne receiver with a frequency tunable local oscillator. For this application, a detector element with a frequency response of tens of MHz (or less) is adequate since the frequency of the local oscillator is tuned close to that of the signal to be received, thus enabling heterodyning to occur at beat frequencies below the frequency limit of the detector element. Accordingly, this method requires tunable light sources and moderately fast detector elements.

The second method involves a fixed-frequency laser local oscillator and a detector element with a "super-fast" response time. The detector element could be a metal-oxide-metal diode with its ultra-high speed of response. The diode is subjected simultaneously to a fixed frequency infrared laser and a frequency tunable microwave radiation source. It has been shown experimentally that with microwave power of tens of milliwatts, the infrared frequency current flowing through the diode can be modulated at the microwave frequency by nearly 100 percent. Accordingly, the alternating current flowing through the diode at each of the infrared frequency side bands is sufficiently large in amplitude to be used as the local oscillator. In this case, the signal to be received is also applied to the same diode. The side-band frequency is tuned close to the signal frequency by tuning the microwave frequency, thus enabling observation of a beat note at a convenient intermediate frequency postamplifier frequency.

It should be noted that this method is applicable to any infrared detector with a subnanosecond response time if it also presents a sufficient amount of nonlinearity to cause a sizeable third order frequency mixing. The three frequencies to be mixed in the detector will be those of the radiation signal, the fixed frequency laser, and the tunable microwave radiation source.

6.5.2.4 Frequency Tuneable Infrared Light Sources as Local Oscillators

As noted above, the local oscillator is an integral part of the detection system in a superheterodyne receiver. Hence, material development for the local oscillators must be seriously considered as a part of a detector development program. The discussion here is limited to frequency tuneable infrared lasers, with examples showing need for further material development.

Frequency tuneable infrared lasers have recently attracted much attention for a variety of potential applications. There are now two types of infrared tuneable lasers, each of which operates close to liquid-He temperature:

- Tuneable injection diode lasers [160]
- Spin-flip Raman lasers [161]

Examples of the diode laser materials are PbSnTe and PbSnSe alloys [160]. These lasers are tuneable within several wavenumbers by changing the temperature, stressing the material, or applying a magnetic field. Their center frequencies can be preselected over a wide range by means of bandgap adjustment through alloy-composition control. They can be manufactured for use over wavelength bands which, so far, extend from about 4.5 to 12 μm but they are not commercially available. These diode lasers appear promising as a versatile tuneable source, but much work needs to be done on material development and diode fabrication (see 6.3.2.2) to improve their reliability and performance. Spin-flip Raman lasers also appear potentially important, but their eventual usefulness as a versatile device can only be assessed after further exploratory work.

Incidentally, in most applications, local oscillator powers in excess of at least several milliwatts are needed.

An attractive alternate method to achieve a tuneable light source capable of room temperature operation is microwave modulation of a fixed frequency gas laser and the generation of radiation at the corresponding side band frequencies. (In this case, infrared frequency tuning can be obtained by tuning the modulation frequency.)

There are a number of well known modulation methods utilizing various types of electro-optical effects in nonlinear crystals. So far, efficient infrared side-band generation has only been achieved at modulation frequencies in the hundreds of MHz region. For a versatile tuneable light source, however, it is important to use modulation frequencies at X- and K-band microwave frequencies so that full advantage can be taken of a much broader range of frequency tuning by using each of the closely spaced laser lines of an oscillating molecular laser band. No serious attempts have yet been made to generate in the infrared a useful amount of side-band power at such high modulation frequencies. Crystals with high electro-optical coefficients are greatly needed. The material homogeneity and the control of impurity over a long crystal length (in excess of several inches) together with a high degree of transparency in the infrared are currently among the major problems. In the 10 μm region CdTe and GaAs are among known materials with highest nonlinear modulation coefficients.[162] Material development in these areas is badly needed.

The use of dielectric waveguides in microwave modulation is another promising method that has been recently proposed.[163] A great deal of work is needed to exploit the full potential of this approach.

It should be stressed that unlike the case of tuneable lasers, the potential of microwave modulators as a practical method for achieving tuneable infrared light sources has not attracted adequate attention.

6.5.3 Parametric Upconvertors

Sensitive and reliable radiation detectors, including imaging systems are available in the visible and ultraviolet regions. Parametric upconversion, followed by direct detection in the visible or the ultraviolet region, has been considered for some time as a candidate for detection of infrared radiation.[164] The infrared radiation is parametrically mixed in a nonlinear crystal with the output of an intense laser, operating in the near-infrared or the visible region; the upconverted radiation is generated at the sum frequency. There are two methods to achieve this: phase-matching in a birefringent crystal and phase-matching in an optical waveguide.

With the phase-matching technique, it is possible to obtain appreciable conversion by utilizing a large length of a suitable crystal. The incident radiation propagates along specific directions in a birefringent crystal, where the corresponding indices of refraction satisfy the phase-matching requirement. Because of dispersion the phase-matching condition limits the usefulness of this technique to radiation over a narrow bandwidth of several wavenumbers. As a result, the application of this technique for an ultimately sensitive infrared thermal detector can be ruled out. Furthermore for infrared radiation over narrow band-widths (e.g., a monochromatic signal), a narrow field of view must be used to maintain the phase matching condition.

The upconversion of $10 \mu m$ laser radiation has attracted attention, mainly because of the $10 \mu m$ CO_2 laser and the atmospheric window in that wavelength region. With the availability of the CO laser operating in the $5 \mu m$ region, and the recent awareness of good atmospheric transmission properties at discrete frequency intervals in that region, the upconversion of the CO lines may also be of interest[150].

Birefringent phase-matched upconversion offers the promise of photon noise-limited imaging without scanning of the image plane and without the necessity of cryogenic cooling. However, the phase-matching requirement, the small size of the usable nonlinear-coefficient materials, and the power-handling capabilities of the known upconvertor materials severely limit the conversion efficiency.

The application of upconvertors includes receivers for pulsed and gated laser illuminators and radars at $10 \mu m$ (or $5 \mu m$). The use of high-intensity pulses of megawatt peak powers enhances the quantum efficiency factor by a sizable amount. Some interest has been shown (at Bell Telephone Laboratories) in birefringent phase-matched upconversion of $10 \mu m$ radiation for laser communication systems. The upconversion of a whole image has been investigated at Itek, Sylvania, NRL, and other laboratories. There is also interest in astrophysical applications in the $10 \mu m$ region. The Nd-YAG laser at $1.06 \mu m$ and ruby at $0.69 \mu m$ have been useful pump sources.

The birefringent crystals must be of low loss. HgS, Ag_3AsS_3 [165] [166] (Proustite) and Ag_3SbS_3 have been used for upconversion of 10 μm radiation. More recently, II-IV-V semiconductors have shown large nonlinear coefficients for 10 μm upconversion.[167-169] Large HgS single crystals are difficult to obtain. $ZnGeP_2$ and $CdGeP_2$ have larger nonlinear coefficients than Ag_3AsS_3, but $ZnGeP_2$ shows substantial absorption in the 1.06 μm region. Similar absorption in GaP was identified with impurities, which have been removed after extensive material research effort.

Upconversion by means of birefringent phase-matching techniques has not yet produced a high enough quantum efficiency to compete seriously with other infrared detectors. Considerable materials research is still required before a realistic assessment can be made of the ultimate potential of the parametric upconvertors. This is a productive area for exploratory research and development since efforts in developing the necessary nonlinear materials will be useful not only for upconvertors, but also in other applications (e.g., as modulators).

Waveguide phase-matching is an entirely different approach to upconversion. It involves the use of optical dispersion inside the guide. Phase-matching can thus be obtained in materials such as GaAs that would ordinarily not be phase-matchable. Due to this control, broad-band ($\Delta\lambda \approx$ 1 μm) operation is possible. Long interaction lengths can be used with very narrow pump beams. To avoid scattering into undesired modes, low order waveguide modes well separated in frequency must be used.[170] Coupling of the incident light into these guides is a difficult problem and is currently under investigation. Despite the difficulties, impressive upconversion quantum efficiencies of about 2 x 10^{-2} have been observed in individual waveguides.[170]

In principle, these guides could be incorporated in linear arrays using epitaxial techniques; slab guides can also be used. They should be ideal for integration with semiconductor diode pumps. With integrated optical circuit techniques, a cheap scanning detection system without cooling may be achievable.

Work with waveguide techniques is a recent development of potential importance. New approaches and ideas need to be explored before systems applications can be fully understood. This approach is highly promising.

6.5.4 Discussion

With the advent of lasers, a variety of new military and civilian applications have become possible. Practical realization of the potentially important applications is dependent on success in the development of novel detection methods. The development of some of these methods suffers from a lack of adequate attention to establish firmly their limitations as well as their capabilities. Examples include frequency tuneable superheterodyne receivers in the infrared, detection methods having very short time resolutions for the exploitation of subnanosecond pulses in the 5 and 10 μm regions, metal-metal oxide-metal point contact tunneling diodes, and some aspects of the parametric upconvertors.

In superheterodyne receivers, the mixer element as well as the laser local oscillator is an integral part of the detection system. It is recommended that emphasis be given to development of high-speed detectors in the 5 and 10 μm regions. Most conventional detectors are potentially capable of high-speed operation but very few are currently available for use in the 5 and 10 μm regions. As for the local oscillators, tuneable infrared lasers with continuous wave powers in excess of tens of milliwatts are greatly needed. Tuneable lasers are not commercially available. A potentially important method of obtaining a room-temperature tuneable source for local oscillator applications is microwave modulation of an infrared laser with a high depth of modulation to obtain sufficient side-band powers. For this purpose high-quality single crystals with high electro-optic coefficients are needed. Development of high-purity single-crystal GaAs and CdTe with high resistivity and low loss in the 5 and 10 μm regions is urgently needed for modulators (and numerous other applications). Attention also should be given to the potential of dielectric waveguides for modulation purposes.

It also is recommended that emphasis be placed on developing the full capability of the infrared metal-metal oxide-metal tunnelling diode. This will require undertaking further exploratory research of the detailed mechanisms and the exact material needs and may require controlled experimentation with clean surfaces under high vacuum. Furthermore, attention should be given to the possibility of making an array of detectors of this type, sufficiently rugged for field operation. Methods of improving the coupling of radiation to the diodes also should be explored.

Upconversion by phase-matching techniques applied to a host of birefringent materials has not produced the quantum efficiency necessary to compete seriously with infrared detectors. Considerable materials research is still required before a realistic assessment can be made of the potential capability of this method. The necessary technology to produce the required nonlinear materials will be useful not only for upconvertors but also in numerous other applications, such as modulators, switches, isolators, etc. Emphasis should be placed on purifying III-V compounds. High-purity upconvertor materials like $ZnGeP_2$ with low loss at $10\,\mu m$ are needed. Materials with a chalcopyrite-like structure (like $ZnGeP_2$) have promise for replacing Proustite as an upconvertor, and an exploratory material development program in this area is desirable.

Upconvertors using waveguide phase-matching methods offer promise. These guides may be used in linear arrays. The application of epitaxial techniques and slab waveguides is recommended. An exploratory program in this area may be combined with the development of microwave modulators which employ infrared dielectric waveguide methods.

6.6 Infrared Imaging

A topic of increasing importance is that of infrared imaging systems. The conventional approach is to use linear arrays of photoconductive detectors such as Ge:Hg or $Hg_{0.8}Cd_{0.2}Te$ which are mechanically scanned across the scene by moving

mirrors. Recommendations concerning array development will be found in the discussions of selected materials.

This section deals with three other imaging methods. These include intrinsic and extrinsic photoconductive vidicons, the pyroelectric vidicon, and mosaics, i.e., two-dimentional arrays. A discussion of charge-coupled imaging devices will be found in 5.5.2. See 5.4.3.4 and 5.4.4 for a discussion of photodiode imaging arrays.

6.6.1 Intrinsic and Extrinsic Photoconductive Vidicon Targets

Research and development of television camera tubes for use in the infrared has been carried out for many years. A major objective has been to achieve passive imaging whereby the camera senses only the natural heat radiation emitted by various objects in a scene.

Two types of vidicon targets have been studied extensively: narrow bandgap intrinsic photoconductors, and wider bandgap materials doped with suitable impurity states within the gap. Both types must be cooled to provide the high dark resistivity required for vidicon operation. Generally the intrinsic types exhibit high sensitivity due to the larger number of absorbing centers. The extrinsic types have better stability and a vari ety of response wavelengths can be achieved by introducing various dopants into the host material.

The first type of successful infrared camera tube employed either a sulfidized lead oxide layer or a porous evaporated lead sulfide material for imaging response to wavelengths up to $2 \mu m$. This was reported by Morton and Forgue about a decade after its development.[171] Tubes of this type are commercially available.

Sensing layers for the longer wavelength atmospheric windows have also been available for several years. Surfaces employing either amorphous intrinsic materials or suitably doped single-crystal material for extrinsic response have been used successfully. Either type of material may be used as a photoconductor in an

electron beam scanning tube; the first type of material may be used as a bolometric layer. Both devices have been able to image objects at temperatures only slightly different from the ambient temperature. Good speed of response has been observed and limiting resolutions over 500 TV lines have been observed at higher radiation levels.

A major difficulty in passive imaging is the low energy contrast available from infrared scenes; often, there is only a slight temperature variation between two objects that must be distinguished. Local variations in the "dark" background can be much larger than the signal variations in the scene. Any technique used to increase the image contrast also increases these unwanted "shading" variations. To some extent, shading is associated with material variation in the target. Consequently, materials research to produce photoconductors with improved uniformity can result in better imaging tubes. One approach is to make an intrinsic photoconductor from a single-crystal material such as InSb. A large area, thin, single-crystal film might be expected to have less variation than an amorphous film. There are also indications that local variations in factors which affect the current can contribute to shading. A special tube with a rotatable target showed that not all of the background shading rotated with the target. Therefore, research in electron optics also may lead to improved tubes.

At present, shading limits the quality of infrared vidicons since, in a small area, a high degree of sensitivity and contrast enhancement can be achieved with intrinsic photoconductive targets. Other areas that should be investigated are improving the stability and reproducibility of photosensitive layers.

It is recommended that research be continued on methods of improving the uniformity and sensitivity of intrinsic photoconductors suitable for application in infrared vidicons.

6.6.2 Pyroelectric Vidicon Targets

A vidicon camera with a sensing target that consists of a thin sheet of pyroelectric material offers the possibility of imaging a scene having temperature variance of about a degree, by its own thermal radiation. Such a system, although lacking the relatively high quantum efficiency of photoconductive target vidicons, has the merit of requiring no cooling and could be inexpensive.

In the pyroelectric effect, a polarization charge is developed when the temperature of the material changes. Under a steady flux of thermal radiation, the temperature equilibrates in a thermal time constant, and no further charge is produced. Thus, for a steady state signal it is essential that the input thermal flux be chopped by a constant temperature shutter. The signal that is detected is then a difference signal between two successive exposures to the scene and the shutter.

Thermal emission from a scene at, for example, 300° K where a difference of 1° K is to be detected contains a large undesired background flux compared with the temperature difference signal. It is an advantage of the pyroelectric effect that this background does not give rise to an electronic signal, although it does give some noise. The quantum efficiency of a pyroelectric material may be defined as the surface polarization charge per incident photon. For triglycine sulfate, the currently favored pyroelectrical material, the efficiency is about 10^{-6} for 10 μm radiation. Hence, if there were not ameliorating factors in the slightly different mode of detection, the pyroelectric vidicon would be hopelessly uncompetitive with the cooled photoconductive vidicon.

From an analysis of a typical device, the following requirements for pyroelectric vidicon operation have emerged.

6.6.2.1 Thermal Considerations

The pyroelectric vidicon differs from other devices in requiring that the time constant be larger than the signal (shutter) period for good response. A thermally isolated film is required for the target, preferably self-supporting so that the absorbed heat is not shared with a substrate.

6.6.2.2 Leakage Current

On each passage of the electron sensing beam past a target element, the target surface potential is lowered to near that of the cathode. If subsequent readings are not to be saturated by this process, it is necessary to leak electrons away from the target surface between readings. It can be shown that the minimum leakage current that can be employed without loss of signal depends upon the velocity distribution of the sensing electron beam.

6.6.2.3 Noise Equivalent Signal

The method of target current amplification is generally noisier than that of return beam detection since there may be appreciable amplifier noise in addition to the beam noise. Recent results on metal-oxide-semiconductor devices made from silicon on sapphire transistors have shown a large improvement in their noise figure to above that of the Junction Field-Effect Transistor. Use of these transistors with target pickup should allow the noise equivalent temperature to drop to that of the return beam system, or possibly even lower, since the return beam loss factor is no longer present. Careful design of these amplifiers is required, including use of negative feedback, to take advantage of the low inherent noise.

The material parameters appear in the noise equivalent temperature as $P_s \epsilon^{-\frac{1}{2}}$ (where P_s is the pyroelectric coefficient and ϵ is the dielectric constant); this may be used as a figure of merit when the noise is beam-limited. Increasing the target area gives an advantage proportional to the linear dimensions; decreasing the thickness only gives an advantage inversely as the square root of the thickness.

The noise temperatures discussed above have been derived under idealized conditions and represent rather optimistic expectations. In particular, the beam current may have to be increased, in practice, well above the ideal value to accommodate inhomogeneities in the target leakage current since the beam current per unit area of target must be larger than the greatest local value of leakage current per unit area. It is uncertain whether targets of the desired area of 4 cm^2 can be made of sufficiently uniform thickness and properties.

6.6.2.4 Polycrystalline Target

It was suggested that polycrystalline films might be made to have a greater uniformity of thickness and of pyroelectric coefficient than single-crystal wafers and that they might have a better controlled resistivity to give a uniform leakage current. These advantages must be balanced against the loss of effective pyroelectric coefficient due to random orientation of the crystals. From a simple analysis, there seems to be some advantage in using cubic material since the polarization tends to be nearer the normal. However, this particular advantage does not make lead zirconate titanate (PZT) comparable with TGS, since the figure of merit, P_s (eff) $\epsilon^{-\frac{1}{2}}$, is still three times better for polycrystalline TGS than for the best reported PZT. An advantage of PZT, which may dominate in practice, however, is the ability to control its conductivity within a desirable range by doping.

It appears that there is no fundamental barrier to constructing an image camera that could detect temperature differences of 0.2° C or less in relatively slow moving scenes with a modest spatial resolution. Since the construction of such a camera and its associated image storage and processing equipment is of a complexity comparable to that for a normal TV camera, and since the pyroelectric tube requires no cooling, such a thermal imaging camera would be less expensive than currently marketed equipment and may find a number of industrial, medical, and military applications. Currently the primary technical problem appears to be that of providing a uniform leakage of charge collected on the target face. Solutions to this may require modified, slightly conducting, pyroelectric material to be developed or a careful provision of leakage paths external to the target material.

It is recommended that research be continued in evaluating the properites of selected pyroelectric materials such as TGS, PLZT, and others for use as vidicon targets. Although the development of a high-performance pyroelectric vidicon will be difficult, the advantages associated with the lack of a cooling requirement warrant a moderate level of effort.

6.6.3 Mosaics

The present state of the art in solid state infrared image sensors is limited to linear photosensor arrays using narrow bandgap semiconductors as the photosensitive elements and conventional silicon devices for the signal switching or scanning functions. The two important advantages of two-dimentional or mosaic sensors are the elimination of mechanical scanring and the possibility of signal integration for a full frame time. To take advantage of the higher sensitivity resulting from the signal integration time for a full frame time, the infrared photosensor elements must be capable of low dark current operation. Another essential characteristic for a mosaic sensor array is a high degree of uniformity in the sensitivity of its signal detection elements.

The magnitude of the effort required for the development of infrared mosaic sensors having spectral response in the 2 to 14 μm range can be assessed by comparison with the state of the art of silicon mosaic sensors. It should be noted that in spite of the enormous effort in silicon device technology, silicon mosaics are still in the R & D stage and the sizes for such arrays are on the order of 100 x 100 resolution elements. Fabrication yields, requirements for uniform sensitivity of the signal detector elements, and switching noise associated with the scanning or signal extraction from two-dimensional arrays are some of the technological problems limiting the useful size of the present silicon mosaic sensors. Self-scanning charge-coupled silicon sensors are presently being considered as a promising new approach for solid state two-dimensional image sensors (see 5.5.2 for related discussion).

308

Infrared mosaic sensors can be visualized in two forms:

- Structures incorporating narrow bandgap materials as the photo-sensor elements and more conventional silicon devices, preferably in large-scale integration form, for signal extraction and, for signal storage functions

- Monolithic structures where the signal detection and the signal extraction are accomplished by devices integrated on single narrow-bandgap semiconductors

Research on the materials and technology for the first category of infrared mosaic sensors should be directed toward development of techniques by which the narrow bandgap semiconductor, such as a III-V binary or a ternary alloy compound, may be incorporated in a silicon LSI array. An example of one class of compounds that might be considered for this purpose comprises InAs, InSb, and $InAs_{1-x}Sb_x$. Development of liquid-phase or vapor-phase technologies by which epitaxial layers of suitable III-V compounds may be deposited on silicon is an example of a practical subgoal for research in this area.

The second class of monolithic infrared mosaic sensors will require major technological efforts leading towards development of a monolithic circuit technology for a narrow bandgap semiconductor having optical absorption bands in the desired infrared spectrum, such as the 3 to 5 μm or 8 to 14 μm atmospheric windows. Research in this area will require the development of appropriate materials. Viable subgoals for research in this area are the development of p-n junctions, bipolar transistors, field-effect junction transistors and Schottky barrier devices for the narrow bandgap semiconductors that are of interest for infrared radiation detection. Another class of long range goals in this area can well be the development of surface passivation techniques and the metal-insulator-semiconductor structures for insulated-gate field-effect transistors to be made from the narrow bandgap semicondcutors. Research on the monolithic HgCdTe line

sensors is an example of this type of research.

In light of this review, it is concluded that most research on infrared mosaic sensors should find earlier fall-outs in the area of linear infrared sensors. Furthermore, the merits of each research project on the infrared mosaic sensors should be evaluated from the point of view of its impact on the device technology that is needed in this area as well as its potential of achieving the desired system performance goals.

It is recommended that a level of effort, commensurate with the risks involved in developing high-density mosaics, be contirued.

6.7 Conclusions and Recommendations

6.7.1 Introduction

Although several novel detection methods have been discovered, those of principal importance to DoD will continue to be photoconductivity (intrinsic and extrinsic) and the photovoltaic effect. Photoconductivity has the advantage over the photovoltaic effect of simplicity of preparation and geometric considerations and of a larger group of usable materials since amphoteric conductivity is not required. The photovoltaic effect is preferred where the biasing required by photoconductors is a disadvantage. Intrinsic photoconductivity with its higher operating temperature is usually preferable to extrinsic photoconductivity. A direct gap semiconductor is to be preferred over an indirect one because of the steeper absorption edge, allowing a thinner detector.

The most important new intrinsic materials are HgCdTe and PbSnTe. The energy gap range of the former allows operation over virtually the entire spectrum, whereas that of the latter is confined to wavelengths greater than $5 \mu m$. The ability to purify HgCdTe sufficiently allows both photoconductive and photovoltaic devices to be made, whereas PbSnTe is generally operated in the photovoltaic mode.

6.7.2 Conclusion on HgCdTe Alloys

The spectral intervals of interest for HgCdTe infrared detectors are principally 1 to $3\,\mu$m, 3 to $5\,\mu$m, 8 to $14\,\mu$m, and 20 to $30\,\mu$m. The 1 to $3\,\mu$m range is of interest for missile-plume detection and engine-tailpipe detection and for multi-spectral radiometry for earth resources mapping. The 3 to $5\,\mu$m interval is of interest for missile and jet-engine-plume detection and thermal imagery of terrain and ambient temperature objects. In the latter instance, operation at dry ice temperature ($195°$ K) or above eases the cooling requirements. The 8 to $14\,\mu$m interval is the primary one for thermal imagery of terrain and objects at temperatures near that of the earth. Although cooling to $77°$ K is required, HgCdTe detectors operating in this spectral range provided superior detection capability to those in the 3 to $5\,\mu$m range when employed against an earth background. The 20 to $30\,\mu$m interval is of interest for detecting objects against cold space backgrounds.

HgCdTe is the best material for use in the 8 to $14\,\mu$m thermal mapping applications. It operates in the photoconductive mode at $77°$ K and is background limited in these applications. The principal problem is providing large areas, e.g., at least $1\ cm^{2}$, of sufficient uniformity in both composition and purity so that the performance of detectors in an array varies by no more than about 10 percent. This can be done on a selected basis, but the yield is low. The problem is complex since the manner whereby the various foreign impurity atoms and stoichiometric defects cause changes in the lifetime of the free carriers through various recombination and trapping mechanisms is not clear.

Much less effort has to be expended in preparing and evaluating HgCdTe for use in 1 to $3\,\mu$m, 3 to $5\,\mu$m and 20 to $30\,\mu$m applications. It appears now that it is the best material for the 1 to $3\,\mu$m and 3 to $5\,\mu$m applications, based on selected detector devices. It is certainly one of the best materials for the 20 to $30\,\mu$m application. Much basic research remains to be done on compositions suitable for these applications. As in the 8 to $14\,\mu$m application, the principal problems are uniformity and understanding of the trapping and recombination mechanisms.

<u>Recommendation</u> (Priority 1)

Research on HgCdTe alloys aimed at the following should be supported:

- Exploiting all ranges of composition, with special emphasis on those providing response in the 1 to $3\,\mu m$, 3 to $5\,\mu m$, 8 to $14\,\mu m$, and 20 to $30\,\mu m$ spectral intervals.

- Studying the fundamental electrical and optical properties of the alloys in all composition ranges, with emphasis on determining the trapping and recombination mechanism.

- Developing growth methods, including but not limited to liquid-phase epitaxy, that can provide crystals of at least 1 inch diameter, of high purity, and uniform in both composition and purity. The application is for high density arrays.

6.7.3 Conclusion on PbSnTe Alloys

The spectral intervals of interest for PbSnTe infrared detectors are 8 to $14\,\mu m$ and 20 to $30\,\mu m$. To date, it has not been possible to purify PbSnTe sufficiently to allow high-performance photoconductive detector operation, so that operation has been in the photovoltaic mode. Although, in general, the responsitivities are much less for photovoltaic detectors than for photoconductive thereby placing more stringent operational requirements on the amplifier, the elimination of a bias supply offers an advantage in some applications where weight and power are of concern.

The requirements for array uniformity impose purity and compositional uniformity requirements on PbSnTe similar to those for HgCdTe. Since BLIP limited PbSnTe detectors can be produced for 8 to $14\,\mu m$ earth background applications, the uniformity requirements are really yield requirements. Methods are needed for providing $1\ cm^2$ cross-sectional areas sufficiently uniform in both purity and composition so that all important detector parameters are uniform within 10 percent. A similar need exists for material suitable for use in 20 to $30\,\mu m$ applications. For compositions suitable for both applications, the nature of the trapping and recombination mechanisms requires elucidation.

Recommendation (Priority 1)

Research on PbSnTe alloys aimed at the following should be supported:

- Exploiting all ranges of composition, with special emphasis on detection in the 8 to 14 μm spectral ranges.

- Studying the fundamental electrical and optical properties of the alloy in all composition ranges, with emphasis on elucidating the trapping and recombination mechanisms.

- Studying growth methods, including but not limited to liquid phase epitaxy aimed at providing crystals of at least one inch diameter of sufficiently high purity and appropriately uniform in both composition and purity. The application is for high density arrays.

6.7.4 Conclusion on Doped Silicon Extrinsic Photoconductors

The most important extrinsic materials of current interest in the infrared are Si:P, Si:As, Si:Sb, Si:Bi, Si:B, Si:Aℓ, Si:Ga and Si:In. Except for Si:In, all respond at wavelengths between 15 and 30 μm. Thus, they are of use in cold background applications. The potential ability to fabricate large arrays in the same chip with integrated preamplifiers and multiplex switches is of obvious importance. The relatively high concentrations of the dopants compared to those in extrinsic Ge allows detector element thickness of about 100 μm, an important advantage in arrays, where crosstalk is a problem.

Recommendation (Priority 1)

Research directed toward exploiting the high density array-integrated circuit potential of extrinsic photoconductors of Si:P, Si:As, Si:Sb, Si:Bi, Si:Aℓ, Si:Ga and Si:In should be supported. The research should seek to determine which material is the best for the 20 to 30 μm detector application. Methods of preparing broad area (1 cm^2) single crystals of the best material and evaluating the potential for large high density arrays should be supported. The development of integrated circuits within the array chip, operating at the array temperature, should be supported (see 6.3.4.2).

6.7.5 Conclusion on Doped Germanium Extrinsic Photoconductors

Extrinsic Ge photoconductive detectors have been studied for two decades. The most important material today is Ge:Hg, which responds in the 8 to 14 μm spectral interval. The requirement for cooling the Ge:Hg detector to below 30° K reduces the utility since the alloy detectors HgCdTe and PbSnTe operating in the same spectral interval need to be cooled only to 77° K. Two other extrinsic detectors of importance for operating in the 20 to 30 μm interval are Ge:Cd and Ge:Cu. Alloy detectors operating in this same interval require cooling to well below 77° K, just as do Ge:Cd and Ge:Cu. All extrinsic Ge detectors have relatively low optical absorption coefficients, requiring the detector length to be much higher than that of the extrinsic Si detectors. A real advantage of the extrinsic Ge detectors over the alloys is the ability to adjust the response time through varying the concentration of selected compensation centers.

Recommendation (Priority 2)

Research should be continued on extrinsic Ge for use in the 8 to 14 μm and 20 to 30 μm intervals. The materials of primary interest are Ge:Hg for the former and Ge:Cd and Ge:Cu for the latter. The need for radiation hardening should be kept in mind. The studies should concentrate on the mechanisms of recombination and trapping (see 6.3.4.1.1).

6.7.6 Conclusion on Ternary Diamond-Like Semiconductors

A new class of materials of potential importance to infrared detection is the ternary diamond-like semiconductors. These have been intensively studied in the Soviet Union but largely ignored in the United States. Of special interest are the non-defect diamond-like ternaries including members of the $A^{II}B^{IV}C_2^V$, $A_2^I B^{IV} C_3^{VI}$, $A^I B^{III} C_2^{VI}$, $A_3^I B^V C_4^{VI}$, and $A^I B_2^{IV} C_3^V$ families, whose known members total more than 50 and whose energy gaps cover nearly all of the visible and infrared portions of the spectrum. Because of their simple nature it should ultimately be possible to prepare large uniform arrays of these materials at less cost than arrays of the alloy semiconductors.

The compounds of primary interest are those whose energy bandgaps are appropriate for operations in the 1 to 3 μm, 3 to 5 μm, 8 to 14 μm, and 20 to 30 μm spectral interval. Basic studies of growth and evaluation of the electrical and optical properties of many of these compounds are lacking so that the best compound for each application is not now known. Little or no contract support has been available to exploit these materials.

Recommendation (Priority 2)

An intensive program should be initiated to explore methods for preparing single crystals of promising ternary diamond-like semiconductors whose energy gaps permit operation in the 1 to 3 μm, 3 to 5 μm, 8 to 14 μm, and 20 to 30 μm spectral interval. The studies should emphasize growth of single crystals sufficiently uniform to yield high-density detector arrays over an area of approximately 1 cm^2. The electrical and optical properties of the materials should be evaluated as functions of temperature. The operable recombination trapping mechanisms should be elucidated. P-n junctions should be prepared and evaluated. The potentialities of the compounds for use in photoconductive and photovoltaic detectors should be determined. Throughout the program, the ultimate need for very uniform, very low cost, high-density arrays for each of the four spectral regions should weight the decisions on choice of materials, methods of growth, mode of detector operation, etc.

6.7.7 Conclusion on InAs and InSb Arrays

InAs and InSb are of interest for detector applications in the 1 to 3 μm and 3 to 5 μm regions, respectively. High-density detector arrays of high performance and whose parameters of interest within 10 percent of nominal are required. Variations in purity do not presently permit a high yield of such arrays. Liquid-phase epitaxy is a promising growth method for obtaining the necessary material uniformity. Photovoltaic detectors requiring p-n junctions are desirable for some applications.

Recommendation (Priority 2)

Research should be supported in the use of liquid phase epitaxy to produce single crystals of InSb and InAs of at least 1 cm^2 cross sectional area for use in high-density arrays of both materials. The required purity is approximately 10^{12} impurities cm^{-3} for photovoltaic ones. Methods of preparing p-n junctions in the epitaxial layers should be explored. The electrical and optical properties of the layers should be evaluated, with emphasis on an understanding of the recombination and trapping mechanisms. The suitability of the layers for use as photoconductive and photovoltaic infrared detectors should be ascertained.

6.7.8 Conclusion on Pyroelectric Detector Materials

The most promising uncooled, wavelength-independent detector is the pyro-electric one. It is applicable not only as a single element but in arrays and vidicons. It is of particular use for thermal imaging applications. The key to the pyroelectric detector is the choice of ferroelectric material. The one usually employed is triglycine sulfate. Others of interest are deuterated triglycine sulfate, triglycine fluoberyllate, strontium barium niobate, and lanthanum-doped lead zirconate titanate. The best detectors today are about an order of magnitude away from the theoretical room temperature background limit.

Recommendation (Priority 2)

Research should be supported on improving existing ferroelectric materials, and searching for new ones for use in pyroelectric detectors. The emphasis should be on materials useful for large-array thermal imaging applications. The detectivity should approach the background limit for thermal detectors against an earth background. Methods of preparing single and polycrystalline samples, attaching electrodes to these samples, and evaluating the performance of these samples as detectors should be supported.

6.7.9 Conclusion on Materials for Thermal Imaging

A need exists for two-dimensional arrays, or mosaics, for use in imaging applications. These are especially important for use in the 2 to 5 μm and 8 to 14 μm intervals. It is desirable that the associated electronics be fabricated within the same chip; this will probably not be accomplished in the near future in any material other than Si. Among the newer methods of signal detection and readout are those of the bucket-brigade and charge-coupled device.

Recommendation (Priority 2)

Long-term support should be given to research on methods and materials suitable for thermal imaging mosaics. New signal readout schemes such as charge-coupled devices and bucket-brigades should be investigated. The materials of interest are PbS, InAs, PbSe, and InSb in the 2 to 5 μm interval and HgCdTe and

PbSnTe in the 8 to 14 μm interval. Methods should be developed for preparing the associated electronics within the mosaic chip, analogous to large-scale integration employed for Si circuits.

6.7.10 Conclusion on Materials for Laser Detectors in 5 μm and 10 μm Wavelength Regions

With the advent of the laser, a variety of new military as well as civilian applications have become possible. Presently, practical realizations of the many potentially important applications are heavily dependent on successes in the development of novel detection methods. Most of the conventional detectors are potentially capable of high speed operation, but very few are currently available for use in the 5 and 10 μm regions. The development of some of these methods suffers from a lack of sufficient work to establish firmly their limitations as well as their full capability. Examples include:

- Frequency tuneable superheterodyne receivers in the infrared.
- Detection method with very short time resolution for the exploitation of subnanosecond pulses in the 5 and 10 μm regions.
- Metal-metal oxide-metal point contact tunneling diodes and parametric upconverters.

Tuneable infrared lasers with continuous wave powers in excess of tens of milliwatts are needed for local oscillators. A potentially important method for local oscillator applications is microwave modulation of an infrared laser with a high depth of modulation to obtain sufficient side-band power. For this purpose high-quality single crystals with high electro-optic coefficients are urgently needed.

Upconversion by phase-matching techniques applied to many birefringent materials has not produced a high level of quantum efficiency to compete seriously with other infrared detectors. However, considerable materials research is still required before a realistic assessment can be made of the ultimate potential of this method.

<u>Recommendation</u> (Priority 2)

It is recommended that support be provided for the development of high-speed detectors useful as laser detectors in the 5 and 10 μm regions. Research should be conducted on high-purity single-crystal GaAs and CdTe with high resistivity and low loss in the 5 and 10 μm regions for use in modulators (and numerous other applications). Attention should also be given to exploration of the potential of dielectric waveguides for modulation purposes.

The full capability of the infrared metal-metal oxide-metal tunnelling diodes should be determined. Exploratory research aimed at understanding the detailed mechanism of operation and the exact material needs should be strongly encouraged. This may require controlled experimentation with clean surfaces under high vacuum. Furthermore, attention should also be given to the possibility of making an array of detectors of this type sufficiently rugged for field operation. Methods of improving the coupling of radiation to the diodes should also be explored.

Research should be supported on nonlinear materials for use in phase-matched upconvertors. Purification of III-V compounds should be studied. New ternary diamond-like materials including $ZnGeP_2$ should be synthesized and evaluated for use in phase-matched upconversion. Waveguided phase-matching methods used with linear arrays should be studied, with emphasis on epitaxial techniques and slab waveguides.

6.7.11 Conclusion on Lead Chalcogenide Film Detector Arrays

Although the lead chalcogenides, PbS, PbSe, and PbTe have been exploited as infrared detector materials for two decades or more, they are still of technological interest. PbS is useful in high-density arrays for missile-plume detection and as individual elements for jet-engine-tailpipe detection in the 1 to 3 μm region. PbSe is useful in high-density arrays for both missile-plume detection and thermal mapping in the 3 to 5 μm region. PbTe would find application similar to PbSe if high-performance detectors could be made. The standard methods for preparing polycrystalline thin films of the lead chalcogenides by evaporation and chemical deposition have been

thoroughly studied. Recent studies of epitaxial methods of single-crystal film preparation have shown promise.

Recommendation (Priority 3)

Basic research on epitaxial methods for preparing thin films of the lead chalcogenides should be undertaken. The requirement for high density detector arrays dictates that the detector performance parameter uniformity shall be within 10 percent over a 1 cm^2 area. Studies of the optical and electrical properties of the layers, with emphasis on recombination and trapping, should be undertaken. The preparation of p-n junctions and Schottky barriers for use in photovoltaic detectors should be undertaken (see 6.3.1.1.4).

6.7.12 Conclusion on InAsSb Alloys

Homogeneous polycrystalline n-type $InAs_x Sb_{1-x}$ films can be grown in the composition range between $x = 0$ and $x = 0.3$. It is not certain that good single-phase crystalline layers can be synthesized in the composition range $0.3 < x < 0.75$, and yet it is of considerable interest because the fundamental bandgap reaches its minimum near the middle and not near one of the extremes. If the purity and compositional uniformity of the alloy having the minimum bandgap were superior to those of HgCdTe and PbSnTe, it would be of interest for 8 to $14\,\mu m$ detector applications, but there is no evidence that this is true. The InAsSb alloys should be considered as a backup for the 8 to $14\,\mu m$ HgCdTe and PbSnTe alloys.

Recommendation (Priority 3)

Research on the growth of alloys of InAsSb in the minimum bandgap range should be pursued. It should be aimed at obtaining high purity and extreme uniformity in composition; it should be coupled with evaluation of the material for infrared detector applications (see 6.3.2.3.3).

6.7.13 Conclusion on Materials for Pyromagnetic Detectors

Pyromagnetic detectors are competitive with pyroelectric and other thermal detectors for use in uncooled thermal imaging detectors. These are less important than the pyroelectric detectors because of the additional complexity afforded by the magnetic requirements. The key to the pyromagnetic detector is the pyromagnetic material. Of the known materials MnAs has the highest pyromagnetic coefficient, but as noted in 6.4.2, the best detectors have been made from gadolinium.

Recommendation (Priority 3)

Research should be supported on preparing and evaluating the properties of pyromagnetic materials for use in thermal imaging applications. A demonstration of potential superiority of the pyromagnetic detector to pyroelectric detector for some application should be a precondition for pyromagnetic detector device development.

6.7.14 Conclusion on Amorphous Semiconductors

Amorphous semiconductors could be important in infrared technology. They promise resistance to high energy radiation damage. They can be made in bulk and large-area evaporated film form, and have properties which imply their feasibility in infrared detectors as single elements, arrays, optical switches, image tubes requiring large area film detectors, and possibly even multi-color infrared tubes.

Recommendation (Priority 3)

Basic research on amorphous materials should be supported at a modest level with emphasis on their potential as infrared detectors. Since they cannot compete for all applications with crystalline semiconductor infrared detectors; attention should be directed toward applications that take advantage of their strong points, such as high energy radiation resistance. Work on large arrays and imaging devices should be deferred until single-element detectors with high detectivity have been demonstrated (see 6.4.5.3).

6.7.15 Conclusion on Infrared Vidicon Materials

A need has existed for many years for an infrared camera tube of the vidicon type. The key to the performance is the target that must meet requirements on resistivity, dielectric constant, sensitivity, and uniformity. In spite of an effort of almost two decades, there is no useful infrared vidicon today. Of the two classes of interest, photoconductive and pyroelectric, the pyroelectric is the more promising.

Recommendation (Priority 3)

Research should continue on materials useful for photoconductive and pyroelectric vidicons. Because of the long and largely unsuccessful attempt to develop a photoconductive vidicon, concentration and future efforts should be centered on pyroelectric detectors. Materials such as triglycine sulfate, strontium barium niobate, lanthanum-doped lead zirconate titanate, and others should be prepared in thin layers suitable for use as vidicon targets. The research should be coordinated with that on pyroelectric detectors for use in arrays.

6.7.16 Conclusion on Schottky-Barrier Detectors

Hot-electron Schottky-barrier detectors provide fast response, avalanche multiplication, and spectral response beyond the absorption edge of the semiconductor from which they are made. They should find application as laser detectors (see 6.3.7).

Recommendation (Priority 3)

Research should be continued on hot-electron Schottky-barrier detectors with emphasis on their use as laser detectors (see 5.6.2.9).

6.7.17 Conclusion on Heterojunction Detectors

In principle the heterojunction photodetector should have a higher detection efficiency than a p-n homojunction photodetector. In practice this has not been found to be true, probably due to recombination centers arising from lattice

321

mismatch at the interface. There seems to be little likelihood of a general solution
to this problem (see 6.3.6).

Recommendation

Work on heterojunction photodetectors for the 2 to 200 μm interval should
not be supported. See Section 5.5.1.5 and Recommendations in 5.6.1.6 of Chapter 5
regarding heterojunction photocathodes for use in the 0.1 to 2.0 μm interval.

6.7.18 Conclusion on PbGeTe Alloys

Alloys of small amounts of GeTe (up to 6 percent) in PbTe allow the
fabrication of detectors of high sensitivity and of shorter wavelength cut off
than pure PbTe; such photovoltaic detectors could have specialized application in
the 3 to 5 μm region.

Recommendation (Priority 3)

Research on PbGeTe alloys should be supported on a moderate level in
order to discover any advantages they might have over pure PbTe and, in particular,
to seek out what effects the large dielectric constant and its variation might have
on the detector operation. Possible advantages that might accrue from a ferroelectric
detector should be investigated.

322

6.8 References

1. See, for example, R. L. Williams, Infr. Phys. $\underline{8}$, 337 (1968).

2. See for example, L. K. Anderson and B. J. McMurtry, Appl. Optics $\underline{5}$, 1573 (1966); R. B. Emmons, J. Appl. Phys. $\underline{38}$, 3705 (1967).

3. J. C. Bose, U. S. Patent 755,840 (1904).

4. R. A. Smith, F. E. Jones, and R. P. Chasmar, The Detection and Measurement of Infrared Radiation, Clarendon Press, Oxford, 1957.

5. T. S. Moss, Proc IRE $\underline{43}$, 1869 (1955).

6. R. J. Cashman, Proc. IRE $\underline{47}$, 1471 (1959).

7. D. E. Bode in Physics of Thin Films edited by G. Hass and R. E. Thup, Academic Press, New York, 1966, Vol. 3, p. 275.

8. S. Espevik, C. H. Wu, and R. H. Bube, J. Appl. Phys. $\underline{42}$, 3513 (1971).

9. See for example, J. L. Davis and M. K. Norr, J. Appl. Phys. $\underline{37}$, 1670 (1966).

10. J. W. Wagner and A. G. Thompson, J. Electrochem. Soc. $\underline{117}$, 936 (1970).

11. J. N. Zemel in Solid State Surface Science, Vol. 1, ed. by Mino Green, Marcel Dekker, New York, 1969, p. 291.

12. R. B. Schoolar, Preparation and Properties of Epitaxial PbS Infrared Detectors, NOLTR 71-223 (1971).

13. For a recent review see Richard Dalven, Infrared Physics $\underline{9}$, 141 (1969)

14. D. L. Mitchell, E. D. Palik, and J. N. Zemel, Physics of Semiconductors; Proc. 7th International Conference, Paris 1964, ed. by M. Hulin, Academic Press, New York, 1964, p. 325.

15. R. B. Schoolar and J. R. Lowney, J. Vac. Sci. Technol. $\underline{8}$, 224 (1971).

16. H. Holloway and E. M. Logothetis, J. Appl. Phys. $\underline{42}$, 4522 (1971).

17. R. B. Schoolar, Appl. Phys. Lett. $\underline{16}$, 446 (1970).

18. G. G. Sumner and L. L. Reynolds, J. Vac. Sci. Technol. $\underline{6}$, 493 (1969).

19. R. B. Schoolar and J. R. Dixon, Phys. Rev. $\underline{137}$, A667 (1965); H. R. Riedl and R. B. Schoolar, Phys. Rev. $\underline{131}$, 2082 (1963).

20. W. W. Scanlon, J. Phys. Chem. Solids $\underline{8}$, 423 (1959).

21. J. N. Zemel, J. D. Jensen, and R. B. Schoolar, Phys. Rev. $\underline{140}$, A330 (1965).

22. J. P. Donnelly, T. C. Harman, and A. G. Foyt, Appl. Phys. Lett. 18, 259 (1971).

23. D. G. Simon, R. B. Schoolar, H. R. Riedl (private communication, 1971).

24. E. M. Logothetis, H. Holloway, A. J. Varga and E. Wilkes, Appl. Phys. Lett. 19, 318 (1971).

25. K. W. Nill, A. R. Calawa, T. C. Harman, and J. N. Walpole, Appl. Phys. Lett. 16, 375 (1970).

26. C. Hilsum and A. C. Rose-Innes, Semiconducting III-V Compounds, Macmillan, New York, 1961.

27. P. W. Kruse, Indium Antimonide Photoconductive and Photoelectromagnetic Detectors, in Semiconductors and Semi-Metals, ed. by R. K. Willardson and A. C. Beer, Academic Press, New York, 1970, pp. 15-83.

28. T. S. Blakemore, Semiconductor Statistics, Pergamon Press, New York. 1962.

29. K. F. Hulme and J. B. Mullin, Solid State Electronics 5, 211 (1962).

30. I. Melngailis and A. R. Calawa, J. Electrochem. Soc. 113, 58 (1966).

31. R. Gremmelmaier, Z. Naturforsch. 11a, 511 (1958).

32. D. Effer, J. Electrochem. Soc. 108, 357 (1961).

33. D. Effer and G. Antell, J. Electrochem. Soc. 107, 252 (1960).

34. G. R. Cronin and S. R. Borrello, J. Electrochem. Soc. 114, 1078 (1967).

35. G. R. Cronin, R. W. Conrad, and S. R. Borrello, J. Electrochem. Soc. 113, 1336 (1966).

36. M. A. C. S. Brown and P. Porteous, British J. Appl. Phys. 18, 1527 (1967).

37. G. A. Antypas, J. Electrochem. Soc. 117, 1383 (1970).

38. G. B. Stringfellow and P. E. Greene, J. Electrochem. Soc. 118, 805 (1971).

39. D. Long and J. L. Schmit, Mercury-Cadmium Telluride and Closely Related Alloys (for Intrinsic Infrared Detectors) in Semiconductors and Semi-Metals, Vol. 5, ed. by R. K. Willardson and A. C. Beer, Academic Press, New York, 1970, pp. 175-255. This is a comprehensive review of the subject and serves as the basic reference for most of this review.

324

40. J. D. Wiley and R. N. Dexter, Phys. Rev. 181, 1181 (1969).

41. P. W. Kruse, D. Long, and O. N. Tufte, Proc. Third International Conf. on Photoconductivity, ed. by E. M. Pell, Pergamon Press, New York, 1971, pp. 223-229.

42. J. L. Schmit and C. J. Speerschneider, Infrared Physics 8, 247 (1968).

43. J. L. Schmit and E. L. Stelzer (unpublished results).

44. A. G. Foyt, T. C. Harman, and J. P. Donnelly, Appl. Phys. Lett. 18, 321 (1971).

45. B. E. Bartlett, D. E. Charlton, W. E. Dunn, P. C. Ellen, M.D. Jenner, and M. H. Jervis, Infrared Physics 9, 35 (1969).

46. J. O. Dimmock, I. Melngailis, and A. J. Strauss, Phys. Rev. Lett. 26, 1193 (1966).

47. J. O. Dimmock, in The Physics of Semi-Metals and Narrow-Gap Semiconductors, ed. by D. L. Carter and R. T. Bate, Pergamon Press, Oxford, 1972, p. 319.

48. A. R. Calawa, T. C. Harman, M. Finn, and P. Youtz, Trans. AIME 242, 374 (1968).

49. J. W. Wagner and R. K. Willardson, Trans. AIME 242, 366 (1968).

50. J. F. Butler, A. R. Calawa, and T. C. Harman, Appl. Phys. Lett. 9, 427 (1966).

51. G. A. Antcliffe and J. S. Wrobel, Technical Report 08-70-38, Texas Instruments, June, 1970.

52. A good review of the device work is presented by I. Melngailis and T. C. Harman in Semiconductors and Semi-Metals, Vol. 5, ed. by R. K. Willardson and A. C. Beer, Academic Press, New York, 1970, p. 111.

53. R. F. Bis, A. S. Rodolakis, and J. N. Zemel, Rev. Sci. Instr. 36, 1926 (1965); E. M. Logothetis and H. Holloway, J. Appl. Phys. 43, 256 (1972).

54. E. G. Bylander, Mater. Sci. Eng. 1, 190 (1966).

55. R. F. Bis, J. R. Dixon, and J. R. Lowney, to be published.

56. J. N. Zemel, University of Pennsylvania, private communication.

57. I. Melngailis and T. C. Harman, Appl. Phys. Lett 13, 180 (1968).

58. D. Long and J. L. Schmit, in Semiconductors and Semi-Metals, Vol. 5, ed. by R. K. Willardson and A. C. Beer, Academic Press, New York, 1970.

59. J. W. Wagner and R. K. Willardson, Trans. AIME 242, 366 (1968).

60. E. M. Logothetis and H. Holloway, Solid State Commun. 8, 1937 (1970).

61. J. Donnelly, T. Harman, and A. Foyt, Lincoln Laboratory Report No. ESD-TR-71-20, p. 1, (1971).

62. K. Nill, J. Walpole, A. Calawa, and T. Harman, J. Phys. Chem. Solids (to be published).

63. W. M. Coderre and J. C. Woolley, Can. J. Phys. 46, 1207 (1968).

64. I. Kudman and L. Ekstrom, J. Appl. Phys. 39, 3385 (1968).

65. A. G. Thompson and J. C. Woolley, Can. J. Phys. 45, 255 (1967).

66. J. C. Woolley and J. Warner, Can. J. Phys. 42, 1879 (1964).

67. E. K. Mueller and J. L. Richards, J. Appl. Phys. 35, 1233 (1964).

68. G. B. Stringfellow and P. E. Greene, J. Electrochem. Soc. 118, 805 (1971).

69. H. H. Wieder, private communication.

70. A. R. Clawson, D. L. Lile and H. H. Wieder, J. Vac. Sci. Tech. (1972).

71. D. K. Hohnke, H. Holloway, and S. Kaiser, J. Phys. Chem. Solids, 33, 2053 (1972).

72. R. T. Bate, private communication.

73. G. A. Antcliffe, S. G. Parker, and R. T. Bate, Appl. Phys. Lett. 21, 505 (1972).

74. G. A. Antcliffe, private communication.

75. J. S. Wrobel, G. R. Pruett, M. A. Kinch, S. R. Borrello, and R. D. Juarros, Proc. IRIS Detector Specialty Group Meeting, p. 79, March 1972.

76. L. I. Berger and V. D. Prochukhan, Ternary Diamond-Like Semiconductors, Consultants Bureau, New York, 1969.

77. N. A. Goryunova and E. Parthe, Mater. Scien. and Eng., No. 2, 1 (1967).

78. A. S. Borshchevskii, N. A. Goryunova, F. P. Kesamanly and D. N. Nasledov, Phys. Stat. Sol. 21, 9 (1967).

326

79. N. A. Goryunova, A. S. Borshchevskii, and D. N. Tretiakov, in Semiconductors and Semi-Metals, Vol. 4. ed. by R. K. Willardson and A. C. Beer, Academic Press, New York 1968, p. 3.

80. D. N. Nasledov and N. A. Goryunova, eds., Soviet Research in New Semiconductor Materials, Consultants Bureau, New York, 1965.

81. F. P. Kesamanly, et al. Sov. Phys.-Doklady 10, 743 (1966).

82. F. M. Gashimzade, Sov. Phys. - Solid State 5, 875 (1963).

83. G. F. Karavaev, A. S. Poplavnoi, and V. A. Chaldyshev, Sov. Phys. - Semicond. 2, 93 (1968).

84. N. A. Goryunova and V. I. Sokolova, Izv. Mold. Filiala Akad. Nauk SSSR No. 3 (69), 31 (1960).

85. L. S. Palatnik et al., Fiz. Tverd. Tela 4, 1430 (1962).

86. N. A. Goryunova, A. V. Voitsekhovskii, and V. D. Prochukhan, Vest. Leningrad Gos. Univ. 10, 156 (1962).

87. F. F. Kharakhorin and V. M. Petrov, Fiz. Tverd. Tela 6, 2867 (1964).

88. L. S. Palatnik, Yu. F. Komnik, and V. M. Kashkin, All-Union Conference on Semiconducting Compounds, Izv. AN SSSR, Moscow (1961), p. 51.

89. R. Annamamedov, et al, in Chemical Bonds in Semiconductors and Thermodynamics, N. N. Sirota, ed., Consultants Bureau, New York (1968), p. 240.

90. H. F. Matare', Electrochem. Soc. Mtg., Chicago (1954).

91. B. Tell, J. L. Shay and H. M. Kasper, J. Appl. Phys. 43, 2469 (1972); and references listed therein.

92. N. A. Goryunova, et al.,Sov. Phys. - Solid State 7, 1060 (1965).

93. M. L. Belle, et al.,Sov. Phys. - Doklady 10, 641 (1966).

94. N. A. Goryunova, I. I. Tychina, and R. Yu. Khansevarov, Sov. Phys. - Semicond. 1, 110 (1967).

95. B. Ray, A. J. Payne, and G. J. Burrell, Phys. Stat. Sol. 35, 197 (1969).

96. F. P. Kesamanly, Yu. V. Rud and S. V. Slobodchikov, Sov. Phys.- Doklady 10, 336 (1965).

97. M. L. Schultz, Infrared Phys. 4, 93 (1964).

98. Fundamentals of Amorphous Semiconductors, Report of the Ad Hoc Committee on the Fundamentals of Amorphous Semiconductors, National Academy of Sciences, Washington, 1972.

99. A. F. Ioffe and A. R. Regel, in Progress in Semiconductors, Vol. 4, Wiley, New York, 1960.

100. S. R. Ovshinsky, Phys. Rev. Lett. 21, 1450 (1968).

101. T. S. Moss, Photoconductivity in the Elements, Butterworths Scientific Publication, London, 1952.

102. P. Scharnhorst and H. R. Riedl, Proceedings of the Special Meeting on Unconventional Infrared Detectors, ONR Report, USNEL, San Diego, April 1971.

103. S. G. Bishop and W. J. Moore, Proceedings of the Special Meeting on Unconventional Infrared Detectors, ONR Report, USNEL, San Diego, April 1971.

104. M. Guntersdorfer, J. Appl. Phys. 42, 2566 (1971).

105. K. Weiser, R. Fischer, and M. H. Brodsky, Proc. 10th Inter. Conf. Phys. Semiconductors, Cambridge, Massachusetts, 1970, p. 667.

106. R. Fischer, U. Heim, F. Stern and K. Weiser, Phys. Rev. Lett. 26, 1182 (1971).

107. D. L. Bowman and J. C. Schottmiller, J. Appl. Phys. 39, 1659 (1968).

108. J. Feinleib and S. R. Ovshinsky, J. Noncryst. Sol. 4, 564 (1970).

109. A. I. Gubanov, Zh. Tekh. Fiz. 20, 1287 (1950).
See also A. V. Ioffe, Zh. Tekh. Fiz. 18, 1498 (1948) and W. Shockley U. S. Patent 2, 569,347 (Sept. 25, 1951).

110. H. Kroemer, Proc. IRE 45, 1535 (1957).

111. R. Ruth, J. Marinace, and W. Dunlap, J. Appl. Phys. 31, 995 (1960).

112. M. Wolf, Proc. IRE 48, 1246 (1960).

113. R. G. Schulze, J. Appl. Phys, 37, 4295 (1966).

114. W. G. Oldham, Thesis, Carnegie Institute of Technology (May 1963).

328

115. W. G. Oldham and A. G. Milnes, Solid-State Electron 6, 121 (1963) and Solid-State Electron. 7, 153 (1964).

116. R. L. Anderson, Solid-State Electron. 5, 341 (1962).

117. See for instance, R. L. Anderson, Ph. D. Dissertation, Syracuse University (December 1959); J. C. Marinace, IBM J. Res. Dev. 4, 248 (1960); J. P. Donnelly, Ph. D. Dissertation; B. Agusta and R. L. Anderson, J. Appl. Phys. 36, 206 (1965); A. Lopez and R. L. Anderson, Solid-State Electron. 7, 695 (1964); S. S. Perlman and D. L. Feucht, Solid State Electron. 7, 911 (1964).

118. P. W. Kruse and R. G. Schulze in Proc. Third Photoconductivity Conf. Stanford, August 1969, ed. by E. M. Pell, Pergamon Press, New York, 1971, p. 403.

119. P. W. Kruse, F. C. Pribble, and R. G. Schulze, J. Appl. Phys. 38, 1718 (1967).

120. L. J. Van Ruyven, Thesis,Technical University of Eindhoven (Sept. 1964).

121. G. Zeidenbergs and R. L. Anderson, Solid-State Electron 9, 1 (1966).

122. W. G. Oldham and A. G. Milnes, Solid-State Electron. 6, 12 (1963).

123 T. Yamato, Japan J. Appl. Phys. 4, 541 (1965).

124. H. J. Hovel, Appl. Phys. Lett. 17, 141 (1970).

125. S. Fujita, S. Arai, K. Itoh, F. Moriai and T. Sakaguchi, Appl. Phys. Lett. 20, 317 (1972).

126. Proceedings of the International Conference on the Physics and Chemistry of Semiconductor Heterojunctions and Layer Structures, Akadamiai Kiado, Budapest, Hungary, 1971.

127. R. J. Archer and J. Cohen, Air Force Cambridge Research Laboratories Reports Nos. AFCRL-68-0651 (1968) and AFCRL-69-0287 (1969).

128. R. J. Archer and J. Cohen, Device Research Conference, Rochester, New York (1969).

129. V. E. Vickers, Appl. Opt. 10, 2190 (1971).

130. V. L. Dalal, J. Appl. Phys. 42, 2274 (1971).

131. S. R. Ducket, Phys. Rev. 166, 302 (1968).

132. F. D. Shepherd, Jr., A. C. Yang and R. W. Taylor, Proc. IEEE 58, 1160 (1970).

133. H. P. Beerman, IEEE Trans. on Electr. Dev. ED-16, 554 (1969).

134. R. W. Astheimer and F. Schwarz, Appl. Opt. 7, 1687 (1968).

135. R. W. Astheimer and S. Weiner, Application Notes for Pyroelectric Detectors, Barnes Engineering Company, Stamford, Conn., 1971, Bulletin 2-611.

136. A. M. Glass, J. Appl. Phys. 40, 4699 (1969).

137. S. T. Liu, J. D. Heaps, and O. N. Tufte, The Pyroelectric Properties of the Lanthanum-Doped PLZT Ceramics, Ferroelectrics 3, (1972).

138. H. P. Beerman, Ferroelectrics 2, 123 (1971).

139. P. J. Lock, Appl. Phys. Lett. 19, 390 (1971).

140. R. J. Phelan, R. J. Mahler, and A. R. Cook, Appl. Phys. Lett. 19, 337 (1971).

141. E. H. Putley and J. H. Ludlow, "Pyroelectric Detectors", presented at Electro-Optical Systems Design Conference, Brighton, England, March, 1971. To be published in Conference Proceedings.

142. R. W. Bene and R. M. Walser, "Pyromagnetic Detectors" in Proceedings of the Special Meeting on Unconventional Infrared Detectors, U. S. Naval Electronics Lab., San Diego, Calif., April 1971.

143. R. M. Walser, R. W. Bene, and R. E. Caruthers, IEEE Trans. on Electr. Dev. ED-18, 309 (1971).

144. E. D. Hinkley and P. L. Kelley, Science 171, 635 (1971).

145. M. C. Teich, R. J. Keyes, and R. H. Kingston, Appl. Phys. Lett. 9, 357 (1966).

146. G. Biernson and R. F. Lucy, Proc. IEEE 51, 202 (1963).

147. L. O. Hocker, D. R. Sokoloff, V. Daneu, A. Szoke and A. Javan, Appl. Phys. Lett. 12, 401 (1968).

148. R. L. Abrams and W. B. Gandrud, Proceedings of the Special Meeting on Unconventional Infrared Detectors, March 1971, San Diego. Published by University of Michigan, Willow Run Laboratories, April, 1971.

149. T. Gilmartin, H. A. Bostic and L. J. Sullivan, Proceedings of NEREM Conference (Nov. 1970), p. 168.

150 T. McClatchey, AFCRL Report 71-0370, July 1971.

151. For a related discussion see A. F. Milton and A. D. Schnitzler, IDA Research paper, p. 581, (IDA Log No. Hq. 70-10983), p. 27, (1970).

152. E. D. Hinkley, T. C. Harman, and Charles Freed, Appl. Phys. Lett. 13, 49 (1968).

153. C. Verie and M. Sirieix, IEEE J. Quant. Electronics QE 8, 180 (1972); I. Melngailis, Proceedings of Detector Specialty Group Meeting (u), March 1971, San Diego, Calif., Published by University of Michigan, Willow Run Lab., Aug. 1971 (Contract #N0014-67-A-0181-0031). For HgCdTe detector operation in the 3 to 8 μm region, see ref. 44.

154. D. R. Sokoloff, A. Sanchez, R. M. Osgood and A. Javan, Appl. Phys. Lett. 17, 257 (1970). See also: V. Daneu, D. R. Sokloff, A. Sanchez and A. Javan, Appl. Phys. Lett. 15, 398 (1969).

155. For a review of early work see: A. Javan, Ann. New York Academy of Sciences 168, 715 (1970).

156. K. M. Evenson, J. S. Wells, L. M. Matarrese and L. B. Elwell, Appl. Phys. Lett. 16, 159 (1970). See also K. M. Evenson, J. S. Wells and L. M. Matarrese, Appl. Phys. Lett. 16, 251 (1970).

157. A. Sommerfeld and H. Bethe, Handbuch der physik, Vol. 2412, ed. by H. Geiger and K. Schell, Julius Springer-Verlag, Berlin, 1933, p. 450.

158 See for instance John G. Simmons, J. Appl. Phys. 34, 1793, 2581 (1963).

159. Samuel I. Green, J. Appl. Phys. 42, 1166 (1971).

160. J. O. Dimmock, I. Melngailis, and A. J. Strauss, Phys. Rev. Lett. 16, 1193 (1966); J. F. Butler, A. R. Calawa, and T. C. Harman, Appl. Phys. Lett. 9, 427 (1966): For a review see T. C. Harman, J. Phys. Chem. Solids, in press.

161. C. K. N. Patel, and E. D. Shaw, Phys. Rev. Lett. 27, 451, (1970); S. A. Mooradian, S. R. J. Brueck, and F. A. Blum, Appl. Phys. Lett. 17, 481 (1970).

162. James E. Kiefer and Amnon Yariv, Appl. Phys. Lett. 15, 26 1969 .

163. For a demonstration of this method applied to modulation of a visible laser,
see D. P. McNutt and J. H. Harris, Applied Optics 11, 2757 1971 .
For a theoretical discussion applied to the 10 μm region, see: W. B. Gandrud,
IEEE J. Quant. Electr. QE-7, 596 (1971).

164. See for instance H. A. Smith and C. H. Townes, Polarization Matière et
Rayonnement, p. 467 (1969).

165. J. Warner, Appl. Phys. Lett. 12, 222 (1968).

166. W. B. Gandrud and G. D. Boyd, Optics Commun. 1, 187 (1969).

167. G. D. Boyd, W. B. Gandrud, and E. Buehler, Appl. Phys. Lett. 18, 446 (1971).

168. G. D. Boyd, E. Buehler, and F. G. Storz, Appl. Phys. Lett. 18, 301 (1971).

169. G. D. Boyd, E. Buehler, F. G. Storz and J. H. Wernick, IEEE J. Quant.
Electr. QE-8, 419 (1972).

170. D. B. Anderson, J. T. Boyd, and J. D. McMullen, Proceedings of the
Symposium on Submillimeter Waves, Polytechnic Institute of Brooklyn,
March 1970, pp. 191-210; see also D. Hall, A. Yariv and E. Garmire, Appl.
Phys. Lett. 17, 127 (1970).

171. G. Morton and S. V. Forgue, Proc. IRE 47, 1607 (1959).

DETECTORS FOR RADIATION OF WAVELENGTHS FROM 1 cm to 200 μm

7.1 Introduction

In the long wavelength end of the 1 cm to 100 μm region (e.g. the milli-meter wave region from 1 cm to about 1 mm), semiconductor diodes have been used extensively as frequency mixer elements and detectors since the advent of millimeter wave generators. The development of a high-quality mixer diode in this region for very low noise figure receivers is being actively pursued. Presently, the optimum performance of receiver systems is limited by the conversion loss, which is generally dependent on the processing and fabrication of the diode package as a circuit element in the radio frequency mixer circuit design.[1,2] As an example of the best contem-porary performance, a mixer using a Schottky-barrier diode fabricated on n-type epitaxial gallium arsenide exhibited single side-band conversion loss as low as 4 dB at 55 GHz[1].

The interest in developing mixer elements for receiver systems to detect in the 1 mm to 100 μm range (the submillimeter region) is relatively new and is due to the availability of many laser local oscillators in this region. However, a number of submillimeter wave detectors have been under development for some time with fairly broad-band characteristics capable of responding to a sizeable portion of the 1 mm to 100 μm region.

The potential applications of low noise receivers in the submillimeter region include astrophysical spectroscopic observations (such as the studies of molecular or atomic lines in the interstellar space or in the solar corona, the ob-servation of the well known background stellar continuum, etc.). Both of these areas are vast fields of study with some potential practical applications and where much can be done with the availability of versatile submillimeter wave detectors and mixer elements.

To indicate examples of the areas requiring material research and de-velopment, several types of detectors are described below.

7.2 Extrinsic Photoconductors in the Submillimeter Region

In an extrinsic photoconductor, the photoionization of neutral impurities at a low temperature is responsible for its photoconductivity. The long wavelength response limit of these devices depends on the impurity ionization energy. In Ge doped with Group III or V impurities, this limit lies at about 120 μm.[3] There are several semiconductors, such as InSb, InAs, or GaAs where the impurity levels are expected to be shallower than in Ge. These materials may permit development of extrinsic photoconductive devices capable of operating in the submillimeter region. The critical factor is the control of impurity content to allow de-ionization of shallow impurity centers at low temperatures.

With the development of vapor- and liquid-phase epitaxial techniques, it has become possible to prepare layers of GaAs of the required high purity.[4] In this material, the electrical characteristics at temperatures between 4° and 300° K are dominated by shallow-donor impurities with ionization energies in the 4 to 6 meV range.

In the long wavelength tail of the detectivity versus wavelength curve, a two-step process plays a major role extending the tail considerably beyond that determined by the energy separation between the donor's ground state and the conduction band.[4] In this case, an electron is first excited from the ground state into the first excited state of the donor and is then thermally transferred into the conduction band. This effect extends the photoconductivity of the GaAs beyond the 214 μm limit (corresponding to the energy spacing between donor ground state and the conduction band). A maximum detectivity of 8×10^{11} cm W^{-1} (Hz)$^{\frac{1}{2}}$ has been obtained at 2×10^{14} cm^{-3} donor concentration and $(N_A / N_D) = 0.2$.[5] The donor has not been positively identified. This detectivity is about an order of magnitude better than that generally obtained with the InSb hot electron bolometer. A comparison of the results obtained from these two detectors is difficult to make since the detectivity measurements were probably made under different conditions.

The device speed of response is important for its use as a mixer element in a submillimeter superheterodyne receiver. As noted already, practically, the response limit is determined by the carrier lifetime arising from impact ionization of the shallow impurity le   A lifetime as short as a few nsec has been determined for the GaAs. So far, the measured time constant has been limited by the resistance-capacitance time constant of the device package; this has given about a 40 MHz frequency response limit. Accordingly, the present device can be used as a mixer for detection of a radiation signal within 40 MHz of the local oscillator frequency.

7.3 Hot Electron Bolometers

Free-carrier absorption is observed in most semiconductors at wavelengths longer than the intrinsic absorption edge. Normally, this absorption does not give rise to photoconductivity because it produces an intraband transistion with no resulting change in the number of free carriers. In addition, the hot electrons excited by the radiation very quickly transfer energy to the lattice and return to equilibrium. At very low temperatures, however, the lattice coupling is weak and electrons can retain an energy (effective temperature) that is large compared to that of the lattice. When this occurs, the average electron mobility changes and there are resulting changes in conductivity. In order to observe this effect, high material purity and high electron mobility are required. To date, hot-electron bolometer operation has been observed in both n-type InSb and n-type Ge at near liquid helium temperatures. The hot-electron bolometers were first proposed by Rollin and developed by Kinch and Rollin in InSb[6,7] Unlike photoconductive detectors they do not have a sharp cut-off in detectivity at long wavelengths; instead their detectivity remains essentially constant for longer wavelengths and falls off proportional to λ^2 at shorter wavelengths. The short wavelength characteristic follows directly from the classical Drude theory for free-carrier absorption where

$$\alpha \propto \sigma , \tag{7.1}$$

and the conductivity variation with frequency is

$$\sigma = \frac{ne^2 \tau_e}{m^*} (1 + \omega^2 \tau_e^2)^{-1}, \qquad (7.2)$$

where α is the optical absorption coefficient, n is the free electron density, e is the electronic charge, τ_e is the electronic scattering time, m* is the electron effective mass, and ω is the angular frequency. To date the shortest wavelength operation has been obtained using InSb where

$$\omega \tau_e \approx 1 \text{ at } \lambda = 1.6 \text{ mm at } 4° \text{ K}.$$

Usable sensitivities have extended to a wavelength of approximately 100 μm.

Shorter wavelength operation was obtained by Putley who proposed increasing the short wavelength absorption coefficient by cyclotron resonance in a magnetic field. In a magnetic field, the spectral response becomes narrow band with typical bandwidths of the order of 5 percent of nominal centered at the cyclotron resonance frequency. For InSb resonance occurs at 100 μm for a 14 KG field and shifts to 26 μm in a 76 KG field.[8] There is some controversy as to whether the response in high magnetic fields is a true hot electron response, an impurity photoconductive response or combination of both.[8,9,10]

Reported typical response times are about 10^{-7} sec for broadband detection. However, in order to improve sensitivity in amplifier-noise-limited cases, several workers have increased the responsivity by incorporating a superconducting transformer resulting in bandwidths of the order of 10^3 Hz.

For hot-electron bolometers operated as video detectors, NEP's ranging from 1.3 x 10^{-13} W(Hz)$^{-\frac{1}{2}}$ to 3 x 10^{-13} W(Hz)$^{-\frac{1}{2}}$ have been reported.[6,7] The limiting noise mechanisms have been identified as Johnson noise and fluctuation in the exchange of energy between electrons, the lattice, and the applied electric field.[7,11] For a heterodyne mixer, NEP's ranging from 8 x 10^{-21} W(Hz)$^{-\frac{1}{2}}$ have been reported with local-oscillator noise-limited performance.[12]

A material purity (or equivalent compensation) level of 10^{13} impurities cm^{-3}, as well as high mobility and very low temperatures, are required for hot electron bolometer operation. The purity requirement, thus far, has limited practical devices to the use of Ge and InSb. The functional mode suggests considerable sensitivity to radiation damage. Despite these problems, the hot-electron bolometer is a viable and reproducible broadband detector for operation in the 100 μm to 10 mm region.

7.4 Josephson Detectors

In 1962, Josephson predicted the existence of superconducting zero-voltage tunnel currents between coupled superconductors.[13] The Josephson effect has been observed experimentally in both metal-insulator-metal thin film and metal-metal point contact structures.[14,15] Further, it has been found that these devices have an energy-dependent photoresponse which peaks near the single particle energy gap for normal electrons in a superconductor.

A superconductor below the transition point may be treated as made up of two interpenetrating electron fluids, one consisting of unpaired or "normal electrons" that are scattered by, and relax to, the ion lattice as in ordinary metallic conduction processes, and a second consisting of strongly correlated electron Cooper pairs (see Section 3.3.3.2) having superfluid properties inter alia, without dissipation.[16] Below the superconducting transition temperature, pairing of electrons is favored. It has been found that electron pairs have a temperature-dependent binding energy corresponding to the energy gap for normal electrons. When two superconductors are separated by a weak barrier, such as a thin insulating film, the electron matrix element for tunneling can be large enough to allow coupled electron wave function correlation on both sides of the barrier. Absorption of electromagnetic energy affects (a) the ratio of normal to paired electrons, and (b) the phase relation between Cooper pairs on opposite sides of the junction.

The simplest Josephson detection process takes place when incident photons are absorbed by Cooper pairs, which in turn are excited to the normal state: this results in a reduction of the zero-voltage tunneling current. The output signal is observed by measuring the drop in short circuit current of the device.

A more complex resonant process occurs when the Josephson junction is biased. When a voltage, V, is applied to the junction the relative phase of paired electron wave functions on opposite sides of the junction changes with time. The phase change, $\frac{d\phi}{dt}$, is given by

$$2\pi \frac{d\phi}{dt} = \frac{2eV}{h},$$ (7.3)

where e is the electron charge and h is Planck's constant.

This change of phase with time gives rise to a sinusoidal variation of the zero-voltage current having frequency

$$\nu_i = \frac{2eV}{h},$$ (7.4)

Further, the rate of change of $\frac{d\phi}{dt}$, is limited by the tunneling properties of the junction so that, in principle, the voltage in equation 7.3 can be varied rapidly in time. In practice, if electromagnetic energy is incident on the junction, the sinusoidal current of frequency ν_i is modulated at the frequency of the incident radiation, ν_{rf}, and side bands are formed at

$$\nu = \nu_i \pm n \, \nu_{rf}$$ (7.5)

$$n = 0, 1, 2, \ldots \quad .$$

A side band will occur at zero frequency whenever

$$V_{DC} = \frac{h}{2e} n \, \nu_{rf} \, .$$

Thus, the presence of incident electromagnetic radiation can be detected by discreet changes in the junction static volt-ampere characteristic.[17]

NEPs of 10^{-13} to 10^{-15} W(Hz)$^{-\frac{1}{2}}$ have been reported for Josephson detectors. Most workers report amplifier-noise-limited conditions. Although limitations on detector performance due to inherent noise have not yet been reached the coherent self-radiation implicit in equation 7.3 could represent one such limit.

The best sensitivity is obtained near wavelengths corresponding to the normal electron energy gap. This has limited operation to wavelengths longer than 100 μm. Utility at shorter wavelengths requires discovery of superconductors with higher critical temperatures.

In a recent publication, the response of superconducting weak links to photons is analyzed. It is shown that, in principle, this should allow detection of single photons.[18]

The frequency response of these devices is determined by tunneling parameters; 10^{-11} second risetimes seem possible. Generally Josephson detectors are quite fragile. Point contacts are subject to vibration damage and thin-film devices are subject to burn out. The Josephson junctions are operated at cryogenic temperatures, often below 4° K. The junction current is self limited by quenching from its own magnetic field. This phenomenon limits formation of uniform junction currents and there is a corresponding penetration depth of about 100 μm. Probably because of these various problems, the Josephson detector has been limited to laboratory use. Recently, interest in these detectors appears to have lessened. It is uncertain whether this is due to general research cutbacks, practical device difficulties or the rather limited utilization of the 1 cm to 100 μm spectral band.

In the laboratory, the Josephson junction has had several important applications. It is being used to determine fundamental constants. (Note that equation 7.3 is geometry independent). It has been used to measure voltage in the 10^{-12} volt

range and it has been used to measure magnetic fields in the 10^{-9} gauss range.

7.5 Metal-Metal Oxide-Metal Tunneling Detector

It has been known for some time that an assembly comprising a metal whisker in contact with a metal post responds to microwave radiation, i.e., a voltage is found to develop across it as the radiation is applied.[19] Depending on the type of contact, the response may simply originate (as is often the case) from a thermoelectric effect with a relatively slow speed of response. But a long response time limits the usefulness of the element as a mixer or frequency multiplier. It has been shown that it is possible to obtain a contact with very high speed of response. The first demonstration of this possibility was achieved in 1968 when it was shown that a contact could be formed which resulted in an assembly with frequency of response as high as 10^{12} Hz.[20] Later experiments have shown the possibility of obtaining a contact corresponding to a frequency of response exceeding about 10^{14} Hz (see Section 6.5).[21] Incidentally, a contact which is found to be as fast as, e.g., 10^{12} Hz, does not prove, in practice, to give a device with a much faster response speed. This is apparently also affected by factors such as the type of contact and the resulting resistance capacitance value.

In a mixer element, an ultra-high speed of response is of particular importance in the submillimeter region, mainly because of lack of frequency tuneability of the reliable laser sources as local oscillators. On the other hand, in the millimeter wave region, frequency-tunable microwave generators are readily available. This is because a mixer element with a moderate speed of response (e.g. tens of MHz) is adequate for use in a millimeter wave heterodyne receiver where frequency tuneability over a wide range can be obtained by tuning the local oscillator. For example, a hot electron bolometer with a moderate speed is an excellent mixer in a tuneable milimeter wave receiver. It is doubtful that a metal-metal oxide-metal diode can compete with other existing millimeter wave mixers. However, in submillimeter wave applications (and in the shorter wavelength region - see Section 6.5.2.2) the metal-metal oxide-metal diode's ultra-high speed of response,

together with its ability to operate at room temperature, makes it potentially attractive. In an initial test, with no precautions taken to optimize the coupling of the radiation to the metal-metal oxide-metal mixer diode, it has been possible to show that 10^{-14} watts at one Hz band-width may be detected for a case where the signal frequency differed from that of the laser local oscillator by 71 GHz. (In this test, the local oscillator and the detected signals were the 337 μm and 311 μm hydrogen cyanide laser lines obtained from two different laser units). For example, improvements appear likely by means of better coupling of the radiation to the diode to reduce the conversion loss and to obtain a local oscillator-limited noise performance.

Interest in using the diode as mixer and frequency multiplier in the submillimeter (and shorter) wavelength regions is relatively recent. As yet there has been no concentrated effort to understand the detailed behavior of the diode, and little has been done to produce a rugged unit for field operation.

7.6 Conclusions and Recommendations

7.6.1 Conclusion on Metallic Far Infrared Detectors

Two important devices of attractive capabilities are the Josephson junction and the room-temperature metal-metal oxide-metal diodes used as mixer elements for submillimeter receivers.

Recommendation (Priority 2)

Research on techniques for making rugged metal-metal oxide-metal diodes (or Josephson junctions) and understanding their performance as circuit elements should be supported.

7.6.^ Conclusion on Extrinsic Photoconductors

High-purity semiconductors, with shallow impurities, capable of extrinsic photoconductivity in the submillimeter region can be of importance to detection in this range. The existing GaAs photoconductive diode is not readily available to users.

Recommendation (Priority 3)

Use of the "existing" GaAs photoconductive diode should be encouraged. New material studies should await the demonstration of compelling need.

7.6.3 Conclusion on InSb Hot Electron Bolometer

Hot-electron bolometers are important detectors that require material purity and compensation levels $\leq 10^{13}$ impurities cm^{-3} as well as high mobility. Because of limited use, there has not been a strong need for further development.

Recommendation (Priority 3)

Research on the improvement of mobility and decrase of compensation in InSb used for hot electron bolometers is recommended at a modest level.

7.7 References

1. B. J. Clifton, W. T. Lindley, R. W. Chick and R. A. Cohen, Proceedings of Conference on High Frequency Generation and Amplification, 1971, Cornell University (to be published).

2. M. R. Barber, IEEE Trans. Microwave Theory Tech., MTT-15, 629-635, Nov. 1967.

3. E. H. Putley, Phys. Stat. Solidi, 6, 571 (1964).

4. G. E. Stillman, C. M. Wolfe, I. Melngailis, C. P. Parker, P. E. Tannenwald and J. O. Dimmock, Appl. Phys. Letters, 13, 83 (1968)

5. G. Stillman, C. M. Wolfe and J. O. Dimmock: Proceedings of the Symposium on Submillimeter Waves, Polytechnic Institute of Brooklyn, March 1970.

6. B. V. Rollin, Proc. Phys. Soc. (London) 77, 1102 (1961).

7. M. A. Kinch and B. V. Rollin, Brit. J. Appl. Phys. 15, 672 (1963).

8. E. H. Putley, Applied Optics 4, 649 (1965).

9. E. H. Putley, J. Phys. Chem. Solids, 22, 241 (1961).

10. R. A. Smith, Applied Optics, 4, 621 (1965).

11. M. A. Kinch, Applied Physics Letters, 12, 78, (1968).

12. T. G. Phillips, (private communication).

13. B. D. Josephson, Phys. Letters, 1, 251 (1962).

14. F. W. Anderson and J. M. Powell, Phys. Rev. Letters, 10, 230 (1963).

15. S. Shapiro, Phys. Rev. Letters, 11, 80 (1963).

16. D. N. Langenberg, et al, Proc. IEEE, 54, 560 (1966).

17. S. Shapiro, Proc. of the Special Meeting on Unconventional Infrared Detectors, Willow Run Laboratories, Univ. of Michigan, p. 27, April 1971.

18. R. Chiao, Physics Letters, 33A, 177, 1970.

19. J. W. Dees, Microwave Journal, p. 48, Sept. 1966.

20. L. O. Hocker, D. R. Sokoloff, V. Daneu, and A. Javan, Appl. Phys. Letters, 12, 401 (1968).

21. D. R. Sokoloff, A. Sanchez, R. M. Osgood and A. Javan, Appl. Phys. Letters 17, 257 (1970). See also K. M. Evenson, J. S. Wells and L. M. Matarrese, Appl. Phys. Letters 16, 251 (1970).

ABBREVIATIONS

Symbol	Meaning
BLIP	Background Limited Infrared Photoconductors
CCD	Charge Coupled Devices
D*	Detctivity Figure of Merit
FAPE	Field-Assisted Photoemission
FIR	Far Infrared
FLIR	Forward Looking Infrared Systems
FWHM	Full Width At Half Maximum
IMPATT	Transit Time Oscillators
LEFD	Low Energy Electron Diffraction
LSI	Large-Scale Integration
MIS	Metal Insulator-Semiconductor
M-O-M	Metal-Oxide-Metal Diode
MOS	Metal-Oxide Semiconductors
MOSFET	Metal-Oxide Semiconductor Field Effect Transists
NEA	Negative Electron Affinity
NEP	Noise Equivalent Power
PC-EL	Photoconductor-Electroluminescent
PLZT	Lanthanum-Doped Lead Zirconate Titanate
PZT	Lead Zirconate Titanate
RC	Resistance Capacitance
SBN	Strontium Barium Niobate
TEOS	Tetraethylorthosilicate
TGFB	Triglycine Fluoberyllate
TGS	Triglycine Sulfate
TSEM	Transmission Secondary Electron Multiplication